

Experimental Determination of the Frequency  
Spectrum of the Rose Bengal Picosecond  
Fluorescence using Two Beating Ring Dye Lasers

by

Zain Hassan Yamani

A Thesis Presented to the

FACULTY OF THE COLLEGE OF GRADUATE STUDIES

KING FAHD UNIVERSITY OF PETROLEUM & MINERALS

DHAHRAN, SAUDI ARABIA

In Partial Fulfillment of the  
Requirements for the Degree of

**MASTER OF SCIENCE**

In

**PHYSICS**

January, 1993

## **INFORMATION TO USERS**

**This manuscript has been reproduced from the microfilm master. UMI films the text directly from the original or copy submitted. Thus, some thesis and dissertation copies are in typewriter face, while others may be from any type of computer printer.**

**The quality of this reproduction is dependent upon the quality of the copy submitted. Broken or indistinct print, colored or poor quality illustrations and photographs, print bleedthrough, substandard margins, and improper alignment can adversely affect reproduction.**

**In the unlikely event that the author did not send UMI a complete manuscript and there are missing pages, these will be noted. Also, if unauthorized copyright material had to be removed, a note will indicate the deletion.**

**Oversize materials (e.g., maps, drawings, charts) are reproduced by sectioning the original, beginning at the upper left-hand corner and continuing from left to right in equal sections with small overlaps. Each original is also photographed in one exposure and is included in reduced form at the back of the book.**

**Photographs included in the original manuscript have been reproduced xerographically in this copy. Higher quality 6" x 9" black and white photographic prints are available for any photographs or illustrations appearing in this copy for an additional charge. Contact UMI directly to order.**

# **U·M·I**

University Microfilms International  
A Bell & Howell Information Company  
300 North Zeeb Road, Ann Arbor, MI 48106-1346 USA  
313/761-4700 800/521-0600



**Order Number 1354037**

**Experimental determination of the frequency spectrum of the  
rose bengal picosecond fluorescence using two beating ring dye  
lasers**

**Yamani, Zain Hassan, M.S.**

**King Fahd University of Petroleum and Minerals (Saudi Arabia), 1993**

**U·M·I**  
300 N. Zeeb Rd.  
Ann Arbor, MI 48106

---



**EXPERIMENTAL DETERMINATION OF THE  
FREQUENCY SPECTRUM OF THE ROSE  
BENGAL PICOSECOND FLUORESCENCE USING  
TWO BEATING RING DYE LASERS**

by

**Zain Hassan Yamani**

A Thesis Presented to the  
**FACULTY OF COLLEGE OF GRADUATE STUDIES**

In Partial Fulfillment of the Requirements  
for the degree  
**MASTER OF SCIENCE**

IN

**PHYSICS**

**KING FAHD UNIVERSITY  
OF PETROLEUM AND MINERALS**

**Dhahran, Saudi Arabia**

**JANUARY, 1993**

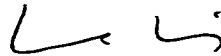
RECEIVED - 9 FEB 1993

KING FAHD UNIVERSITY OF PETROLEUM AND MINERALS  
DHAHRAN 31261, SAUDI ARABIA

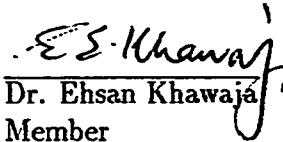
COLLEGE OF GRADUATE STUDIES

This thesis, written by ZAIN HASSAN YAMANI and approved by his Thesis Committee, has been presented to and accepted by the Dean of the College of Graduate Studies, in partial fulfillment of the requirements for the degree of MASTER OF SCIENCE.

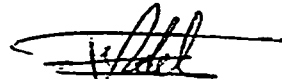
Thesis Committee



Professor UWE Klein  
Thesis Advisor



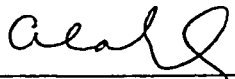
Dr. Ehsan Khawaja  
Member



Dr. Fida Al-Adel  
Member

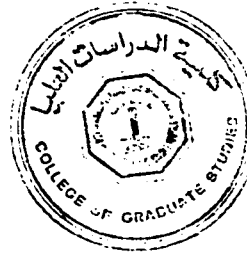


Dr. Abdul-Aziz Al-Harathi  
Department Chairman



Dr. Ala H. Al-Rabeh  
Dean, College of Graduate Studies

Date: January 1993



## ACKNOWLEDGEMENT

Acknowledgement is due to King Fahd University of Petroleum and Minerals for support of this research.

I wish to express my appreciation to Professor UWE Klein who served as my major advisor. I also wish to thank the other members of my Thesis Committee Dr. Ehsan Khawaja and Dr. Fida Al-Adel. I would like to thank Mr. Joe Mastromarino for assisting me in the experimental work.

# Table of Contents

	Page
Acknowledgements .....	iii
List of Tables .....	vii
Abstract .....	viii
I. Introduction .....	1
1.A. Time Resolved Spectroscopy .....	1
1.B. Rose Bengal: A Candidate for Picosecond Lifetime Measurements .....	6
II. Amplitude Demodulation: A Technique to Measure Lifetimes .....	9
2.1 Beating of Two Beams .....	9
2.2 Modulation Depth .....	14
2.3 Fluorescence Lifetime Determination by Amplitude Demodulation .....	18
2.4 Experimental Set-up .....	24
III. PMT Frequency Response Study .....	30
3.1 Introduction .....	30
3.2 Study of Spectrum Analyzer Baseline Subtraction .....	43
3.3 Study of the PMT Frequency Response .....	54
3.3.1. The Effect of Photon Flux Intensity .....	55
3.3.2. The Effect of Focus .....	64

	Page
3.3.3. The Effect of PMT Voltage .....	68
3.3.4. The Effect of Incident Laser Wavelength .....	78
3.3.5. The Effect of Polarization .....	81
Summary .....	83
IV. Rose Bengal Lifetime Determination in Water-Ethanol Mixtures: An Application For Demodulation Spectroscopy .....	84
4.1. Introduction .....	84
4.2. Procedure .....	86
4.3. Remarks .....	90
4.4. Data Manipulation and Error Analysis .....	97
4.4.A. The Lifetime of Rose Bengal in Pure Ethanol .....	97
4.4.B. The Lifetime of Rose Bengal in Water-Ethanol Mixtures .....	109
4.5. The Uncertainty in the Lifetime Measurements .....	141
4.6. The Quenching of Rose Bengal Fluorescence at High Water Concentrations .....	144

	Page
Summary .....	154
Conclusions .....	155
Appendix 1.A PMT Frequency Response Measurements Against Different Parameters .....	156
Appendix 1.B Rose Bengal Fluorescence Frequency Response Spectra at Different Water-Ethanol Mixtures .....	186
Appendix II BASIC Program Listing for Spectrum Analyzer Baseline Subtraction .....	203
References .....	206

## List of Tables

Table	Page
3.1 Spectrum Analyzer Baseline Subtraction .....	51
3.2 DC and AC Ratios at Different Incident Intensities .....	63
4.1 Rose Bengal Fluorescence Lifetimes and Decay Rates .....	139
4.2 Rose Bengal Fluorescence Lifetimes in Pure Water and in Pure Ethanol (Previous Work) ....	140

## THESIS ABSTRACT

FULL NAME OF STUDENT ZAIN HASSAN YAMANI

TITLE OF STUDY EXPERIMENTAL DETERMINATION OF  
THE FREQUENCY SPECTRUM OF THE  
ROSE BENGAL PICOSECOND FLUORESCENCE USING TWO BEATING RING DYE  
LASERS

MAJOR FIELD PHYSICS

DATE OF DEGREE JANUARY, 1993

In this thesis two ring dye lasers have been used to achieve amplitude modulated light of variable frequency.

The amplitude modulated light was used to study the frequency response of an 800 ps risetime photomultiplier against different parameters. The photomultiplier was found not to have a frequency response dependence on intensity of incident light, photocathode illumination shape, laser wavelength (in the range 570–593 nm), and polarization of incident laser beam. The higher frequency components of the response were enhanced with increasing photomultiplier operating voltage.

The amplitude modulated light was also used to perform demodulation spectroscopy on Rose Bengal. By measuring the demodulation in the fluorescence signal, the fluorescence lifetime of Rose Bengal in pure ethanol was found to be  $740 \pm 4$  ps. The lifetime was then determined in mixtures of water and ethanol. The fluorescence lifetime of Rose Bengal was found to monotonically decrease with increasing water concentration, and was found to be  $80 \pm 22$  ps in pure water.

The decay rates of Rose Bengal fluorescence showed a nonlinear dependence on water concentration. This could be explained by a water cluster model.

MASTER OF SCIENCE DEGREE

KING FAHD UNIVERSITY OF PETROLEUM AND MINERALS

Dhahran, Saudi Arabia

January 1993

بسم الله الرحمن الرحيم

## خلاصة الرسالة

اسم الطالب : زين بن حسن بن عبدالله يماني .  
عنوان الدراسة : التحديد المخبري للمطياف الترددي لجزء الروزينغال باستخدام  
ليزرين صبغيين حلقيين .  
التخصص : كلية العلوم ، قسم فيزياء .  
تاريخ الشهادة : ١٤١٣ هـ / ١٩٩٣ م .

لقد تم في هذا البحث الحصول على ضوء متضامن السعة ذو التردد المتغير بواسطة استخدام  
جهازين من ليزر الصبغ الحلقي .

ولقد استخدم الضوء المذكور لدراسة التجاوب الترددي لمضاعف ضوئي ذو زمن تصاعدي  
مقدراه (  $١٠ \times ٨٠٠$  -  $١٢$  ) ثانية تحت تأثير عوامل متعددة .

ولقد وجد بأن التجاوب الترددي للمضاعف الضوئي لايعتمد على أي من شدة ضوء الليزر  
الساقط أو شكله ، أو طول موجته ، أو استقطابيته . ووجد بأن التجاوب الترددي للمضاعف  
الضوئي يتحسن بازدياد الجهد الكهربائي على المضاعف الضوئي .

لقد تم أيضاً استخدام الضوء متضامن السعة لعمل فك تضمين جزئيء الروزينغال وبقياس  
فك التضمين في الانبعاث الجزئيء ، تبين أن مدة حياة الانبعاث الجزئيء لجزئيء الروزينغال في  
الكحول الإيثيلي هو (  $٧٤٠ \pm ٤$  )  $\times ١٠^{-١٢}$  ثانية .

كما تم تحديد مدة حياة الانبعاث للجزئيء المذكور في مخاليط من الماء والكحول الإيثيلي ووجد  
أن مدة حياة الانبعاث لجزئيء الروزينغال يقل تدريجياً بازدياد تركيز الماء في الخليط ، ووجد أن  
الانبعاث في الماء النقي هو (  $٢٢ \pm ٨٠$  )  $\times ١٠^{-١٢}$  ثانية .

ولقد أظهر معدل الانبعاث لجزئيء الروزينغال علاقة غير خطية بالنسبة لتركيز الماء في  
الخليط ، وأمكن تفسير هذا باستخدام نظرية الحزم المائية .

### درجة الماجستير في العلوم

جامعة الملك فهد للبترول والمعادن

الظهران - المملكة العربية السعودية

شعبان ١٤١٣ هـ - يناير ١٩٩٣ م

# CHAPTER 1

## INTRODUCTION

### A. Time Resolved Spectroscopy

Atomic or molecular spectroscopy is the science that studies transitions between different electronic, vibrational, and rotational states in atoms and molecules.

Time resolved spectroscopy is the branch of spectroscopy that is concerned with the rates at which different transitions take place. A lifetime of a transition is a measure of how long a molecule remains in the excited state of that particular transition. The transition rate, on the other hand, is a measure of how fast the transition occurs.

In the early 1970's, before laser applications to spectroscopy were well established, the most common technique for time resolved spectroscopy in the nanosecond range was the use of a fast spark gap lamp to create short excitation pulses. The time difference between excitation and the detection of a single photon was measured with a time to amplitude converter (TAC). Photons whose emission times are represented by a series of varying amplitude TAC outputs are generated from successive excitation pulses [1]. This is called the single photon counting method.

Still, this method was difficult to apply when measuring short times, of the or-

der of nanoseconds, with spark gap lamps because of the comparatively long pulse width. Other problems include: the exponential tailing in the falling edge of the flash, small number of photons per unit wavelength, and low repetition rates [1].

By the mid 1970's, lasers were well established in the field of time resolved spectroscopy. There are mainly three experimental methods for time resolved spectroscopy using lasers. These are: Pulsed excitation method, phasefluorometry, and the Hanle effect [2] which is hardly used any more.

In phasefluorometry, the molecules are excited by intensity modulated light. The fluorescence is also modulated with the same frequency, but there is a phase shift with respect to the incident light. This phase shift can be measured, and it is related to the lifetime of the fluorescence. Hence, the lifetime is determined [3,4].

As shorter and shorter laser pulses have been achieved during the last decade, intensive studies have been made on the pulsed excitation method [5]. Using saturable absorbers, pulses in the picoseconds domain have been achieved [6]. In fact, pulses as short as 8 fs have been reported [7].

Most lasers can be pulsed using electro-optical or acousto-optical methods. Pulses that are short in comparison with lifetimes of transitions under study excite molecules. The induced fluorescence can be monitored on an oscilloscope, or by transient recorders with averaging capabilities. Some of the latest techniques that utilize pulses are the laser induced pulsed excitation single photon counting method

[8], the pump probe method [9], and up-conversion [10].

In pump probe, two lasers are used. The first (pump laser) induces a transition from a lower state (usually the ground state) to a state that is to be studied; call it  $S_1$ . In effect, it is pumping the system to the excited state. The second pulsed laser (the probe) is set at an energy that corresponds to a transition from the excited state ( $S_1$ ) to a higher excited state; call it  $S_2$ . When this laser is applied, the amount by which the pulse is absorbed, is related to the population of the state  $S_1$ . If  $S_1$  has a long lifetime, the second pulse will be greatly absorbed. When a delay between the pump and probe pulses is introduced, the absorption is a measure of the population at that delayed time. Hence, the population of the excited state as a function of time is found resulting in the determination of the lifetime of state  $S_1$ .

In Up-Conversion, a special crystal, often called a doubling crystal, generates a second harmonic from the crossing of the fluorescence signal with a delayed laser pulse. Knowing the shape of the pulse, the second harmonic crossing signal may be deconvoluted to yield the shape of the fluorescence as a function of time thereby determining the lifetime of the excited state.

When making a comparison between pulsed excitation methods and phase-fluorometry, one can realize the following. Pulsed methods have the advantage of producing a complete (explicit) time decay curve. This can be very useful

when sorting out mixed emissions especially with the presence of non-exponential decays. Phasefluorometry, on the other hand, usually involves simpler instrumentation. The average excitation power in phasefluorometry is relatively high; hence, there is higher sensitivity when examining weak emissions [11].

Instead of measuring phase shifts, as in phasefluorometry, it is possible to measure demodulation in amplitude modulated fluorescence signals as compared to the excitation signal. The demodulation is also related to the lifetime of the fluorescent state. The major difficulty with this method is in the achievement of stable amplitude modulated excitation sources of great modulation depth.

Until 1984, there were many problems that faced researchers trying to obtain controlled frequency amplitude modulated light. Modulation depths were typically of the order of a few percent, and were strongly dependent on the frequency. Cut off frequencies were low (not more than 1 GHz).

In 1984, Lakowicz was able to make use of the harmonic content of a pulse train to obtain modulated light of discrete frequency. Still, the modulation depth was not constant with frequency, and depended on the width of the pulse [4].

In 1990, two groups<sup>a</sup> were able to obtain high frequency amplitude modulated light. While group (a: Williams et al) had laser wavelength of 1319 nm only [12, 13], group (b: Klein et al) had wavelengths of 280–1000 nm depending on the dyes used in the ring dye lasers. Group (a) had beat frequencies ranging between 6-34 GHz. Group (b), on the other hand, had a much wider range of 1 KHz – 10000 GHz or better with modulation depths of almost 100%.

There are many advantages in using amplitude modulated light. In contrast to the pulsed excitation method, amplitude modulation spectroscopy does not require ideal conditions for transmittance fidelity, and the interference with the investigated sample is low; this is advantageous when working with biological systems [3]. In addition, amplitude modulation spectroscopy may take advantage of the existence of high frequency components detected by a photomultiplier (PMT). Finally, we can select definite transitions using amplitude modulation spectroscopy.

Amplitude modulation spectroscopy may also be referred to as demodulation spectroscopy since it is the demodulation that gives us a measure of the lifetime.

In this thesis, we will work with amplitude modulated light sources of variable frequency. Demodulation spectroscopy will be applied to determine short lifetimes.

---

<sup>a</sup>The two groups are a: Williams et al of the Optical Science Division, Naval Research Laboratory, Washington, D.C., and b: Klein et al of the Laser Research Laboratory in KFUPM.

## B. Rose Bengal: A Candidate for Picosecond Lifetime Measurements

Rose Bengal (RB), the disodium salt of 2, 4, 5, 7-tetraiodo -3',4',5',6'-tetrachloro fluorescein, is a member of the Xanthene dyes. It was originally synthesized to mimic the red colors in bengalis [14]. Rose Bengal has a structure as shown in Figure (1.1). Extensive studies have been made on Rose Bengal. They include rotational diffusion [15], induced photo fragmentation [16], concentration induced changes in the micellar structures [17, 18], and singlet-singlet energy transfer [19] are discussed in literature. A review article about Rose Bengal was published in 1989 [14].

Because of a number of reasons, Rose Bengal holds an important position among dyes.

1. Although intersystem crossing is high in RB, fluorescence is almost always present. Through time resolved fluorescence measurements, one may be able to model different transitions.
2. It is a photodynamic sensitizer.
3. Its spectrum is diagnostic of its immediate environment.
4. The D-line in the sodium vapor lamp can easily excite RB in most solvents in which it is soluble.

A few other reasons are mentioned elsewhere [14].

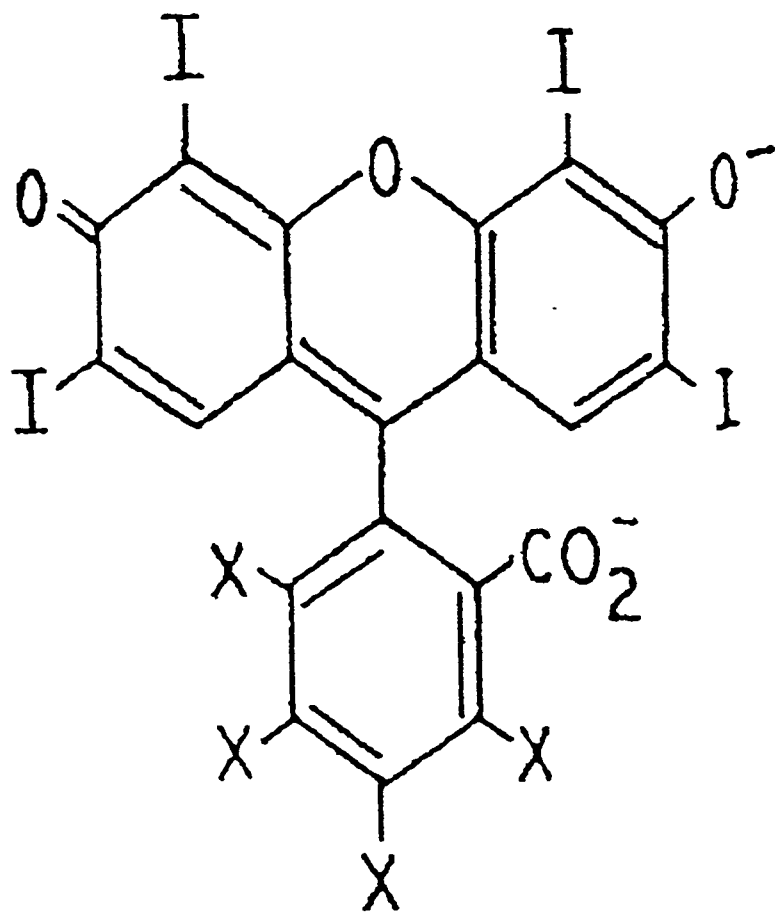


Fig. (1.1): Rose Bengal X = Cl

Still, because the fluorescence lifetimes of Rose Bengal in common solvents is very short, lifetime measurements have been performed only by a few groups; five groups to the best of our knowledge [1, 11, 15, 17, 20]. There has been discrepancy in the results but all published work shows that the fluorescence lifetime of Rose Bengal in water is in the range 75–120 ps, and in ethanol is in the range of 600–840 ps.

In this thesis, it is our intention to achieve amplitude modulated light of variable frequency. This will be used to study photomultiplier (PMT) frequency response characteristics. Specifically, the effects of incident intensity, photocathode illumination shape, PMT operating voltage, incident light wavelength, and polarization on the frequency response of the PMT will be studied.

Demodulation spectroscopy will be used to measure fluorescence lifetimes of Rose Bengal in different water–ethanol mixtures. By taking advantage of high PMT frequency response components, we will measure lifetimes that are, in cases, an order of magnitude shorter than the PMT risetime.

Finally, the variation in Rose Bengal fluorescence lifetimes with different water–ethanol mixtures will be studied.

## CHAPTER 2

### AMPLITUDE DEMODULATION: A TECHNIQUE TO MEASURE LIFETIMES

#### 2.1 Beating of Two Beams

An electromagnetic wave propagating along the  $x$ -direction may be described by:

$$E(x, t) = Ae^{i(kx - \omega t)} \quad (2.1.1)$$

where

- $A$  is the amplitude of the electromagnetic wave
- $E$  is the electric field of the electromagnetic wave
- $\omega$  is the angular frequency of the electromagnetic wave
- $k$  is the wave number of the electromagnetic wave.

If two electromagnetic waves (of the form (2.1.1)) are collinear, then the two waves may be described by:

$$E_1(x, t) = A_1 e^{+i(k_1 x - \omega_1 t)}, \quad E_2(x, t) = A_2 e^{+i(k_2 x - \omega_2 t + \theta)} \quad (2.1.2)$$

$\theta$  is a phase angle

If the two amplitudes  $A_1$  and  $A_2$  are equal then the superposition of the two electromagnetic waves is just the sum  $E(x, t)$ :

$$E(x, t) = A \left[ e^{i(k_1 x - \omega_1 t)} + e^{i(k_2 x - \omega_2 t + \theta)} \right] \quad (2.1.3)$$

At any point  $x_0$

$$E(x_0, t) = A e^{i(k_1 x_0)} \left[ e^{-i\omega_1 t} + e^{-i(\omega_2 t - \phi)} \right] \quad (2.1.4)$$

where  $\phi = \theta + (k_2 - k_1)x_0$  is a constant phase angle.

Therefore,  $E(x_0, t)$  which, at a specific point in space, is a function of time only, can be written:

$$E(t) = K [\cos \omega_1 t - i \sin \omega_1 t + \cos(\omega_2 t - \phi) - i \sin(\omega_2 t - \phi)]; \quad (2.1.5)$$

$K (= A e^{ik_1 x_0})$  is a constant

$$= K [\cos \omega_1 t + \cos(\omega_2 t - \phi) - i(\sin \omega_1 t + \sin(\omega_2 t - \phi))] \quad (2.1.6)$$

But

$$\sin \alpha + \sin \beta = 2 \sin \frac{\alpha + \beta}{2} \cos \frac{\alpha - \beta}{2} \quad (2.1.7)$$

and

$$\cos \alpha + \cos \beta = 2 \cos \frac{\alpha + \beta}{2} \cos \frac{\alpha - \beta}{2} \quad (2.1.8)$$

Therefore,

$$\sin \omega_2 t + \sin(\omega_1 t - \phi) = 2 \sin \frac{(\omega_1 + \omega_2)t - \phi}{2} \cos \frac{(\omega_1 - \omega_2)t + \phi}{2} \quad (2.1.9)$$

and

$$\cos \omega_1 t + \cos(\omega_2 t - \phi) = 2 \cos \frac{(\omega_1 + \omega_2)t - \phi}{2} \cos \frac{(\omega_1 - \omega_2)t + \phi}{2} \quad (2.1.10)$$

Therefore,

$$E(t) = 2K \cos \frac{(\omega_1 - \omega_2)t + \phi}{2} \left[ \cos \frac{(\omega_1 + \omega_2)t - \phi}{2} - i \sin \frac{(\omega_1 + \omega_2)t - \phi}{2} \right] \quad (2.1.11)$$

That is,

$$E(t) = 2K \cos \frac{(\omega_1 - \omega_2)t + \phi}{2} e^{-i\left(\frac{\omega_1 + \omega_2}{2}t - \phi\right)} \quad (2.1.12)$$

The intensity of an electromagnetic wave is  $I = EE^*$ . For the first electromagnetic wave alone,

$$E_1(t) = Ae^{i(k_1x - \omega_1t)}$$

Therefore,

$$I_1(t) = E_1E_1^* = A^2 \quad (2.1.13)$$

For the second electromagnetic wave alone,

$$E_2(t) = Ae^{i(k_2x - \omega_2t + \theta)}$$

Therefore,

$$I_2(t) = E_2E_2^* = A^2 \quad (2.1.14)$$

From Eqs. (2.1.13, 2.1.14),  $I_1$ , and  $I_2$  are constant in time.

However, the intensity of the superposition is (using Eq. (2.1.12)),

$$\begin{aligned} I(t) &= EE^* \\ &= 4K^2 \left[ \cos \frac{(\omega_1 - \omega_2)t + \phi}{2} \right]^2 \end{aligned}$$

But,

$$\cos^2(\alpha/2) = \frac{1 + \cos \alpha}{2}.$$

Therefore,

$$I(t) = 2K^2(1 + \cos[(\omega_1 - \omega_2)t + \phi]) \quad (2.1.15)$$

The resultant intensity is amplitude modulated at an angular frequency  $\omega_1 - \omega_2$ .

In summary, if we have two electromagnetic waves that are collinear and have the same polarization and amplitude, with angular frequencies  $\omega_1$ , and  $\omega_2$ , the intensity of each alone is constant with time. The intensity of their superposition, however, is amplitude modulated at an angular frequency equal to the difference between the two frequencies  $\omega_1$  and  $\omega_2$ . The name beating is referred to this superposition of electromagnetic waves. This can be pictured as in Figure (2.1).

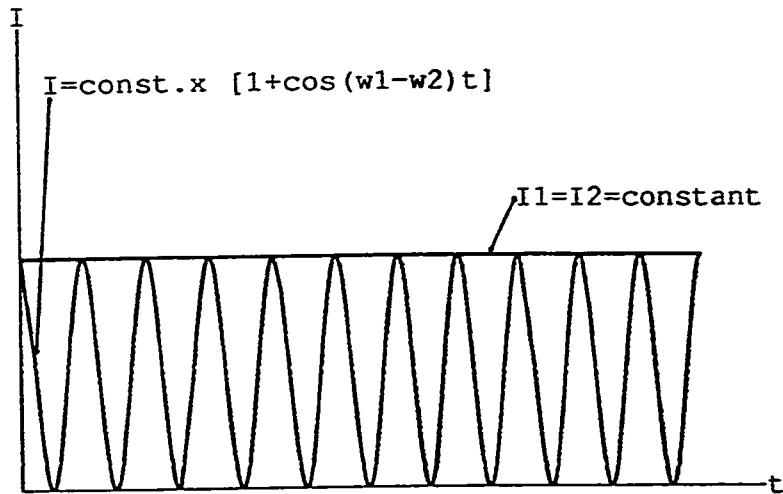


Fig. (2.1): Beating of Two Beams

## 2.2 Modulation Depth

If the time dependence of any system under investigation is described through linear differential equations, the time dependence of the response,  $I_E(t)$ , is given by the convolution integral [3]:

$$I_E(t) = \int_0^t I_a(t - \theta) I_E^\delta(\theta) d\theta \quad (2.2.1)$$

where

$I_a(t)$  is the time dependent excitation

$I_E^\delta(t)$  is the  $\delta$  response of the system

If the excitation source is amplitude modulated with a frequency  $\nu$ , then

$$I_a(t) = A[1 + \alpha \cos \omega t] \quad (2.2.2)$$

where

$$\omega = 2\pi\nu$$

$\alpha$  is ( $0 < \alpha < 1$ ) called the modulation depth of the exciting source.

$\alpha = 1$  means perfect amplitude modulation.

In complex notation,

$$I_a(t) = A[1 - \alpha e^{-i\omega t}] \quad (2.2.3)$$

Substituting Eq.(2.2.3) in Eq. (2.2.1), the response  $I_E(t)$  has the form [3]

$$I_E(t) = B[1 - \beta e^{-i(\omega t - \phi)}] \quad (2.2.4)$$

$\phi$  is a phase shift.

$\beta$  is the modulation depth of the response.

We can see that the response has the same modulation frequency  $\omega$ , but a different modulation depth,  $\beta$ . The response is also shifted by an angle  $\phi$ .

For the simple case of mono-exponential  $\delta$ -response

$$I_E^\delta(t) = \eta e^{-\lambda t} \quad (2.2.5)$$

where  $\lambda$  is the rate associated to the response.

If the response is a fluorescence,  $\lambda$  becomes  $\lambda_F$  (the decay rate of the fluorescence). The lifetime of the fluorescence is the inverse of the decay rate

$$\tau_F = \lambda_F^{-1}. \quad (2.2.6)$$

Substituting (2.2.3, 2.2.4, 2.2.5) in (2.2.1) with the upper limit in the integral going to infinity shows that the phase shift  $\phi$ , and the modulation depth of the response  $\beta$  are given by,

$$\phi = \tan^{-1} \frac{\omega}{\lambda_F}, \quad (2.2.7)$$

$$\beta = \alpha \frac{\lambda_F}{\sqrt{\omega^2 + \lambda_F^2}} \quad (2.2.8)$$

It is clear that  $\beta \leq \alpha$ . That is, the modulation depth of the response is always less than or equal to the modulation depth of the excitation source.

If the modulation source is perfectly amplitude modulated ( $\alpha = 1$ ),

$$\beta^2 = \frac{\lambda^2}{\lambda^2 + \omega^2} \quad (2.2.9)$$

The relation between an amplitude modulated excitation source and its response can be pictured as in Figure (2.2).

If the  $\delta$ -response is complex; i.e.,  $I_E^\delta(t) = \sum_i A_i e^{-\lambda_i t}$  then  $\phi$  and  $\beta$  are given by [3],

$$\phi = \tan^{-1} \left[ \frac{\sum \frac{A_i \omega}{\omega^2 + \lambda_i^2}}{\sum \frac{A_i \lambda_i}{\omega^2 + \lambda_i^2}} \right] \quad (2.2.10)$$

$$\beta = \alpha \left[ \left( \sum \frac{A_i \omega}{\omega^2 + \lambda_i^2} \right)^2 + \left( \sum \frac{A_i \lambda_i}{\omega^2 + \lambda_i^2} \right)^2 \right]^{1/2} \left( \sum \frac{A_i}{\lambda_i} \right)^{-1} \quad (2.2.11)$$

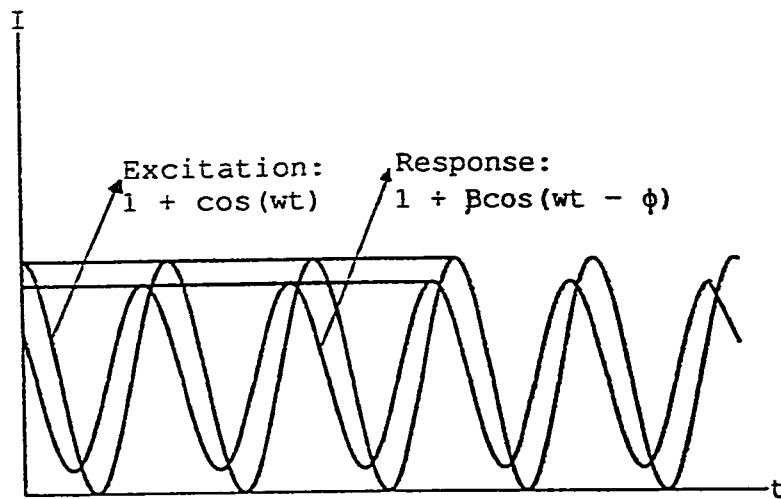


Fig. (2.2): Excitation and Response of Amplitude Modulated Light Incident on a Linear System

### 2.3 Fluorescence Lifetime Determination by Amplitude Demodulation:

As mentioned in Sec. 2.2, if a system has a simple fluorescence decay rate  $\lambda$ , the intensity of the fluorescence has the form

$$I(t) = \eta e^{-\lambda t} \quad (2.3.1)$$

The lifetime  $\tau$  is the inverse of the decay rate

$$\tau = \lambda^{-1} \quad (2.3.2)$$

Therefore,

$$I(t) = \eta e^{-t/\tau} \quad (2.3.3)$$

At time  $t = 0$

$$I(t) = \eta \quad (2.3.4)$$

At time  $t = \tau$

$$I(t) = \eta e^{-1} \approx 0.368 \eta \quad (2.3.5)$$

This means that the lifetime  $\tau$  is the time it takes the fluorescence intensity to drop by a factor  $1/e$ ; i.e., by a factor 0.3678; refer to Figure (2.3).

This lifetime can be experimentally measured using amplitude demodulation in the following way:

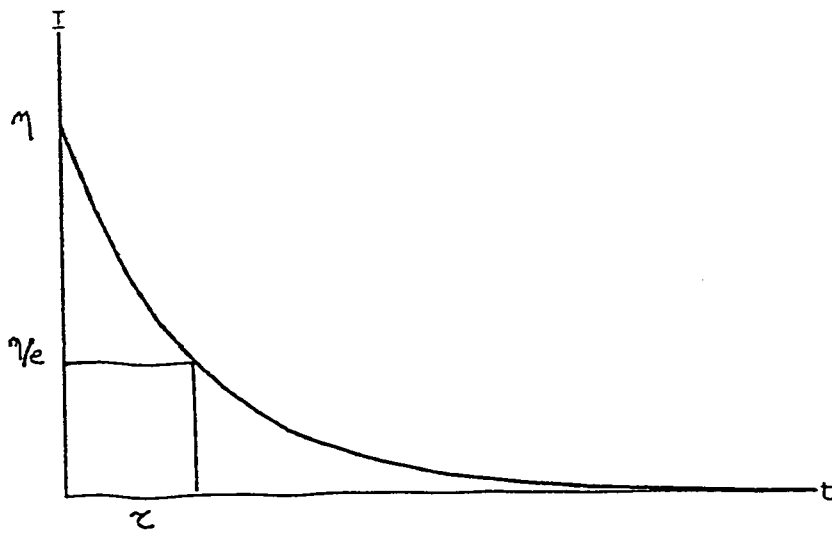


Fig. (2.3): Meaning of Lifetime

If there is an excitation light source which is amplitude modulated at variable frequencies with modulation depth 1, then according to (2.2.3, 2.2.4), the intensity of the excitation source is:

$$I_a(t) = A(1 - e^{-i\omega t}) \quad (2.3.6)$$

and the intensity of the response is:

$$I_E(t) = B(1 - \beta e^{-i(\omega t - \phi)}) \quad (2.3.7)$$

In two steps:

1) The amplitude modulated light source is incident on a scatterer (e.g., diluted milk). The response will be

$$I_0(t) = B_0(1 - \beta_0 e^{-i(\omega t - \phi_0)}) \quad (2.3.8)$$

$B_0$  is the DC value of the scattered signal.

From eq (2.2.8),

$$\beta_0^2 = \frac{\lambda_0^2}{\lambda_0^2 + \omega^2} \quad (2.3.9)$$

But for a perfect scatterer there are no excited states; therefore  $\tau_0 = 0$  and  $\lambda_0$  is infinite. Substituting in 2.3.9, we get  $\beta_0 = 1$  for scatterers. Substituting in 2.3.8

$$I_0(t) = B_0(1 - e^{-i(\omega t - \phi_0)}) \quad (2.3.10)$$

i.e., the amplitude of the AC signal is also  $B_0$ .

2) The amplitude modulated light is incident on the fluorescent sample. The response will be

$$I(t) = B(1 - \beta e^{-i(\omega t - \phi)}) \quad (2.3.11)$$

$B$  is the DC value of the fluorescence signal

$B\beta$  is the AC amplitude of the fluorescence signal.

By monitoring the DC values of the scatterer and the fluorescent sample we determine  $B_0$ , and  $B$ . Measuring the AC amplitudes from the scatterer and fluorescence (call them  $S_0$ , and  $S$  respectively) and dividing the AC signal of the fluorescence by the AC signal of the scatterer we get:

$$\frac{S}{S_0} = \frac{\text{AC signal of fluorescence}}{\text{AC signal of scatterer}} = \frac{B\beta}{B_0} \quad (2.3.12)$$

where

$S$  : is the AC amplitude from fluorescence.

$S_0$  : is the AC amplitude from scatterer.

$B$  : is the DC signal from fluorescence.

$B_0$  : is the DC signal from scatterer.

$S, S_0, B$  and  $B_0$  are determined experimentally and from Eq. (2.3.12)

$$\beta = \frac{B_0 S}{S_0 B} \quad (2.3.13)$$

It is possible to make  $B_0$  equal to  $B$  by varying the intensity of the excitation source until the DC signal from the scattered signal  $B_0$  is equal to that of the fluorescence signal  $B$ . In that case, the modulation depth is

$$\beta = \frac{S}{S_0} \quad (\text{with } B_0 = B) \quad (2.3.14)$$

The modulation depth is the ratio of AC amplitude of the fluorescence to the AC amplitude of the scatterer when the DC voltages are equal. Hence, the modulation depth may be determined experimentally.

Having measured the modulation depth at any specific frequency, and from Eq.

(2.2.9)

$$\beta^2 = \frac{\lambda^2}{\lambda^2 + \omega^2} \quad (2.3.15)$$

we can determine the decay rate  $\lambda$ . This is done by inverting (2.3.15) to get

$$\lambda = \frac{\omega\beta}{\sqrt{1-\beta^2}} = \frac{\omega}{\sqrt{1/\beta^2-1}} \quad (2.3.16)$$

The lifetime  $\tau$  is just  $\lambda^{-1}$

$$\tau = \frac{\sqrt{1-\beta^2}}{\omega\beta} \quad (2.3.17)$$

One needs to realize certain points concerning this procedure in order for

$\beta^2 = \frac{\lambda^2}{\lambda^2 + \omega^2}$  to be applicable.

1. The fluorescent system must have a time dependence that is described by linear differential equations. Only in that case, does the convolution integral apply. Usually, what this means is that the concentration of excited states must be low, and the excited molecules (atoms) do not interact with each other.
2. We are assuming the modulation depth of the exciting source ( $\alpha$ ) to be equal

to unity i.e.  $\alpha = 1$ . If this is not the case, then our equation becomes

$$\beta^2 = \frac{\alpha^2 \lambda^2}{\lambda^2 + \omega^2} \quad (2.3.18)$$

$$\lambda = \frac{\omega \beta}{\sqrt{\alpha^2 - \beta^2}} \quad (2.3.19)$$

and

$$\tau = \frac{\sqrt{\alpha^2 - \beta^2}}{\omega \beta} \quad (2.3.20)$$

If the uncertainty in  $\alpha$  is large, the lifetime cannot be accurately determined.

3. The fluorescence must have a monoexponential decay. In the case of multiexponential decay, more involved equations must be used. This is the case when there is rotational diffusion or when there is more than one type of fluorescent substance in the sample. See before Eqs. (2.2.10, 2.2.11).

## 2.4 Experimental Set-up (Please refer Figure (2.4))

The first step in the experiment is to achieve amplitude modulated light of variable frequency. For this we need two single modes of electromagnetic waves one of frequency  $\nu_1$ , the other of frequency  $\nu_2$ , such that the amplitude modulated light has a frequency  $\nu = |\nu_1 - \nu_2|$ .

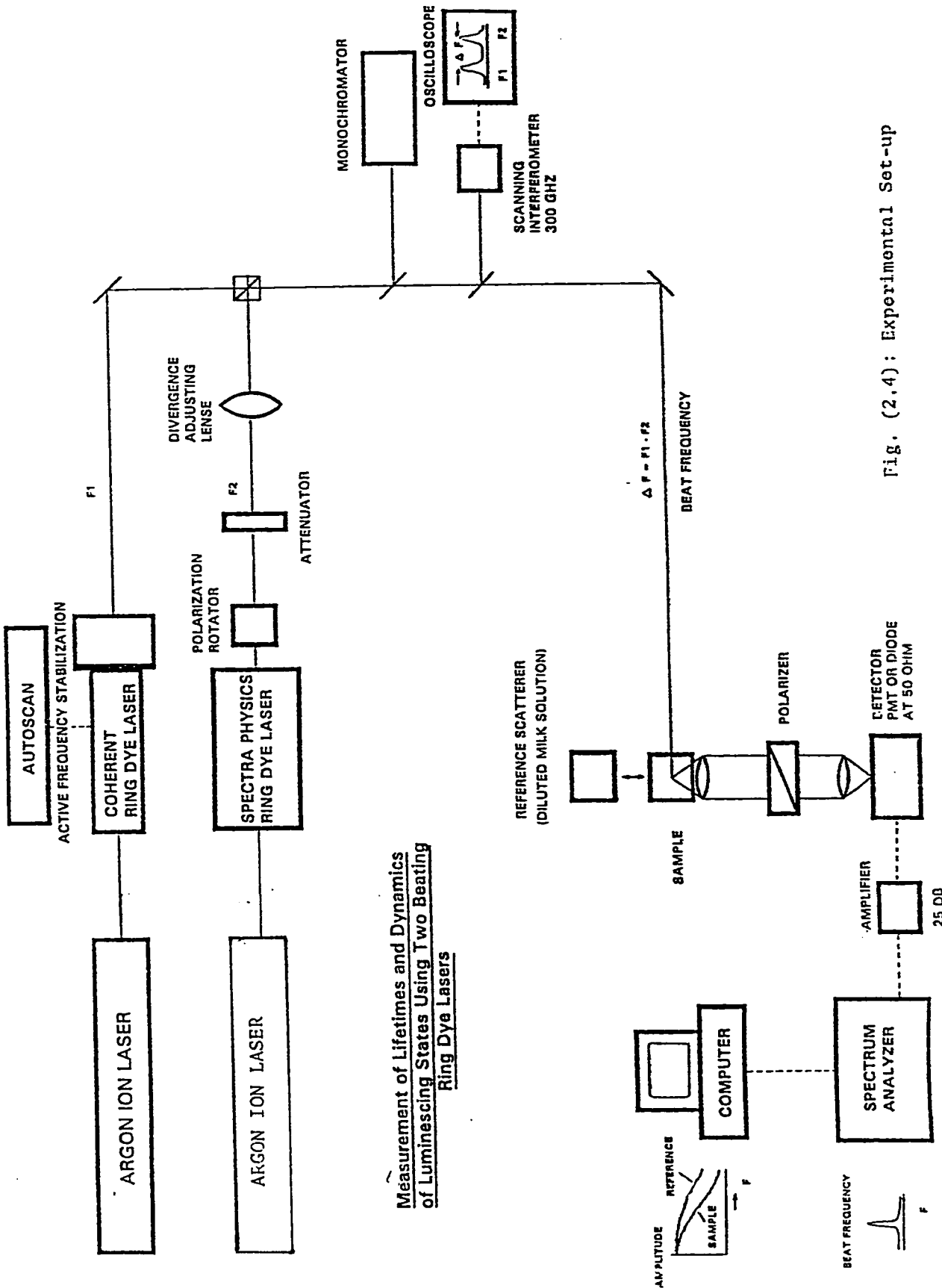
Two single mode narrow band lasers would achieve this. Both lasers must be single mode in order to construct amplitude modulated signal (sect. 2.1). They must be narrow band so that the uncertainty in the modulated signal is as small as possible.

$$\nu = |\nu_1 - \nu_2|$$

$$\Delta\nu = \Delta\nu_1 + \Delta\nu_2$$

The narrower the bandwidth of the two lasers, the finer is the bandwidth of the modulated light. Two narrow band ring dye lasers are used. A Coherent 699-29 Scanning Ring Dye Laser (having a beam frequency of  $F_1$ ) is pumped with a Coherent Innova 100  $Ar^+$  Ion Laser, and a Spectra Physics 380 Ring Dye Laser (having a beam frequency of  $F_2$ ) is pumped with a Spectra Physics 171  $Ar^+$  Ion Laser.

Rodamine 6G is used in the ring dye lasers. This dye has a lasing range between 565 nm and 620 nm. The two beams coming out of the two ring dye lasers must have the same divergence, polarization, and intensity. For this reason, a divergence



Measurement of Lifetimes and Dynamics of Luminescing States Using Two Beating Ring Dye Lasers

Fig. (2.4): Experimental Set-up

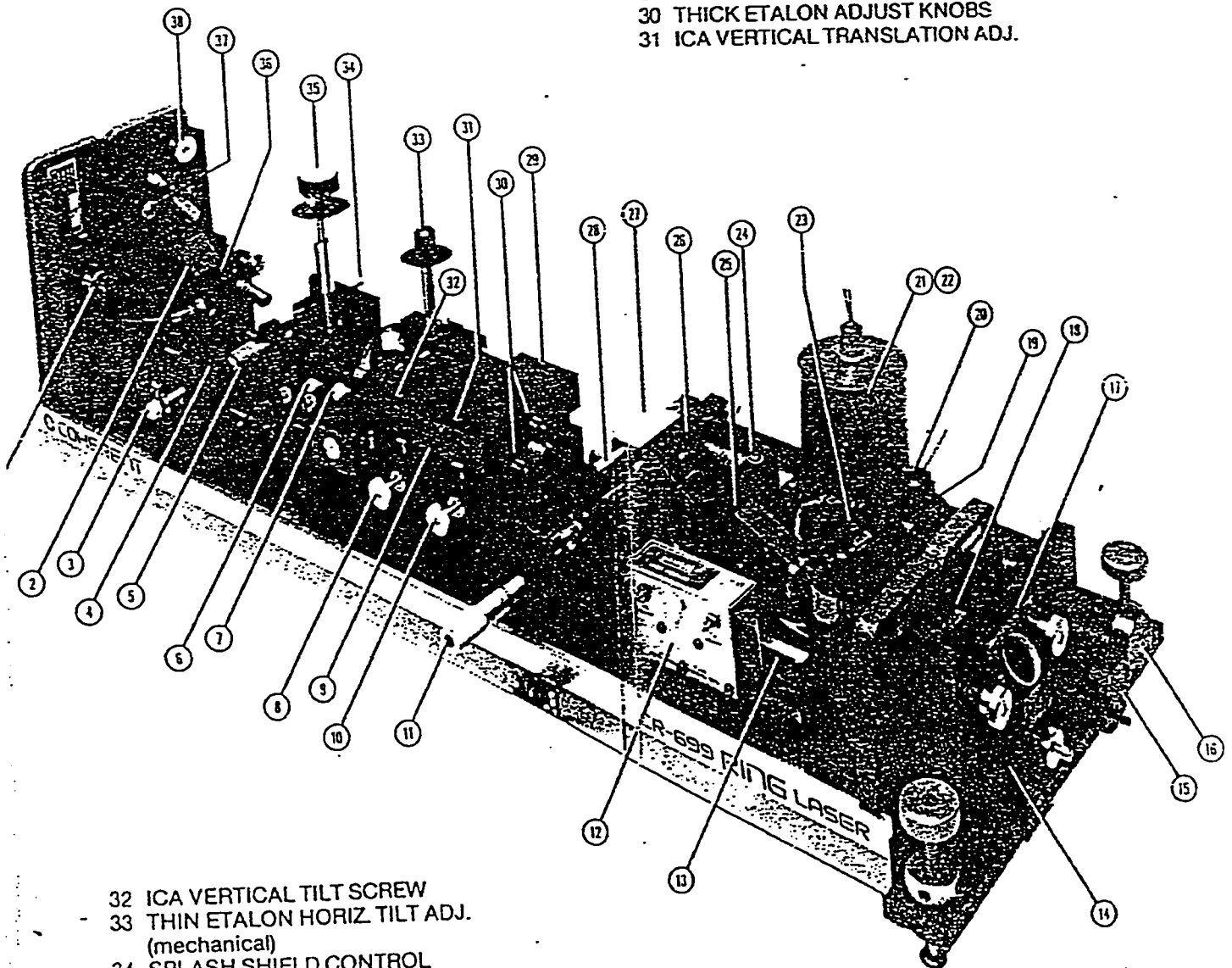
adjusting lens system, a polarization rotator, and an attenuator were used. Ring dye lasers are single mode lasers with very narrow band width. In fact, the 699-29 Coherent ring dye laser has a band width of 500 kHz or less. That is, when it lases with a frequency  $\nu = 5 * 10^{14} \pm 5 * 10^4$  the frequency is defined to 1 in  $10^9$  Hz. The Spectra Physics ring dye laser has a 50 MHz jitter.

The two beams are aligned collinearly by a beam splitter. A monochromator is used to assure that the frequencies of the two beams are close to each other. This is required because the Spectra Physics ring dye laser has no wavemeter control. Then, a 300 GHz scanning interferometer hooked to an oscilloscope is used to establish a frequency difference as small as 1.5 GHz. This can now be detected by the Hewlet Packard HP 8568B Spectrum Analyzer through connection to a fast speed photodiode. As was shown in Sec 2.1, the beat frequency is  $\Delta F = |F_1 - F_2|$  and this achieves amplitude modulated light. The frequency of modulation is controlled by scanning the Coherent 699-29 in frequency ( $F_1$ ).

The autoscan enables us to vary the frequency of the Coherent with a resolution better than 1 MHz. This is done while the Spectra 380 is left to jitter around some desired frequency. In effect, we achieve a variable beat frequency that can be controlled by the autoscan. In our experiment, the beat frequency will be in the range of 20-1050 MHz. In Figure (2.5), we can see the different components of the Coherent ring dye laser.

- 1 150-mm FOLD MIRROR HORIZONTAL ADJ.
- 2 ASTIGMATIC COMPENSATION RHOMB
- 3 NOZZLE HOLDER
- 4 NOZZLE TRANSLATOR ASSEMBLY
- 5 DRIP BOOT
- 6 PUMP MIRROR
- 7 100-mm HIGH REFLECTOR
- 8 ICA HORIZONTAL TILT CONTROL
- 9 INTRACAVITY ASSEMBLY (ICA)
- 10 ICA HORIZONTAL TRANSLATION KNOB
- 11 TUNER MICROMETER ADJUST
- 12 TWEETER TRAP

- 13 INVARI BAR
- 14 INFO. BEAM FOLD MIRROR (25-mmd)
- 15 NORMALIZING BEAM-FOLD MIRROR (12-mmd)
- 16 REF. BEAM-FOLD MIRROR (12-mmd)
- 17 BEAMSPLITTER MOUNTING ASSEMBLY
- 18 OUTPUT COUPLER RETAINING NUT
- 19 OUTPUT MIRROR VERTICAL ADJ.
- 20 OUTPUT MIRROR HORIZONTAL ADJ.
- 21 REF. CAVITY GALVO HOUSING
- 22 REF. CAVITY ASSY. (interferometer)
- 23 GALVO-DRIVE BREWSTER PLATE (woofer)
- 24 OPTICALLY ACTIVE DIODE ELEMENT
- 25 STAIRSTEP RHOMB (pickoff)
- 26 MAGNET ASSY. FOR OPTICAL DIODE
- 27 DETECTOR BLOCK
- 28 BIREFRINGENT FILTER
- 29 ICA ROLL ADJUST SCREW
- 30 THICK ETALON ADJUST KNOBS
- 31 ICA VERTICAL TRANSLATION ADJ.



- 32 ICA VERTICAL TILT SCREW
- 33 THIN ETALON HORIZ TILT ADJ. (mechanical)
- 34 SPLASH SHIELD CONTROL
- 35 PUMP MIRROR VERTICAL TRANSLATION ADJUST
- 36 TWEETER (lower fold mirror, PZT)
- 37 150-mm FOLD MIRROR
- 38 150-mm FOLD MIRROR VERTICAL ADJUST

Fig. (2.5): Components of the Coherent Ring Dye Laser

The amplitude modulated light (beating beam) is incident on a sample. The resultant scattered light and/or fluorescence is then collected and focused on a Hamamatsu Photomultiplier (PMT) after passing through a variable angle polarizer. The PMT has a DC out port and an AC out port. The DC signal is monitored with a digital voltmeter. The AC signal is amplified with a two stage pre-amplifier after which it is taken to the spectrum analyzer. The function of the spectrum analyzer is to store the amplitude of an AC signal at its corresponding frequency over a wide range of frequencies (1 – 1500 MHz). The spectrum analyzer can function in different modes. It can collect data on a linear scale or a logarithmic scale and one can vary the span width of the spectrum analyzer, in addition to many other functions. This variety of functions allows us to easily calibrate the spectrum analyzer and choose the frequency range that most suits a particular experiment with the best possible resolution as will be shown in chapters 3, and 4.

Finally, the data stored on the spectrum analyzer can be transferred to an IBM compatible personal computer by a GPIB card. The PC is used to control the spectrum analyzer and to manipulate and analyze the stored data.

This system (of beating ring dye lasers, interferometer, monochromator, optical elements, PMT, digital voltmeter, spectrum analyzer, and PC computer) has the ability to produce amplitude modulated light of variable frequency. It excites samples under consideration, and detects the response of these samples, after which

the response can be stored and analyzed. This is exactly what we needed in the previous section (sect. 2.3) for the determination of lifetimes.

Because our photodetecting device, the PMT, is a real PMT and not a thought or ideal one, it certainly has limitations, and conditions of best performance. For this reason, we will study the effect of different parameters on the frequency response of the PMT since we will be using light that is amplitude modulated at different frequencies. This is described in the next chapter.

## CHAPTER 3

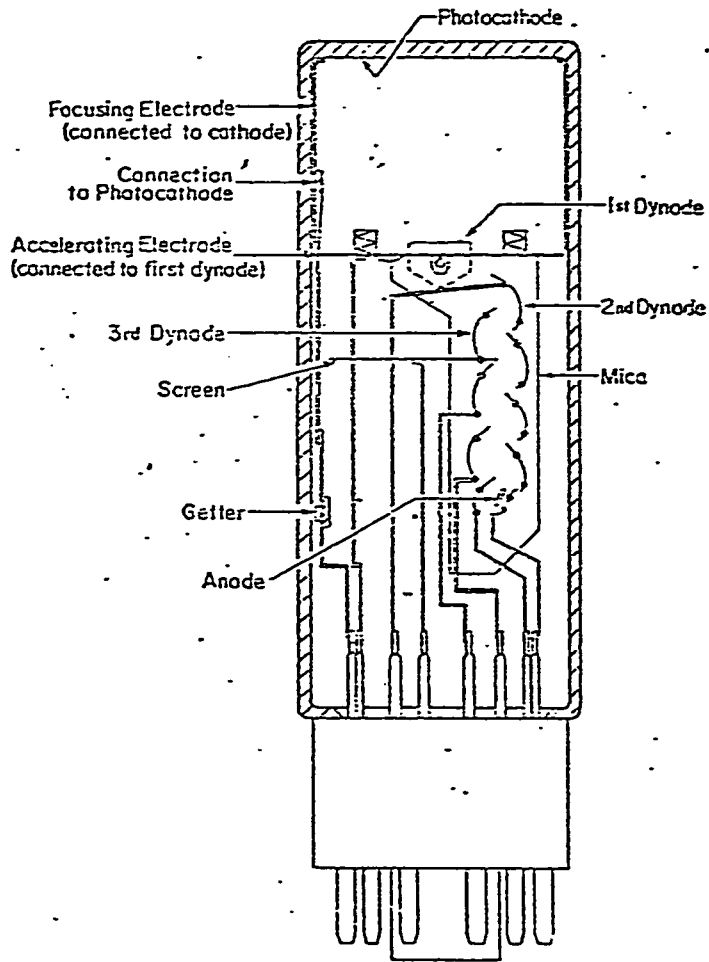
# PMT FREQUENCY RESPONSE STUDY

### 3.1 Introduction

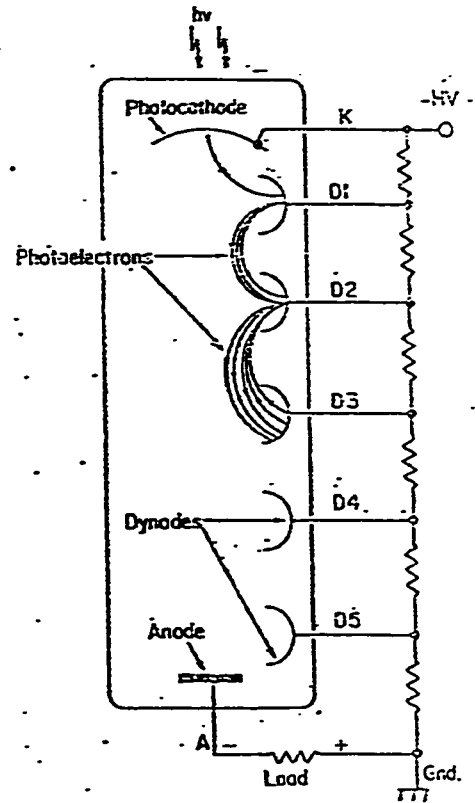
A photomultiplier (PMT) is a device for measuring photon fluxes. It is a tube with a photocathode and a dynode system. The incident photons emit photoelectrons off the photocathode which are multiplied (secondary emission) by a set of dynodes. At the rear end of the tube, there is an anode. A potential difference is applied between the photocathode and the anode. This causes the electrons to accelerate towards the anode and an electric signal is detected. The main parts of a typical PMT are shown in Figure (3.1).

As we have seen in the previous chapter, we have a source of amplitude modulated light which we may call "beating beam". The beating beam has a 'beat frequency' of a few Megahertz to as high as thousands of Gigahertz.

The PMT we are using has, just like any electronic photodetection device, a finite rise time. That is, if the PMT was to be excited by a very short pulse (theoretically a delta pulse), then it would take the PMT some time to reach from 10% of its maximum output current to 90% of its maximum current. This time is called a 'risetime'. The PMT was specified to have a rise time of approximately



Photomultiplier Structure



Photomultiplier tube in principle

Fig. (3.1): Schematic Diagram of a Typical PMT

800 picoseconds  $\equiv$  800 ps.

Working in frequency domain, through Fourier transform, an 800 ps rise time means that the PMT cannot respond to extremely high frequencies. This can be explained through the following (simplified) mathematical model:

A  $\delta$ -pulse in time domain  $f_0(t) = \delta(t)$  would have a Fourier transform  $g_0(\omega) = \text{const.}$ , Figure (3.2). If the PMT had a  $\delta$ -pulse response  $f(t)$  of the form

$$\begin{aligned} f(t) &= H & 0 < t < t_0, & \quad H \text{ is a constant} \\ &= 0 & t > t_0 & \end{aligned} \quad (3.1)$$

then, the Fourier transform of the response would have a shape  $g(\omega)$

$$g(\omega) = \frac{J}{\omega} \sin \omega t_0; \quad J \text{ is a constant.} \quad (3.2)$$

To a first approximation, this is shown in Figure (3.3).

The cut-off frequency is the frequency after which the PMT cannot respond. The cut-off frequency in our simplified model is  $\frac{\pi}{t_0}$ .

As we can see, the higher the cut-off frequency, the shorter (better) the response in time domain is. The converse is also true. A long time response (large  $t_0$ ) means a low cut-off frequency and the system has very little or no response to higher frequencies. This explains the statement: A PMT with a rise time of 800 ps (relatively long time) cannot respond to extremely high frequencies.

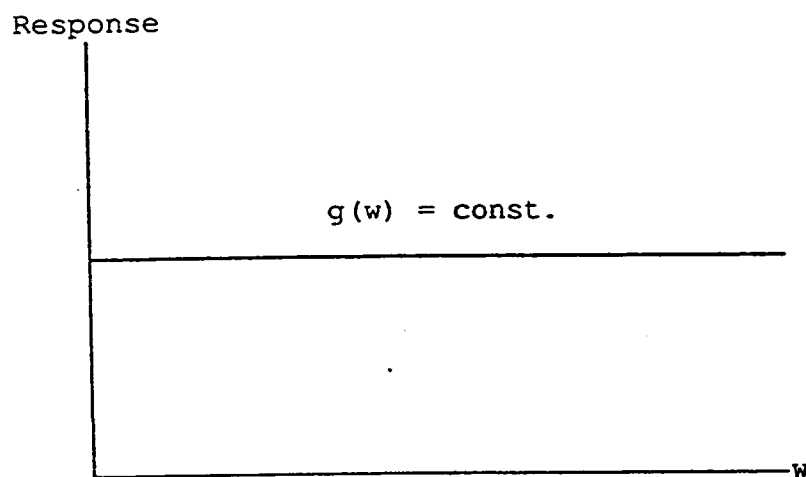
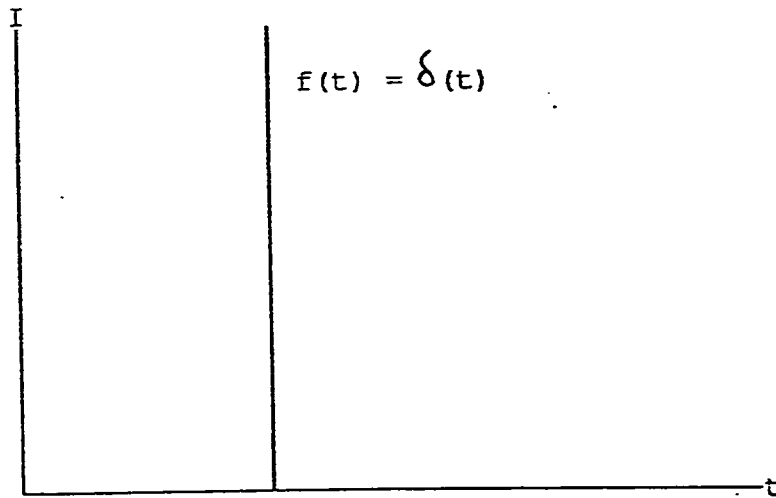


Fig. (3.2): Frequency Response to a Delta Pulse

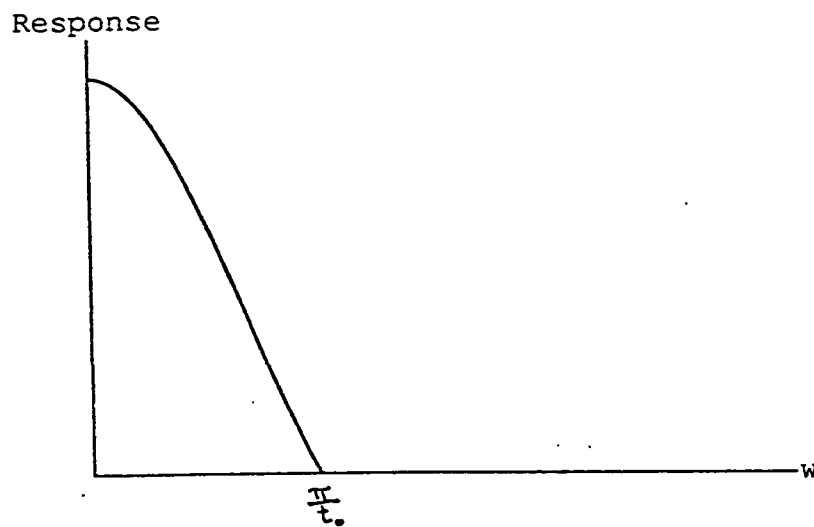
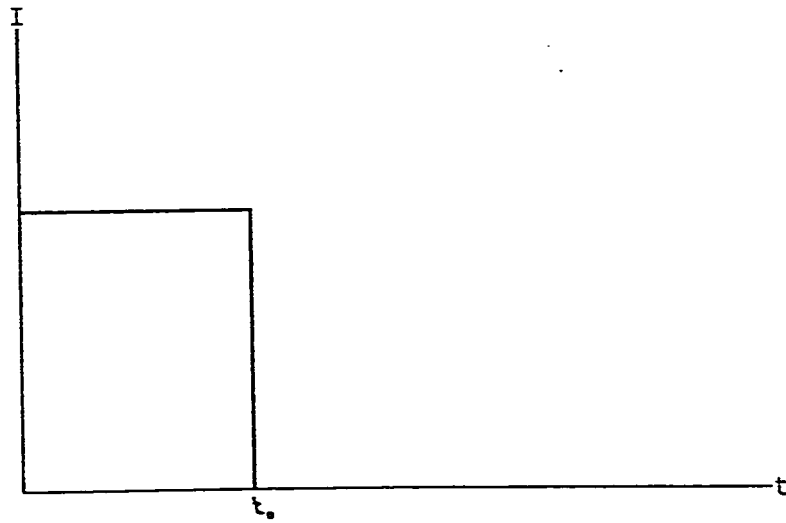


Fig. (3.3): Frequency Response to a Square Pulse

In reality, a typical PMT does not have a simple frequency response of  $\frac{\sin \omega t_0}{\omega}$  instead it has a response as shown in Figure (3.4). To our knowledge a figure like this probably has never been published before.

The procedure for collecting a complete continuous frequency response of a PMT is as follows:

Two beams of frequencies  $\nu_1$ , and  $\nu_2$  are aligned collinearly with the same amplitude, polarization, and divergence. This produces a beating beam of modulation depth equal to unity. The intensity  $I(t)$  is given by (Eq. (2.1.15))

$$I(t) = \text{const.}(1 + \cos(\omega t + \sigma)) \quad (3.3)$$

where

$$\omega = 2\pi\nu; \quad \nu = |\nu_1 - \nu_2|$$

For convenience the phases may be chosen such that  $\sigma = 0$ .

By varying  $\nu_1$ , and  $\nu_2$  we effectively vary the beat frequency ( $\nu$ ). The beating beam is incident on a sample of diluted milk (a scatterer). The scattered light is collected and focused on to the PMT operating at some high voltage, 600 V, for example.

According to Eq. (2.3.6), the exciting source has an intensity  $I_a$ :

$$I_a(t) = A(1 - e^{-i\omega t}); \quad A \text{ is a constant} \quad (3.4)$$

Because the PMT may have different responses at different frequencies, we cannot

FILE NAME: A:PVOLLS600  
DC OUT = 35 MV  
WAVELENGTH = 578.9 nm  
IN-FOCUS

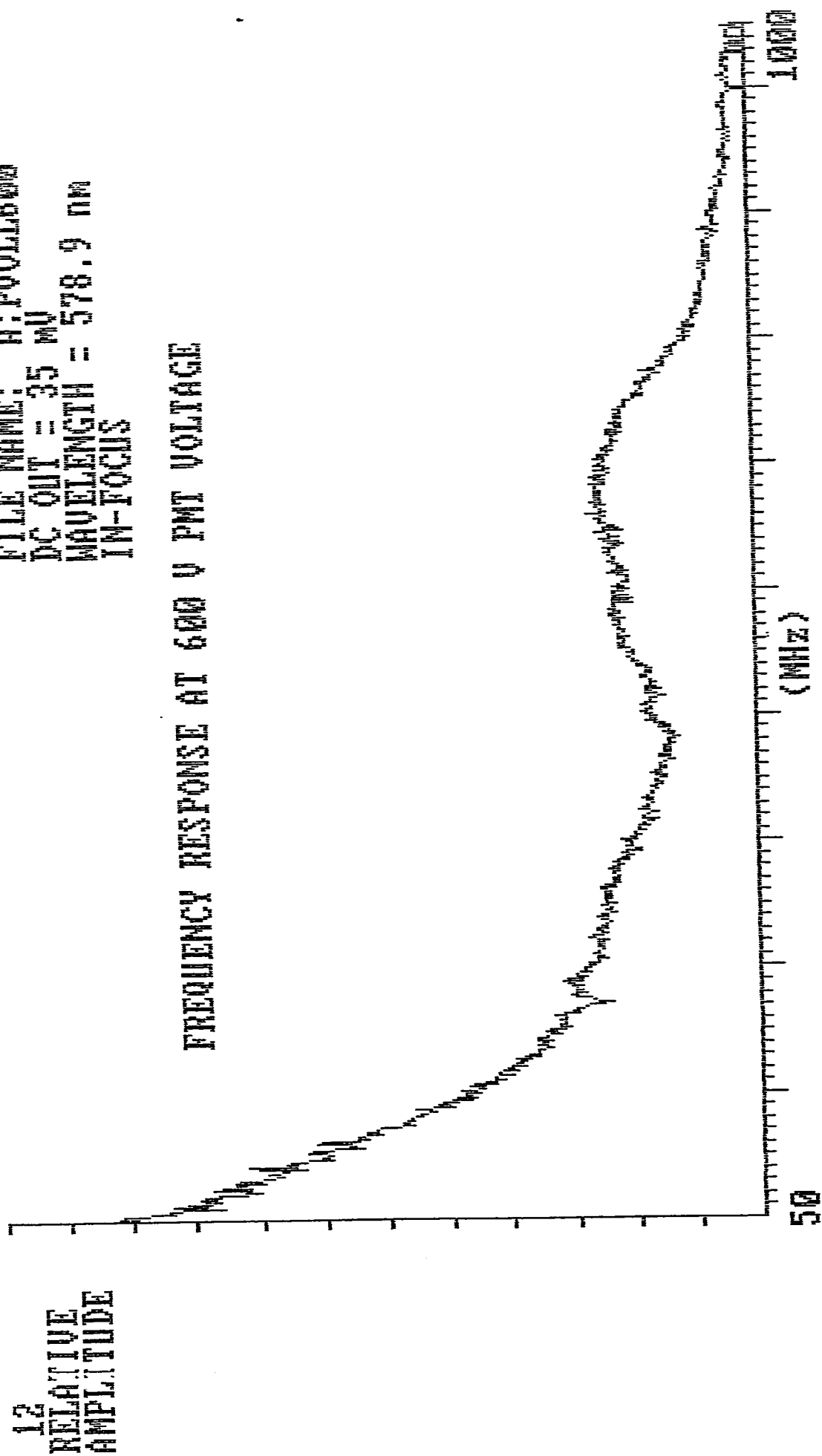


Fig. (3.4)

expect the PMT response to be of the form

$$I_E(t) = B(1 - e^{-i(\omega t - \phi)}) \quad B \text{ is a constant} \quad (3.5)$$

Actually, this would be the response of an ideal (thought) PMT. Instead, the PMT response has the form:

$$I_E(t) = B(r_0 - r(\omega)e^{-i(\omega t - \phi)}) \quad (3.6)$$

where  $r_0$  is the DC response factor and  $r(\omega)$  is the AC response factor at frequency  $\omega$ . Absorbing  $r_0$  in the constant  $B$ , we can rewrite Eq. (3.6) in the form

$$I_E(t) = B(1 - r(\omega)e^{-i(\omega t - \phi)}) \quad (3.7)$$

where  $r(\omega)$  has been redefined to be  $\frac{1}{r_0} r(\omega)$ .

The AC signal is preamplified. The AC signal now has the form (according to Eq. (3.7)).

$$I_{AC}(t) = BF r(\omega) e^{-i(\omega t - \phi)} \quad (3.8)$$

where  $F$  is an amplification factor.

The magnitude of the AC signal is

$$|I_{AC}(t)| = BF r(\omega) = \text{const.} * r(\omega) \quad (3.9)$$

Eq. (3.9) shows that the amplitude of the AC signal is a measure of the AC response factor  $r(\omega)$  where  $\omega$  is the angular beat frequency.

The magnitude of the AC signal is stored on a spectrum analyzer while the beat frequency is varied between 50 to 1000 MHz. The result is a spectrum of the

frequency response  $r(\omega)$  in the range 50–1000 MHz as shown in Figure (3.4). That particular spectrum had the following conditions.

PMT voltage = 600 V

DC out voltage = 35 mV (after amplification by a factor  $\sim 30$ )

Laser wavelength = 579 nm.

The scattered light was focused onto the photocathode.

### Linearity Check

As we have discussed in section 2.3, in order to determine lifetimes, we need to take ratios of AC signals (Eq. (2.3.12)). For that reason, we must make sure that the PMT has a linear signal response, i.e, if the incident flux of photons is increased by a factor  $\gamma$ , then the response signal is also increased by the same factor  $\gamma$ .

$$I_E(t) = B(1 - r(\omega)e^{-i(\omega t - \phi)})$$

$$\gamma I_E(t) = \gamma B(1 + r(\omega)e^{i(\omega t - \phi)})$$

$$\text{When} \quad I_E(t) \rightarrow \gamma I_E(t)$$

$$\text{then} \quad I_{DC} : B \rightarrow \gamma B$$

$$\text{and} \quad I_{AC} : B(\omega) \rightarrow \gamma B r(\omega)$$

It is more convenient to take DC signal linearity checks. This was done at two PMT voltages: 600 V, and 700 V. The results, as one can see from Figure (3.5, 3.6), is that at 600 V PMT voltage, the PMT is linear up to about 35 mV DC out. At 700 V PMT voltage the PMT is linear up to about 30 mV DC. It is to be noted that the value of 30 or 35 mV is not the true DC value at 50  $\Omega$ , but rather an amplified value, for better resolution, by about a factor of 30.

Whenever we run an experiment for lifetime determination, it is necessary to

be at or below 35 mV DC out if the PMT is operating at 600 V and the DC out signal must be at or below 30 mV if the PMT is operating at 700 V.

VOLTAGE LINEARITY STUDY  
VOLTAGE/INTENSITY VS VOLTAGE

ARBITRARY  
UNITS

PMT VOLTAGE = 600 V



VOLTAGE = 34.76 MV

73.426

VOLTAGE (MV)

21.0978

Fig. (3.5)

VOLTAGE LINEARITY STUDY  
VOLTAGE/INTENSITY VS VOLTAGE

PMT VOLTAGE = 700 V

ARBITRARY  
UNITS

VOLTAGE = 29.9922 MV

62.223

VOLTAGE (MV)

7.2701

Fig. (3.6)

### 3.2 Study of Spectrum Analyzer Baseline Subtraction

One of the problems that we faced in the experiment was the fact that the spectrum analyzer's baseline would affect the magnitude of an AC input signal. This was detected by the following way:

Using an external frequency generator, an AC input of certain known amplitude was fed into the spectrum analyzer. Whenever the baseline level was much lower than the external signal, the AC signal recorded on the spectrum analyzer would give the same reading as that generated by the frequency generator. On the other hand, whenever the input signal level was comparable to the spectrum analyzer baseline, the spectrum analyzer would give a reading (an apparent signal level) that was greater than the input signal. For this reason, a calibration of the spectrum analyzer was needed such that what we measure should be the real signal and not an apparent signal.

The spectrum analyzer was left to acquire while the frequency generator scanned through some suitable range of frequencies. This was done at different spectrum analyzer frequency span widths, and at different input signals. Some of these measurements are shown in Figure (3.7-3.12).

It is clear that the effect of the baseline on the real (actual) signal is the same at different frequencies. This can be seen from the figures (Fig. (3.7-3.12)). As the input signal is varied in frequency with constant amplitude, the approximately

1  
RELATIVE  
AMPLITUDE

FILE NAME: A:LSPEC31  
INPUT VOLTAGE 70.7 uV  
SPAN WIDTH 785 - 787 MHZ

### FREQUENCY RESPONSE TO A SIGNAL GENERATOR

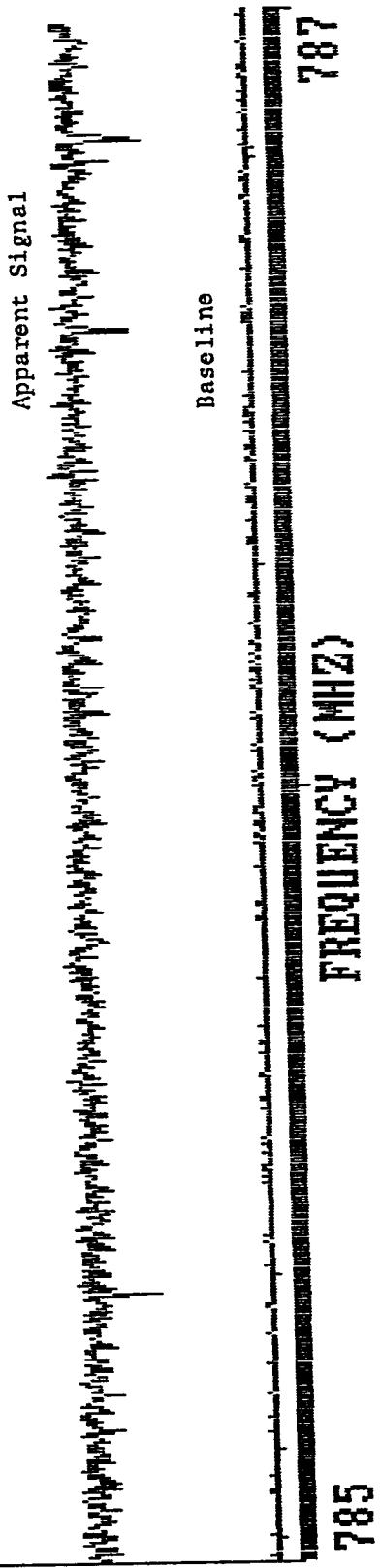


Fig. (3.7)

1  
RELATIVE  
AMPLITUDE

FILE NAME: A:LSPEC22  
INPUT VOLTAGE 70.7 uV  
SPAN WIDTH 780 - 790 MHZ

### FREQUENCY RESPONSE TO A SIGNAL GENERATOR

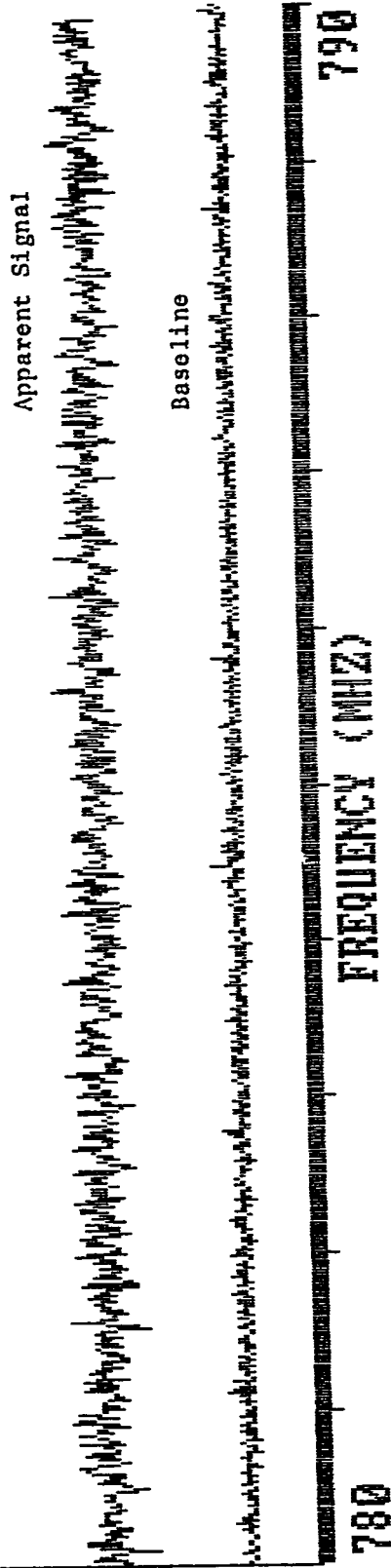


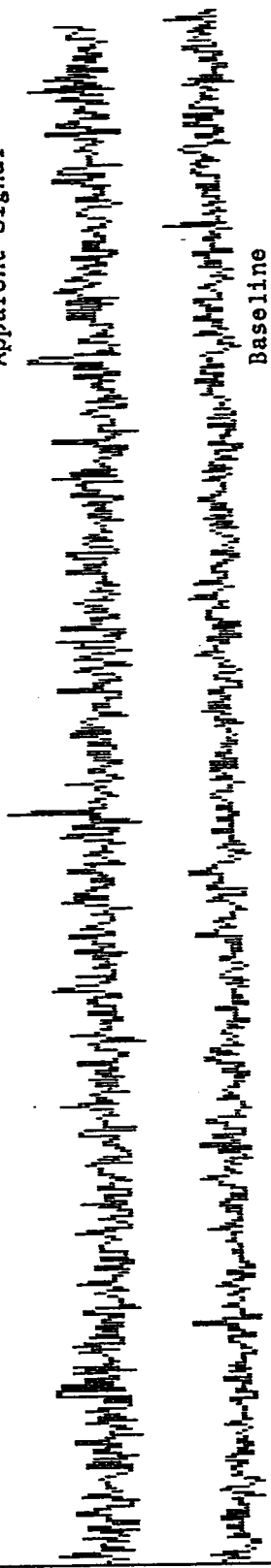
Fig. (3.8)

FILE NAME: A:LSPEC13  
INPUT VOLTAGE 70.7 uV  
SPAN WIDTH 700 - 800 MHZ

### FREQUENCY RESPONSE TO A SIGNAL GENERATOR

1  
RELATIVE  
AMPLITUDE

Apparent Signal



Baseline

700  
FREQUENCY (MHZ)  
800

Fig. (3.9)

FILE NAME: A:LSPEC4  
INPUT VOLTAGE 70.7 uV  
SPAN WIDTH 50 - 990

1  
RELATIVE  
AMPLITUDE

### FREQUENCY RESPONSE TO A SIGNAL GENERATOR

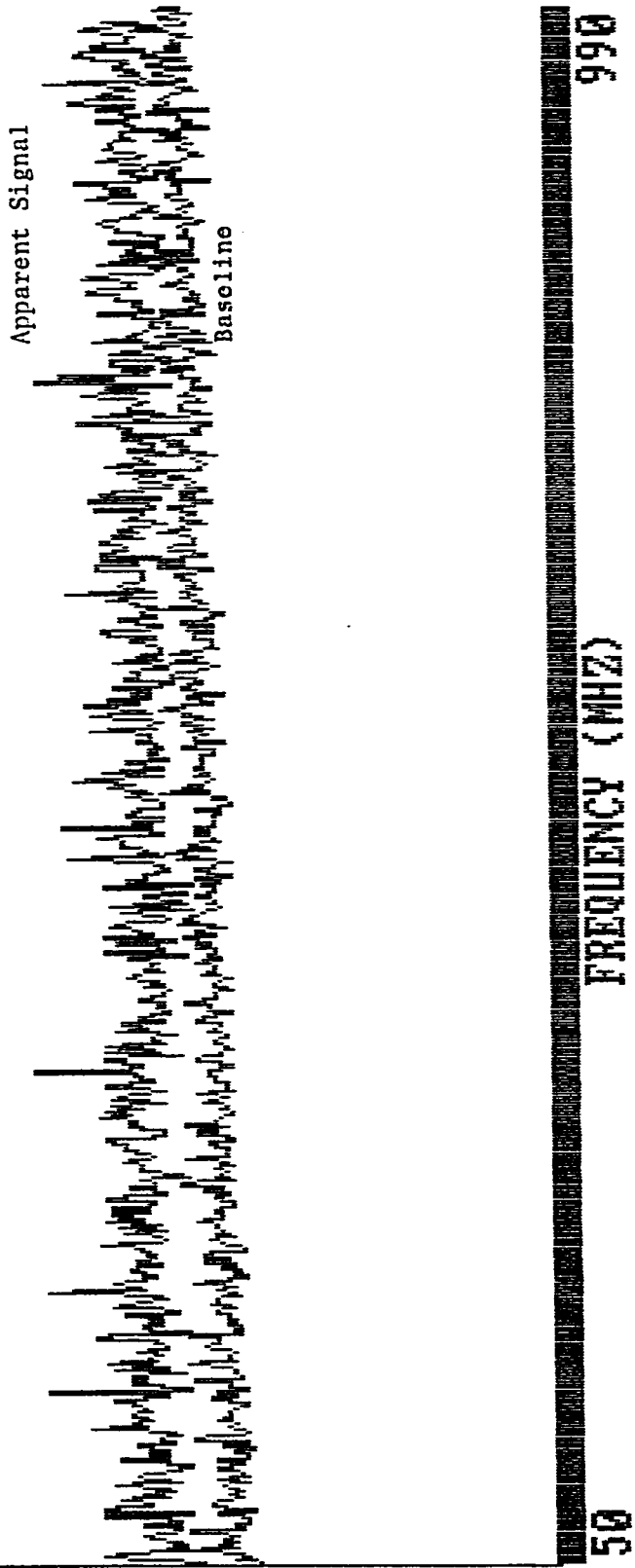


Fig. (3.10)

FILE NAME: A:LSPEC12  
INPUT VOLTAGE 224 uV  
SPAN WIDTH 700 - 800 MHz

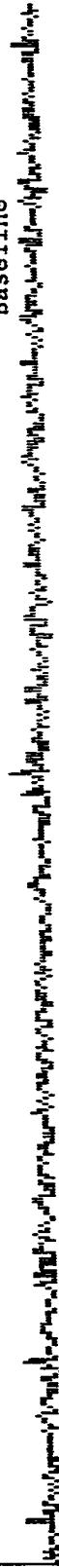
### FREQUENCY RESPONSE TO A SIGNAL GENERATOR

2  
RELATIVE  
AMPLITUDE

Apparent Signal



Baseline



700

FREQUENCY (MHz)

800

Fig. (3.11)

FILE NAME: A:LSPEC3  
INPUT VOLTAGE 224 uV  
SPAN WIDTH 50 - 990

### FREQUENCY RESPONSE TO A SIGNAL GENERATOR

2  
RELATIVE  
AMPLITUDE

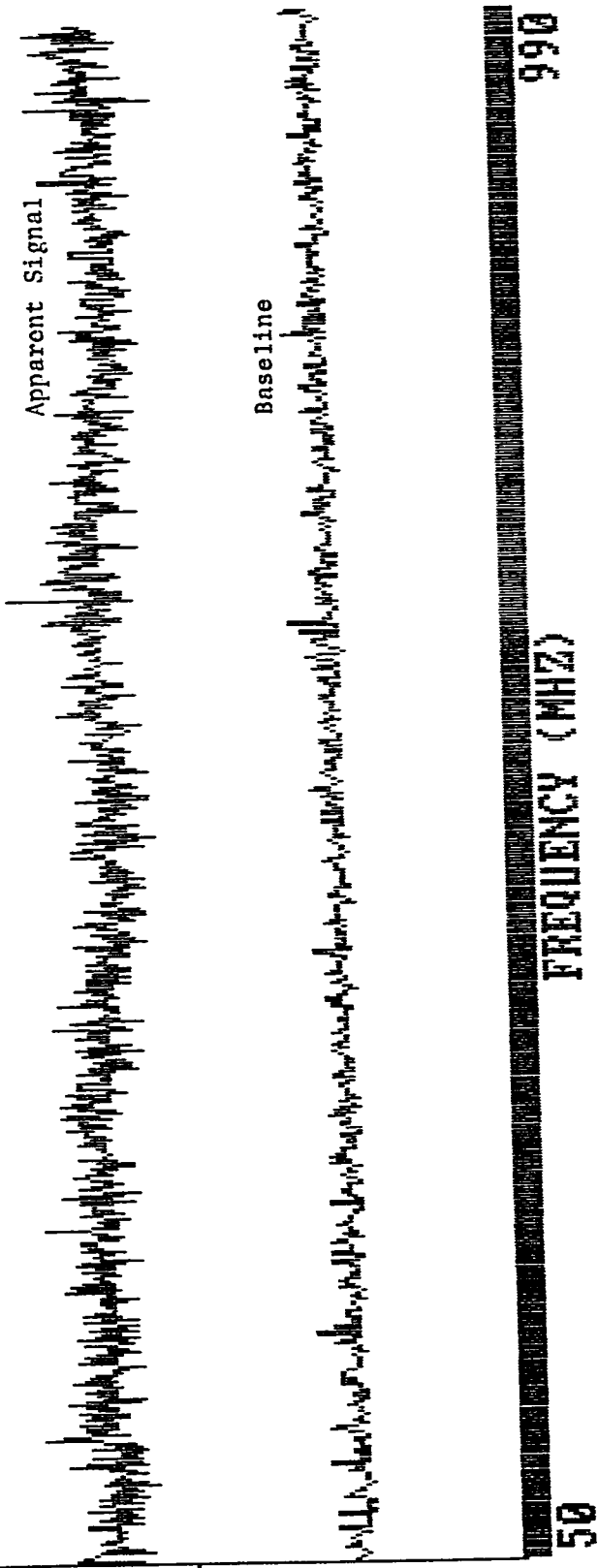


Fig. (3.12)

constant baseline affects the input signal such that to give a constant 'apparent signal' signifying that the effect of the baseline on the real input signal is the same at different frequencies. If the effect was frequency dependent, the constant baseline would affect the constant input signal differently at different frequencies, and the apparent signal would not be constant in frequency.

Since this is not the case, instead, the apparent signal is constant with frequency, we can safely state that the baseline effect on the input signal is frequency independent. Therefore, we can do the calibration at any frequency, and this calibration will hold for all frequencies.

Table (3.1) lists a set of measurements taken at a spectrum analyzer frequency span width of 50–1050 MHz. The baseline was found to be at  $-64.7$  dBm.

dBm is a unit for measuring electric signals. Its relation to millivolts using a  $50 \Omega$  impedance is as follows:

$$mV = 223.6 * 10^{\frac{dBm}{20}}$$

where mV is the electric signal in millivolts and dBm is the dBm value. Actually, dBm is defined by

$$0 \text{ dbm} = 1mW \text{ at } 50\Omega$$

That is, zero dBm is 1 milliwatt at 50 ohm impedance. The less negative the dBm value is, the stronger the signal.

Input Signal from Generator (dBm)	Apparent Signal on Spectrum Analyser (dBm)	Difference Between Apparent Signal and Baseline (dBm)	Difference Between Apparent Signal and Input Signal (dBm)
-60.70	-57.50	7.20	3.20
-61.70	-58.00	6.70	3.70
-62.70	-58.70	6.00	4.00
-63.70	-59.50	5.20	4.20
-64.70	-60.20	4.50	4.50
-65.70	-60.80	3.90	4.90
-66.70	-61.30	3.40	5.40
-67.70	-61.70	3.00	6.00
-68.70	-62.00	2.70	6.70
-69.70	-62.40	2.30	7.30
-70.70	-62.10	2.60	8.60
-71.70	-62.70	2.00	9.00
-74.70	63.70	1.30	11.00
-76.20	-64.50	0.50	11.70

Table (3.1): Spectrum Analyzer Baseline Subtraction

As we can see from Table (3.1), when the input signal level is much higher than the baseline level, the apparent signal is just a little higher than the real input signal from the frequency generator. As we reduce the amplitude of the input signal closer to the baseline level, the apparent signal becomes much higher than the actual input signal. The conclusion is: the closer the apparent values are to the baseline, the more they need to be subtracted. Even when the input signal is lower than the baseline; still, the apparent signal may be higher than the baseline. Table (3.1) shows that whenever the difference between the apparent signal and the baseline is as in column (3), what needs to be subtracted is the corresponding value in column (4). For example, when the difference between the apparent signal and the baseline is 6 dBm, we must subtract 4 dBm from the apparent signal in order to get the actual (real) input signal value. In our table, subtracting 4 dBm from - 58.7 dBm gives the real - 62.7 dBm input signal. A BASIC program was prepared to read a frequency spectrum and compare it with its baseline, and subtract according to Table (3.1). The amount of difference was split into regions, and the subtraction was taken to be linear from the beginning to the end of each region. This is shown in Figure (3.13). When the difference between the apparent signal and the baseline is less than 1 dBm, it means that the actual input signal is more than 10 dBm below baseline. In this case, we set the actual signal to be zero because of unreliability. A listing of the program is in Appendix (II).

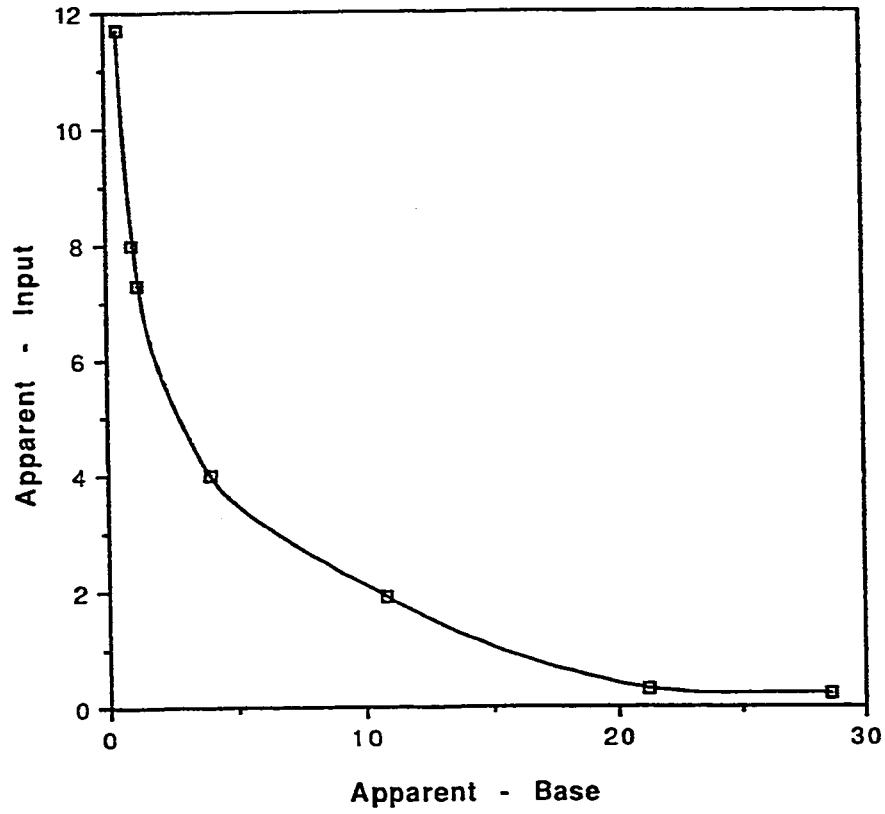


Fig. (3.13): Spectrum Analyser Subtraction Curve

### 3.3 Study of the PMT Frequency Response

The PMT we are using is a Japan-made Hamamatsu model H3284. It is specified to have a rise time of 800 ps. In this part of the thesis, we would like to study the effect of different parameters on the frequency response. Parameters that are of interest include: intensity of photon flux, PMT voltage, focus-non focus illumination of the photocathode, laser wavelength of incident flux, and, finally, polarization.

It should be emphasized that, strictly, the response is not that of the PMT alone; instead, it is the response of the detection system as a whole including: PMT, amplifiers, wires (cables), and spectrum analyzer. The HP 8568B spectrum analyzer is specified to function up to a frequency of 1.5 GHz. Although it operates at frequencies over 2.2 GHz, we will be studying the PMT response in the range 50–1000 MHz. Therefore, the spectrum analyzer should have only a mild effect on the frequency response of the detection system. The electric coaxial cables we are using can handle up to a few GHz. As we use short cable lengths, the frequency response is not altered. In essence, what we are measuring is the frequency response of the PMT with the amplifiers.

We have described in the beginning of this chapter how to acquire a frequency response spectrum. In each part of the study, we will keep different parameters constant while varying one parameter alone. The sets of frequency response spectra are in appendices (IA.1–IA.5).

### 3.3.1. The Effect of Photon Intensity on PMT Frequency Response

In this part of the study, the PMT voltage is held at 600 V (anode 0 V, cathode - 600 V), the wavelength of the ring dye lasers is kept at 588 nm, and the scattered light is focused on to the photocathode. The intensity of the photon flux is varied by adding or removing neutral density filters in the path of the beating beam. The intensity is monitored by the DC out voltage; i.e., when the flux intensity is cut by half the DC out voltage is also cut by half. This is true as long as the PMT has a linear signal response. At this PMT voltage (600 V), it was found (Figure (3.5)) that the PMT is linear to a DC out voltage of 35 mV. The frequency response spectra for 10, 15, 20, 29, 40, 50, and 60 mV DC out voltages are shown in Appendix (I.A.1). The frequency response was taken in the range of 50–1000 MHz. The response at high frequencies is low, and because of the proper subtraction of signals due to the effect of the spectrum analyzer baseline (Sec. 3.2), the magnitude of the signal is artificially taken to zero when the signal is too small to give a reliable value. This happens when the signal is smaller than 70  $\mu$ V. As we can see from the frequency response spectra (Appendix (I.A.1)), the frequency response drops sharply in the region 50–440 MHz. From 440–630 MHz, there is (strangely) an evident increase in response. One would expect that a physical system would have a lower response with increasing frequency. From 630–740 MHz, there is another sharp decrease in response after which the response slowly falls off. The next few plots (Figure (3.14 – 3.19)) in the following pages show the

ratio of frequency responses taken at different DC out voltages as compared to the frequency response taken at 29 mV DC out voltage. In general, we can say that they are approximately constant with frequency. For low DC out voltage; i.e., less than 35 mV, this constant ratio is the same as the ratio of the DC out voltages. This can be safely stated when we realize that there is a  $\pm 1$  mV uncertainty in DC out voltage. Table (3.2) shows a summary of the results.

For higher DC out voltages, i.e., larger than 35 mV, the non-linearity effect is clear as also shown in Table (3.2). Since the ratio of frequency response is constant with frequency within experimental error, the conclusion is that the frequency response of the PMT is intensity independent.

FILE NAME: A:FREST10

1.2  
RELATIVE  
AMPLITUDE

RATIO OF FREQUENCY RESPONSES AT  
10 MV AND 29 MV DC OUT VOLTAGES

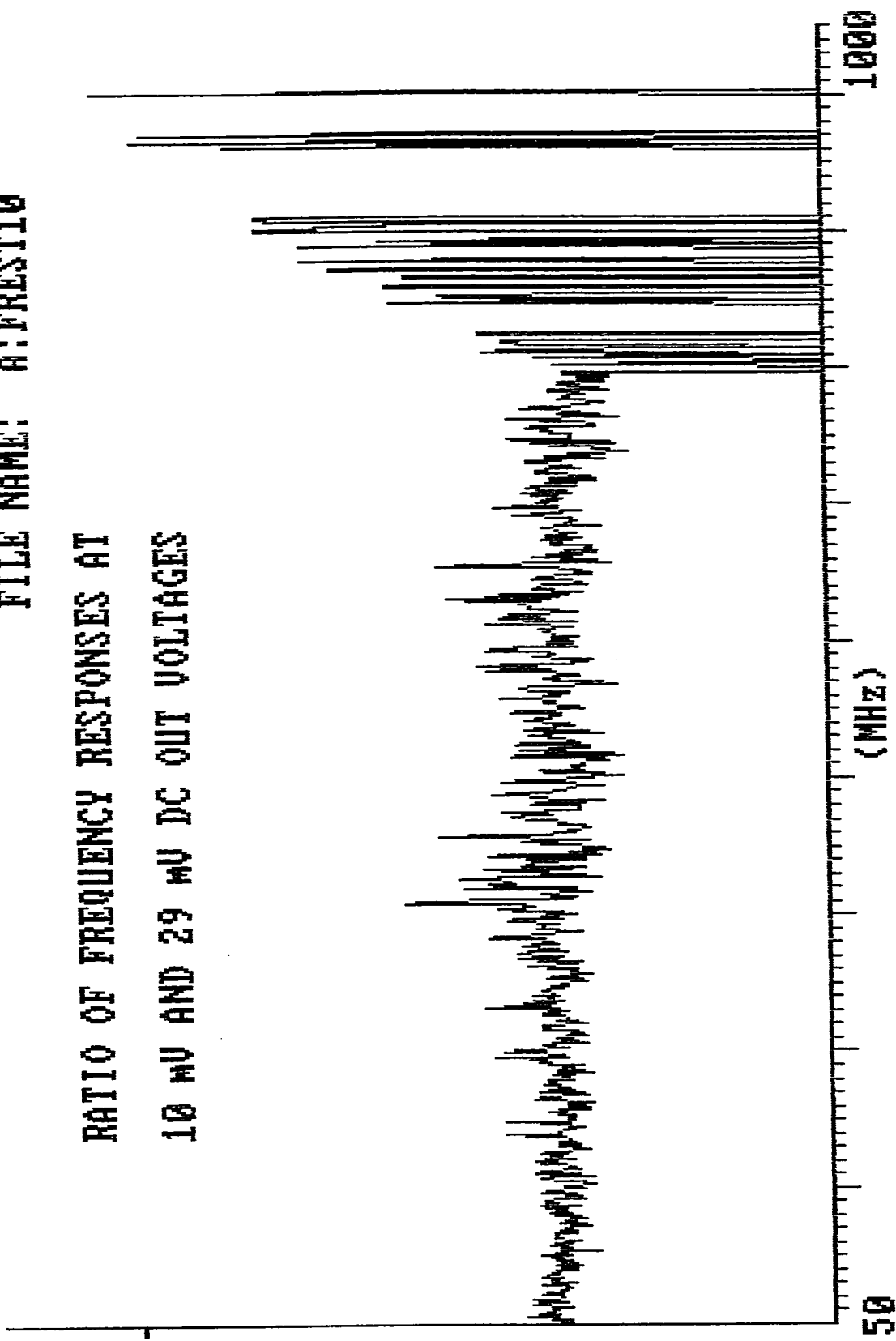


Fig. (3.14)

1.3  
RELATIVE  
AMPLITUDE

FILE NAME: A:FREST15

RATIO OF FREQUENCY RESPONSES AT  
15 MV AND 29 MV DC OUT VOLTAGES

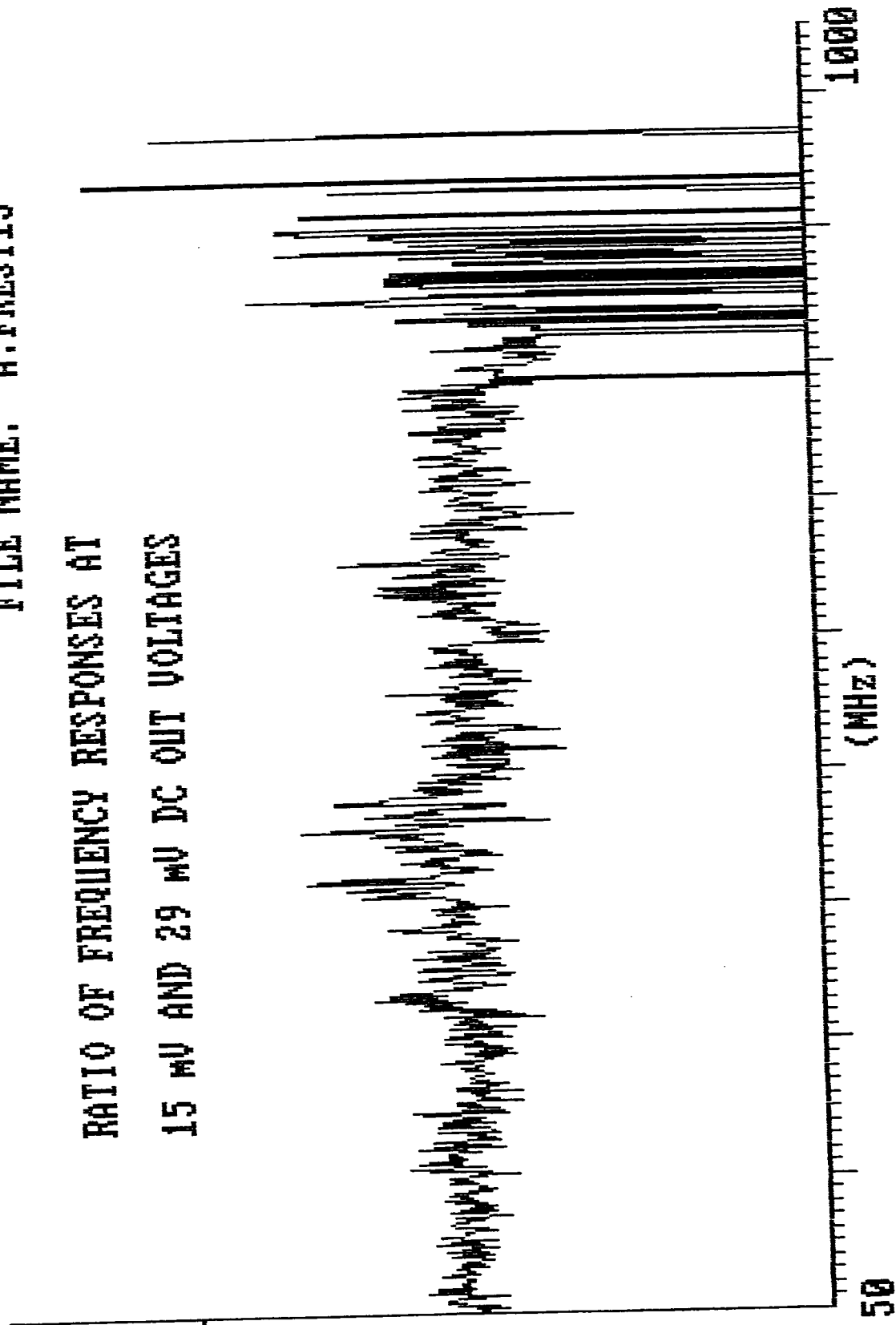


Fig. (3.15)

FILE NAME: A:FREST20

1.2  
RELATIVE  
AMPLITUDE

RATIO OF FREQUENCY RESPONSES AT  
20 MV AND 29 MV DC OUT VOLTAGES

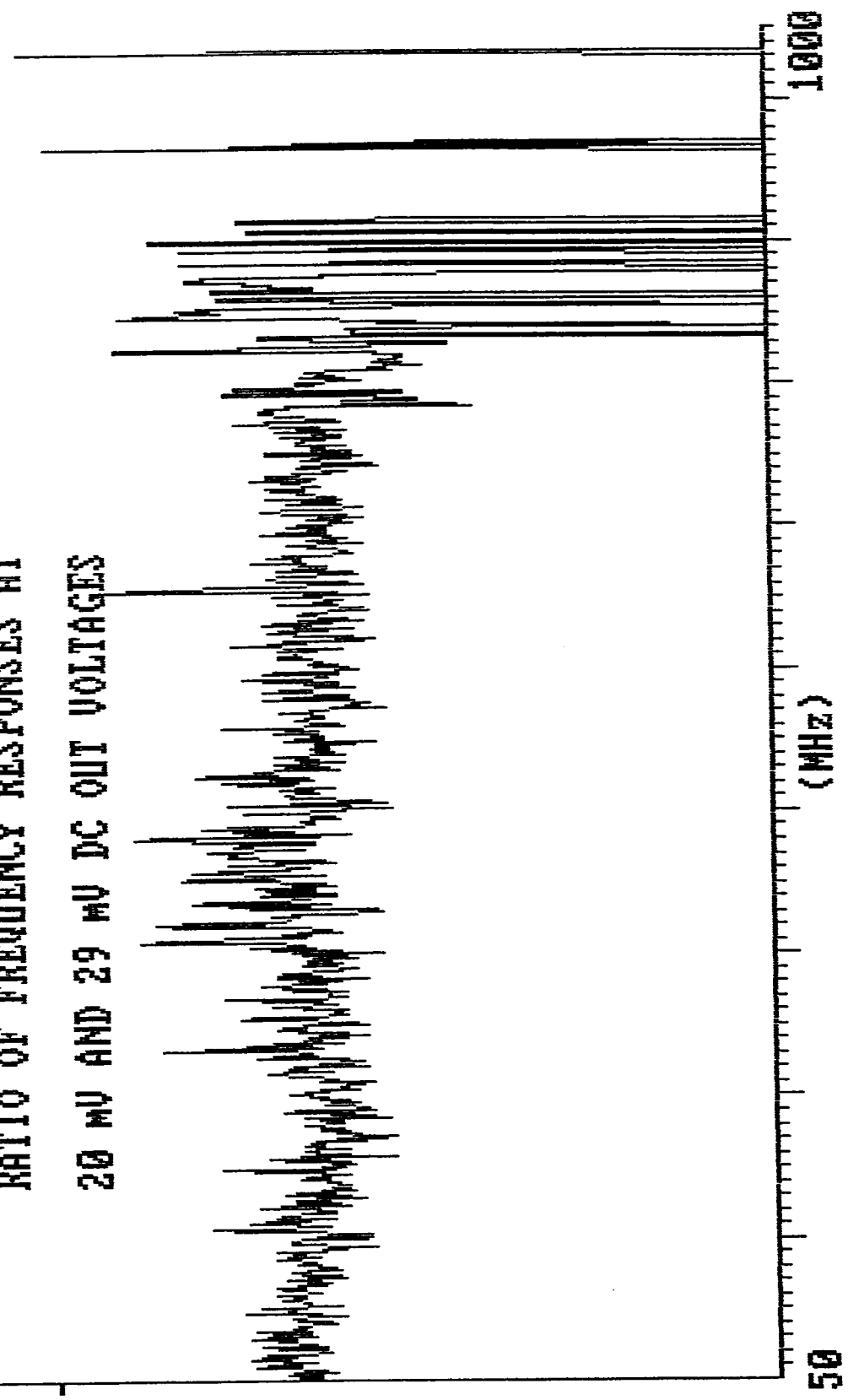


Fig. (3.16)

FILE NAME: A:FREST40

2.7  
RELATIVE  
AMPLITUDE

RATIO OF FREQUENCY RESPONSES AT  
40 MV AND 29 MV DC OUT VOLTAGES

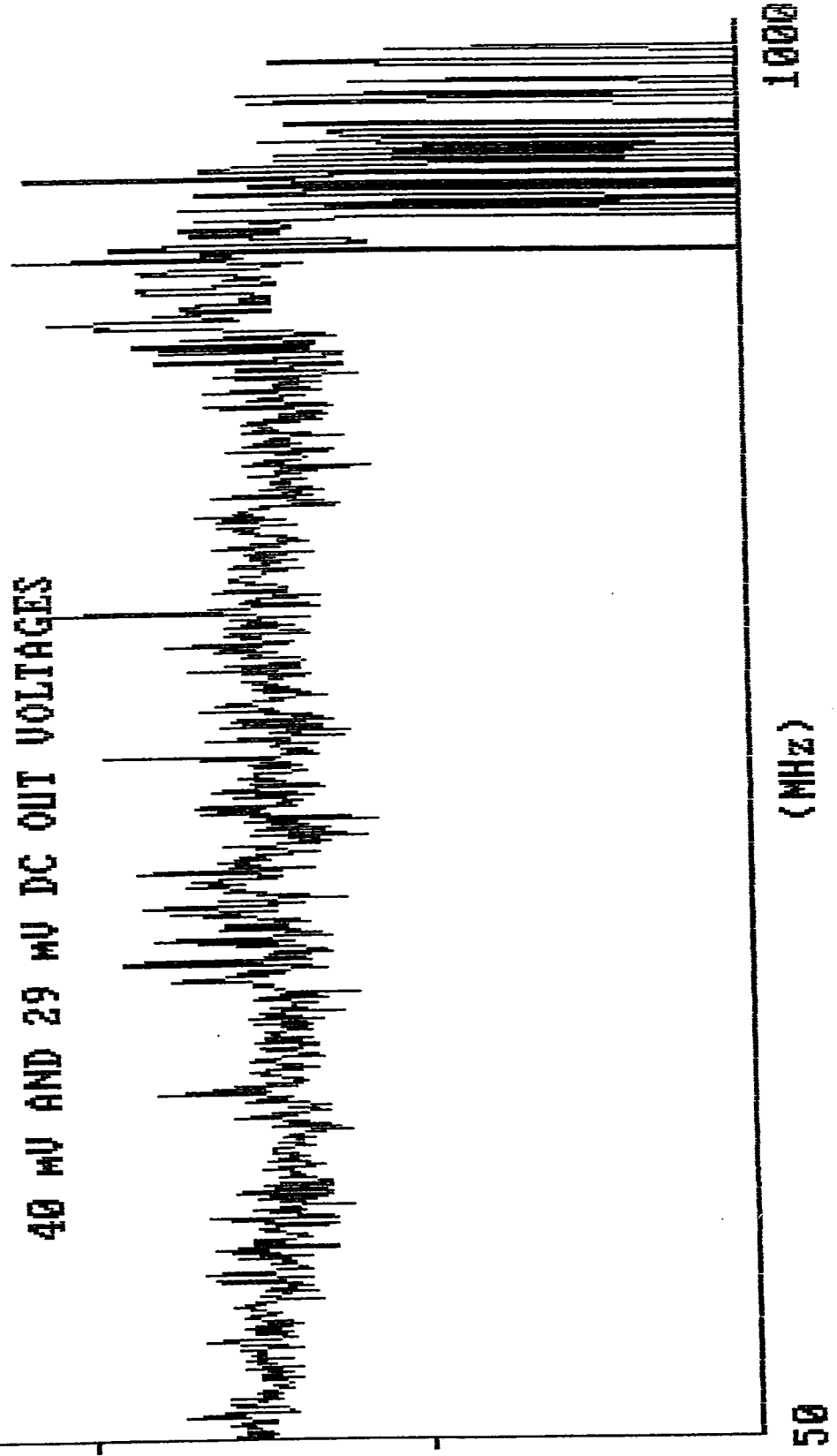


Fig. (3.17)

FILE NAME: A:FREST50

7.2  
RELATIVE  
AMPLITUDE

RATIO OF FREQUENCY RESPONSES AT  
50 MV AND 29 MV DC OUT VOLTAGES

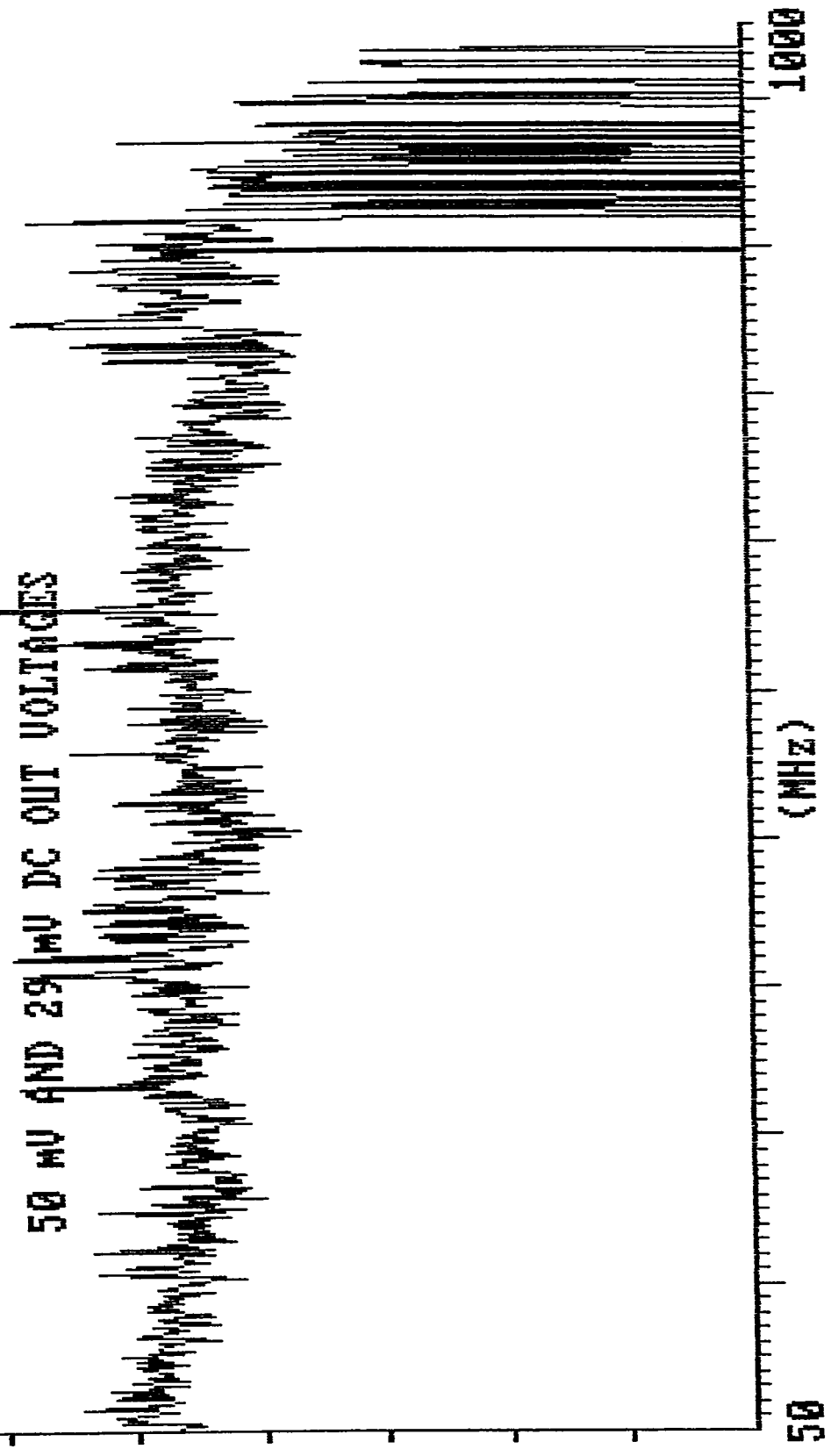
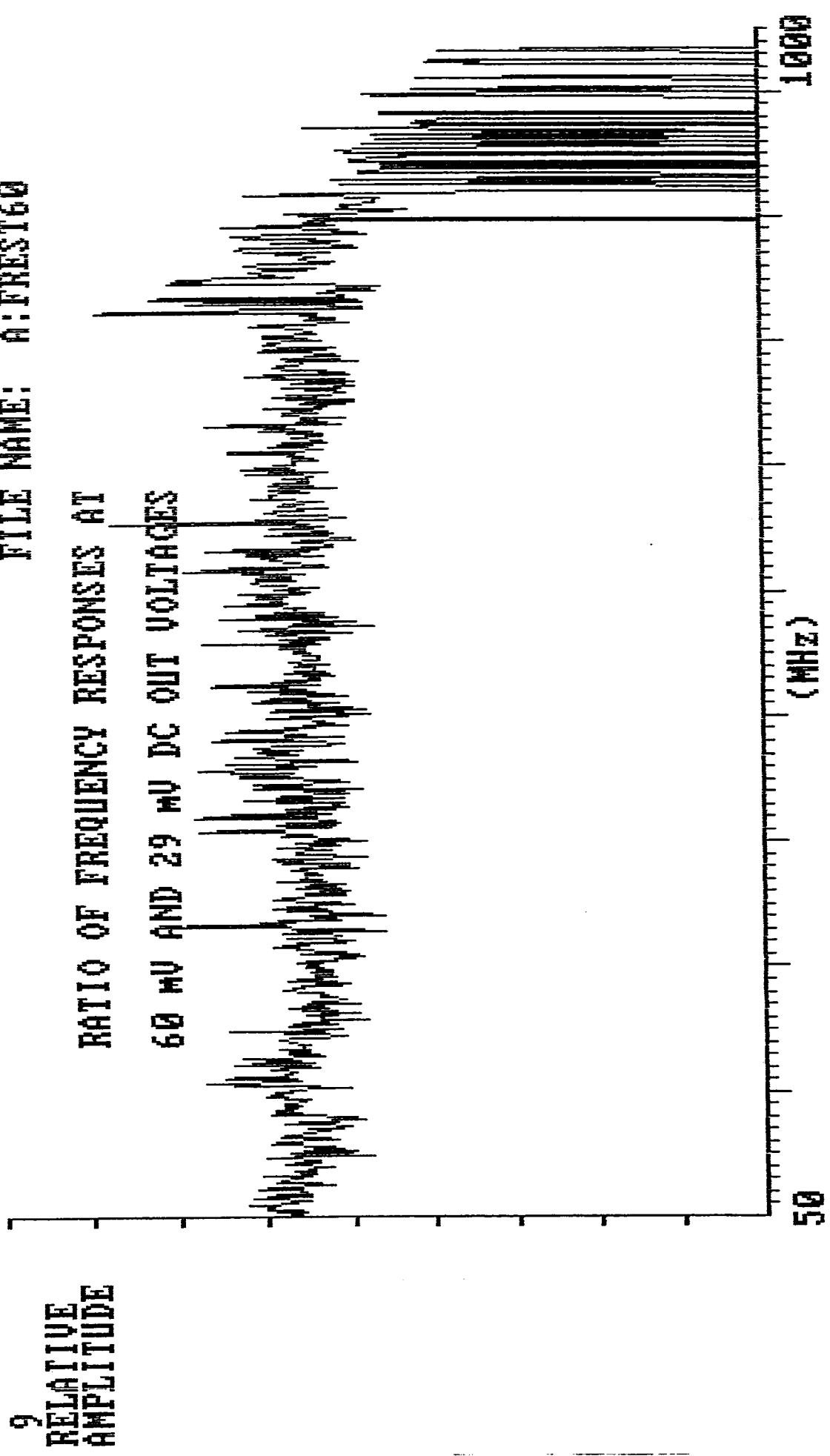


Fig. (3.18)

FILE NAME: A:FREST60



9  
RELATIVE  
AMPLITUDE

RATIO OF FREQUENCY RESPONSES AT  
60 MV AND 29 MV DC OUT VOLTAGES

Fig. (3.19)

DC OUT VOLTAGE(mV)	DC RATIO	AC RATIO	% DIFF
10	0.34	0.36	6
15	0.52	0.55	6
20	0.69	0.67	3
40	1.38	1.55	12
50	1.72	4.8	179
60	2.07	5.8	180

Table (3.2): DC and AC Ratios at Different Incident Densities

### 3.3.2. The Effect of Focus on PMT Frequency Response

The frequency response of the PMT was taken at 600 PMT voltage with a ring dye laser wavelength of 588 nm. This was taken at 20, 29, 40 mV DC out voltages, just as before but with a non-focused arrangement such that the scattered light illuminates a larger portion of the photocathode. These spectra are reported in Appendix (I.A.2).

When comparing the frequency response of the non-focused illumination of photocathode with the focused one, the ratio is as shown in the following plots, (Figure (3.20) – (3.22)). It is clear from the three plots that whether or not the light is focused onto, the photocathode has no effect on the frequency response of the PMT.

FILE NAME: A:NOFOCT20

1.9  
RELATIVE  
AMPLITUDE

RATIO OF FREQUENCY RESPONSES WHEN OUT OF FOCUS AND  
IN FOCUS AT 20 MV DC OUT VOLTAGE

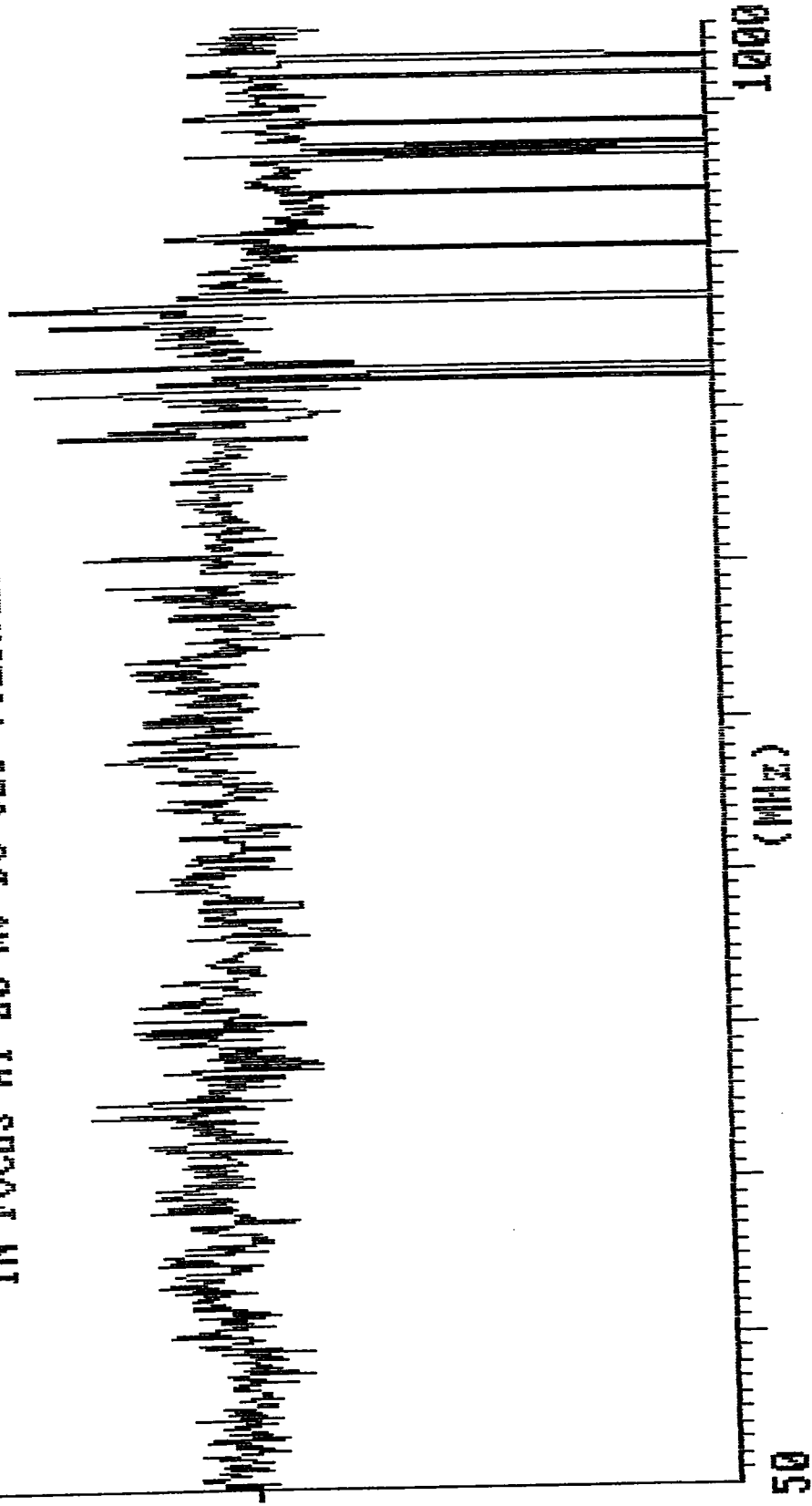


Fig. (3.20)

FILE NAME: A:NOFOCT29

1.9  
RELATIVE  
AMPLITUDE

RATIO OF FREQUENCY RESPONSES WHEN OUT OF FOCUS AND  
IN FOCUS AT 29 MV DC OUT VOLTAGE

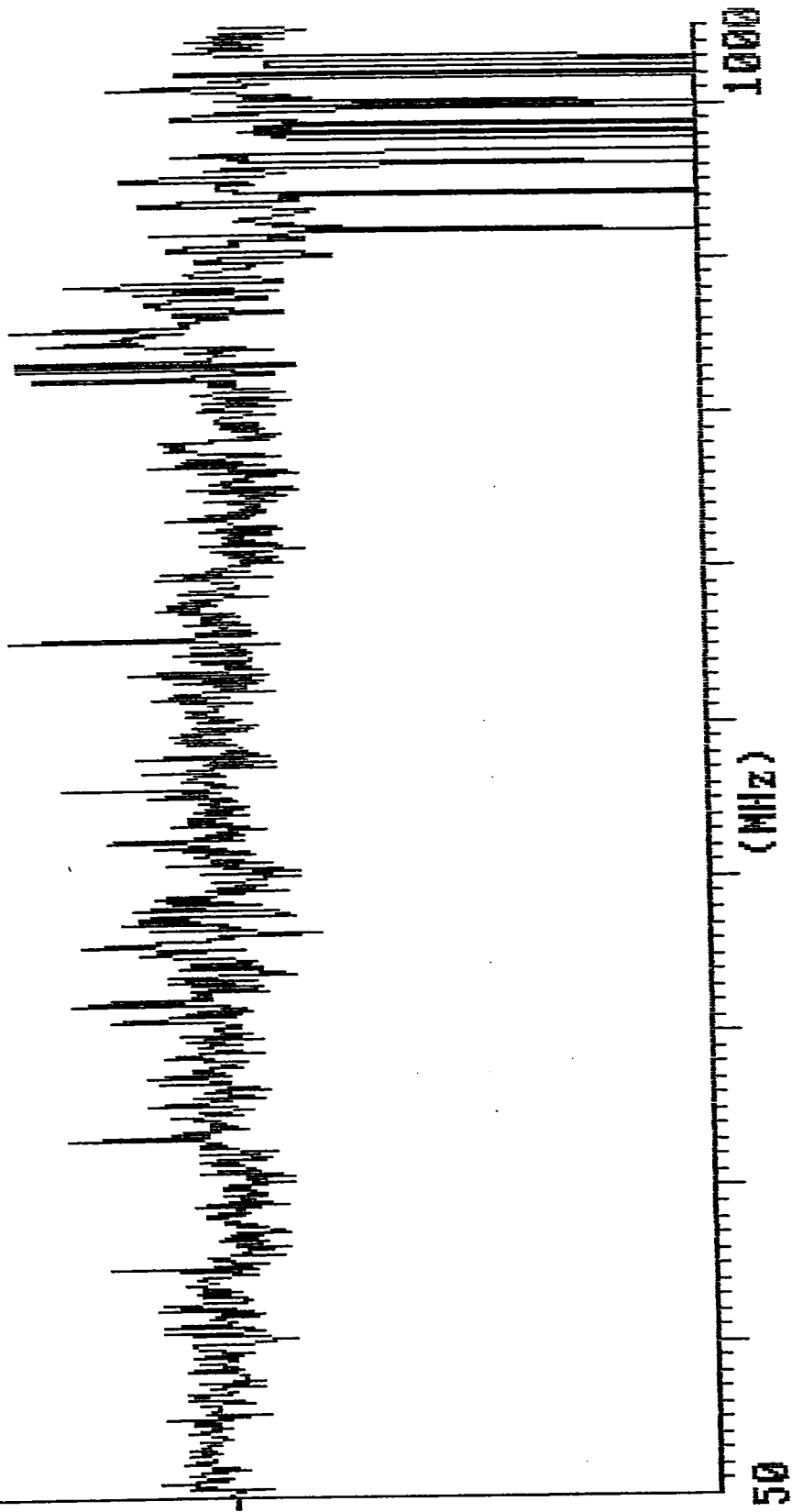


Fig. (3.21)

1.7  
RELATIVE  
AMPLITUDE

FILE NAME: A:NOFOCT40  
RATIO OF FREQUENCY RESPONSES WHEN OUT OF FOCUS AND  
IN FOCUS AT 40 MV DC OUT VOLTAGE

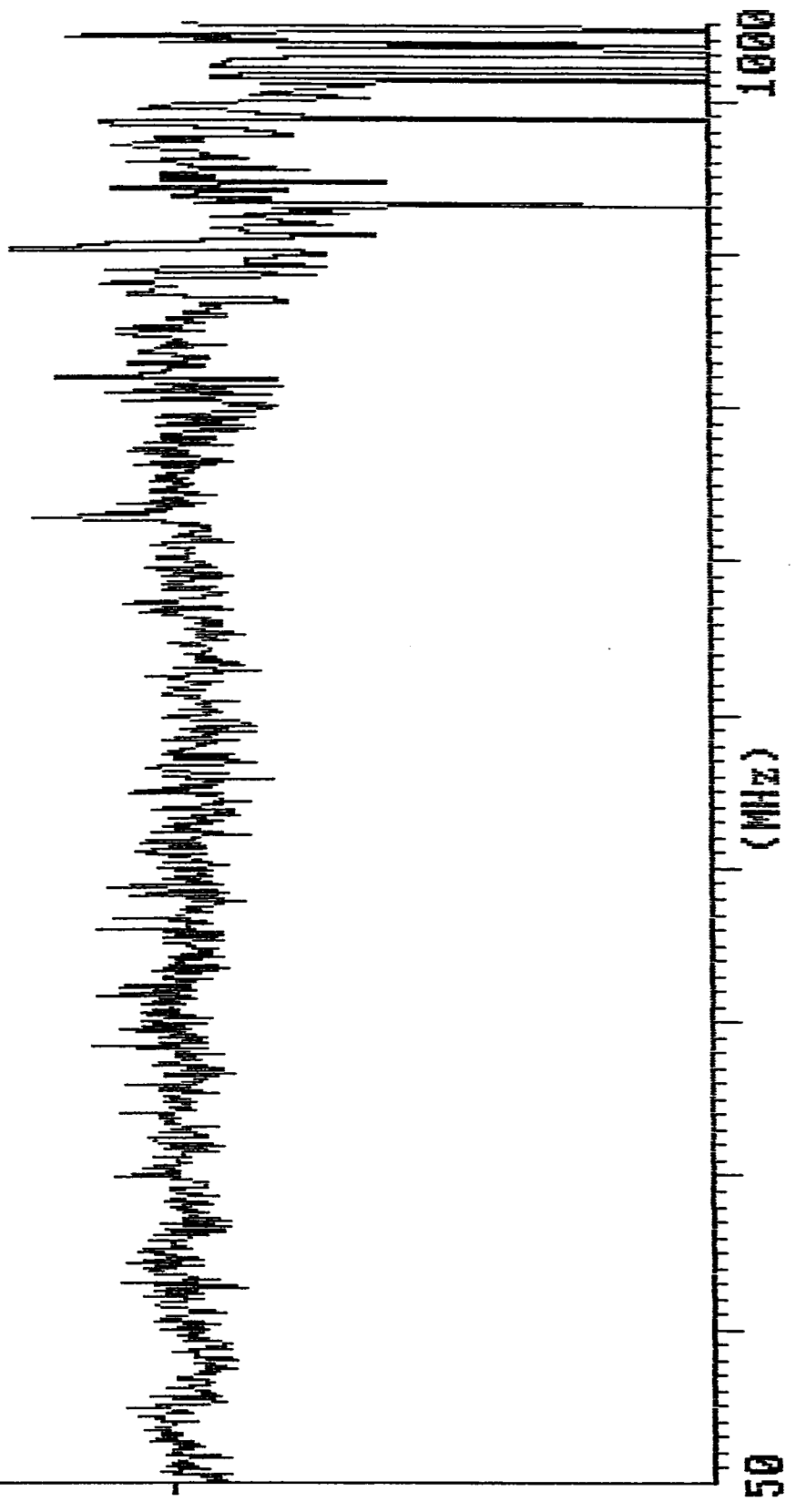


Fig. (3.22)

### 3.3.3. The Effect of PMT Voltage on PMT Frequency Response

At 35 mV DC out voltage, laser wavelength of 579 nm, and in focus arrangement, the frequency response of the PMT was taken while the PMT was operating at 450 V. Then, the frequency response was taken at 500, 550, 575, 600, 625, 650, 675, and 700 V. The frequency response spectra are shown in Appendix (I.A.3).

As the PMT voltage is increased, the PMT becomes more sensitive to high frequencies. This is intuitively expected and can be explained as follows: Let us take some high beat frequency, 1 GHz, for example. Every nanosecond, the intensity of the modulated light is at a crest. After half a nanosecond, the intensity is at a trough. Now, at low PMT voltages, photoelectrons that are emitted from the photocathode due to the incidence of the modulated scattered light are accelerated relatively slowly in comparison with photoelectrons under influence of high PMT voltages. With very low PMT voltages, just as the photoelectrons emitted due to a crest in intensity start accelerating away from the photocathode, half a nanosecond has passed and photoelectrons resembling a trough in intensity are also emitted from the cathode. Both sets of photoelectrons, and accompanying secondary emissions of course, may reach the anode at almost the same time and the signal out of the anode is disturbed. At high PMT voltages, on the other hand, the photoelectrons emitted due to a crest in intensity are quickly accelerated away from the photocathode because of the high potential difference. By the time the

trough in intensity has caused a second set of photoelectrons to be emitted, the first set of photoelectrons, representing the crest, have been quite on their way to the anode, and the signal is clear. This explains why the frequency response at higher frequencies is better at higher PMT voltages. In the following plots (Figure (3.23) – (3.30)), the ratio of frequency responses at 450, 500, 550, 575, 625, 650, 675, and 700 V to the frequency response at 600 V are shown. For PMT voltages less than 600 V, the ratio falls with increasing frequency, while at PMT voltages higher than 600 V, the ratio increases with frequency. This is the expected behavior. An increase in PMT voltage enhances the response at higher frequencies. At the same time the noise also increases with PMT voltage so that one cannot improve the signal to noise ratio above 700 V.

FILE NAME: A:PVOLT450

1.5  
RELATIVE  
AMPLITUDE

RATIO OF FREQUENCY RESPONSES AT  
450 V AND 600 V PMT VOLTAGES

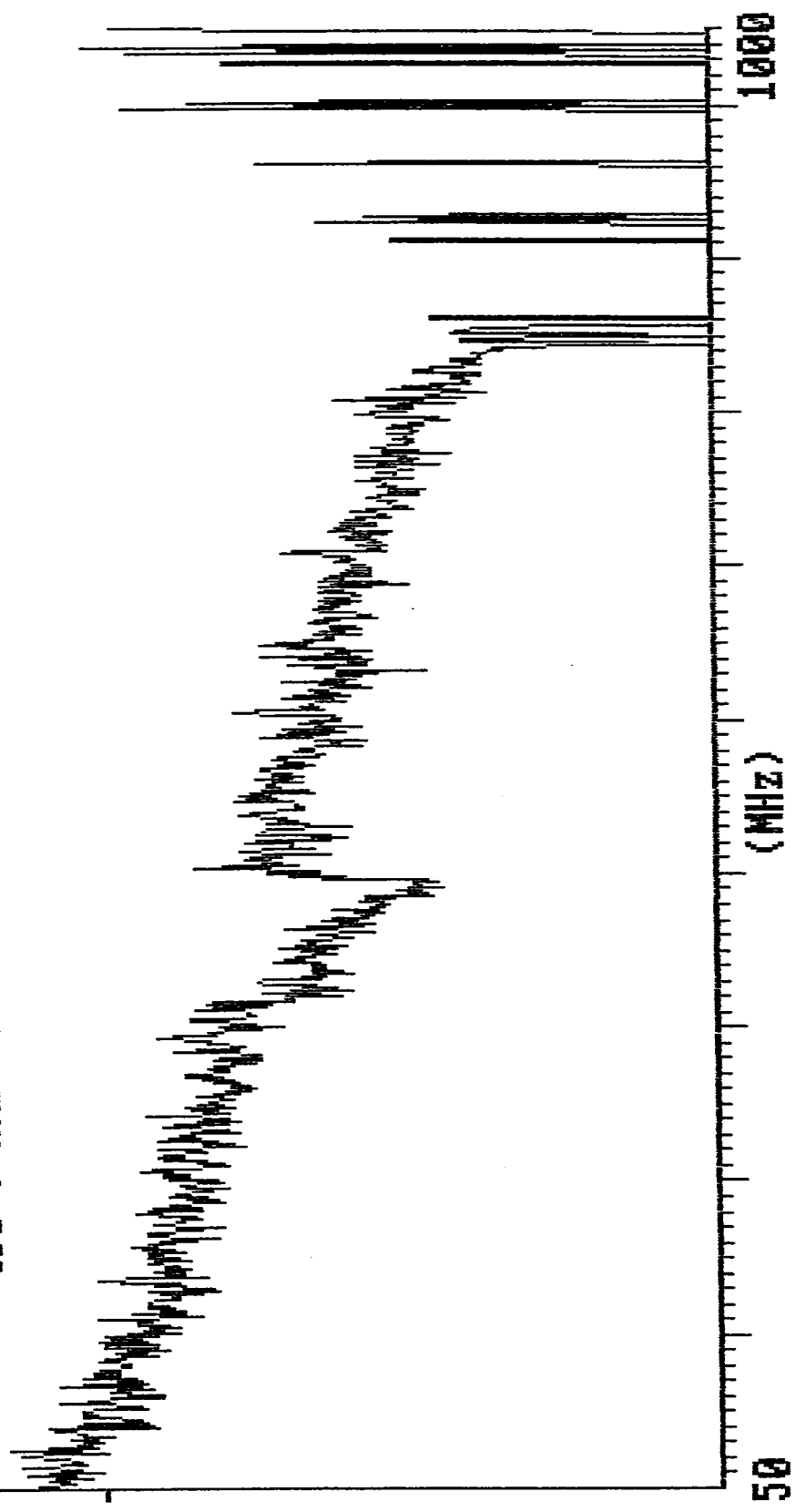


Fig. (3.23)

FILE NAME: 0:PVOLT500

1.5  
RELATIVE  
AMPLITUDE

RATIO OF FREQUENCY RESPONSES AT  
500 V AND 600 V PMT VOLTAGES

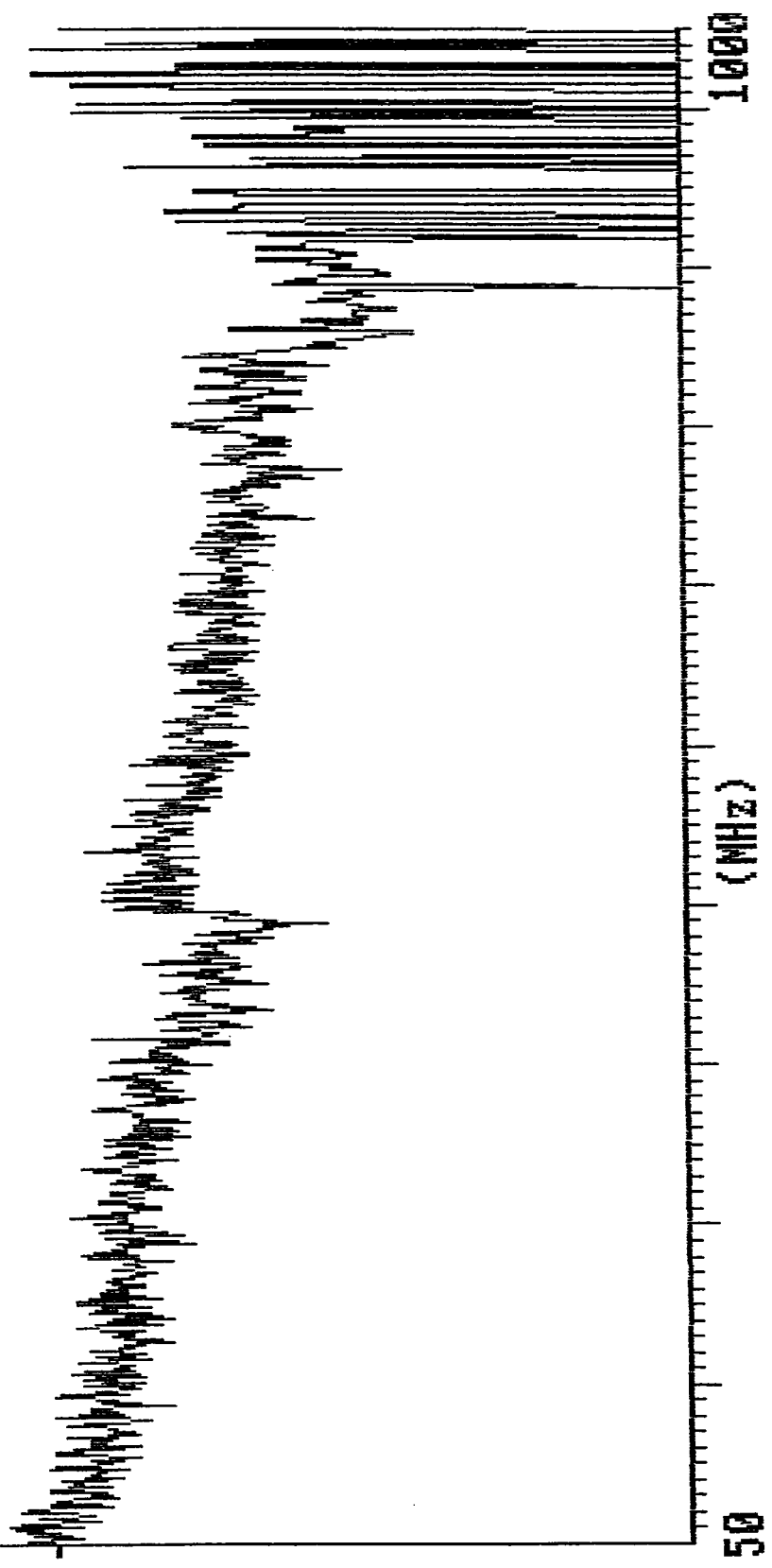


Fig. (3.24)

FILE NAME: A:PVOLT550

RATIO OF FREQUENCY RESPONSES AT  
550 V AND 600 V PMT VOLTAGES

1.7  
RELATIVE  
AMPLITUDE

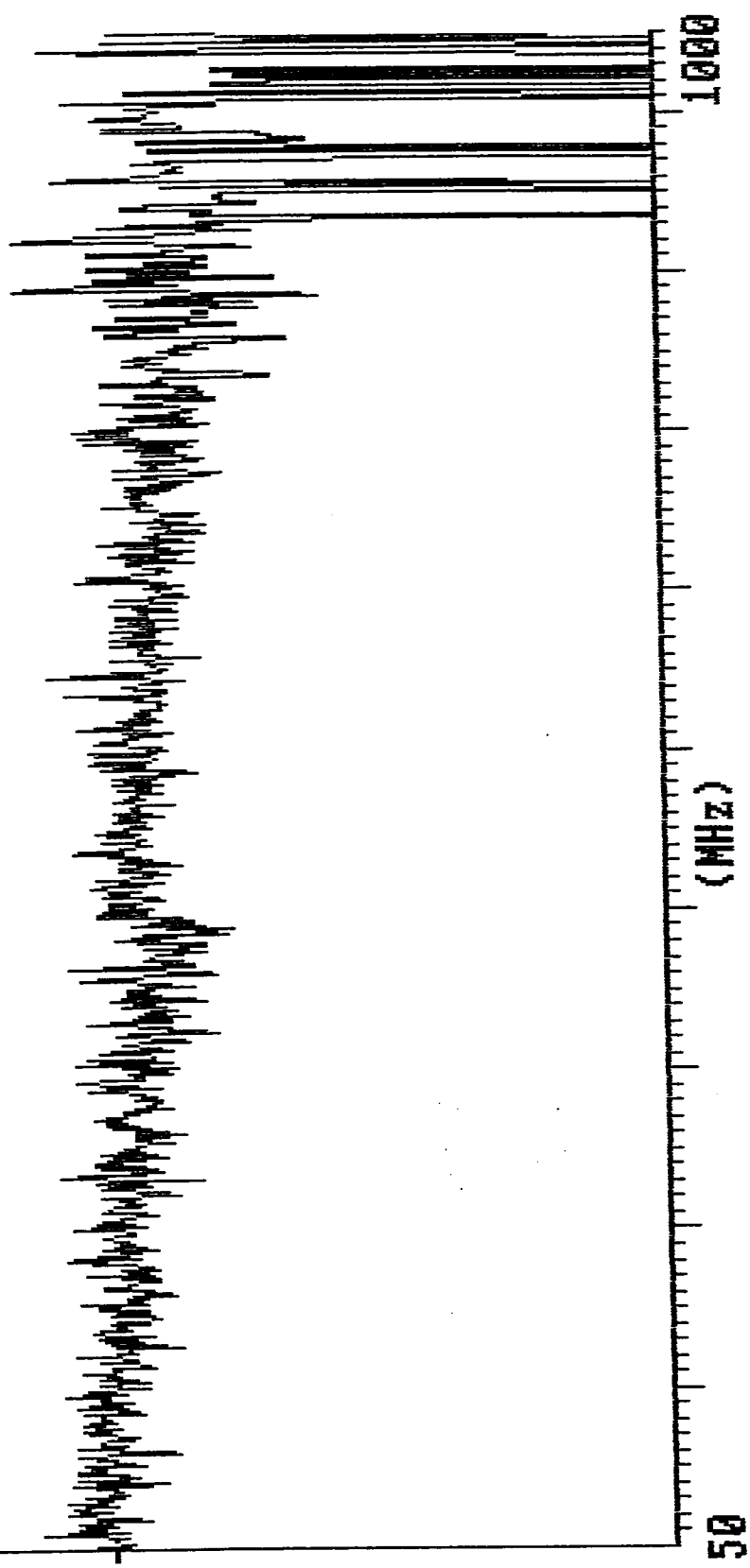


Fig. (3.25)

FILE NAME: A:PVOLT575

<sup>2</sup> RELATIVE AMPLITUDE

RATIO OF FREQUENCY RESPONSES AT  
575 V AND 600 V PMT VOLTAGES

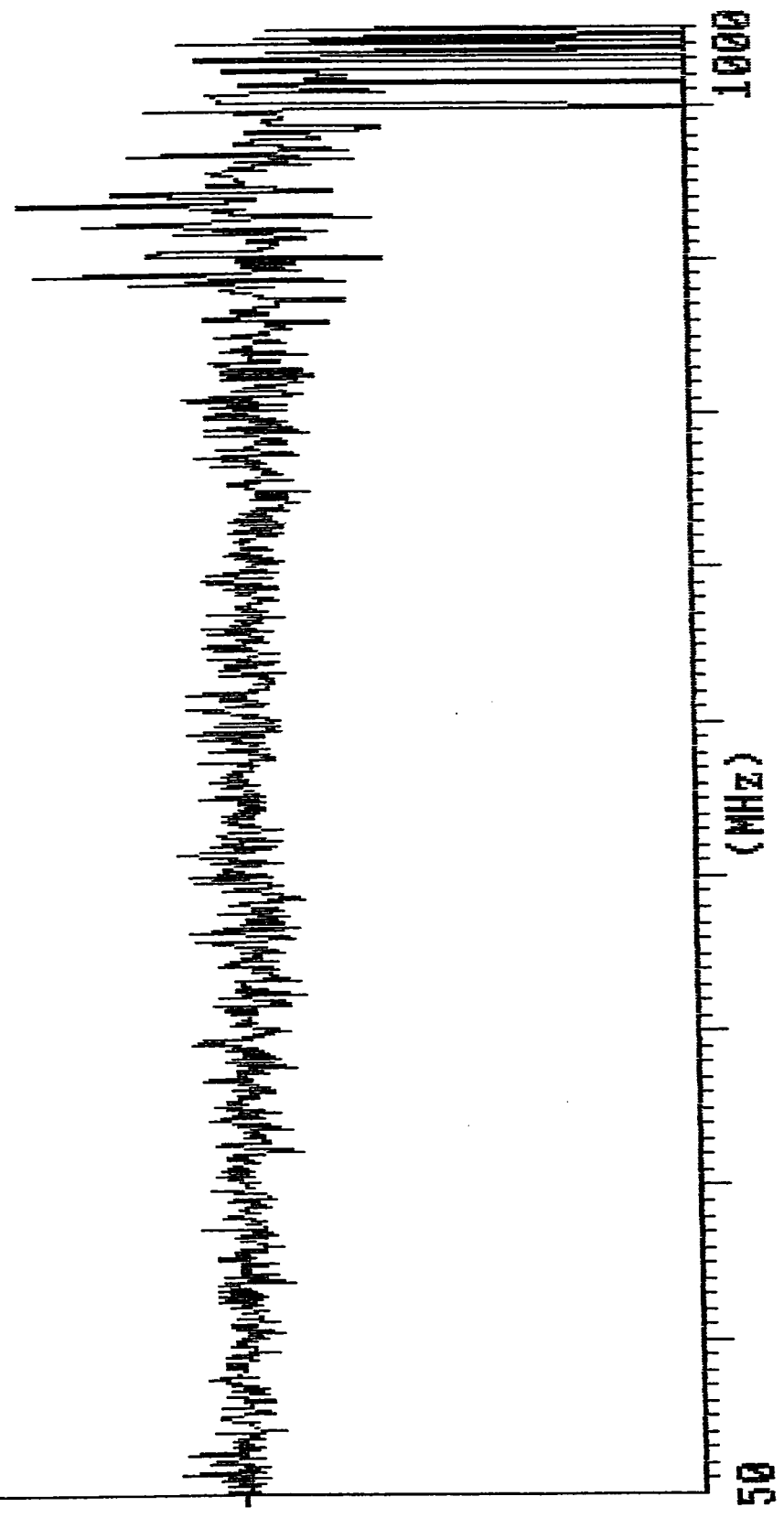


Fig. (3.26)

FILE NAME: A:PVOL1625

<sup>2</sup> RELATIVE  
AMPLITUDE

RATIO OF FREQUENCY RESPONSES AT  
625 V AND 600 V PWT VOLTAGES

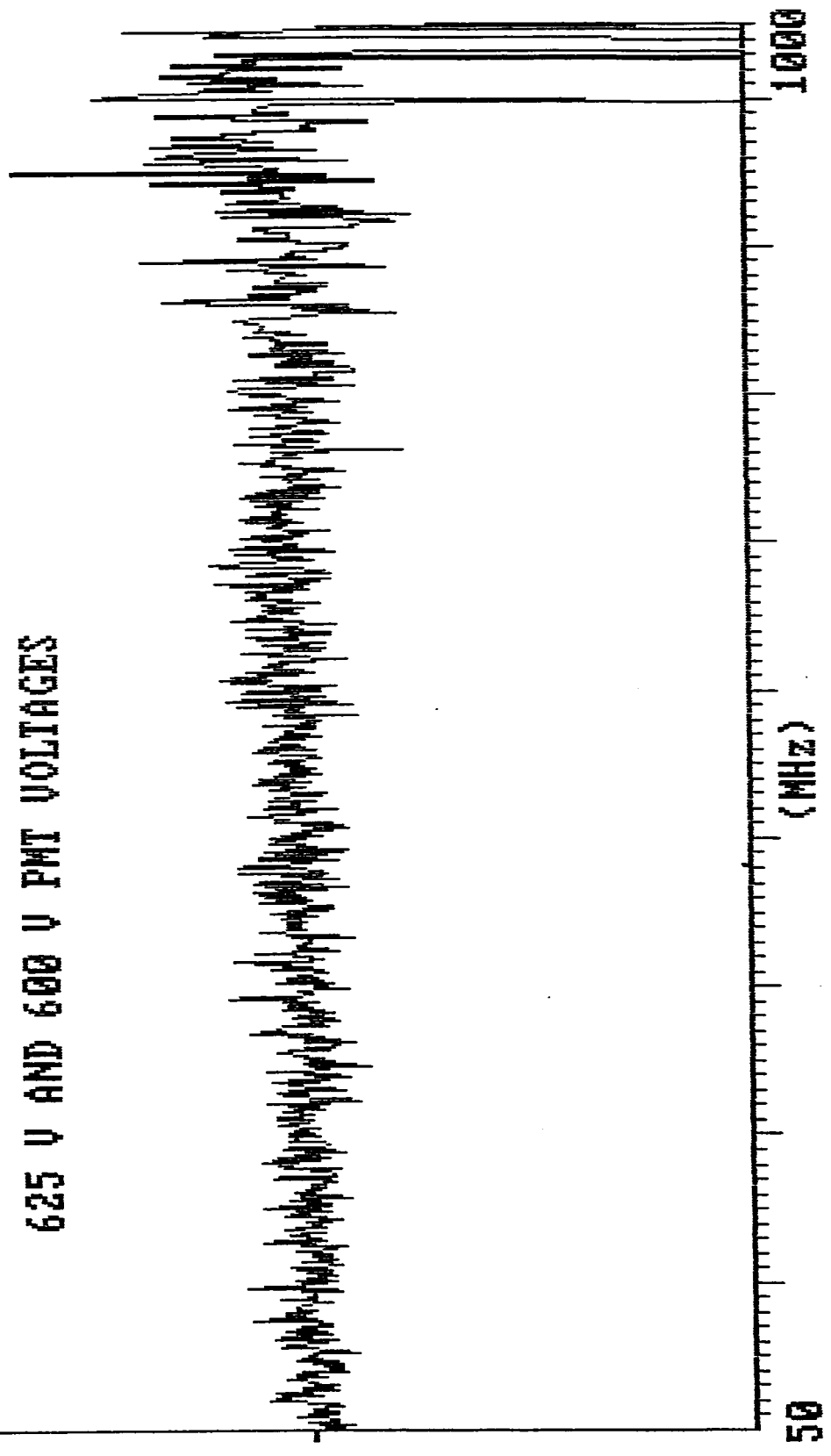


FIG. (3.27)

FILE NAME: A:PVOLT650

2  
RELATIVE  
AMPLITUDE

RATIO OF FREQUENCY RESPONSES AT  
650 V AND 600 V PMT VOLTAGE

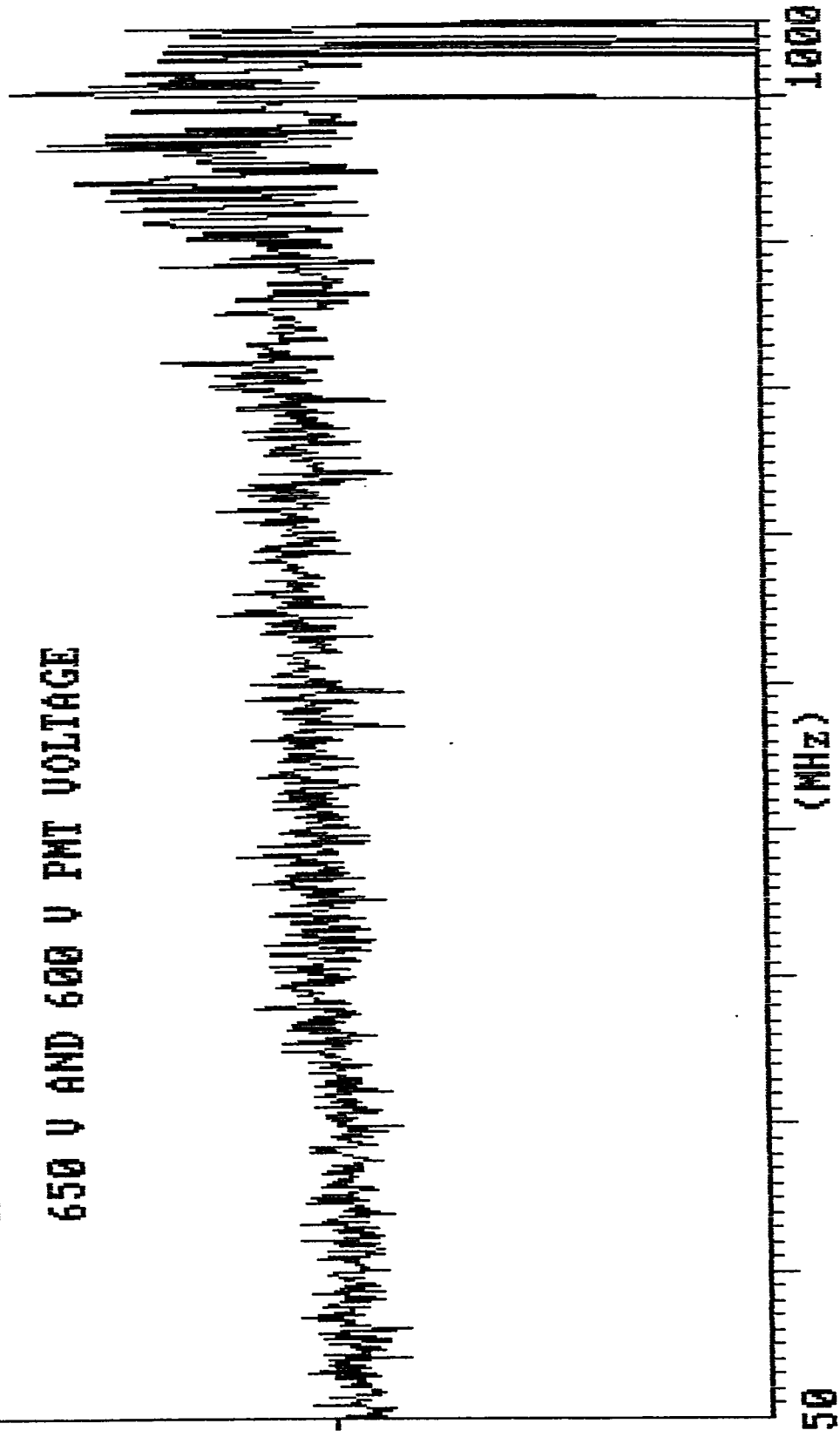


Fig. (3.28)

FILE NAME: A:PVOLT675

2.4  
RELATIVE  
AMPLITUDE

RATIO OF FREQUENCY RESPONSES AT  
675 V AND 600 V PMT VOLTAGES

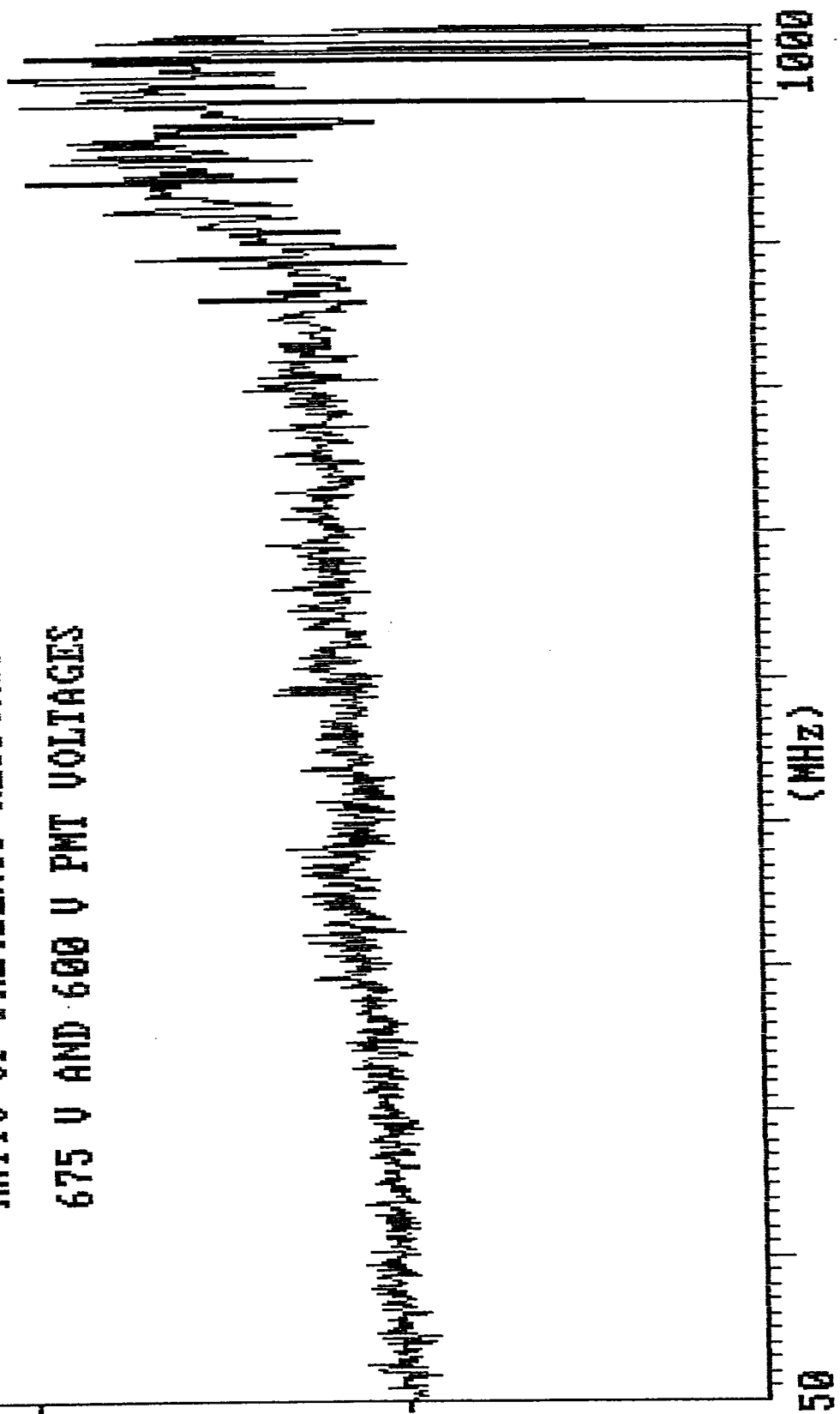


FIG. (3.29)

FILE NAME: A:PVOLT700

2.5  
RELATIVE  
AMPLITUDE

RATIO OF FREQUENCY RESPONSES AT

700 V AND 600 V PMT VOLTAGES

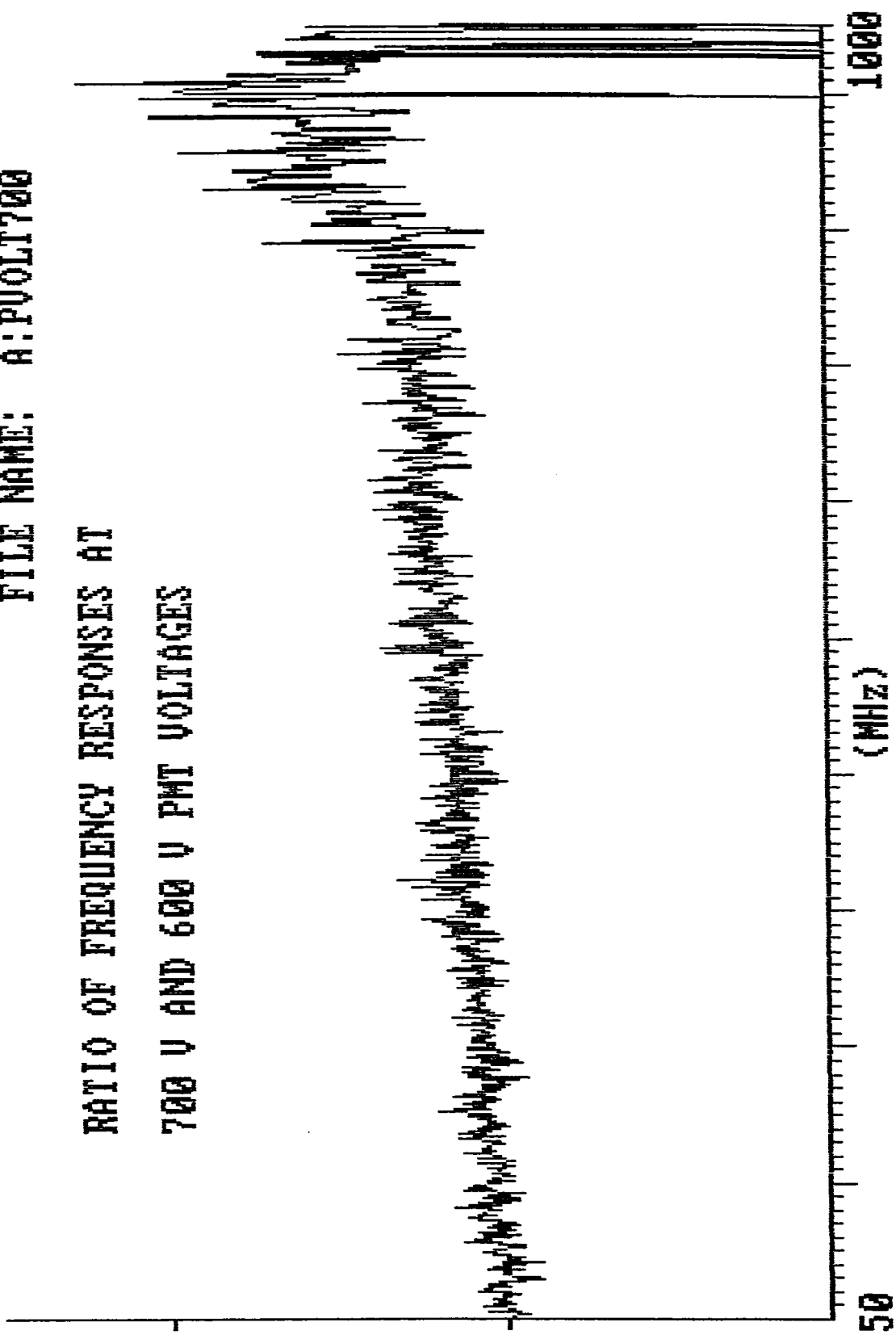


Fig. (3.30)

### 3.3.4. The Effect of Incident Laser Wavelength on the PMT Frequency Response

At 35 mV DC out voltage, 600 V PMT voltage, and in focus arrangement, the frequency response of the PMT was taken with an incident laser wave length of 570 nm once, and once with an incident laser wavelength of 593 nm. The frequency spectrum with these conditions at an incident laser wavelength of 579 nm had already been acquired during the PMT voltage study at 600 V. The spectra are shown in Appendix (I.A.4). Comparing the frequency responses at 570, and 593 nm to that at 579 nm, we get the following two plots (Figure (3.31), (3.32)). It is clear that the laser wavelength dependence for the PMT frequency response is negligible in the range 570-593 nm.

FILE NAME: A:LAMT570

3.4  
RELATIVE  
AMPLITUDE

RATIO OF FREQUENCY RESPONSES AT  
570 NM AND 579 NM LASER WAVELENGTHS

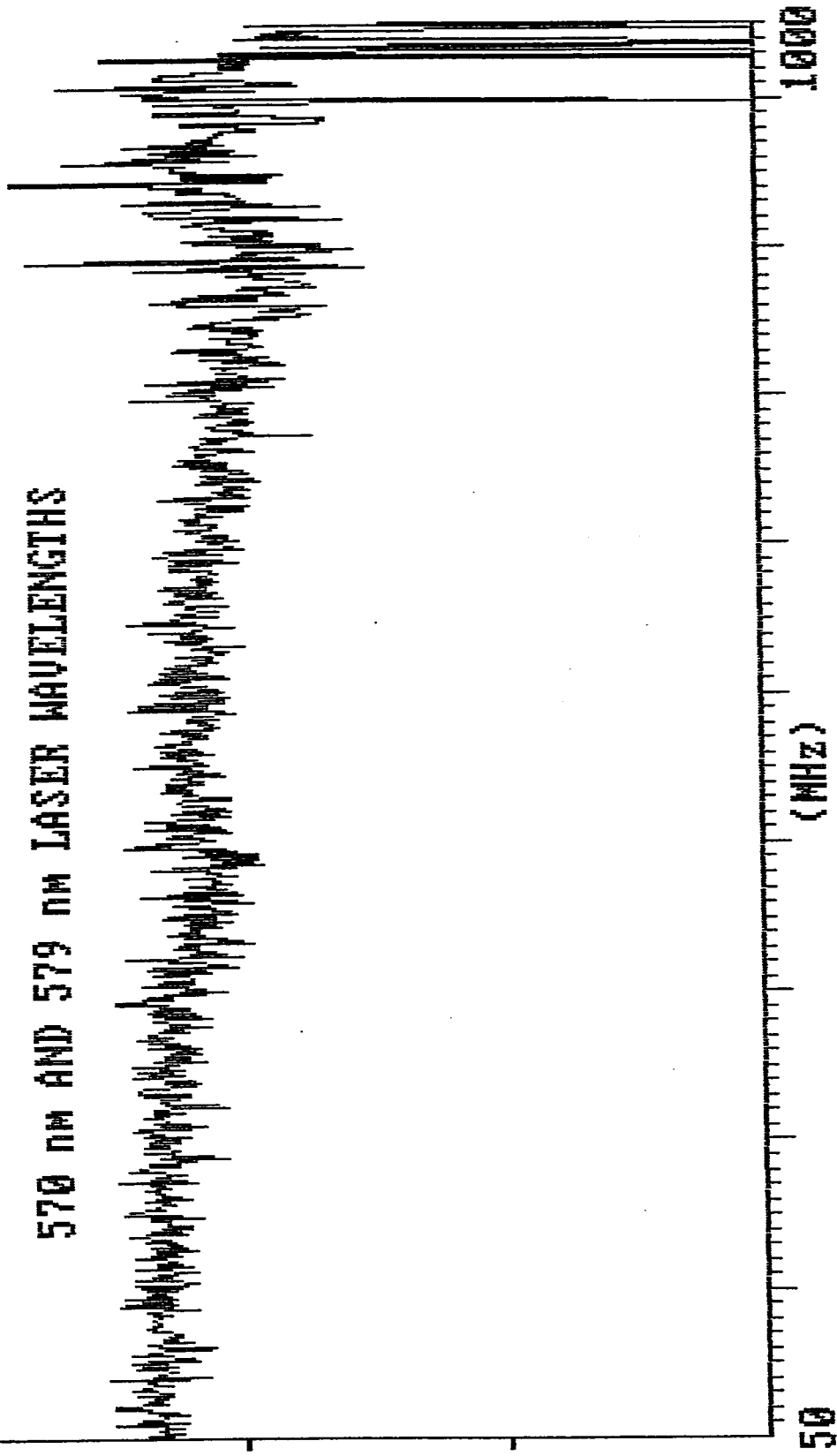


Fig. (3.31)

FILE NAME: A:LAMT593

2:8  
RELATIVE  
AMPLITUDE

RATIO OF FREQUENCY RESPONSES AT

593.4 nm AND 578.9 nm LASER WAVELENGTHS

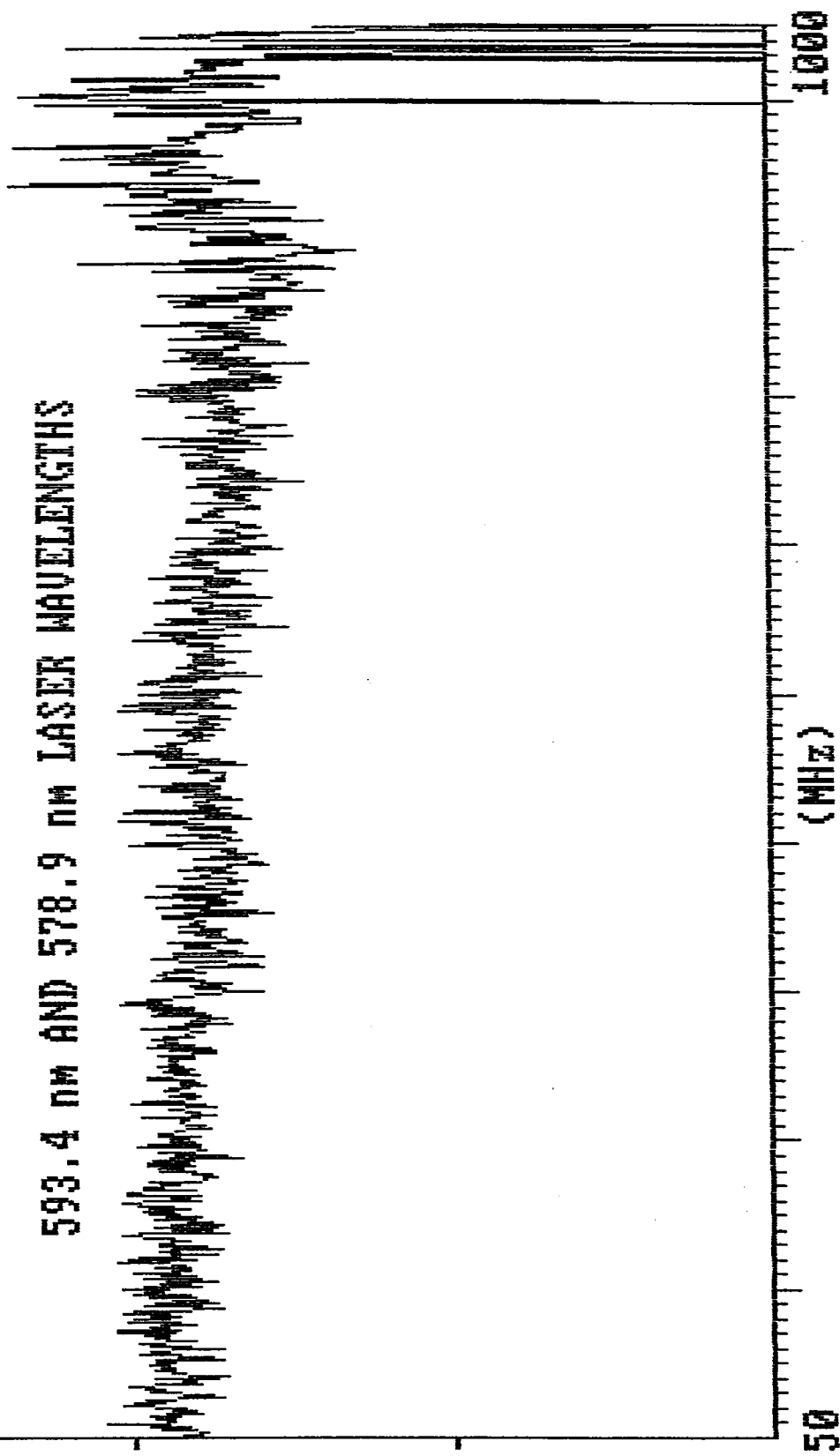


Fig. (3.32)

### 3.3.5. The Effect of Polarization on PMT Frequency Response

At 700 V PMT voltage, 570 nm incident wavelength, 30 mV DC out voltage, and in an in-focus arrangement, the frequency response was taken twice. Once, at a polarization angle  $0^\circ$ , and again at  $90^\circ$ . The two spectra are shown in Appendix (I.A.5). After taking their ratios, the plot is as in Figure(3.33). It is clear that there is no polarization dependence for the PMT frequency response.

FILE NAME: A:REFTPOL

1.8  
RELATIVE  
AMPLITUDE

RATIO OF FREQUENCY RESPONSES OFF A SCATTERER  
WHEN A POLARIZER IS AT 90 AND 0 DEGREES

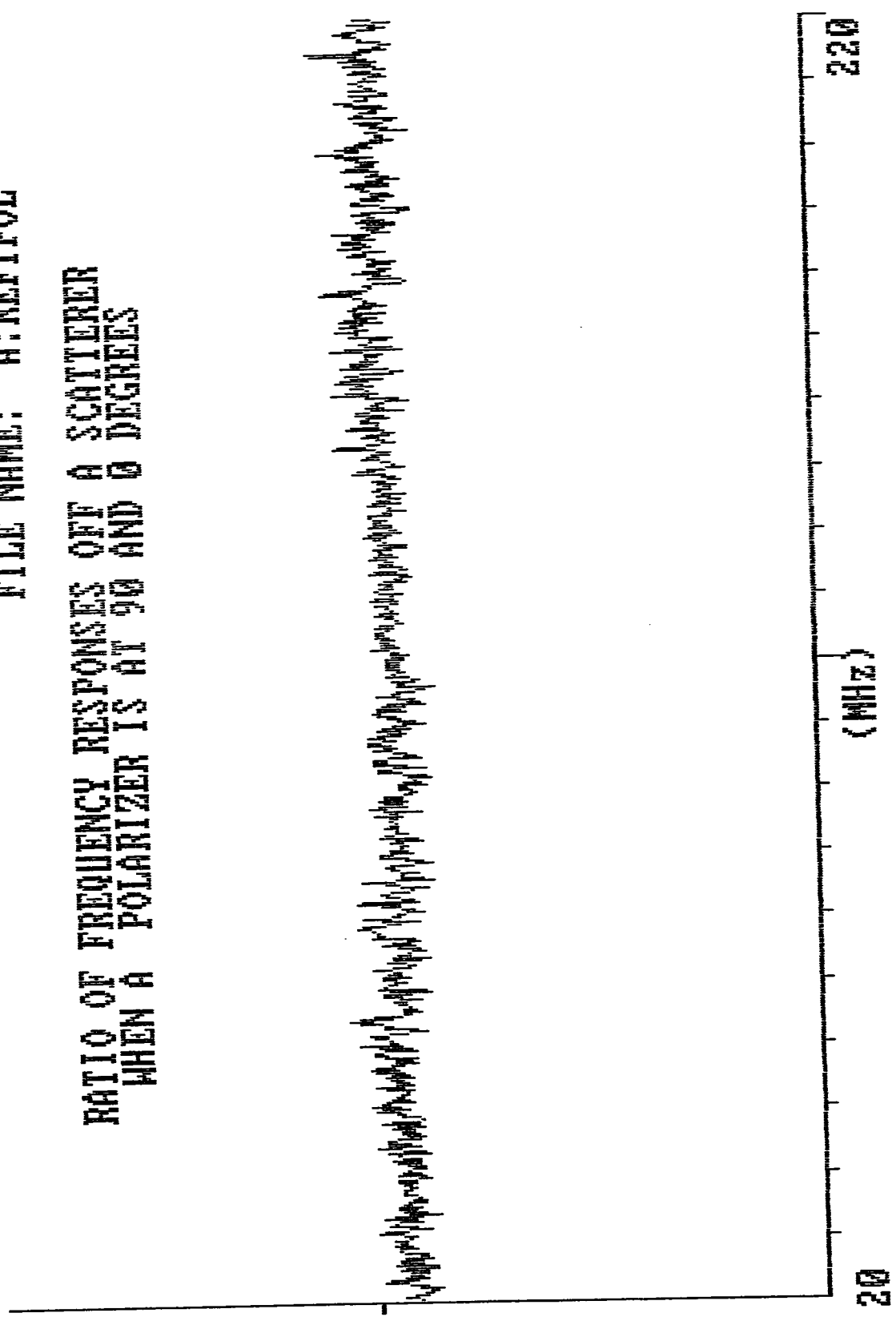


Fig. (5.35)

## Summary

After studying the effect of photon flux intensity, PMT voltage, focus-non focus photocathode illumination, incident flux laser wavelength, and polarization of incident flux, we come up with the following conclusions:

The PMT (Hamamatsu model H3284) we are using, has a high frequency response at low frequencies and drops sharply to less than 11% between 20 and 440 MHz. We observed an increase in the frequency response in the range 400–630 MHz after which the response steadily decreases and becomes too weak to be of use at frequencies above 1100 MHz. The frequency response is independent of the flux intensity, focus-non focus of photocathode illumination, laser wavelength (in the range 570–593 nm), and of polarization.

An increase in the higher components of the frequency response with an increase in PMT voltage was observed. However, due to increasing noise, the signal to noise ratio was not improved above 700 V.

## CHAPTER FOUR

### ROSE BENGAL LIFE-TIME DETERMINATION IN WATER-ETHANOL MIXTURES: AN APPLICATION FOR DEMULATION SPECTROSCOPY

#### 4.1. Introduction

Rose Bengal (RB) is an Xanthene dye whose chemical properties have been studied extensively [14, 16, 18]. In Chapter (1B), we have shown its structure and mentioned some of its properties that give it importance among dyes. Still, because of the short fluorescence lifetime of RB, there have been only a few groups who have determined the lifetime of RB in ethanol or water solutions. There has been discrepancy between different published results [1, 11, 15, 17, 20]. No one, to the best of our knowledge, has studied the effect of different water-ethanol mixtures on the first electronic excited state lifetime of RB.

In this chapter, we will use demodulation spectroscopy to determine and study the fluorescence lifetimes of Rose Bengal in ethanol and in different water-ethanol mixtures.

---

**Review:** It was shown in section 2.1 that a system of two beating ring dye lasers at frequencies  $\nu_1$  and  $\nu_2$  has a beam intensity of the form: (Eq. (2.1.15)).

$$I(t) = \text{const.}(1 + \cos((\omega_1 - \omega_2)t + \phi))$$

We can define our phases such that  $\phi = 0$  and

$$I(t) = \text{const} (1 + \cos((\omega_1 - \omega_2)t) \quad (4.1.1)$$

In section 2.2, it was shown that eq (4.1.1) could be put in the form

$$I = A[1 - e^{-i\omega t}] \quad (4.1.2)$$

where

$$\omega = 2\pi\nu, \quad \nu = |\nu_1 - \nu_2|$$

That is, we have a beating beam of modulation depth ( $\alpha$ ) = 1 and beat frequency  $\nu$ .

It was also shown that if the system under consideration; RB in ethanol for example, had a time dependence that is described by linear differential equations, and if this system had a monoexponential response of the form

$$I_E(t) = \eta e^{-\lambda t} \quad (4.1.3)$$

where  $\lambda$  is the decay rate related to the response, then the response would have an intensity of the form (Eq. 2.2.4)

$$I_E(t) = B[1 - \beta e^{-i(\omega t - \phi)}] \quad (4.1.4)$$

The relation between the modulation depth of the response ( $\beta$ ) and the decay rate of the response ( $\lambda$ ) is (Eq. (2.2.9)):

$$\beta^2 = \frac{\lambda^2}{\lambda^2 + \omega^2} \quad (4.1.5)$$

The modulation depth ( $\beta$ ) approaches unity at lower frequency. As the frequency increases, the modulation depth drops; hence, the name demodulation spectroscopy.

By definition, the relation between the lifetime ( $\tau$ ) and the decay rate ( $\lambda$ ) is: (Eq. 2.2.6)

$$\tau = \frac{1}{\lambda} \quad (4.1.6)$$

In section 2.3, a detailed description of demodulation spectroscopy for the determination of lifetimes was explained.

## 4.2. Procedure

In these few lines we summarize the procedure described in Sect. (2.3) for the determination of fluorescence lifetimes:

1. A beating beam is incident on a scatterer; diluted milk for example. The scattered light has an intensity  $I_0(t)$

$$I_0(t) = B_0(1 - e^{-i(\omega t - \phi_0)}) \quad (4.2.1)$$

where  $B_0$  is a constant amplitude. This would be the case for an ideal (thought) detection system. For a real system, there is a frequency response

factor and Eq. (4.2.1) becomes

$$I_0(t) = B_0(1 - r_0(\omega)e^{-i(\omega t - \phi_0)}) \quad (4.2.2)$$

where  $r_0(\omega)$  is the frequency response factor due to the incidence of scattered light and is a function of frequency.

The DC signal is  $B_0$  and is detected with a digital voltmeter. The AC signal is  $B_0 r_0(\omega)$  and is a function of frequency. It is recorded on a spectrum analyzer.

2. Inserting an orange cut off filter in front of the photocathode to block scattered light, and replacing the scatterer with the fluorescence sample of which one wants to determine its lifetime, the fluorescence will have an intensity  $I(t)$ :

$$I(t) = B(1 - \beta e^{-i(\omega t - \phi)}) \quad (4.2.3)$$

This is true for an ideal PMT. For a real PMT Eq. (4.2.3) becomes

$$I(t) = B(1 - r(\omega)\beta e^{-i(\omega t - \phi)}) \quad (4.2.4)$$

where  $\beta$  is the modulation depth of the fluorescence,  $r(\omega)$  is the frequency response factor of the PMT detection system due to incidence of fluorescence  $B$  is the DC signal. It is monitored with a voltmeter. The AC signal is  $Br(\omega)\beta(\omega)$ . It is recorded on the spectrum analyzer. We have shown in Chapter 3 that the PMT frequency response is independent of intensity,

laser wavelength and polarization. Therefore, if the PMT operating voltage is kept constant in both runs; i.e., with the scatterer and the fluorescence, the response factors  $r_0(\omega)$ , and  $r(\omega)$  are the same.

Dividing the AC signal of the fluorescence ( $S$ ) by the AC signal of the scatters ( $S_0$ ), which were both stored on the spectrum analyzer as a function of frequency, the result is

$$\frac{S(\omega)}{S_0(\omega)} = \frac{B r(\omega) \beta(\omega)}{B_0 r_0(\omega)} = \frac{B \beta(\omega)}{B_0} \quad (4.2.5)$$

because  $r_0(\omega) = r(\omega)$ .

$B_0$  is the DC signal of the scatter.  $S_0(\omega)$  is the AC signal of the scatter at angular beat frequency  $\omega$  ( $\omega = 2\pi|\nu_1 - \nu_2|$ ).  $B$  is the DC signal of the fluorescence.  $S(\omega)$  is the AC signal of the fluorescence at angular beat frequency  $\omega$ .  $\beta(\omega)$  is the modulation depth of the fluorescence.

Inverting Eq. (4.2.5) we get an expression for the modulation depth as a function of beat frequency in terms of purely experimental quantities, i.e.,

$$\beta(\omega) = \frac{B_0 S(\omega)}{B S_0(\omega)} \quad (4.2.6)$$

By varying the intensity of the excitation source until the DC amplitude from the scattered signal is equal to that of the fluorescence signal, we have

$B = B_0$  in which case

$$\beta(\omega) = \frac{S(\omega)}{S_0(\omega)} \quad (\text{with } B = B_0) \quad (4.2.7)$$

This experimentally determines the modulation depth. The modulation depth  $\beta(\omega)$  is the quotient of AC signal amplitude of the fluorescence over the AC signal amplitude from the scatter when the DC out voltages are equal from both fluorescence and scattered light.

3. The lifetime  $\tau$  is related to the decay rate  $\lambda$  by:

$$\tau = \frac{1}{\lambda} \quad (4.2.8)$$

and for monoexponential responses of samples that have time dependence described by linear differential equations, the modulation depth  $\beta(\omega)$  is related to  $\lambda$  by (Eq. 2.2.9)

$$\beta^2 = \frac{\lambda^2}{\lambda^2 + \omega^2} \quad (4.2.9)$$

Combining 4.2.8) with (4.2.9) the fluorescence lifetime is:

$$\tau = \frac{\sqrt{1 - \beta^2(\omega)}}{\omega\beta(\omega)} \quad (4.2.10)$$

and this determines the lifetime experimentally.

### 4.3. Remarks

#### A) Ideal PMT vs Real PMT

It may be instructive to picture the difference between how an ideal PMT would behave in a demodulation spectroscopic experiment and how a real PMT behaves under the same conditions.

An ideal PMT would have response to scattered light (Eq. (4.2.1)):

$$I_0 = B_0(1 - e^{-i(\omega t - \phi_0)})$$

The response to fluorescence would be (Eq. (4.2.3))

$$I = B(1 - \beta e^{-i(\omega t - \phi)})$$

Assuming  $B_0 = B$  (which can be achieved experimentally), the AC scatter signal and AC fluorescence signal would have intensities on the spectrum analyzer as shown in Figure (4.1).

The AC scatter signal would have a constant amplitude with frequency while the AC fluorescence signal would have an amplitude  $B\beta$ :

$$B\beta = \frac{B\lambda}{\sqrt{\lambda^2 + \omega^2}}$$

When  $\omega \ll \lambda$ , the signal has an amplitude of approximately  $B$ . At higher frequencies the fluorescence of the AC fluorescence signal drops as  $\frac{1}{\sqrt{a + \omega^2}}$ ;  $a$  is a constant.

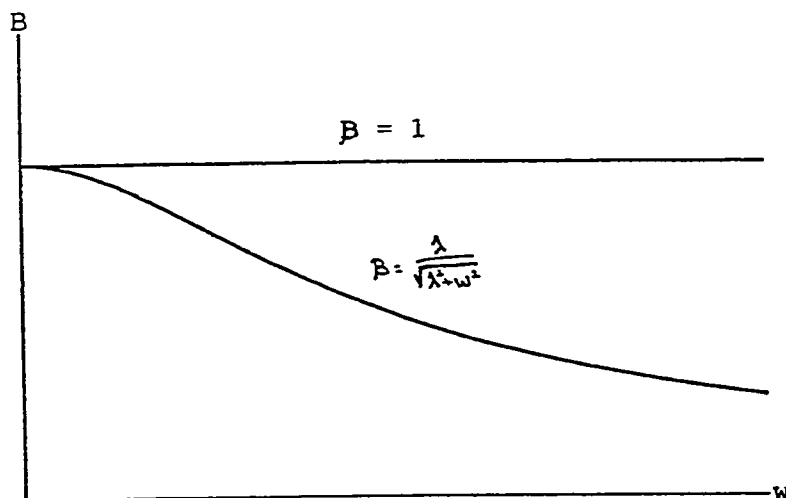


Fig. (4.1): Ideal PMT Behavior in a Demodulation Spectroscopy Experiment

A real PMT, on the other hand, does not have a constant response for all frequencies and the intensity of the scattered light is Eq. (4.2.2)

$$I_0(t) = B_0(1 - r_0(\omega)e^{i(\omega t - \phi_0)})$$

and the fluorescence signal intensity is Eq. (4.2.4)

$$I(t) = B(1 - r(\omega)\beta e^{-i(\omega t - \phi)})$$

Again, with  $B_0 = B$ . If we assume that the response of the PMT is the same to scattered light as it is to fluorescence, which is an acceptable assumption as we have seen in Ch. 3, then the frequency spectrum of the scattered light and of the fluorescence would be recorded on the spectrum analyzer just like in Figure (4.2). This is a real spectrum of a fluorescence signal and scatter signal. Still, their ratio gives the modulation depth  $\left(\beta = \frac{\lambda}{\sqrt{\lambda^2 + \omega^2}}\right)$  as explained in Sec. 4.2.

FREQUENCY RESPONSE TO 1: REFERENCE  
2: RB IN PURE ETHANOL

7  
RELATIVE  
AMPLITUDE

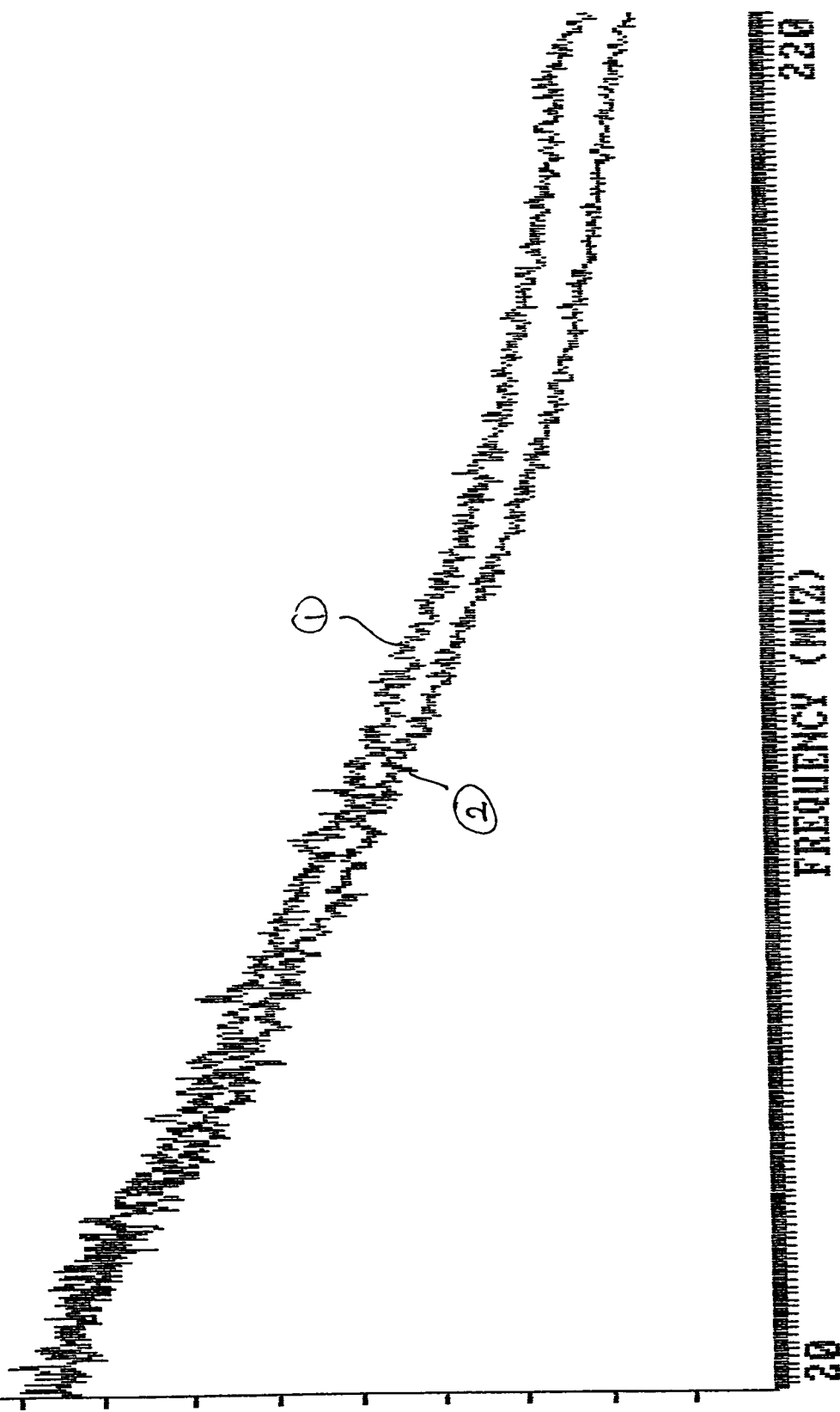


FIG. (4.2)

### B) Monoexponential Decay:

In order for Eq. (4.2.9):  $\beta^2 = \lambda^2/(\lambda^2 + \omega^2)$  to hold the fluorescence must be monoexponential. Therefore, we must be as certain that we have only one type of fluorescence substance in the sample; only Rose Bengal, for example. This is taken care of during the preparation of the solution. The Rose Bengal powder used in the preparation is assumed to have Rose Bengal as the sole fluorescent substance. Another factor that induces a multiexponential decay is rotational diffusion. It can be shown that if a polarizer is adjusted to  $54.7^\circ$  in front of the PMT then rotational diffusion will not introduce multiexponential decays [15].  $54.7^\circ$  is sometimes referred to as 'magic angle' [17].

### C) Linearity of Fluorescence Sample

The relation  $\beta^2 = \frac{\lambda^2}{\lambda^2 + \omega^2}$  was derived from an original convolution integral equation that holds only if the fluorescence system (RB and solvent) has a time dependence that is described by linear differential equations. In order for this to be true the concentration of excited molecules must be small compared with the concentration of the unexcited molecules. In our experiment, we are using Rose Bengal (RB) in water and/or ethanol. The molarity of RB is  $5 \times 10^{-5}M$ . To find the concentration of excited  $RB \equiv RB^*$ , we look at the following reaction:



$RB$  is excited by absorption after which it decays by a decay rate  $\lambda$ . Therefore

$$\frac{d[RB^*]}{dt} = I_{abs} - \lambda[RB^*] \quad (4.3.2)$$

where  $I_{abs}$  is the number of quanta absorbed by  $RB$  molecules per unit time per unit volume. At equilibrium  $\frac{d[RB^*]}{dt} = 0$ , therefore,

$$[RB^*] = \frac{I_{abs}}{\lambda} \quad (4.3.3)$$

$\lambda \approx 10^{10}$  Hz as will be shown near the end of this chapter.  $I_{abs}$  is found in the following way:

The power of the beating beam is approximately 100 mW, it has dimensions of approximately 1 mm radius absorbed in a 1 cm long cell. The wavelength of the beating beams is 570 nm. The greatest concentration of  $RB^*$  will be if we assume that the beating beam is absorbed by  $RB$  molecules only, and that there is complete absorption of the beam. Under these conditions, the amount of energy per photon quantum is:

$$E = \frac{hc}{\lambda} = 3.5 * 10^{-19} \text{ J.}$$

The number of quanta incident per sec is:

$$N = \frac{100 \text{ mJ s}^{-1}}{3.5 * 10^{-19} \text{ J/Quantum}}$$

$$N = 2.9 * 10^{17} \text{ Quanta/sec}$$

The number of quanta density per sec inside the sample cell is

$$n = \frac{2.9 * 10^{17} \text{ Quanta} * \text{s}^{-1}}{\pi(1 \text{ mm})^2 * 1 \text{ cm}} = 9.2 * 10^{18} \frac{\text{Quanta}}{\text{cm}^3 * \text{s}}$$

$$= 9.2 * 10^{21} \text{ Quanta } s^{-1} \ell^{-1}.$$

If the beam is completely absorbed by  $RB$  molecules only, then

$$I_{abs} = 9.2 * 10^{21} s^{-1} \ell^{-1}$$

Now, the concentration of the excited  $RB$  molecules can be calculated using Eq.

(4.3.3)

$$[RB^*] = \frac{9.2 * 10^{21} s^{-1} \ell^{-1}}{10^{10} s^{-1}} = 9.2 * 10^{11} \frac{\text{molecule}}{\ell}$$

In terms of molarity:

$$[RB^*] = \frac{9.2 * 10^{11}}{6.0 * 10^{23}} \simeq 1.5 * 10^{-12} \text{ M}$$

If this is compared with  $[RB] = 5 * 10^{-5} \text{ M}$ , we see that the concentration of excited  $RB^*$  is eight orders of magnitude less than the concentration of  $RB$ ; i.e.,

$$\frac{[RB^*]}{[RB]} = 3 * 10^{-8}$$

This ensures linearity behavior of the solution.

## 4.4 Data Manipulation And Error Analysis

### A) The Fluorescence Lifetime of Rose Bengal in Pure Ethanol

We have summarized the procedure for fluorescence lifetime determination through demodulation spectroscopy in Sec. 4.2. In the following we will describe the determination of the fluorescence lifetime of Rose Bengal in pure ethanol.

1. **Data Acquiring & Baseline Effect Subtraction:** At 600 V PMT operating voltage, 30 mV DC out voltage, and 570 nm laser wavelength, the frequency response of  $1 * 10^{-5}$  M *RB* in pure ethanol in the region of 20 – 220 MHz is acquired and is stored in the spectrum analyzer. The data is then transferred to a PC computer. The baseline of the spectrum analyzer is also recorded and transferred to the PC. The effect of the baseline on the fluorescence frequency response is subtracted as described in Sec. 3.2. Under the same conditions, with diluted milk replacing the fluorescence sample, the frequency response is acquired and transferred to the PC. Again, the spectrum analyzer baseline is recorded and transferred to the PC. The effect of the baseline on the scatter frequency spectrum is subtracted.

2. **Linearization:** Since the spectrum analyzer is set to acquire in dBm (logarithmic) mode, we must now linearize the (properly subtracted) frequency response data. The properly subtracted, linearized data for the fluorescence sample

is shown in Figure (4.3). The equally treated data from the diluted milk scatter is shown in Figure (4.4). We will call this: reference frequency response.

**3. The Modulation Depth:** As we have shown, in Sec. 4.2, the ratio of the fluorescence frequency response to its corresponding reference frequency response is the modulation depth  $\beta(\omega)$ . This is shown in Figure (4.5). The demodulation with increasing frequency is evident. The modulation depth should have the form

$$\beta = \frac{\lambda}{\sqrt{\lambda^2 + \omega^2}}$$

**4. Linear Regression:** Looking at Eq. (4.2.9),

$$\beta^2(\omega) = \frac{\lambda^2}{\lambda^2 + \omega^2} \quad (4.4.1)$$

where  $\lambda$  is the decay rate and  $\omega = 2\pi\nu$  and  $\nu$  is the beat frequency.

As the beat frequency approaches zero, the modulation depth  $\beta(\omega)$  approaches unity. Due to possible mismatch in conditions under which the sample and its reference are acquired, the modulation depth at zero beat frequency will be some multiple ( $\xi$ ) of unity. For example, this is the case when there is a mismatch in the DC output voltages in the two runs. Therefore,  $\beta \rightarrow \xi\beta$  and Eq. (4.4.1) becomes

$$\beta^2 = \frac{\xi^2 \lambda^2}{\lambda^2 + \omega^2} \quad (4.4.2)$$

Inverting Eq. (4.4.2)

$$\frac{1}{\beta^2} = \frac{1}{\xi^2} + \frac{1}{\xi^2 \lambda^2} \omega^2 \quad (4.4.3)$$

By plotting  $\frac{1}{\beta^2}$  vs.  $\omega^2$ , the vertical intercept  $H$  is

$$H = \frac{1}{\xi^2} \quad (4.4.4)$$

and the slope  $M$  is

$$M = \frac{1}{\xi^2 \lambda^2} \quad (4.4.5)$$

Using a two-parameter fit of  $\frac{1}{\beta^2}$  vs.  $\omega^2$  the best fit values of  $H$  and  $M$  are determined as follows:

If  $X_i$  is defined to be the  $i$ -th value of  $\omega^2$ , and  $Y_i$  is defined to be the corresponding value of  $\frac{1}{\beta^2(\omega)}$ , then the equation under consideration is [21]:

$$H + MX_i = Y_i \quad (4.4.6)$$

$H$  is given by:

$$H = \frac{1}{D} (\sum X_i^2 \sum Y_i - \sum X_i \sum X_i Y_i) \quad (4.4.7)$$

$M$  is given by:

$$M = \frac{1}{D} (-\sum X_i \sum Y_i + P \sum X_i Y_i) \quad (4.4.8)$$

where

$$D = P \sum X_i^2 - (\sum X_i)^2 \quad (4.4.9)$$

and  $P$  is the number of different values of the independent variable  $X_i$ .

Using (4.4.4, 4.4.5),

$$M = H/\lambda^2 \quad (4.4.10)$$

but  $\lambda = \frac{1}{\tau}$ ; therefore

$$\tau = \sqrt{\frac{M}{H}} \quad (4.4.11)$$

And this determines the lifetime ( $\tau$ ).

In Figure (4.6), the two-parameter linear regression best fit is shown.

The slope  $M$  is found to be

$$M = 0.360 * (\text{GHz})^{-2}$$

The vertical intercept  $H$  is found to be

$$H = \frac{1}{\beta^2(0)} = 0.678$$

Therefore,

$$\begin{aligned} \tau &= \sqrt{\frac{0.360}{0.678}} \quad (\text{GHz})^{-1} \\ &= 0.728 \quad 10^{-9} \text{ s} \\ &= 728 \quad \text{ps} \\ \lambda &= \frac{1}{\tau} = 1.37 \quad \text{GHz} \end{aligned}$$

Figure (4.7) shows a plot of the modulation depth along with the best fit of the modulation depth found from the linear regression of  $\frac{1}{\beta^2}$  vs  $\omega^2$ . The fit is very good, and the standard deviation is found to be 0.03. Figure (4.8) is a plot of the residuals as a function of frequency. The scatter around the mean is approximately symmetric, and this suggests that we have only random (statistical) errors.

FILE NAME: B:ROSEL2  
DC OUT = 30 MV  
WAVELENGTH = 570 nm  
PMT VOLTAGE = 600 V

FREQUENCY RESPONSE OF ROSEL BENGAL  
IN 0 % WATER AND 100 % ETHANOL

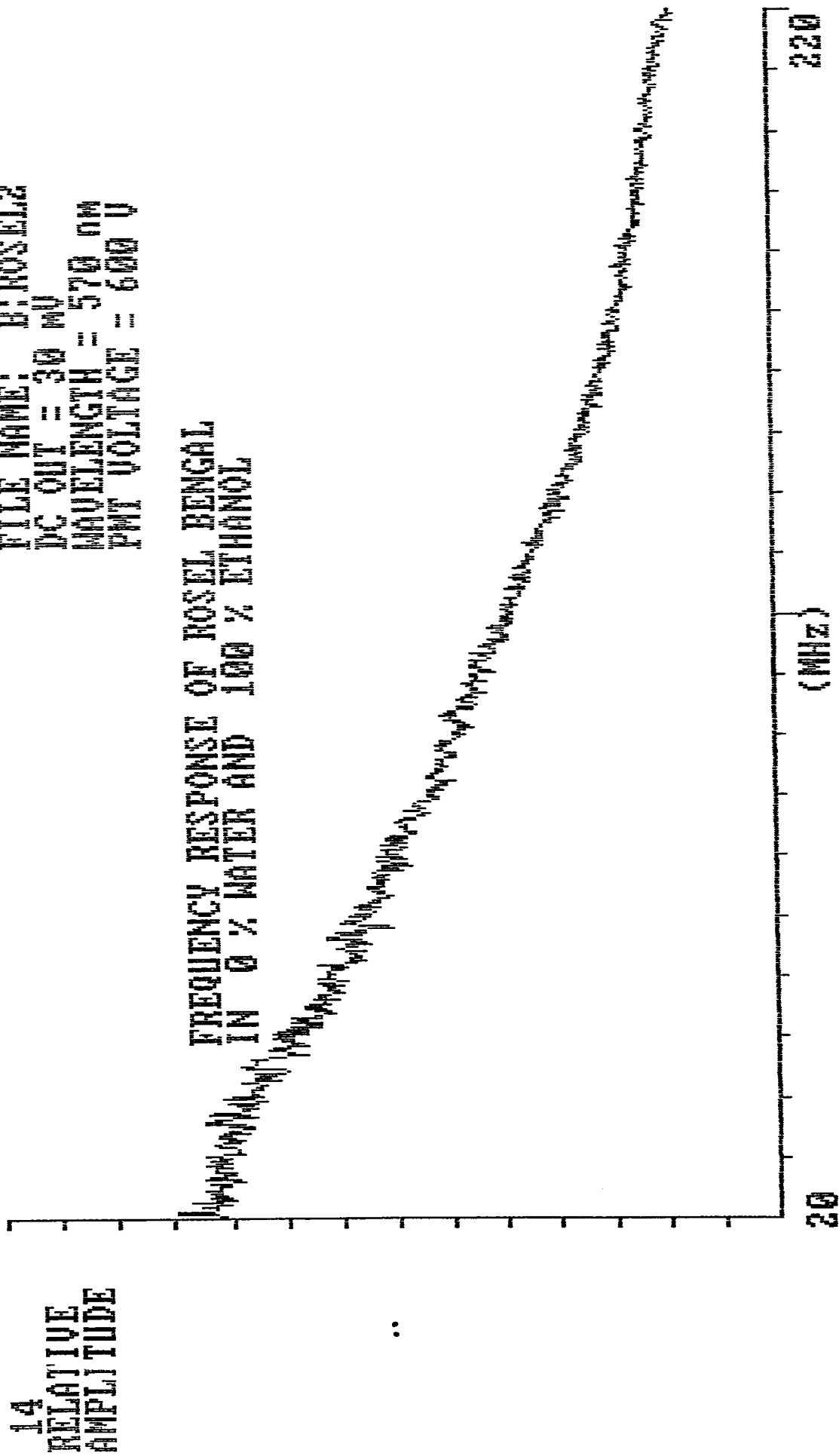


FIG. (4.3)

FILE NAME: B:REFL2  
DC OUT = 30 MV  
WAVELENGTH = 570 nm  
PMT VOLTAGE = 600 V

12  
RELATIVE  
AMPLITUDE

FREQUENCY RESPONSE OF REFERENCE FOR ROSEL2

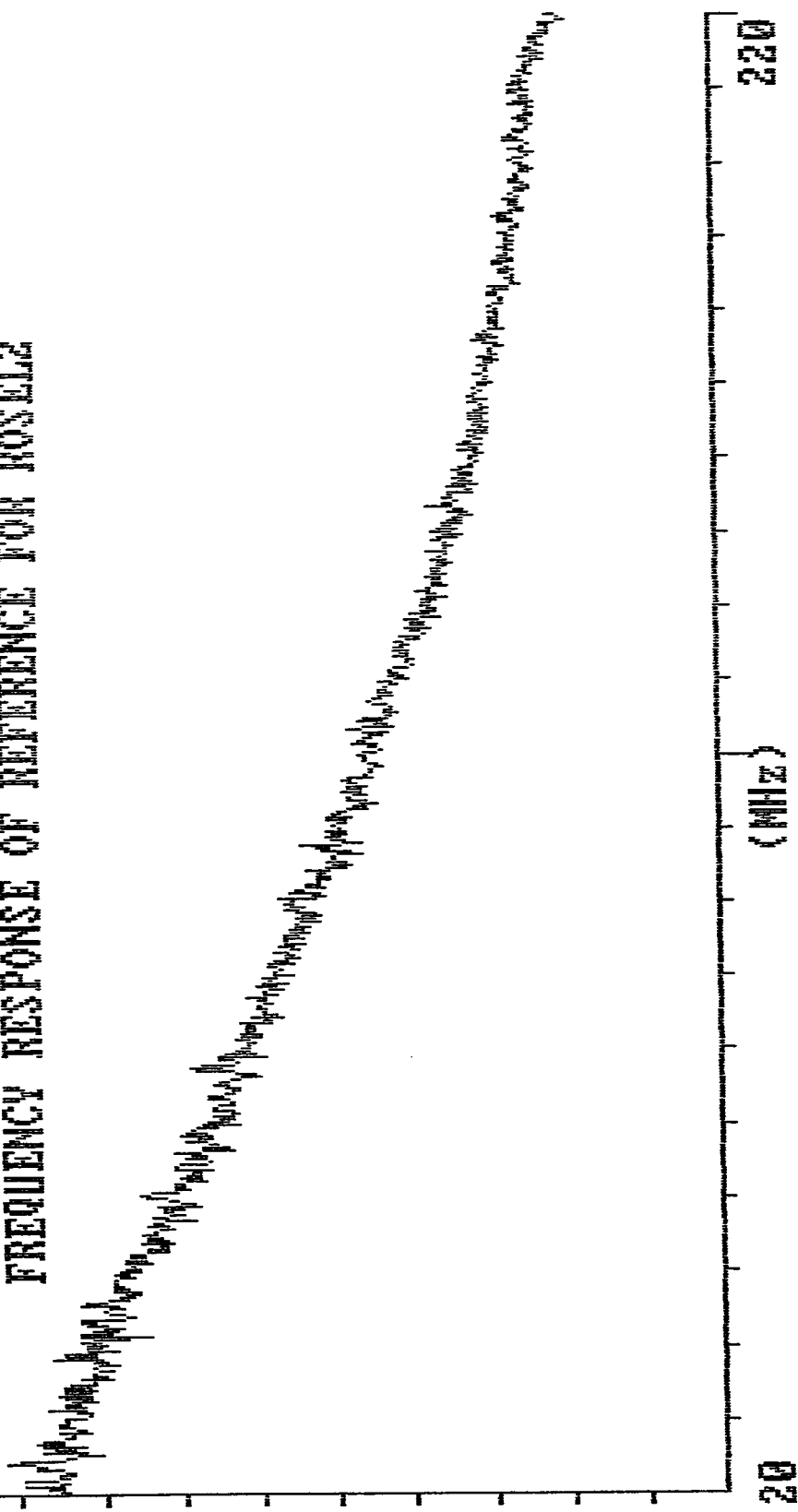


Fig. (4.4)

DEMODULATION FOR  
RB IN PURE ETHANOL

FILENAME: B:ROSET2

MODULATION  
DEPTH

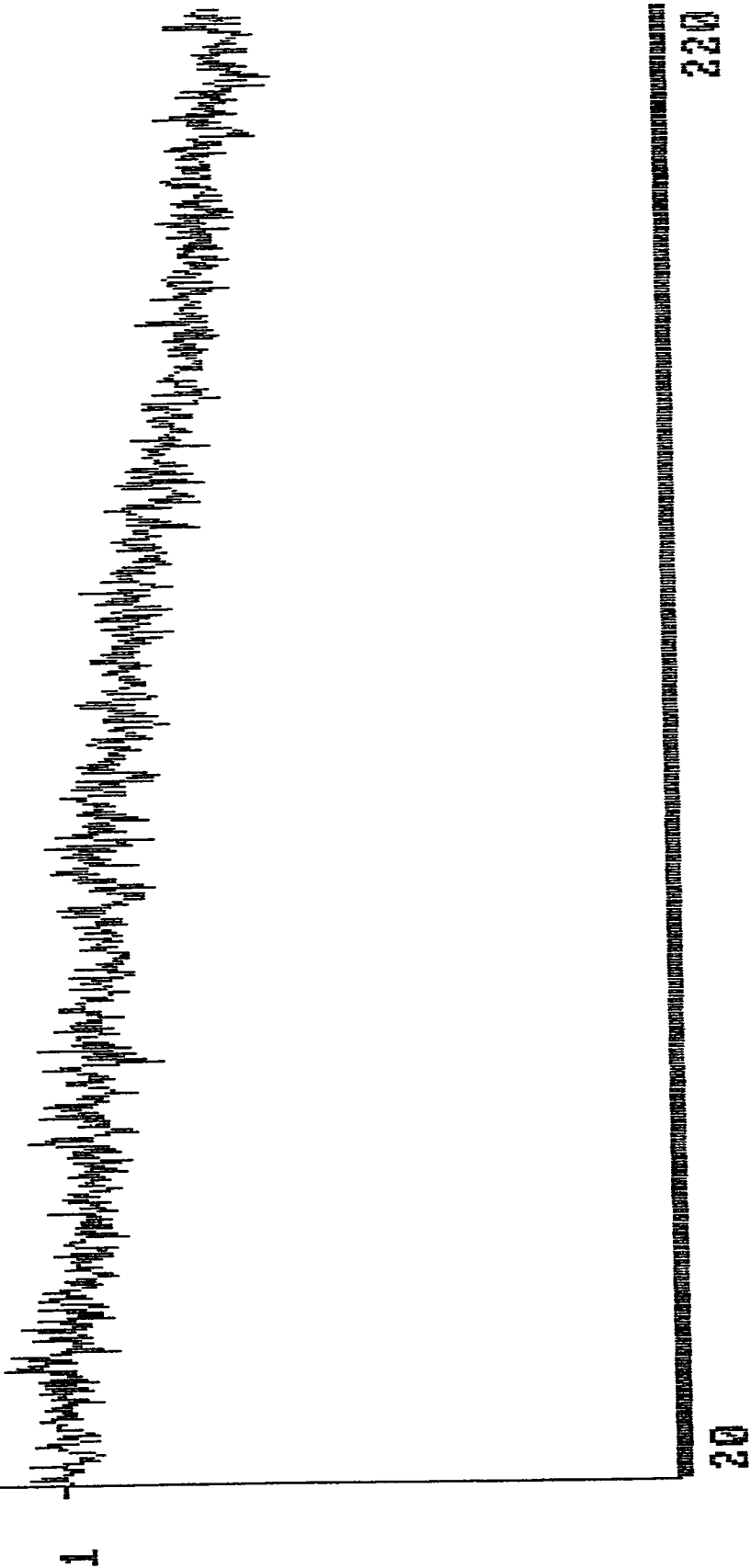


Fig. (4.5)

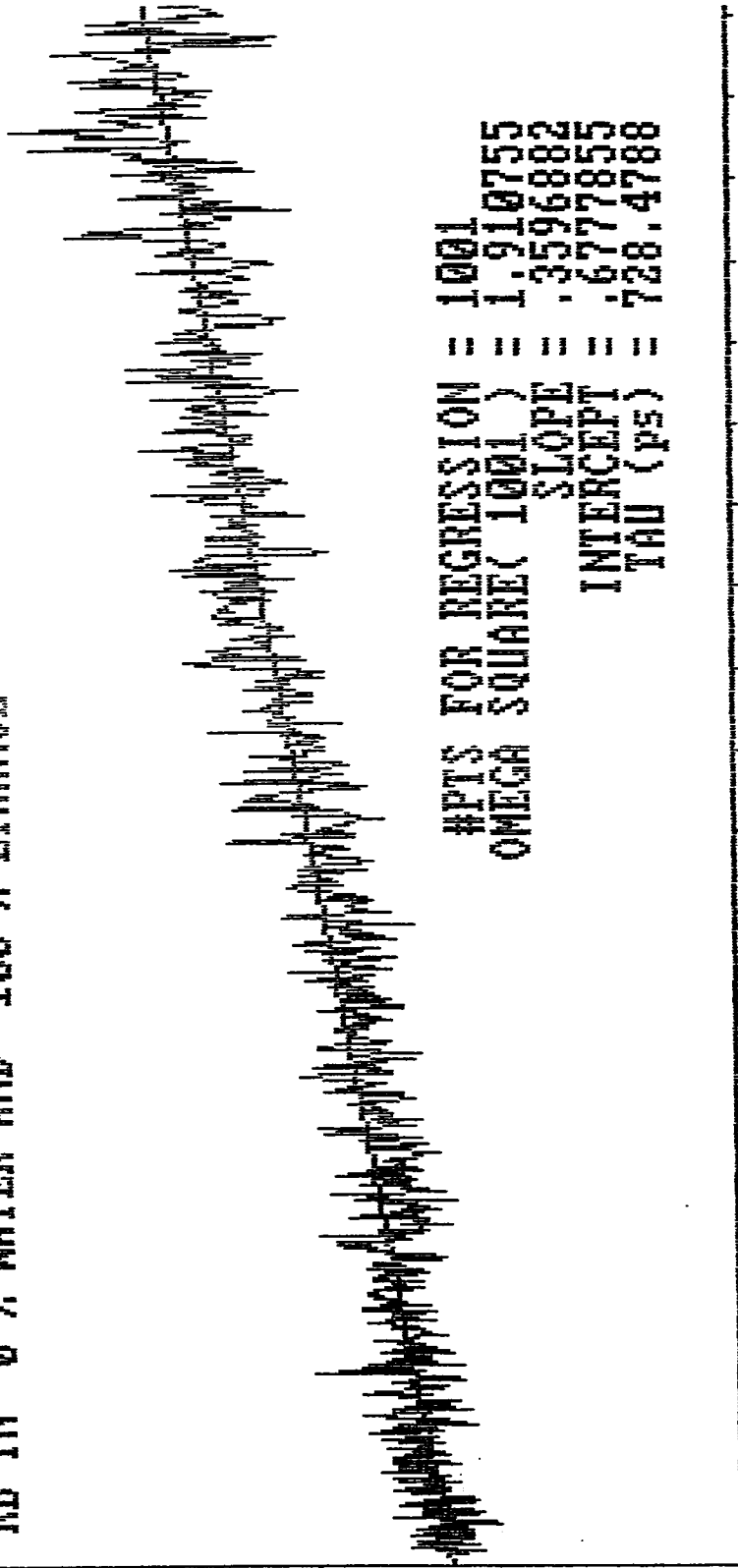
2.313712

ONE OVER BETA SQUARE

FILE NAME: B:ROSET2

FREQUENCY RANGE (MHZ): 20 - 220

RB IN 0 % WATER AND 100 % ETHANOL

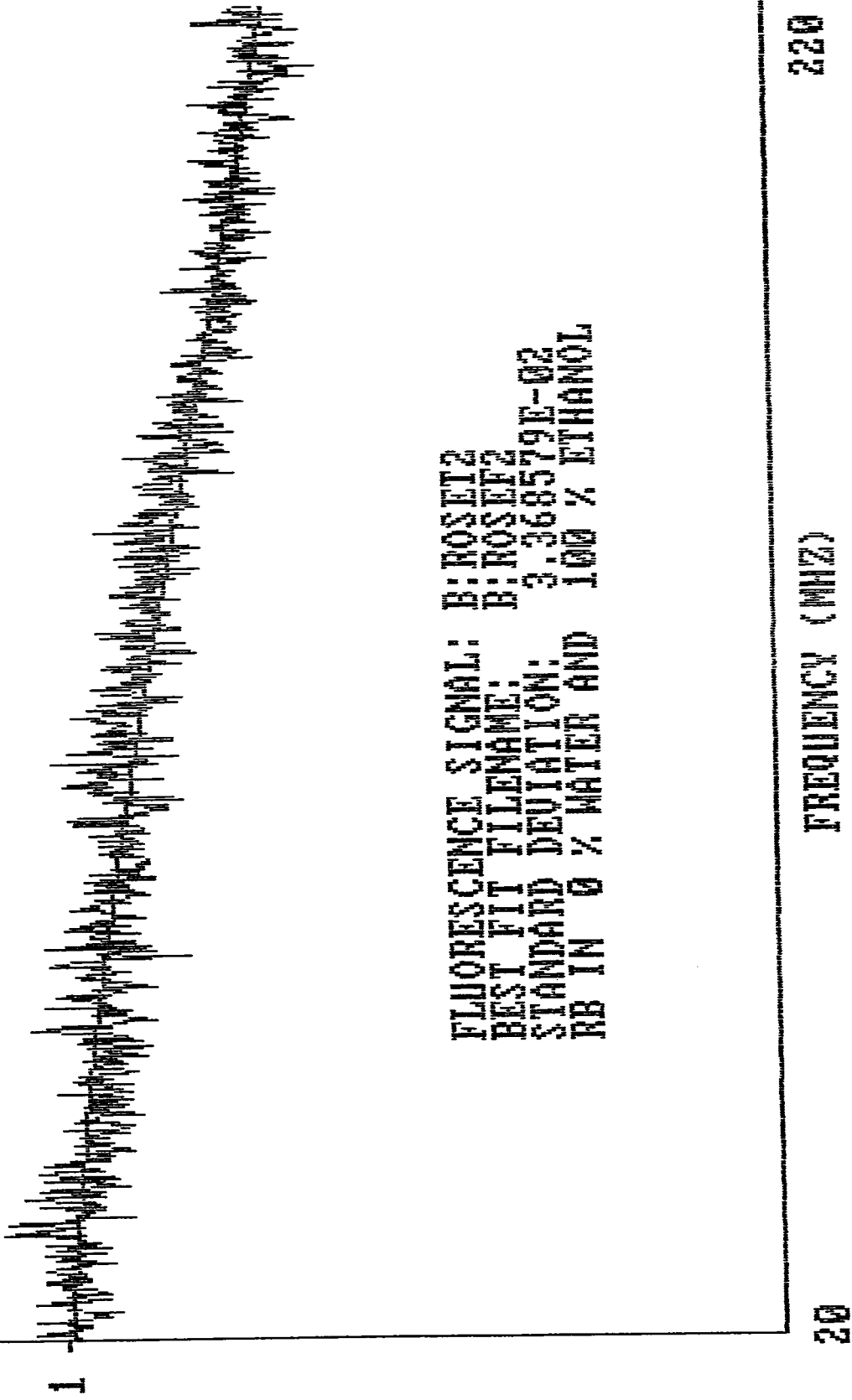


#PTS FOR REGRESSION = 1001  
 OMEGA SQUARE( 1001 ) = 1.910755  
 SLOPE = .3596882  
 INTERCEPT = .6777855  
 TAU (PS) = 728.4788

0 OMEGA SQUARE (GHZ \* GHZ) 1.910755

Fig. (4.6)

MODULATION  
DEPTH



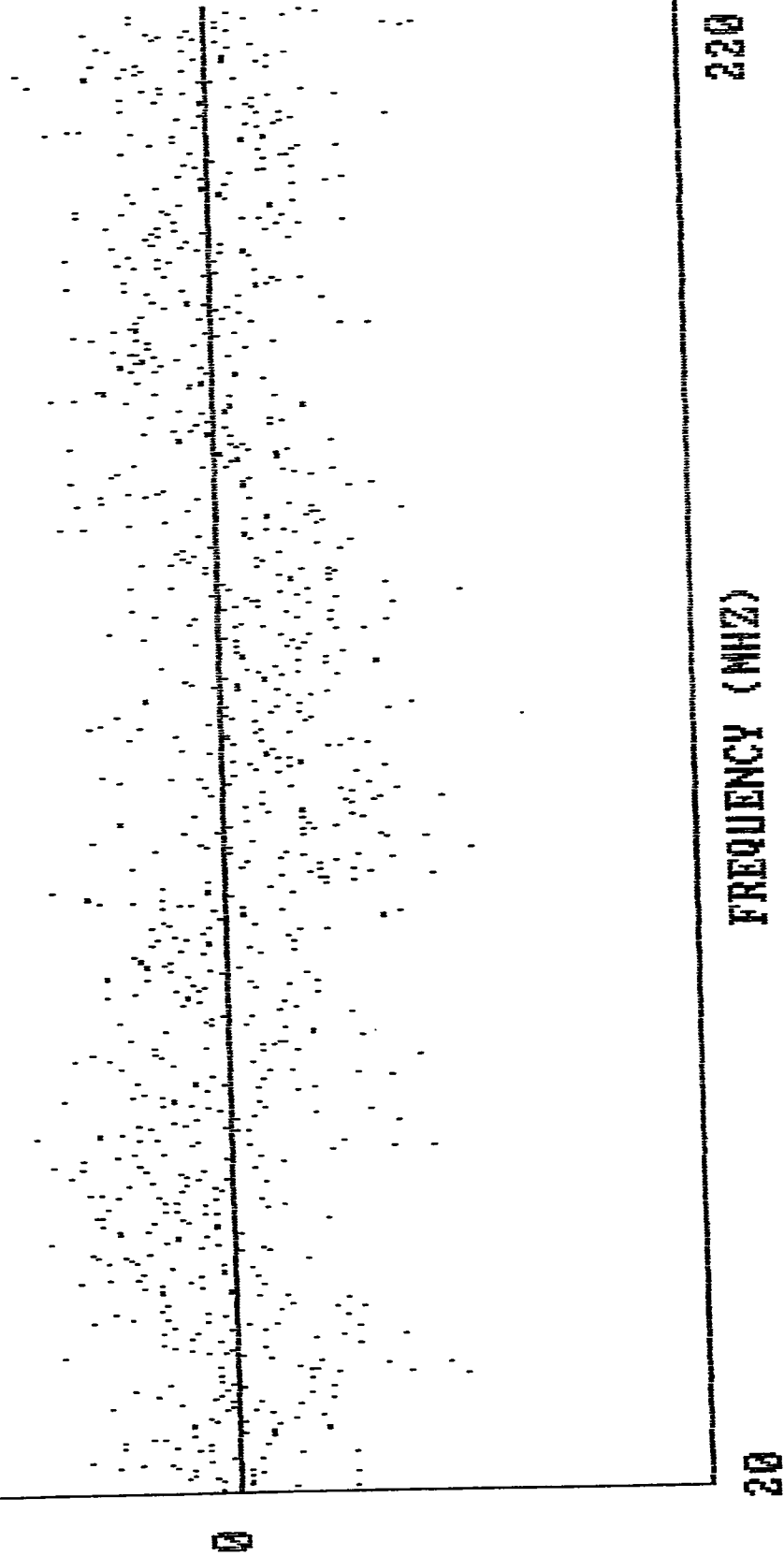
FLUORESCENCE SIGNAL: B:ROSET2  
BEST FIT FILENAME: B:ROSET2  
STANDARD DEVIATION: 3.368579E-02  
RB IN 0 % WATER AND 100 % ETHANOL

Fig. (4.7)

.4140902

RESIDUALS  
FLUORESCENCE SIGNAL: B:ROSET2  
BEST FIT FILENAME: B:ROSET2

RB IN. 0 % WATER AND 100 % ETHANOL



-.4140902

Fig. (4.8)

5. **Error Analysis:** In the two-parameter linear regression fit, the lifetime ( $\tau$ ) was related to the best fit slope ( $M$ ) and best fit vertical intercept ( $H$ ) by Eq. (4.4.11):

$$\tau = \sqrt{\frac{M}{H}}$$

Under complete matching in conditions of which the scattered light and the fluorescence are detected,  $\frac{1}{\xi^2} = H$  should be identically equal to unity. In this case the lifetime ( $\tau$ ) is the square root of the slope.

$$\tau = \sqrt{M} \quad (H = 1, \sigma_H = 0 \quad \text{under complete matching conditions})$$

In this case  $\frac{\sigma_\tau}{\tau} = \frac{1}{2} \frac{\sigma_M}{M}$ . In reality, there is a mismatch in conditions under which fluorescence and reference signals are detected; therefore,  $H \neq 1$ ,  $\sigma_H \neq 0$ . Instead, the relative uncertainty in the lifetime  $\frac{\sigma_\tau}{\tau}$  is:

$$\frac{\sigma_\tau}{\tau} = \frac{1}{2} \left( \frac{\sigma_M}{M} + \frac{\sigma_H}{H} \right) \quad (4.4.12)$$

where we have taken  $M$ , and  $H$  to be uncorrelated. Actually,  $M$ , and  $H$  are correlated, and Eq. (4.4.12) gives an upper limit to the relative uncertainty of the lifetime.

The values of  $\sigma_M$ , and  $\sigma_H$  are found from the two-parameter fit as follows [21]:

$$\sigma_H = \left( \frac{1}{D} \sum X_i^2 \right)^{1/2} \left( \frac{\sum \delta_i^2}{P-n} \right)^{1/2} \quad (4.4.13)$$

and

$$\delta_M = \left( \frac{P}{D} \right)^{1/2} \left( \frac{\sum \delta_i^2}{P-n} \right)^{1/2} \quad (4.4.14)$$

where  $P, D$ , and  $X_i$  have been defined (Eq. (4.4.6 – 4.4.9)),  $n$  is the number of parameters ( $n = 2$  for a two-parameter fit), and  $\delta_i$  is the difference between the measured value  $Y_i$  and the best fitted value of  $Y$  at the  $i$ -th point.

In all our calculations, we are taking the weights of our measurements to be equal to unity.

As a result,  $\tau, M, H, \sigma_M, \sigma_H$  are known. Substituting in Eq. (4.4.12), a value for the absolute uncertainty in lifetime  $\sigma_\tau$  may now be found.

In addition, since  $\tau = \frac{1}{\lambda}$ ,

$$\frac{\sigma_\tau}{\tau} = \frac{\sigma_\lambda}{\lambda} \quad (4.4.15)$$

$\tau, \lambda$ , and  $\sigma_\tau$  are known, and the absolute uncertainty in decay rate can be calculated.

In the specific example of  $1.0 * 10^{-5} M$  RB in pure ethanol

$$M = 0.3597(\text{GHz})^{-2}, \quad H = 0.6778$$

$$\sigma_M = 3.84 * 10^{-3} (\text{GHz})^{-2}, \quad \sigma_H = 4.28 * 10^{-3}$$

Therefore

$$\tau = \sqrt{\frac{M}{H}} = 728.5 \text{ ps}, \quad \sigma_\tau = 6.2 \text{ ps}$$

$$\lambda = \frac{1}{\tau} = 1.373 \text{ GHz}, \quad \sigma_\lambda = 1.2 * 10^{-2} \text{ GHz}$$

## B) The Fluorescence Lifetime of Rose Bengal in Water-Ethanol Mixture:

The same procedure of data acquiring, proper subtraction, linearization, dividing sample signal by reference signal, and finally making a two-parameter best fit to get a value for the fluorescence lifetime from the slope and vertical intercept is done with other samples of Rose Bengal in water-ethanol mixtures. For every sample there must be a reference with which the signal is to be compared. The linearized data is shown in Appendix (I.B).

Figures (4.9 - 4.35) show the results of linear regression with the value of the slope, vertical intercept and lifetimes. The samples were  $5 * 10^{-5}$  M *RB* in water-ethanol mixtures. The percentage of water was 0, 12.5, 25, 40, 50, 60, 75, 87.5, and 100% by volume respectively. The figures show how well the linear regression fits the demodulation data and show the distribution of residuals as a function of frequency for the different samples.

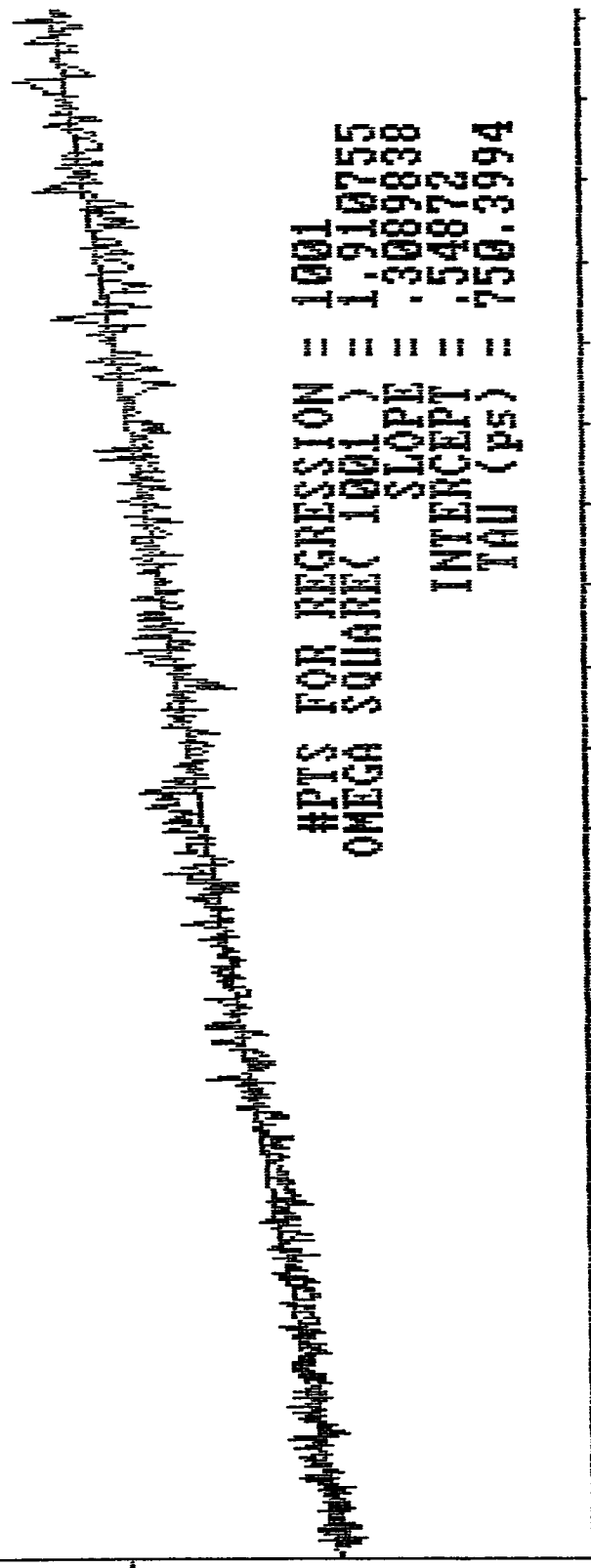
2.132401

ONE OVER BETA SQUARE

FILE NAME: B:RBT0001

FREQUENCY RANGE (MHZ): 20 - 220

RB IN 0 % WATER AND 100 % ETHANOL



OMEGA SQUARE (GHZ \* GHZ)

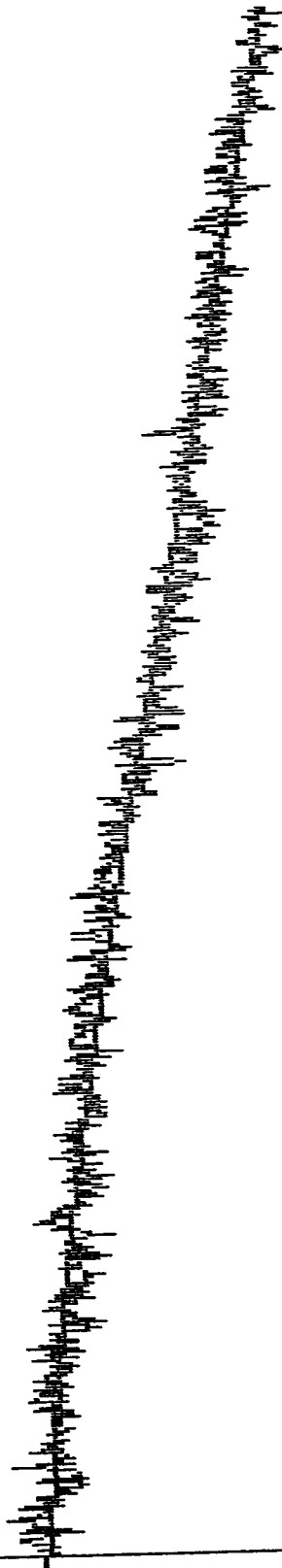
1.910755

0

Fig. (4.9)

MODULATION  
DEPTH

1



FLUORESCENCE SIGNAL: B:RBTF0001  
BEST FIT FILENAME: B:RBTF0001  
STANDARD DEVIATION: 1.786066E-02  
RB IN 0 % WATER AND 100 % ETHANOL

220

FREQUENCY (MHZ)

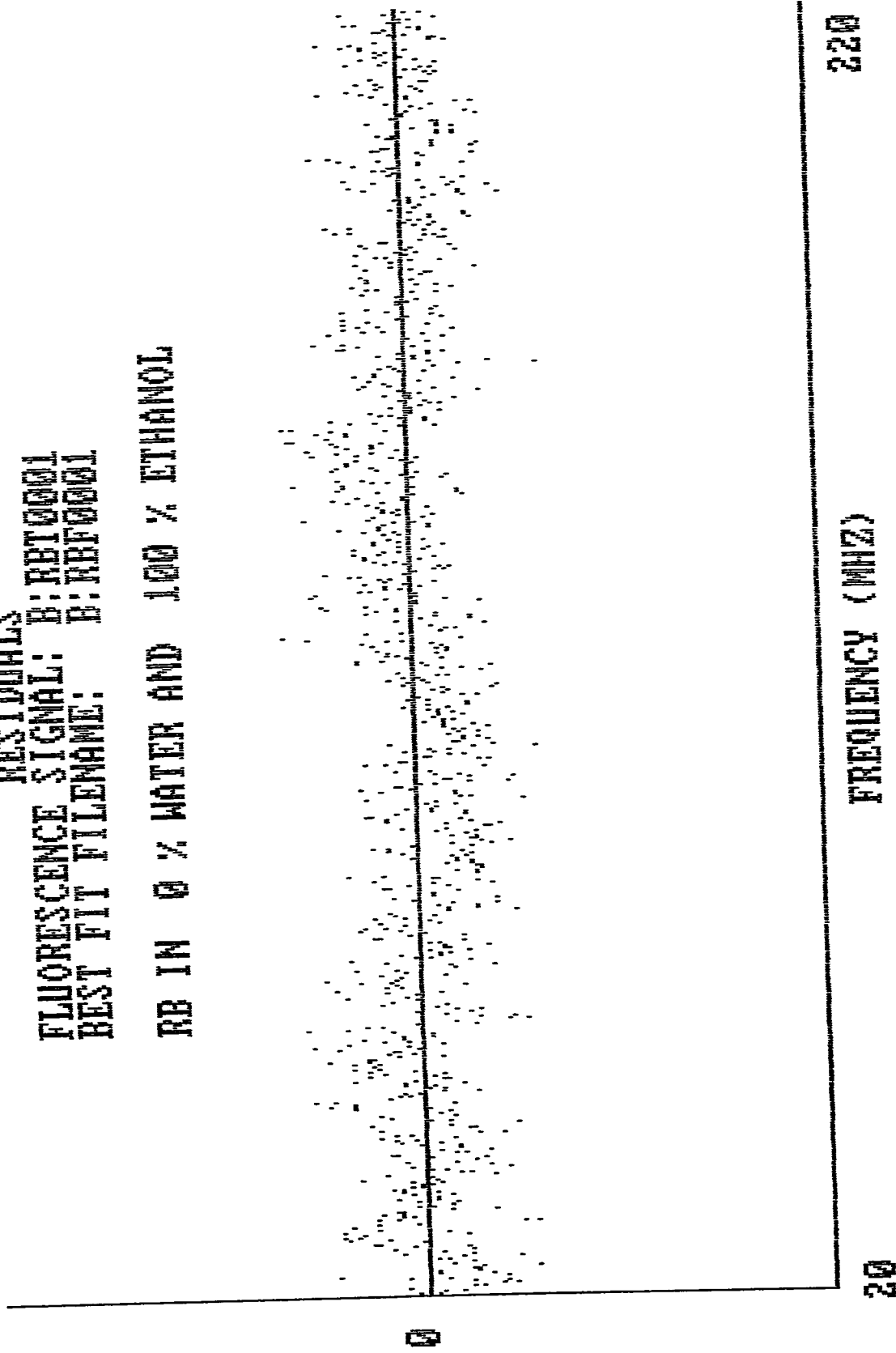
20

Fig. (4.10)

.3540074

RESIDUALS  
FLUORESCENCE SIGNAL: B:RBTF0001  
BEST FIT FILENAME: B:RBTF0001

RB IN 0 % WATER AND 100 % ETHANOL



-.3540074

Fig. (4.11)

5.656574

ONE OVER BETA SQUARE

FILE NAME: B:RBT0131

FREQUENCY RANGE (MHZ): 50 - 550

RB IN 12.5 % WATER AND 87.5 % ETHANOL

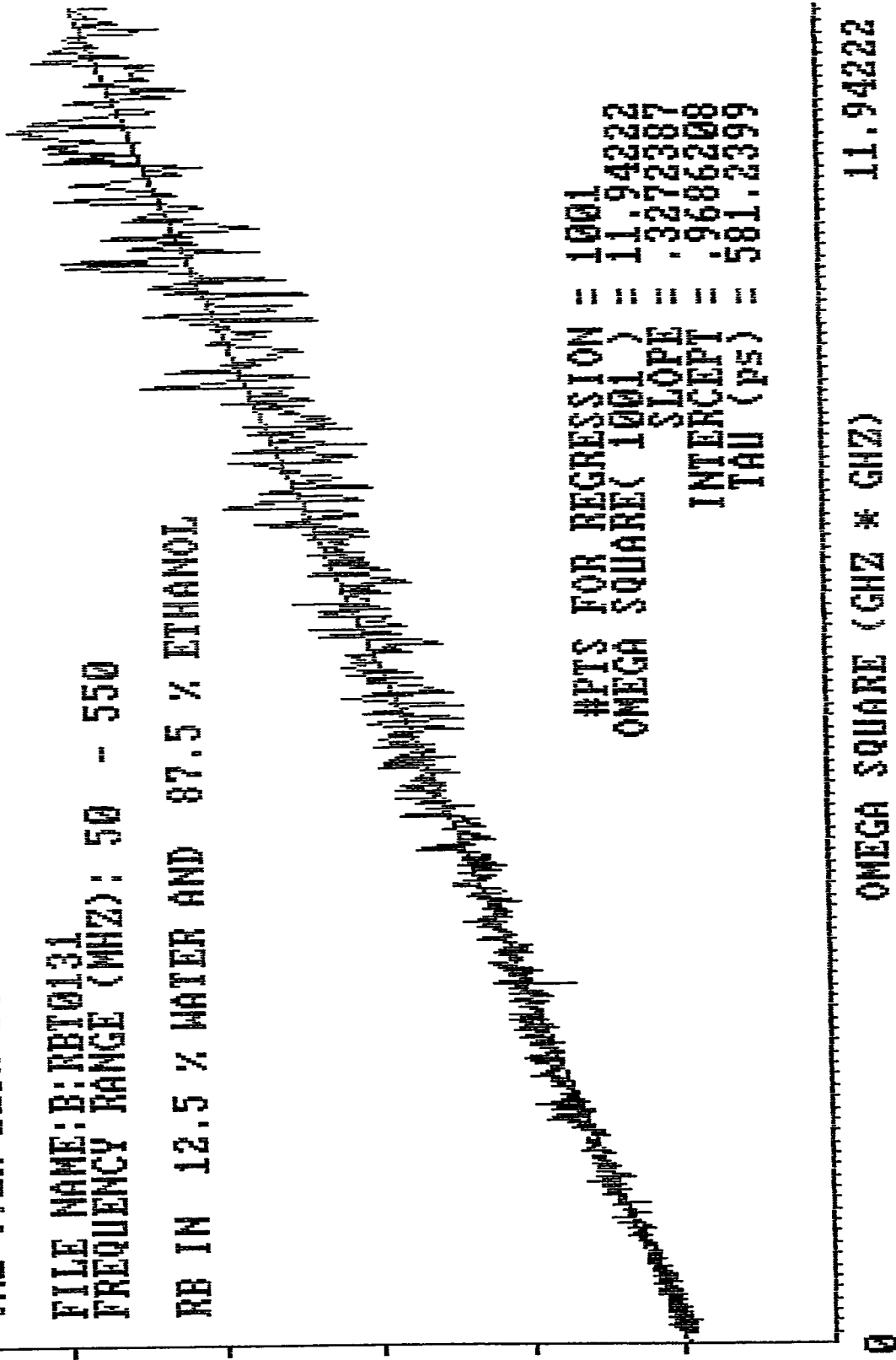
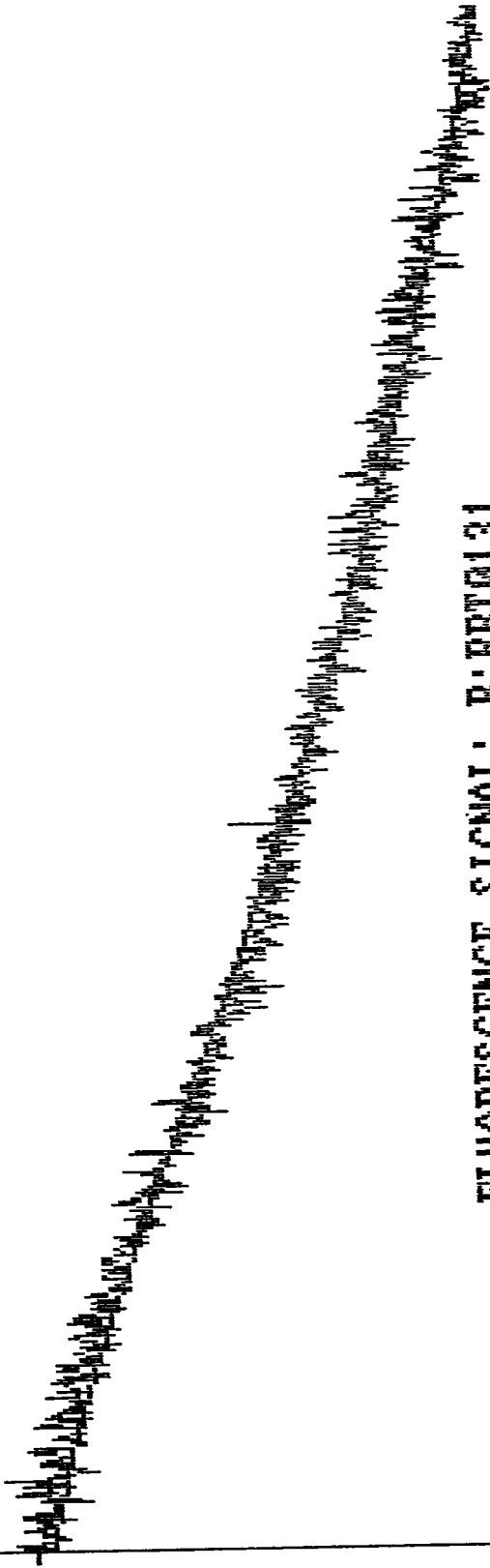


Fig. (4.12)

MODULATION  
DEPTH

1



FLUORESCENCE SIGNAL: B:RBFB0131  
BEST FIT FILENAME: B:RBFB0131  
STANDARD DEVIATION: 0.728543  
RB IN 12.5 % WATER AND 87.5 % ETHANOL

50

FREQUENCY (MHZ)

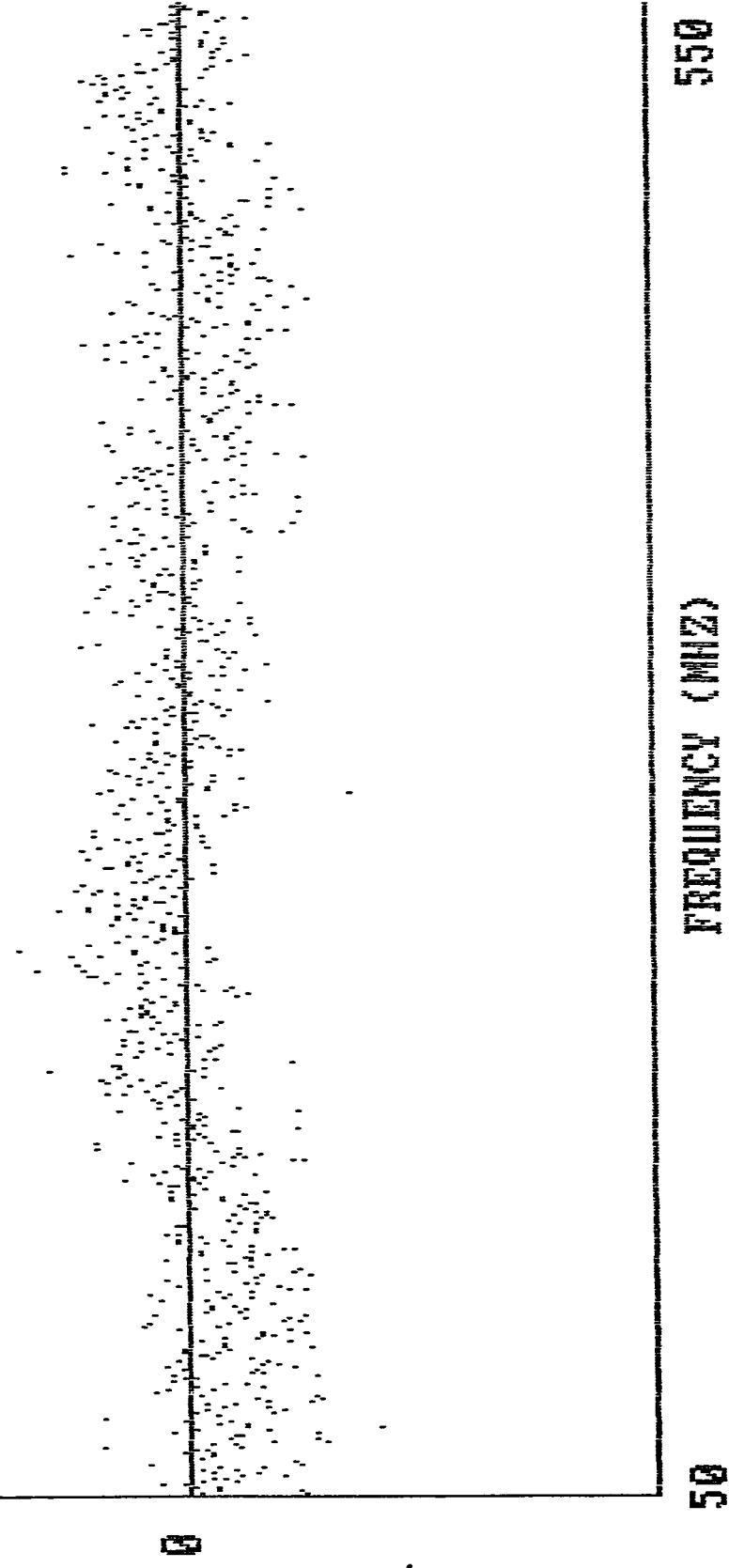
550

Fig. (4.13)

.360981

RESIDUALS  
FLUORESCENCE SIGNAL: B:RBFO131  
BEST FIT FILENAME: B:RBFO131

RB IN 12.5 % WATER AND 87.5 % ETHANOL



.360981

4.264371

ONE OVER BETA SQUARE

FILE NAME: B:RB10251  
FREQUENCY RANGE (MHZ): 50 - 550

RB IN 25 % WATER AND 75 % ETHANOL

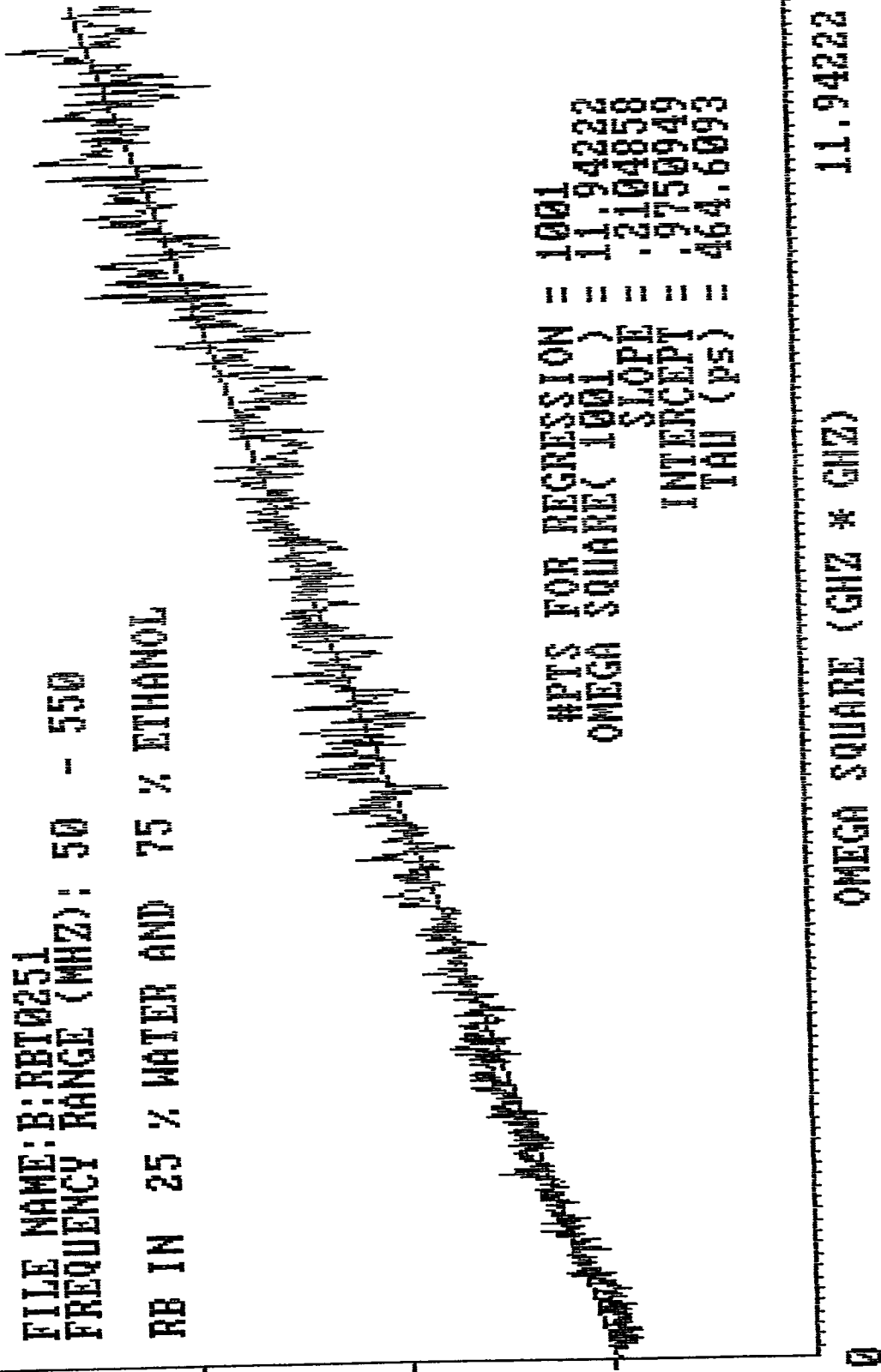
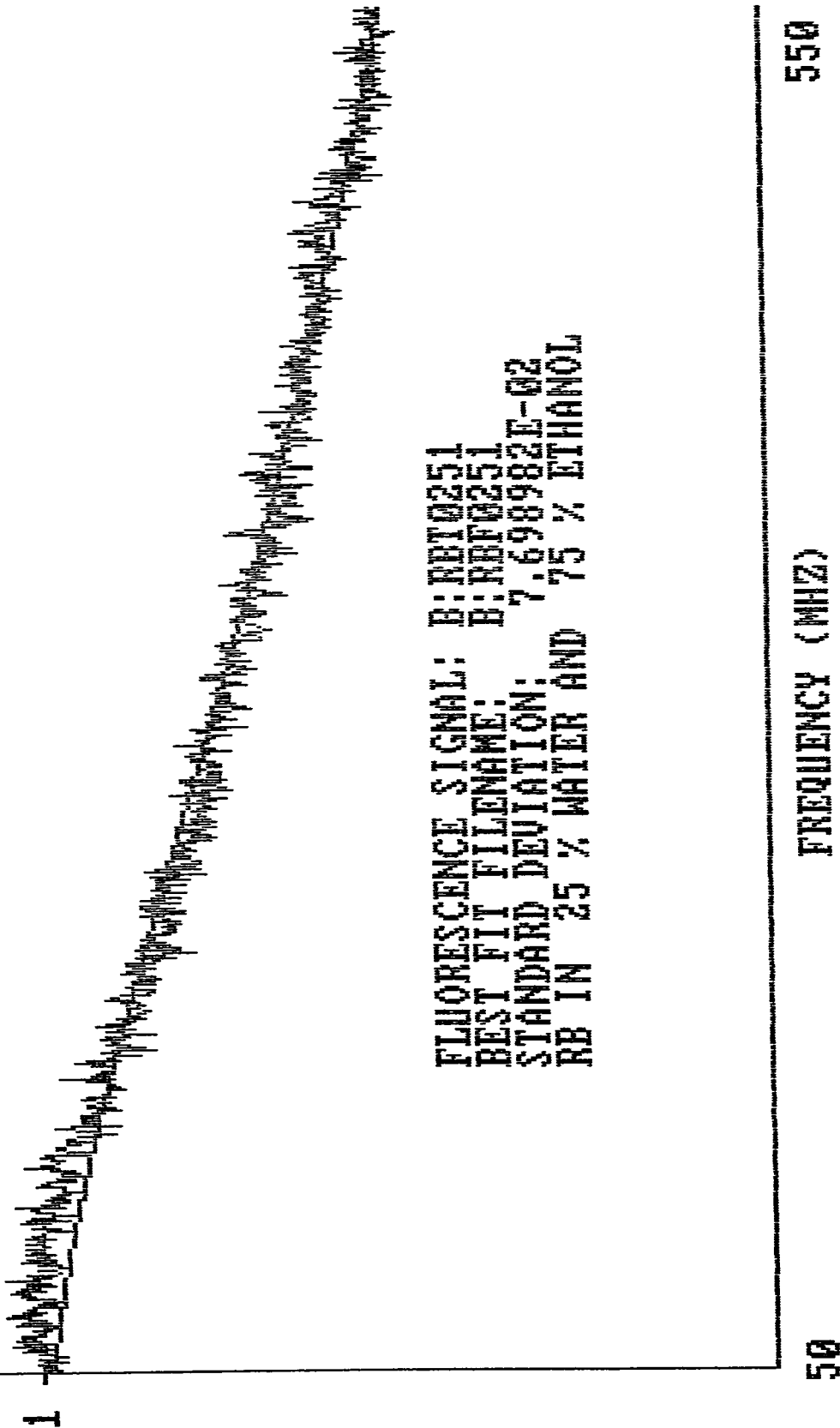


Fig. (4.15)

MODULATION  
DEPTH



FLUORESCENCE SIGNAL: B:NBFO251  
BEST FIT FILENAME: B:NBFO251  
STANDARD DEVIATION: 7.698982E-02  
RB IN 25 % WATER AND 75 % ETHANOL

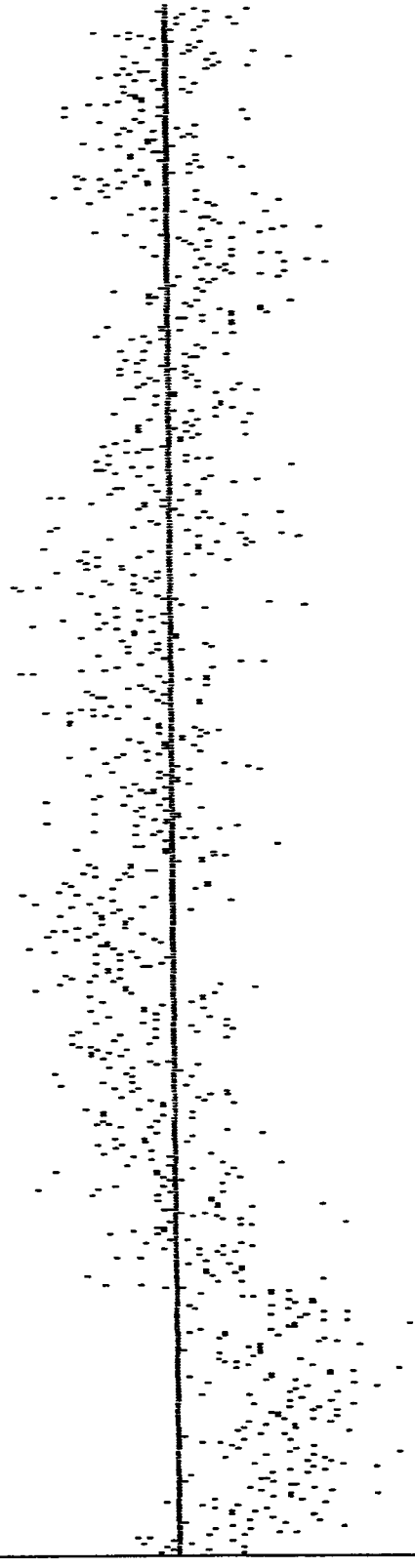
Fig. (4.16)

.3658229

RESIDUALS  
FLUORESCENCE SIGNAL: B:RBT0251  
BEST FIT FILENAME: B:RBF0251

RB IN 25 % WATER AND 75 % ETHANOL

0



-.3658229

50

FREQUENCY (MHZ)

550

Fig. (4.17)

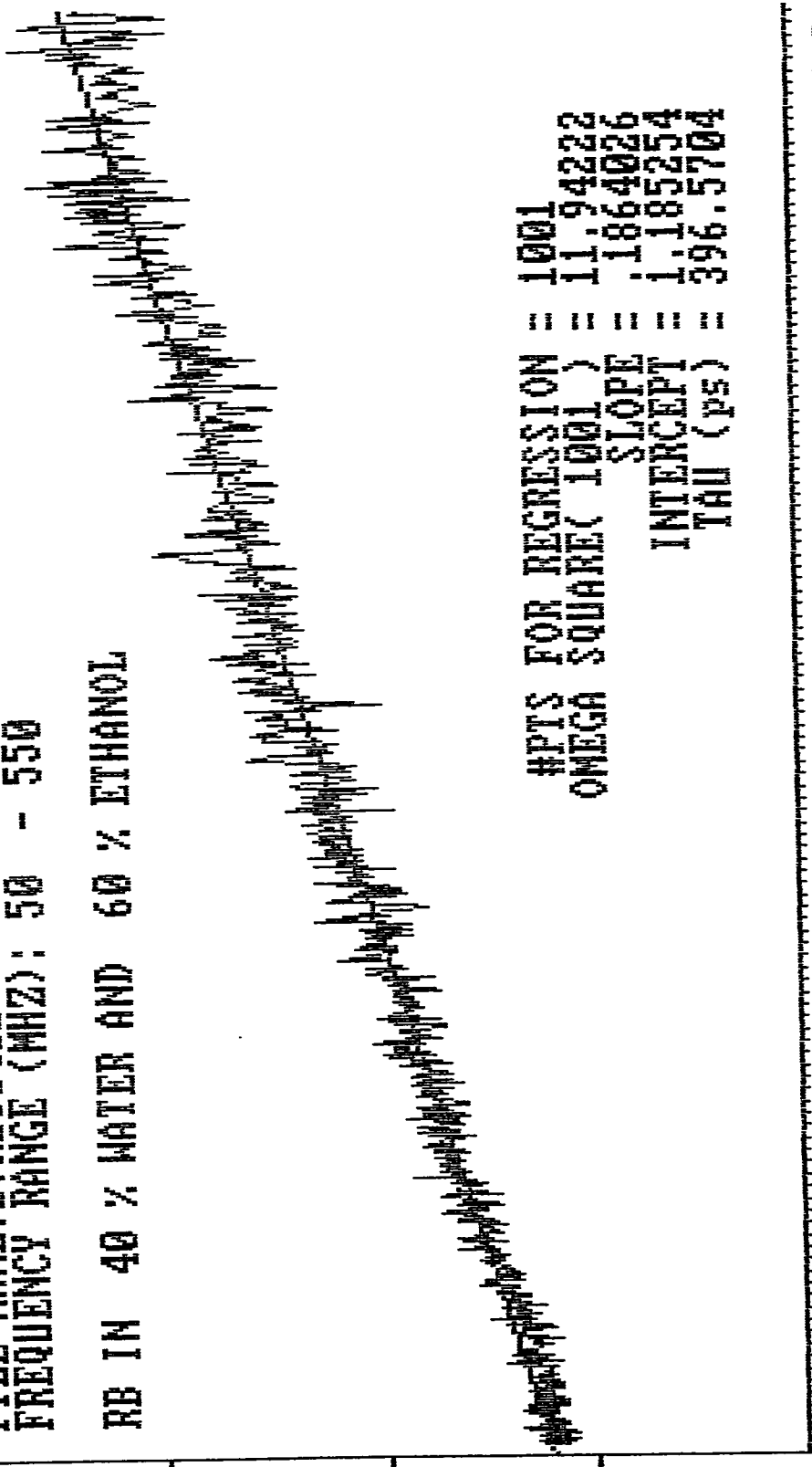
4.331708

ONE OVER BETA SQUARE

FILE NAME: B:NB10401

FREQUENCY RANGE (MHZ): 50 - 550

RB IN 40 % WATER AND 60 % ETHANOL



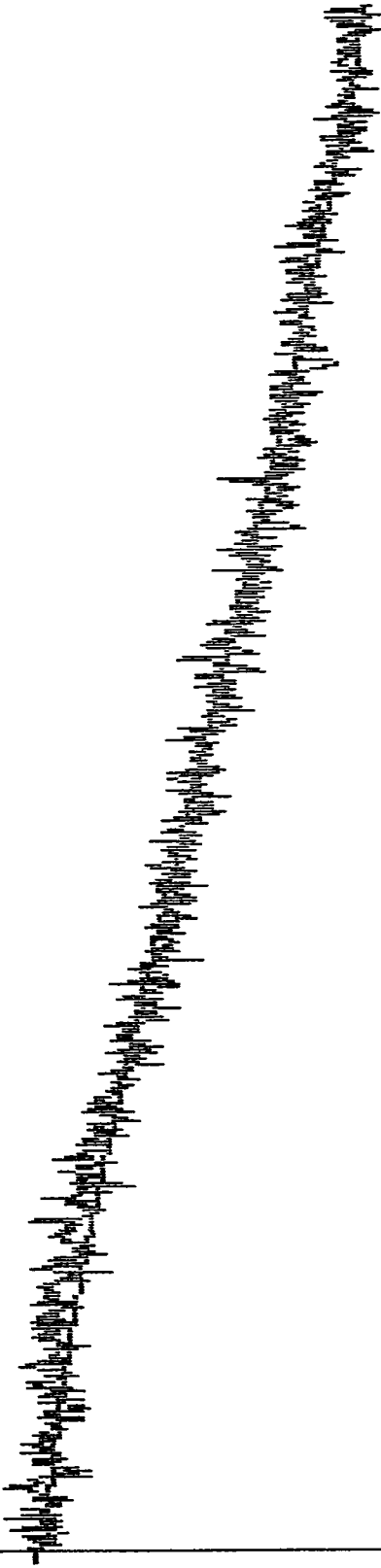
#PTS FOR REGRESSION = 1001  
OMEGA SQUARE( 1001 ) = 11.94222  
SLOPE = .1864026  
INTERCEPT = 1.185254  
TAU (ps) = 396.5704

OMEGA SQUARE (GHZ \* GHZ) 11.94222

Fig. (4.18)

MODULATION  
DEPTH

1



FLUORESCENCE SIGNAL: B:RBFD401  
BEST FIT FILENAME: B:RBFD401  
STANDARD DEVIATION: 7.971616E-02  
RB IN 40 % WATER AND 60 % ETHANOL

50

FREQUENCY (MHZ)

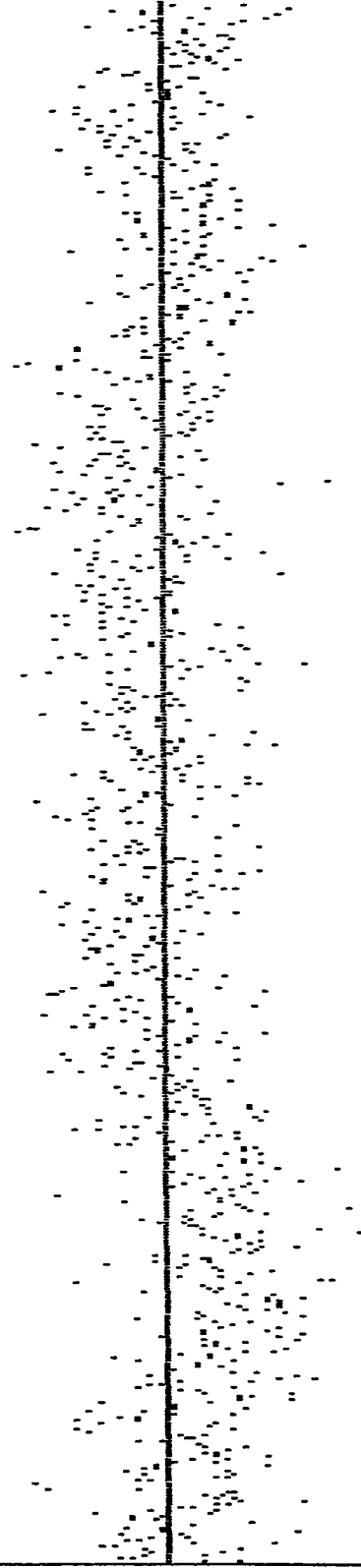
550

Fig. (4.19)

.3584015

RESIDUALS  
FLUORESCENCE SIGNAL: B:RBT0401  
BEST FIT FILENAME: B:RBF0401

RB IN 40 % WATER AND 60 % ETHANOL



-.3584015

FREQUENCY (MHZ)

550

50

Fig. (4.20)

2.851398

ONE OVER BETA SQUARE

FILE NAME: A:RBT0501  
FREQUENCY RANGE (MHZ): 50 - 550

RB IN 50 % WATER AND 50 % ETHANOL

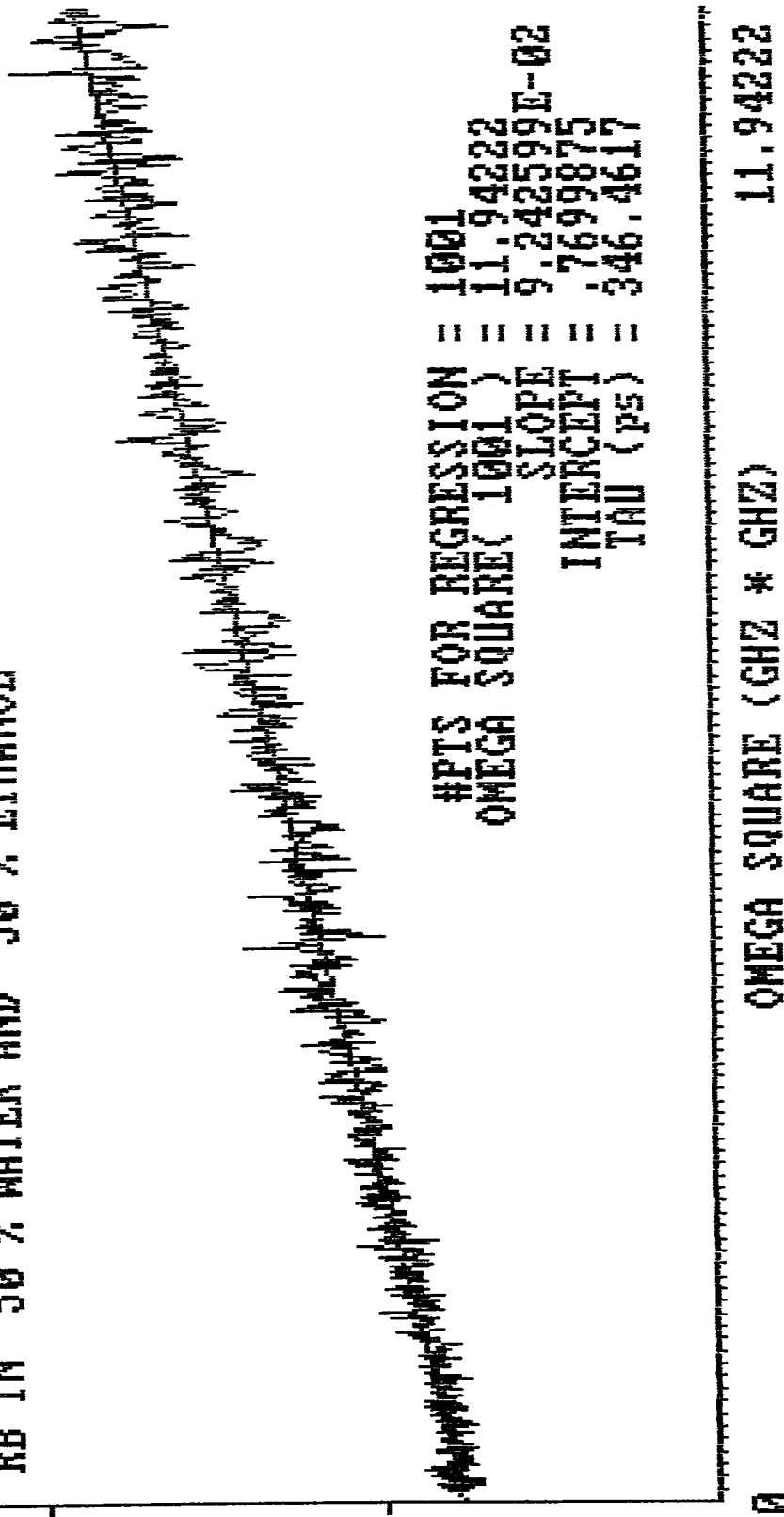
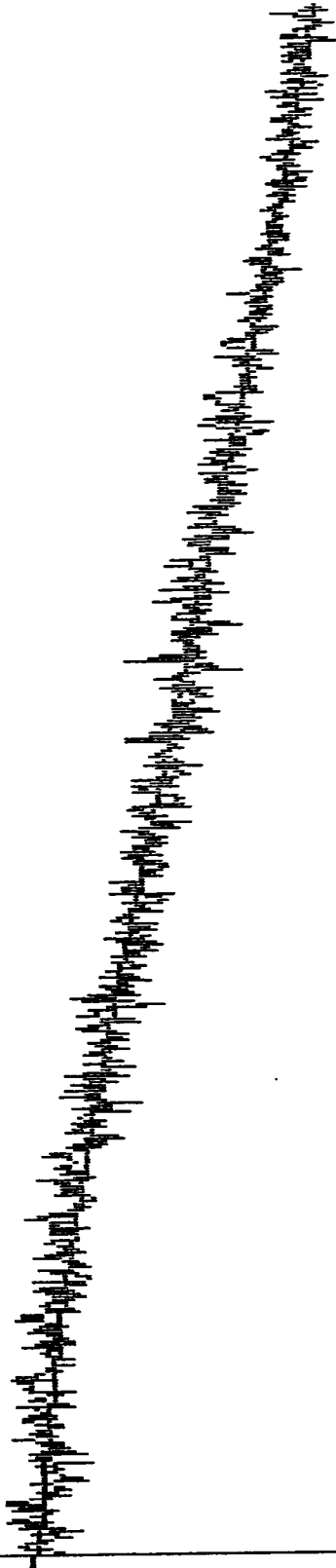


Fig. (4.21)

MODULATION  
DEPTH

1



FLUORESCENCE SIGNAL: B: RBT0501  
BEST FIT FILENAME: B: RBF0501  
STANDARD DEVIATION: 8.212615E-02  
RB IN 50 % WATER AND 50 % ETHANOL

50

FREQUENCY (MHZ)

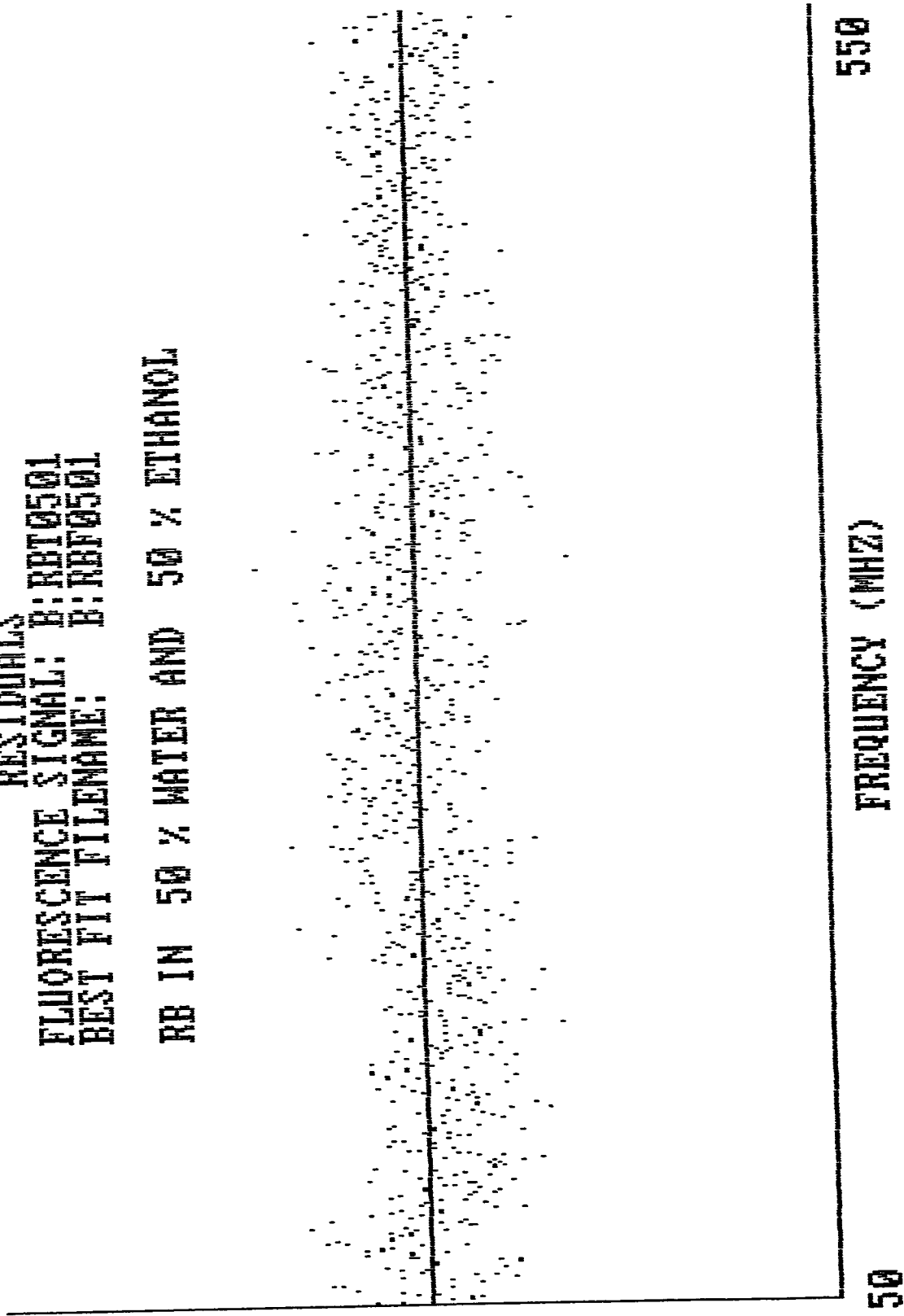
550

Fig. (4.22)

.3688083

RESIDUALS  
FLUORESCENCE SIGNAL: B:RRT0501  
BEST FIT FILENAME: B:RRT0501

RB IN 50 % WATER AND 50 % ETHANOL



-.3688083

Fig. (4.23)

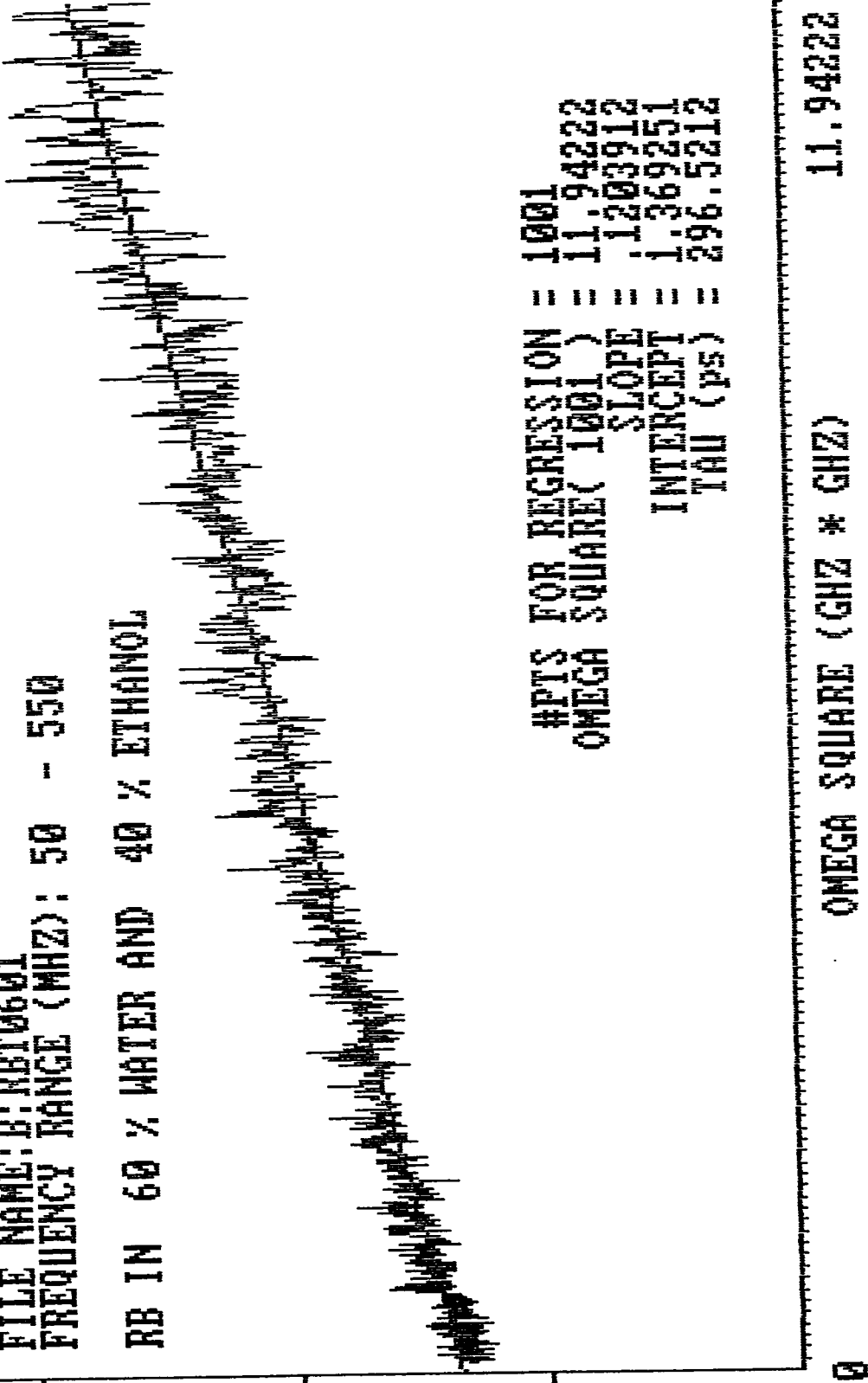
3.503044

ONE OVER BETA SQUARE

FILE NAME: B:RBT0601

FREQUENCY RANGE (MHZ): 50 - 550

RB IN 60 % WATER AND 40 % ETHANOL

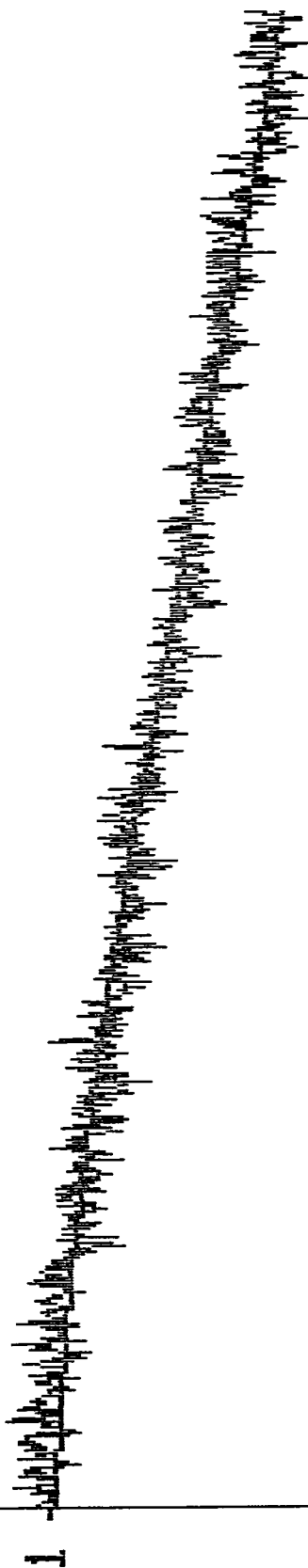


#PTS FOR REGRESSION = 1001  
 OMEGA SQUARE( 1001 ) = 11.94222  
                   SLOPE = 1.203912  
                   INTERCEPT = 1.369251  
                   TAU (ps) = 296.5212

OMEGA SQUARE (GHZ \* GHZ)                    11.94222

Fig. (4.24)

MODULATION  
DEPTH



FLUORESCENCE SIGNAL: B:RBTF0601  
BEST FIT FILENAME: B:RBTF0601  
STANDARD DEVIATION: 8.496508E-02  
RB IN 60 % WATER AND 40 % ETHANOL

550

FREQUENCY (MHZ)

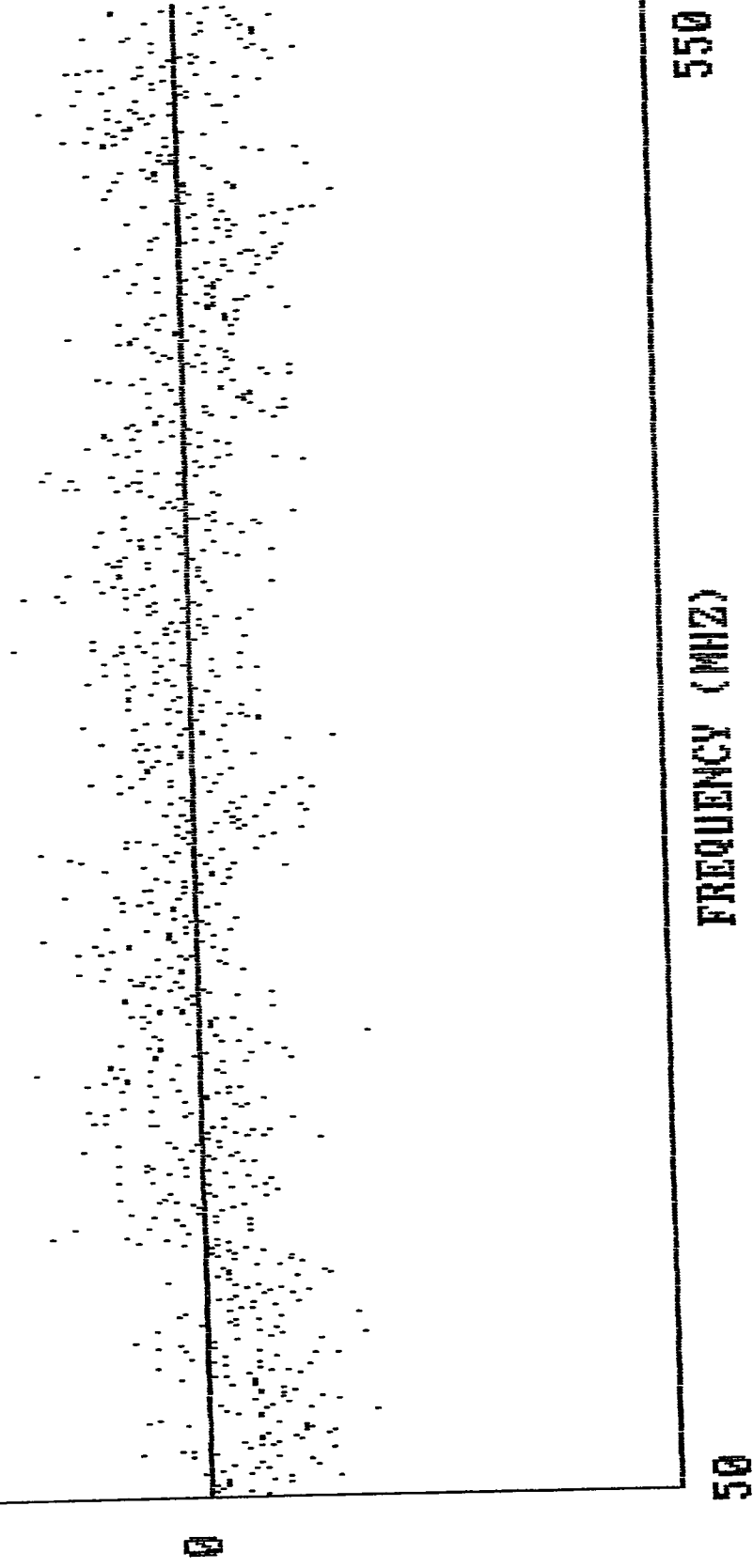
50

Fig. (4.25)

.3682264

RESIDUALS  
FLUORESCENCE SIGNAL: B:RBT0601  
BEST FIT FILENAME: B:RBT0601

RB IN 60 % WATER AND 40 % ETHANOL



-.3682264

Fig. (4.26)

3.055889

ONE OVER BETA SQUARE

FILE NAME: B:RBT07512  
FREQUENCY RANGE (MHZ): 50 - 550

RB IN 75 % WATER AND 25 % ETHANOL

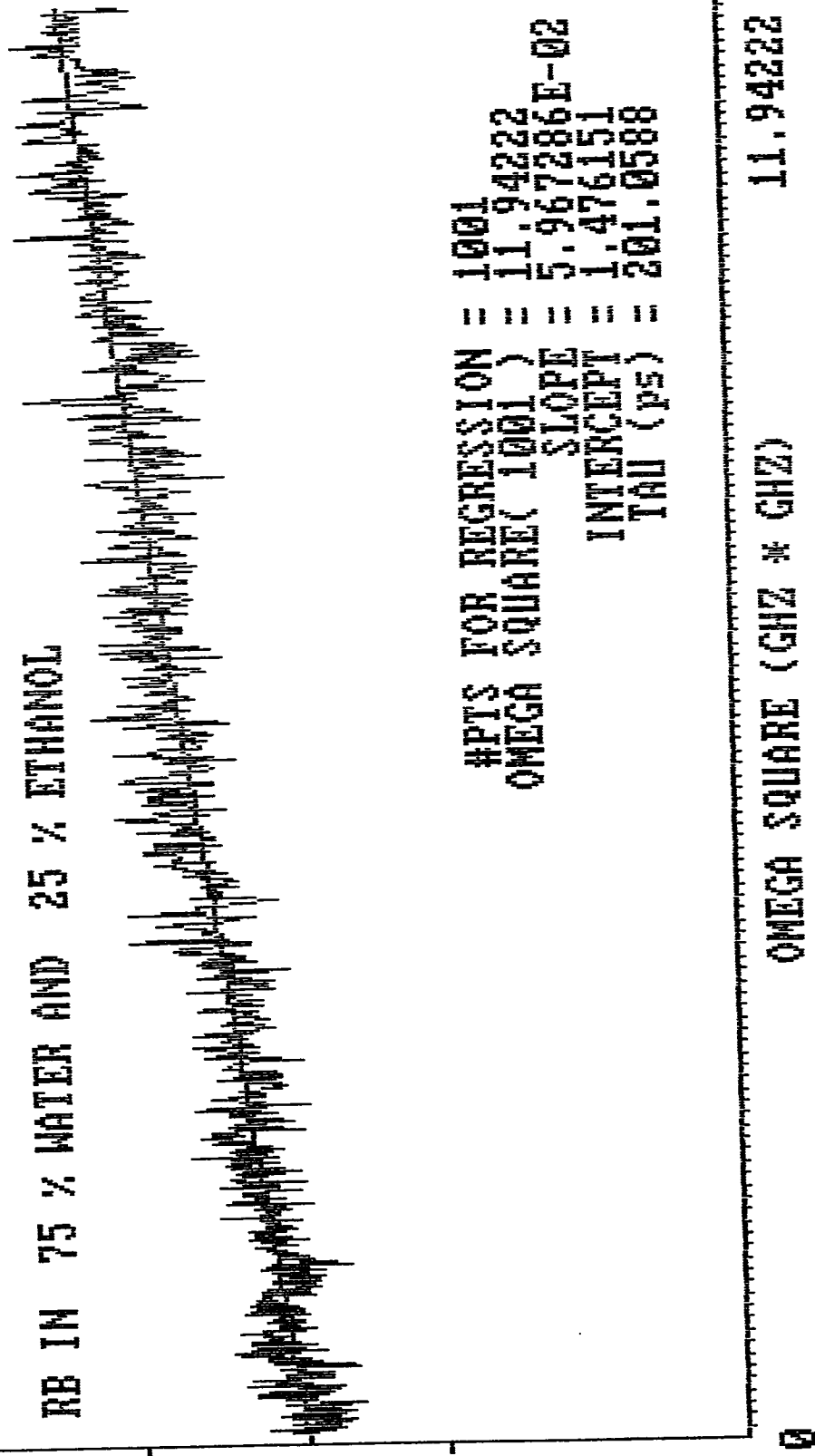
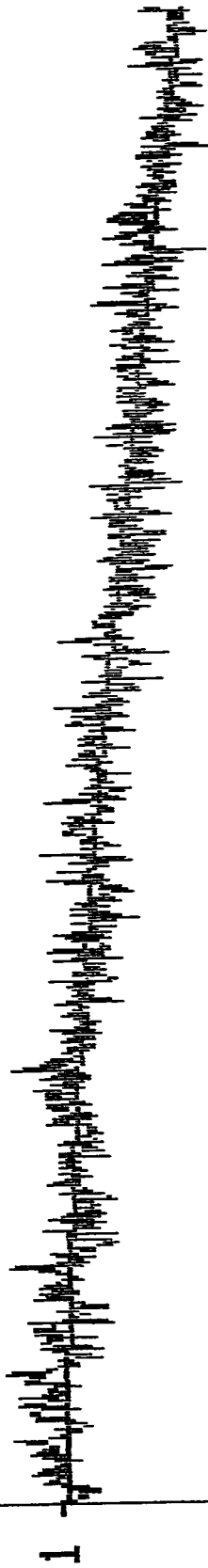


Fig. (4.27)

MODULATION  
DEPTH



FLUORESCENCE SIGNAL: B: RBT07512  
BEST FIT FILENAME: B: RBF07512  
STANDARD DEVIATION: .0881649  
RB IN 75 % WATER AND 25 % ETHANOL

50

FREQUENCY (MHZ)

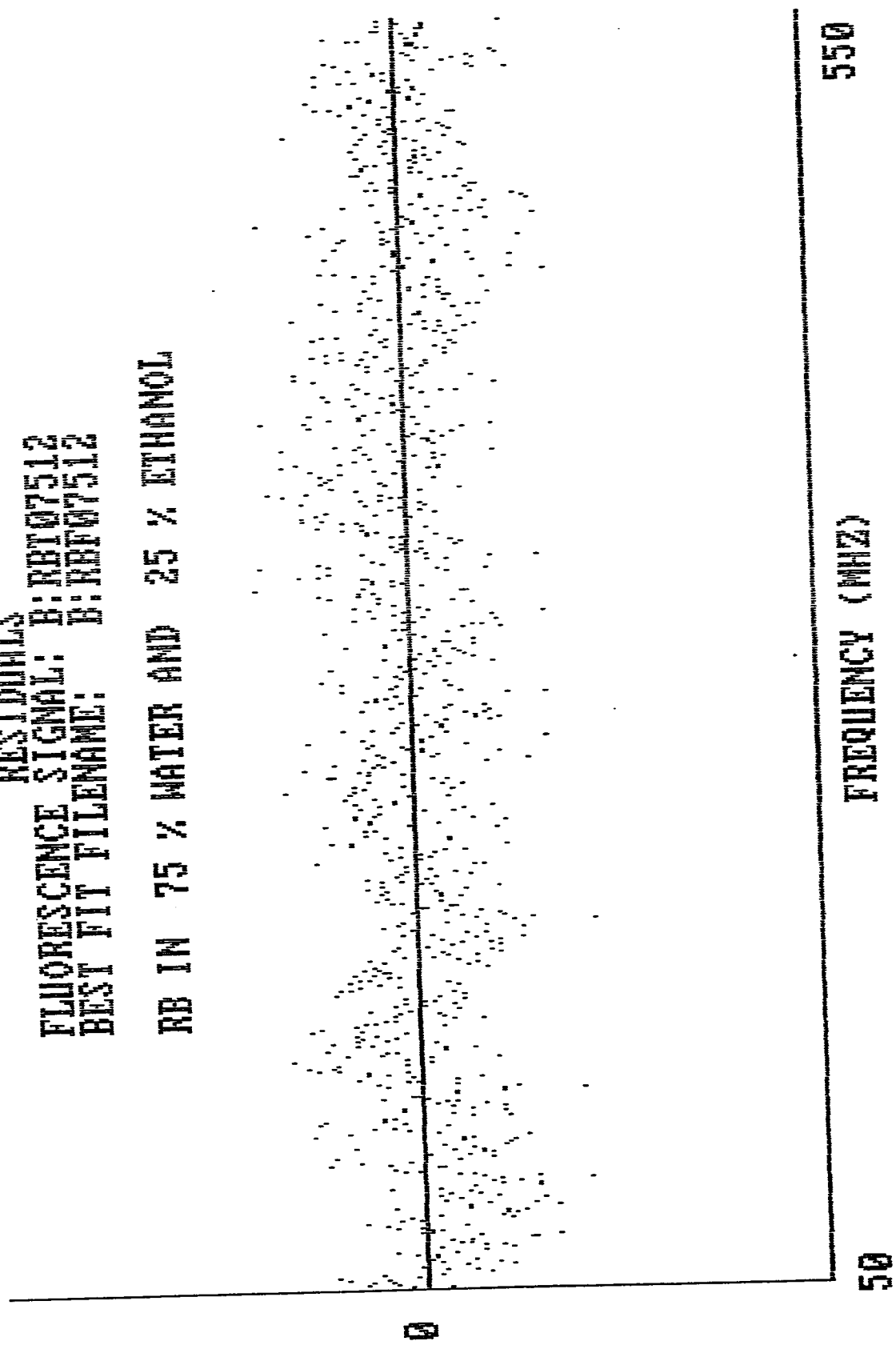
550

Fig. (4.28)

.3670329

RESIDUALS  
FLUORESCENCE SIGNAL: B:RBT07512  
BEST FIT FILENAME: B:RFF07512

RB IN 75 % WATER AND 25 % ETHANOL



-.3670329

Fig. (4.29)

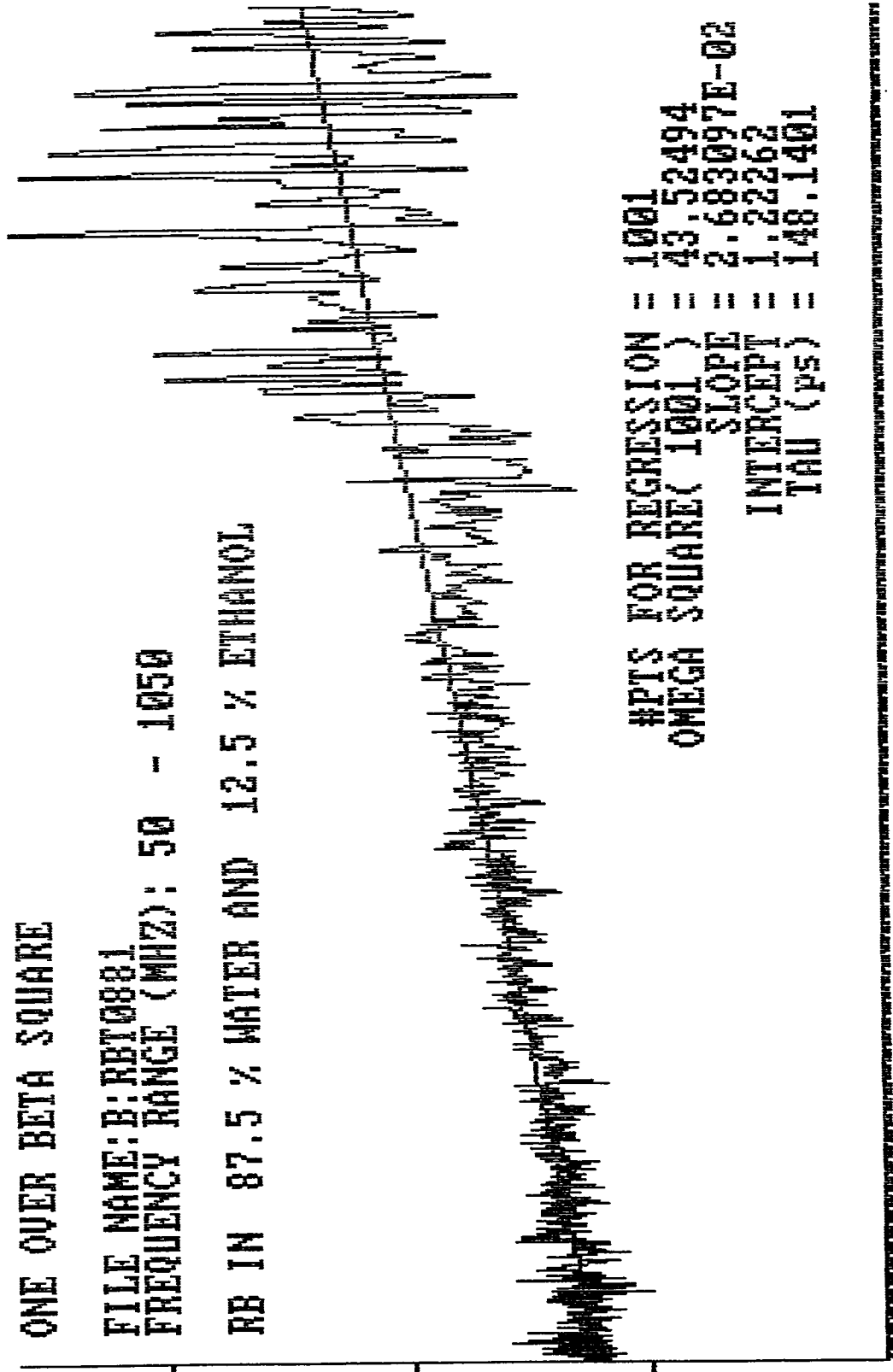
3.609176

ONE OVER BETA SQUARE

FILE NAME: B:RBT0881

FREQUENCY RANGE (MHZ): 50 - 1050

RB IN 87.5 % WATER AND 12.5 % ETHANOL



#PTS FOR REGRESSION = 1001  
 OMEGA SQUARE( 1001 ) = 43.52494  
 SLOPE = 2.683097E-02  
 INTERCEPT = 1.22262  
 TAU (PS) = 148.1401

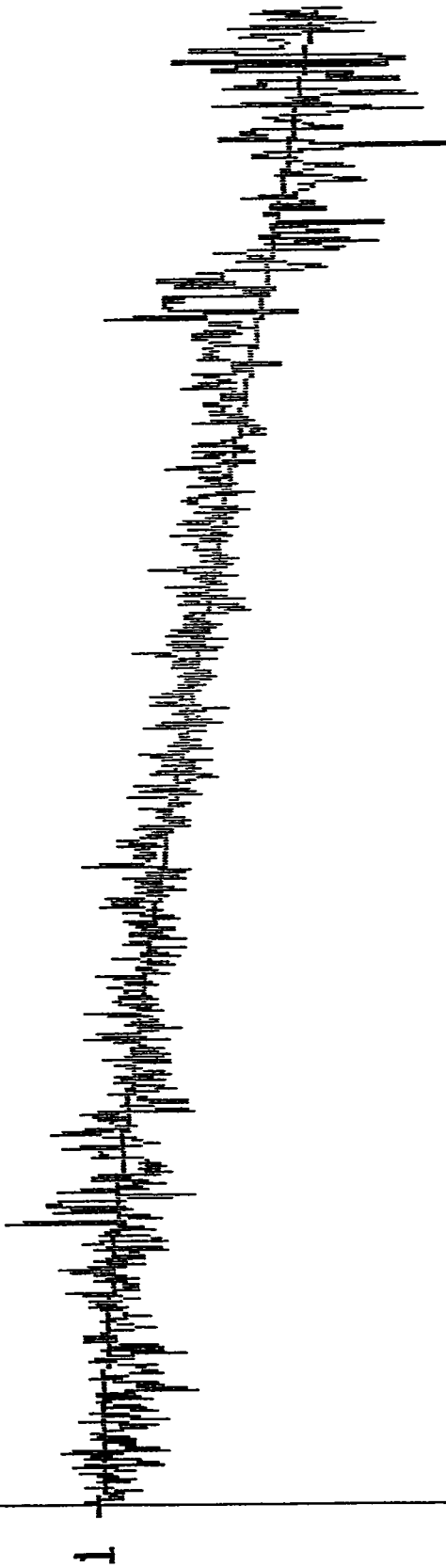
OMEGA SQUARE (GHZ \* GHZ)

43.52494

0

Fig. (4.30)

MODULATION  
DEPTH



FLUORESCENCE SIGNAL: B: RBT0881  
BEST FIT FILENAME: B: RBF0881  
STANDARD DEVIATION: 9.832372E-02  
RB IN 87.5 % WATER AND 12.5 % ETHANOL

1050

FREQUENCY (MHZ)

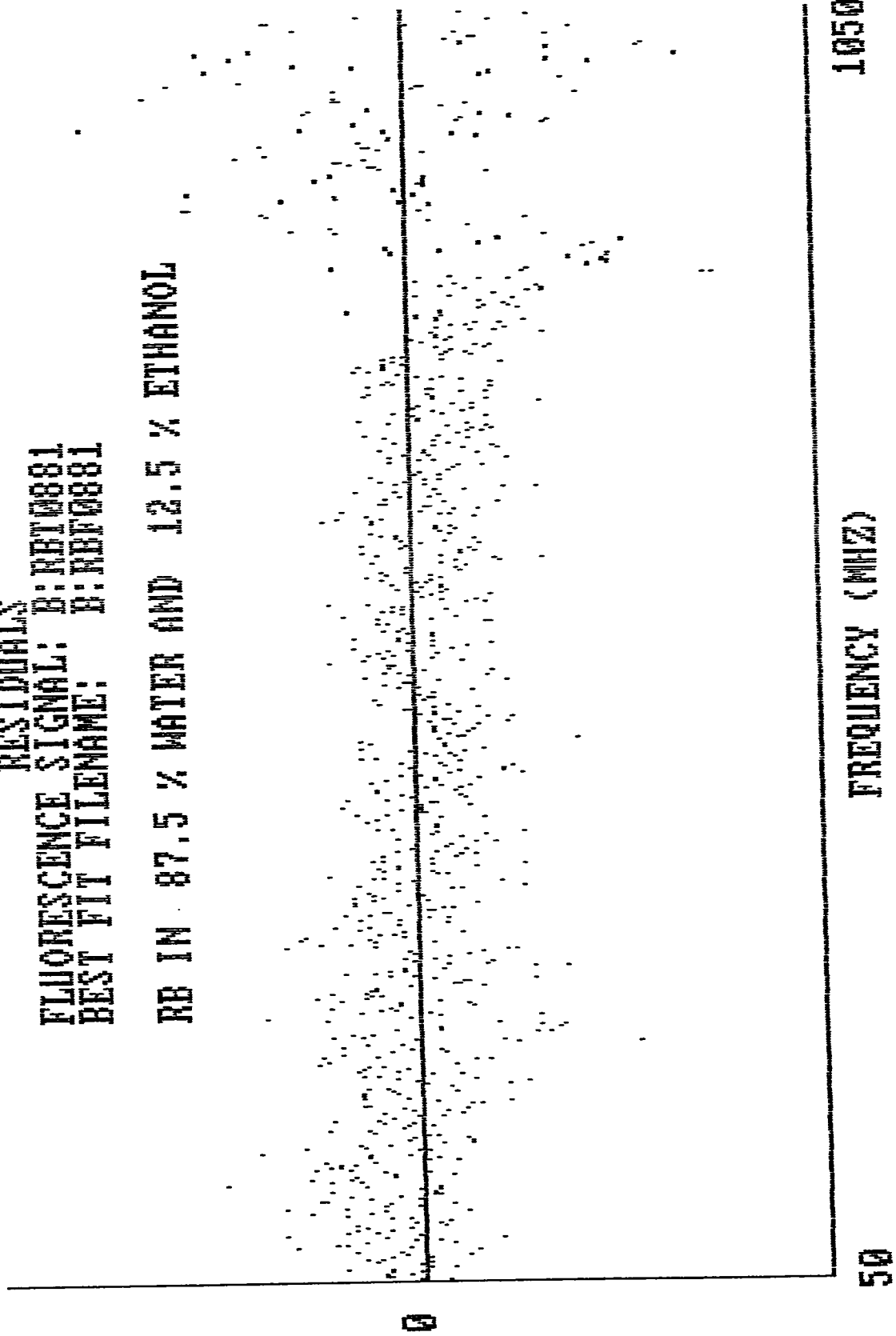
50

Fig. (4.31)

.4891537

RESIDUALS  
FLUORESCENCE SIGNAL: B:RHY0881  
BEST FIT FILENAME: B:RHY0881

RB IN 87.5 % WATER AND 12.5 % ETHANOL



-.4891537

Fig. (4.52)

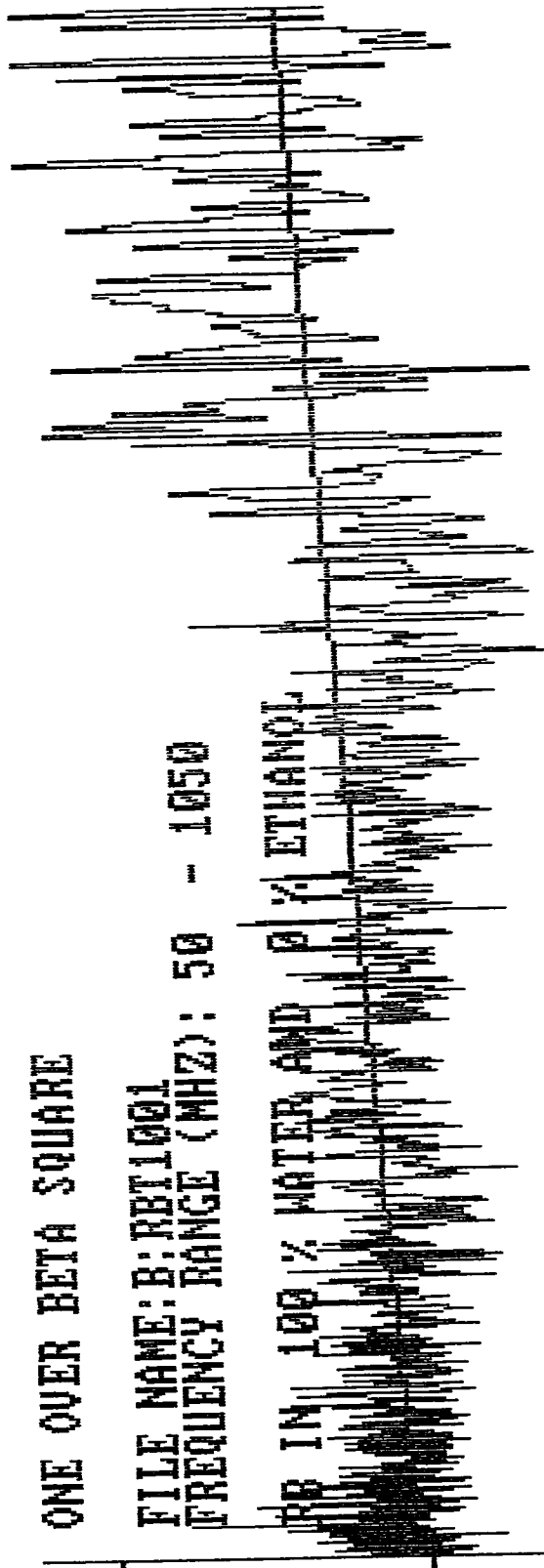
3.251645

ONE OVER BETA SQUARE

FILE NAME: B:RBI1001

FREQUENCY RANGE (MHZ): 50 - 1050

RD IN 100 % WATER AND 0 % ETHANOL



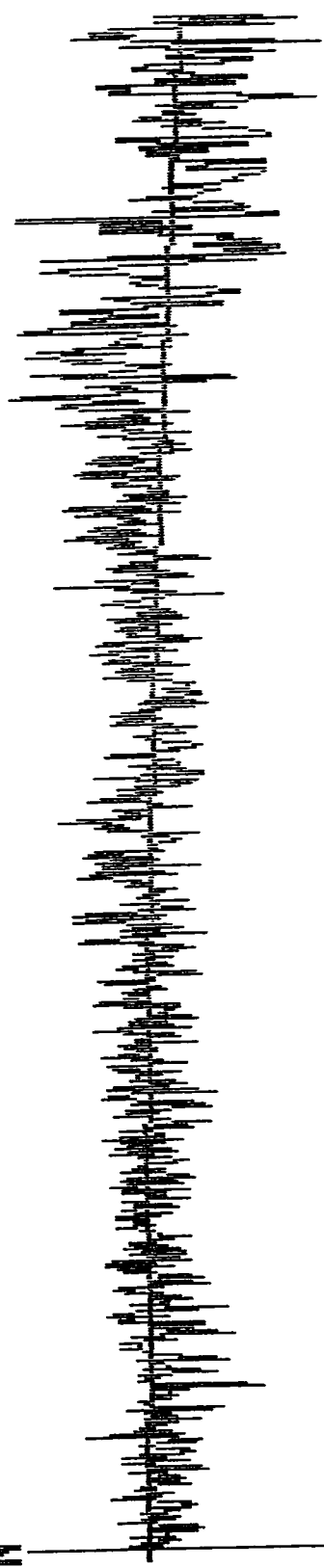
#PTS FOR REGRESSION = 1001  
 OMEGA SQUARE( 1001 ) = 43.52494  
 SLOPE = 8.077114E-03  
 INTERCEPT = 2.048992  
 TAU (PS) = 62.78531

OMEGA SQUARE (GHZ \* GHZ) 43.52494

Fig. (4.33)

MODULATION  
DEPTH

1



FLUORESCENCE SIGNAL: B:RBFI001  
BEST FIT FILENAME: B:RBFI001  
STANDARD DEVIATION: .11111991  
RB IN 100 % WATER AND 0 % ETHANOL

50

FREQUENCY (MHZ)

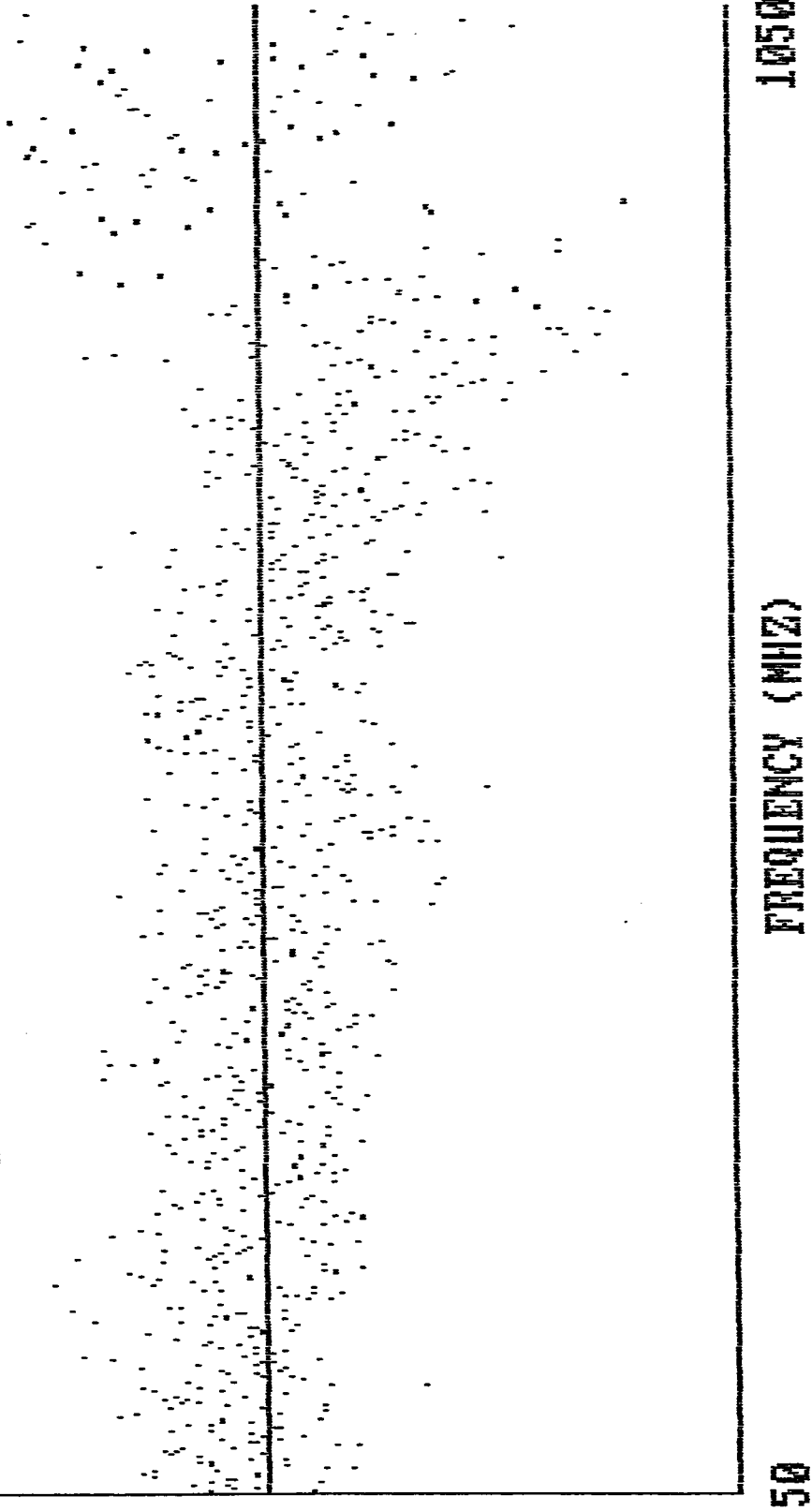
1050

Fig. (4.34)

.4692625

RESIDUALS  
FLUORESCENCE SIGNAL: B:RBT1001  
BEST FIT FILENAME: B:RBT1001

RB IN 100 % WATER AND 0 % ETHANOL



-.4692625

Fig. (4.35)

In Figure (4.36), the frequency responses of RB in 25% water, and RB in 60% water are plotted on one graph along with their reference frequency response. The demodulation is strongest in the sample of RB in 25% water indicating that its fluorescence lifetime is longer than the sample of RB in 60% water. This can be seen by looking at the relation (Eq. (4.2.9)):

$$\beta^2 = \frac{\lambda^2}{\lambda^2 + \omega^2}$$

At any given frequency, a stronger demodulation means a smaller  $\beta^2$  which means a smaller decay rate  $\lambda$  indicating a longer fluorescence lifetime. From this argument and from Figure (4.36), we conclude that the fluorescence lifetime of RB in 25% water is longer than in 60% water. For quantitative analysis we repeat the two-parameter linear regression (Eq. (4.4.3 – 4.4.11)). The result is that the fluorescence lifetime of RB in 25% water is 465 ps and becomes much shorter ( $\approx$  297 ps) in 60% water.

The fluorescence lifetimes and decay rates of RB in water-ethanol mixtures is tabulated in Table (4.1). Eqn. (4.4.3 – 4.4.15) were used to find  $\tau, \lambda, \delta_\tau,$  and  $\sigma_\lambda$ .

The fluorescence lifetimes of RB in pure ethanol and RB in pure water have been measured by five groups. Their results along with our values are reported in Table (4.2).

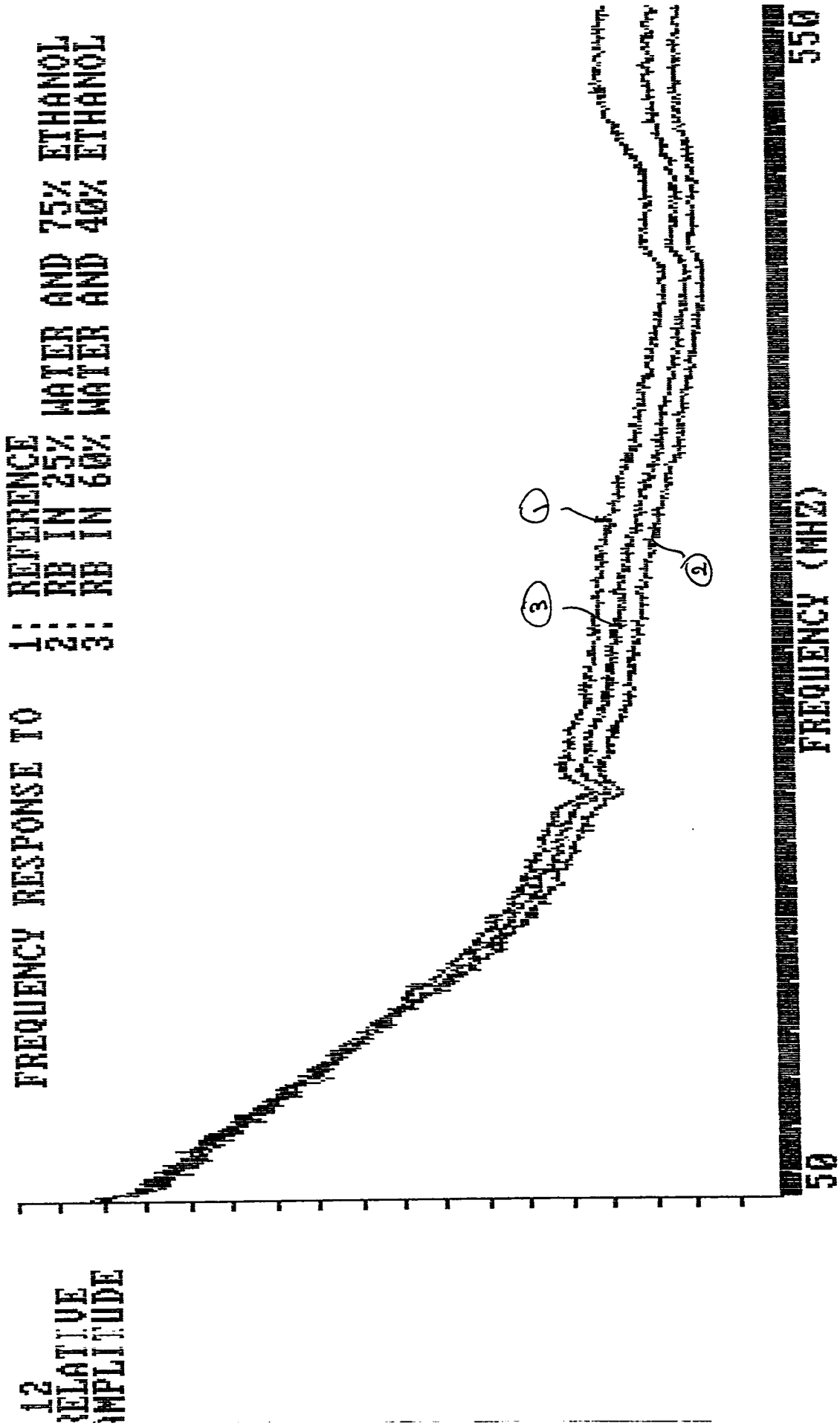


Fig. (4.36)

fil name	% water vol.	Slope-M. (GHz)	$\sigma_M$ (GHz)	Intercept-H.	$\sigma_H$	$\tau$ (ps)	$\sigma_\tau$ (ps)	$\lambda$ (GHz)	$\sigma_\lambda$ (GHz)
FOSET2	0	0.3597	0.0038	0.6778	0.0043	728.5	6.2	1.373	0.0117
R3T0001	0	0.309	0.0017	0.5487	0.0019	750.4	3.3	1.333	0.0059
R3T0131	12.5	0.3272	0.0089	0.9686	0.0016	581.2	8.4	1.72	0.0249
RBT0251	25	0.2105	0.0064	0.9751	0.0012	464.6	7.4	2.152	0.0342
RBT0401	40	0.1864	0.0058	1.185	0.001	396.6	6.3	2.521	0.0403
RBT0501	50	0.0924	0.003	0.7699	0.0005	346.6	5.8	2.888	0.048
PBT0601	60	0.1204	0.0053	1.369	0.0009	296.5	6.6	3.372	0.0751
R3T07512	75	0.0597	0.0045	1.476	0.0008	201.1	7.6	4.974	0.189
FBT0881	87.5	0.0268	0.0112	1.223	0.0006	148.1	31.1	6.75	1.416
FOSET14	100	0.00347	0.0073	0.979	0.0004	59.6	62.6	16.788	17.655
FBT1001	100	0.00808	0.0122	2.049	0.0008	62.8	47.4	15.927	12.036
RBT10012	100	0.0127	0.0075	1.075	0.0004	108.7	31.9	9.2	2.7
RBT10017	100	0.00241	0.00326	0.597	0.0002	63.6	42.9	15.724	10.608

Table (4.1) : Rose Bengal Fluorescence Lifetimes and Decay Rates  
in Water-Ethanol Mixtures.

LIFETIME IN WATER (ps)	LIFETIME IN ETHANOL (ps)	GROUP/CITATION
100	836	FLEMING/[15]
79 +/- 11	610	RODGERS/[17]
25	660 +/- 40	DORSEY/[11]
115 +/- 7	732	SPEARS/[1]
88	710	SMALL/[20]
80 +/- 22	740 +/- 4	Present Work

Table (4.2): Rose Bengal Fluorescence Lifetime in Pure Water and in Pure Ethanol. (Previous Work)

## 4.5. The Uncertainty in the Lifetime Measurements

As we have mentioned in the beginning of this chapter, the PMT we are using has a risetime of approximately 800 ps. However, we can see from Table (4.1) that the uncertainty of lifetimes shorter than the PMT rise time may be as small as 1%. This is the case with a  $10^{-5}$  M solution of RB in pure ethanol. The lifetime is 728 ps with a 6 ps uncertainty.

Uncertainty in lifetime measurements is less than 4% as long as the lifetime is longer than 200 ps (approximately 1/4 of the PMT rise time). This is an astonishing result. Previously, researchers were not able to detect fluorescence lifetimes with high precision if the lifetimes were shorter than the PMT rise time. Deconvolution, taking into account the shape of the pulse, was always accompanied by considerable uncertainty. In our system, on the other hand, one can detect lifetimes that are shorter than the PMT rise time with remarkable certainty. This is because the individual differentials of the frequency response are contributing to the lifetime measurement. The high frequency response components, although comparatively small in magnitude, can still be taken advantage of by measuring the demodulation in these components. This leads to the detection of short events as mentioned in Sec. 3.1. It was discussed that, high frequency response components lead to the detection of short events. Ideally, infinitely high frequency response components can measure infinitesimally short events.

In pulsed excitation method, an integral over the frequency spectrum of the PMT is taken to represent events in time domain. Because the higher frequency components are small in magnitude, they hardly contribute to the integral and their effect of measuring short events is diminished.

The value of fluorescence lifetime of a  $10^{-5}$  M solution of RB in pure ethanol was found to be  $728.5 \pm 6.2$  ps. It was measured again with a  $5 * 10^{-5}$  M solution of RB in pure ethanol. The result was  $\tau = 750.4 \pm 3.3$  ps. We can see that the two values are approximately within  $2\sigma$  from each other; i.e.,  $729 + 2 * 6 \approx 750 - 2 * 3$ . Therefore, the accepted value of RB fluorescence lifetime in pure ethanol is  $739.5 \pm 4.4$  ps. However, the slight difference in the lifetimes may also be caused by a small concentration dependence of the lifetimes.

As the lifetimes get shorter and shorter, i.e., less than 200 ps, the certainty becomes less. This is because with short lifetimes, the demodulation at comparatively high frequencies is still small. This can be seen from Eq. (4.2.9)

$$\beta^2 = \frac{\lambda^2}{\lambda^2 + \omega^2}$$

For example, a 100 ps lifetime yields modulation depth of 0.85 (little demodulation) at 1000 MHz. Because our PMT hardly has a frequency response at such a high frequency, the extent to which the demodulation can be accurately determined is small. In fact, we have shown in Chapter (3) that when the amplified AC signal is less than  $40 \mu\text{V}$  the signal is 'artificially' recorded to be zero because of

unreliability. This is the case with our PMT at frequencies greater than 1000 MHz.

It is clear from Table (4.2), that the value of  $80 \pm 22$  ps for RB fluorescence lifetime in pure water could be stated with this precision only because of the fact that the measurements were taken a number of times. A set of three measurements was found to have an average lifetime  $\tau = 63$  with uncertainty  $\sigma = 47$  ps. Another set of measurements had an average  $\tau = 109$  ps,  $\sigma = 32$  ps.

A single measurement gave  $\tau = 60$  ps;  $\sigma = 63$  ps

Another single measurement gave  $\tau = 64$  ps;  $\sigma = 43$  ps

The average lifetime  $\bar{\tau}$  and standard deviation  $\sigma$  are found to be

$$\bar{\tau} = \frac{1}{8} \sum_{i=1}^8 \tau_i = \frac{3 * 63 + 3 * 109 + 60 + 64}{8} = 79.7 \text{ ps}$$

$$\sigma \leq \frac{\sigma_{\max}}{\sqrt{8}} = 22.1 \text{ ps}$$

From this analysis, and looking at Table (4.1), we can state that although our PMT cannot accurately detect lifetimes shorter than 100 ps, it certainly can measure lifetimes as short as 200 ps (which is a fraction of the PMT rise time) with remarkable experimental certainty.

## 4.6 The Quenching of Rose Bengal Fluorescence at High Water Concentrations

From Table (4.1), we can clearly see a monotonic decrease in RB lifetimes with increasing water concentrations.

Plotting lifetime vs percentage of water by volume, we get Figure (4.37).

In chemical reactions, it is the decay rate that is of greater interest. It is a measure of the speed of a reaction. According to different models, the dependence of decay rate on molar concentration of water or on mole fraction of water gives direct interpretations.

Plotting the decay rates vs. molar concentration of water we get Figure (4.38).

Plotting the decay rate vs. mole fraction we get Figure (4.39).

As can be seen in Figure (4.38), the decay rate of RB increases with water concentration. At the same time, this is accompanied by a decrease in the fluorescence quantum yield as was seen from steady-state fluorescence measurements. This means that water is enhancing the transition of excited Rose Bengal through channels other than fluorescence. Excited Rose Bengal has three main channels through which it can relax. These are fluorescence (F1), intersystem crossing (ISC), and radiationless transition (RT). These transitions are shown in Figure (4.40). Because RB is surrounded by water molecules, these molecules interact with ex-

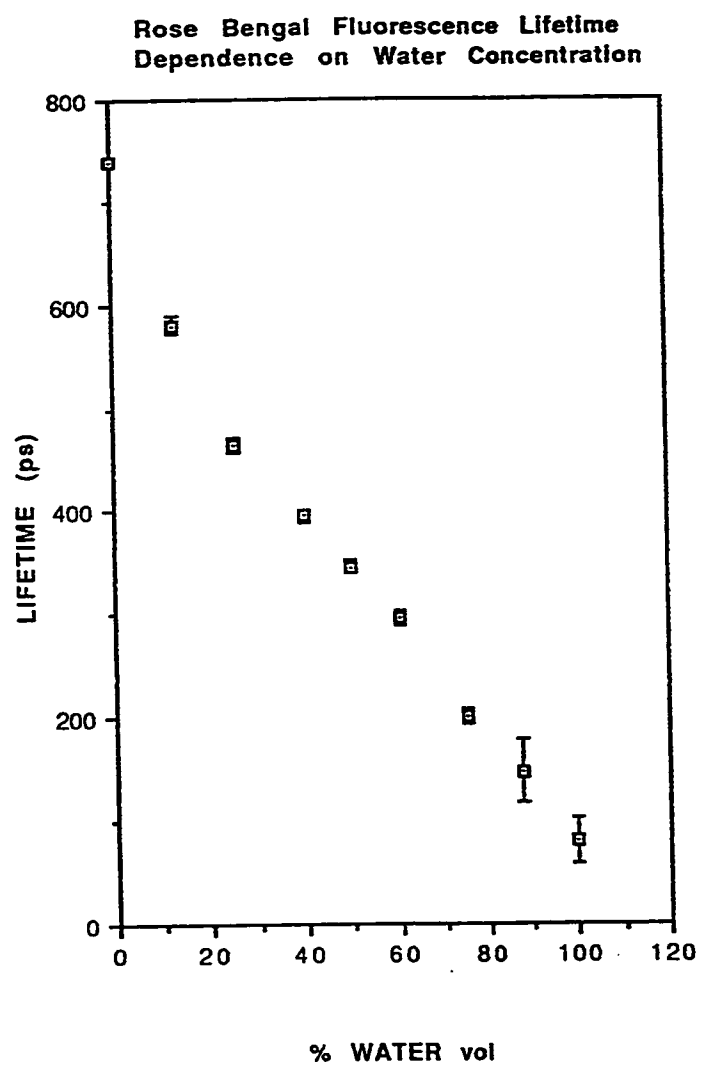


Fig. (4.37)

Rose Bengal Decay Rate Dependence  
on Water Concentration

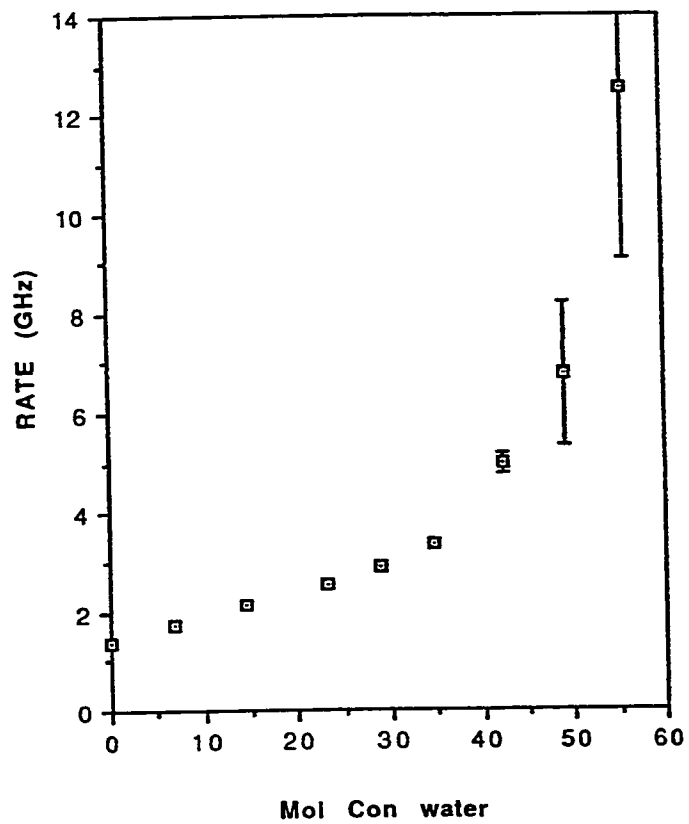


Fig. (4.38)

Rose Bengal Decay Rate Dependence  
on Water Concentration

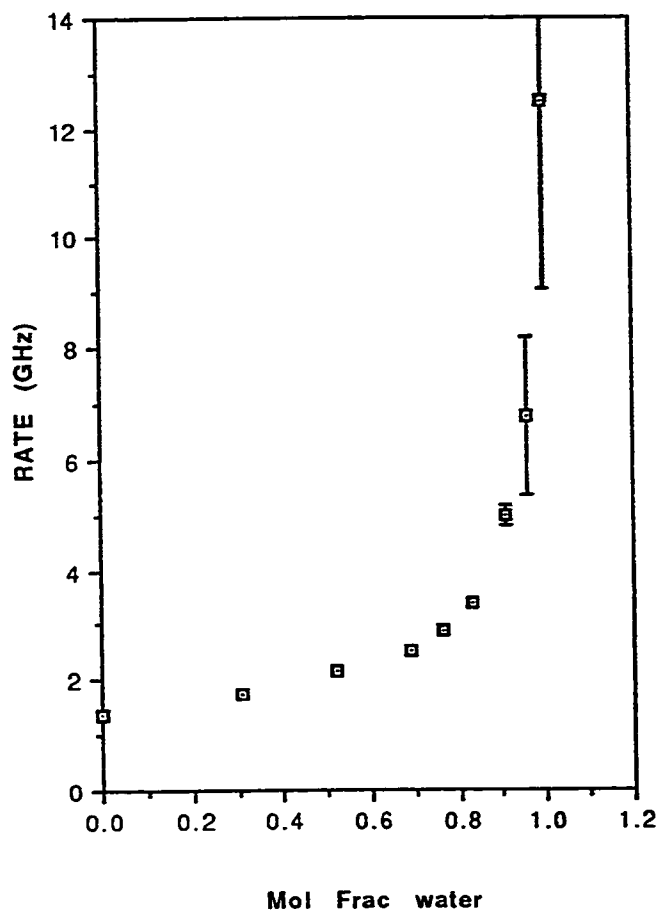


Fig. (4.39)

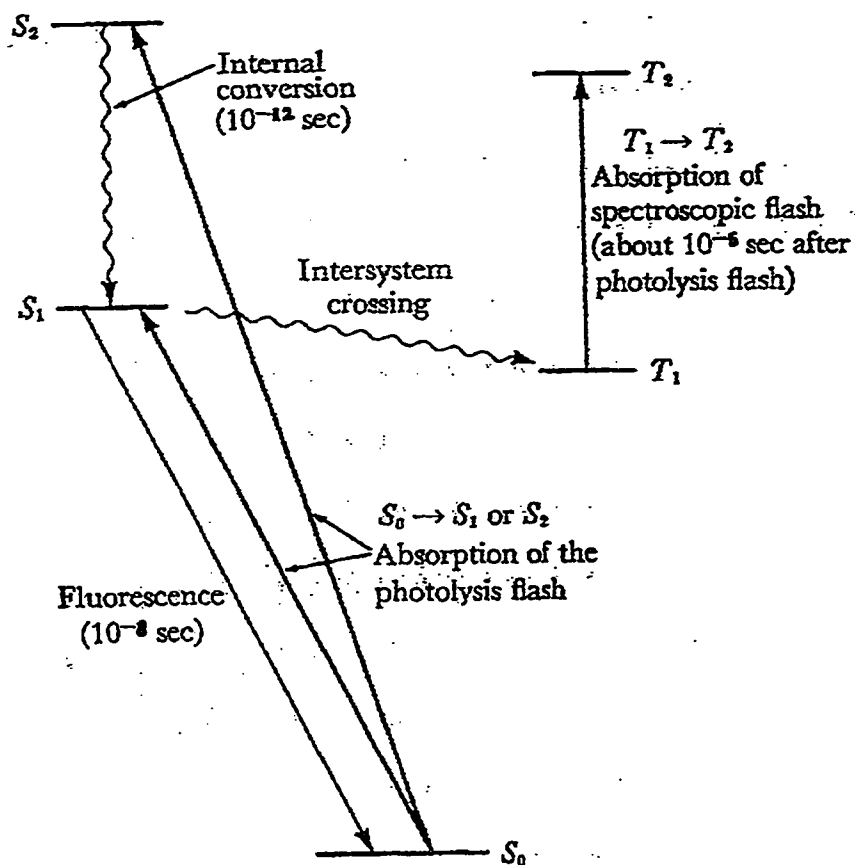


Fig. (4.40): Transitions Involved in Photolysis Studies

cited RB ( $RB^*$ ) by collisions (and even through slight bonding). These collisions induce quenching of the  $RB^*$  fluorescence.

If the three main channels due to RB alone have a transition rate  $k_0$ , and if the collision rate is taken to be linear with molar concentration of water; then the total decay rate  $\lambda$  is

$$\lambda = k_0 + k_1[H_2O] \quad ; k_1 \text{ is the collision rate constant} \quad (4.6.1)$$

As can be seen from Figure (4.38), in the range of 0 – 30 Mol/l, the decay rate dependence on water concentration is approximately linear. The slope is found to be  $0.0533 \text{ GHz}(\text{Mol/l})^{-1}$ . When the molar concentration is higher than 35 Mol/l, there is clearly a non-linear dependence of decay rate on water concentration. This suggests that a nonlinear term needs to be added to the decay rate ( $\lambda$ ).

As a model we can picture the situation as follows.  $RB^*$  is in an environment of water of some concentration  $M$ . Consider the water molecules to be in dynamic equilibrium with water clusters of four water molecules. The idea of water cluster enhancement to chemical reactions has been studied [22-26]. The accepted model is that water forms clusters of the form  $(H_2O)_{4\pm 1}$ .



Therefore,

$$B = KA^4 \quad (4.6.3)$$

where

$$B = [(H_2O)_4]$$

$$A = [H_2O]$$

$$K = k/k' \quad \text{is the equilibrium constant}$$

Conservation of water concentration in the sample implies that:

$$M = A + 4B \quad (4.6.4)$$

Instead of Eq. (4.6.1) in the case of linear collisional dependence, we now have another term in the expression for the decay rate ( $\lambda$ ):

$$\lambda = k_0 + k_1A + k_2B \quad (4.6.5)$$

The term  $k_2B$  describes the enhanced quenching of the RB fluorescence due to collisions with water clusters.

By rearranging Eq. (4.6.5) and using Eq. (4.6.3, 4.6.4),  $\lambda$  may be put in the following form

$$\lambda = k_0 + k_1A + k_2B \quad (4.6.6)$$

$$= k_0 + k_1A + k_2KA^4 \quad (4.6.7)$$

$$= k_0 + k_1A + 4k_1KA^4 - 4k_1KA^4 + k_2KA^4 \quad (4.6.8)$$

$$= k_0 + k_1(A + 4KA^4) + (k_2 - 4k_1)KA^4 \quad (4.6.9)$$

$$= k_0 + k_1M + (k_2 - 4k_1)KA^4 \quad (4.6.10)$$

$k_0$  (in our case 1.35) is the value of the vertical intercepts of the curve.

$k_1$  to a first order approximation is the slope of the curve in the linear region ( $M = 0 - 30$  Mol/l).

At the different molar concentration, we try to fit the values of the molar concentrations ( $M$ ) and their corresponding decay rates ( $\lambda$ ) to get best fits for  $k_2$ , and  $K$ . If the fit is not satisfactory, the values of  $k_2$ ,  $K$  are used to get a better estimate of  $k_1$  and the iterative procedure is continued until an acceptable fit is processed. A plot of the data points with the best fit is shown in Figure (4.41).

For our data we got.

$$\begin{aligned} k_0 &= 1.351 \text{ GHz} \\ k_1 &= 0.0355 \text{ GHz(Mol/l)}^{-1} \\ k_2 &= 92 \text{ GHz(Mol/l)}^{-1} \\ K &= 7 * 10^{-9} \text{ (Mol/l)}^{-3} \end{aligned} \quad (4.6.11)$$

The standard deviation is:

$$\sigma = 0.138 \quad (\text{the error bars are taken into consideration})$$

In this fit:

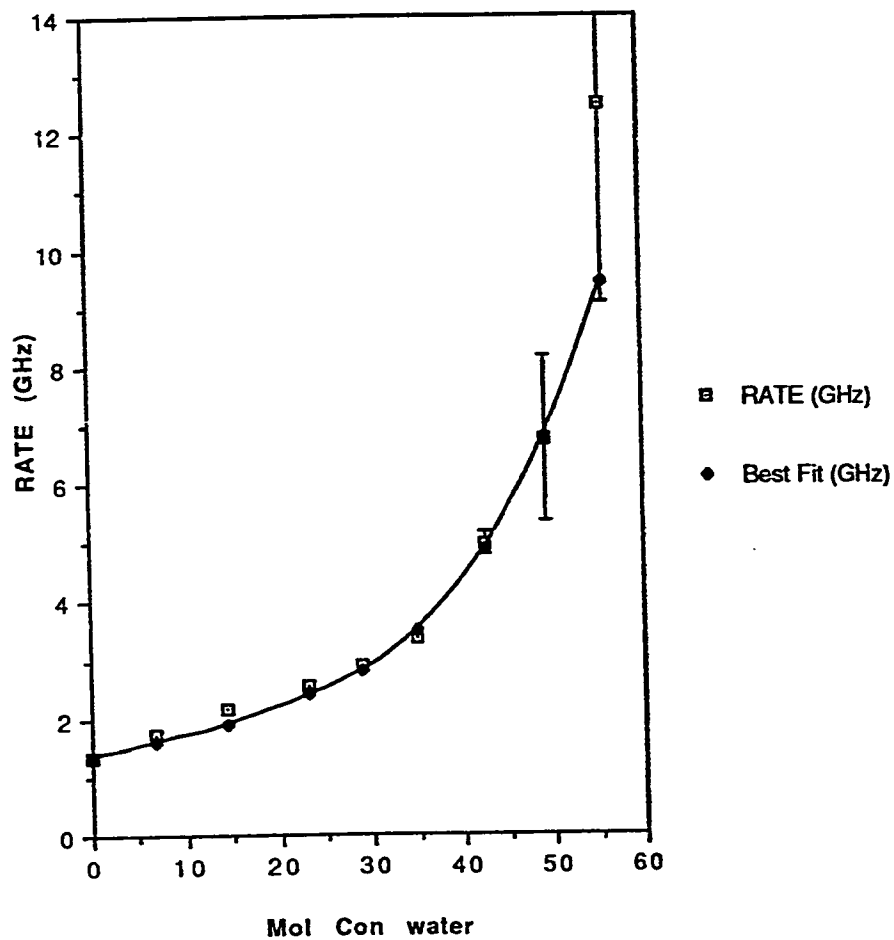
$k_0$  is the rate of transition due to the different channels in RB alone.

$k_1$  is a measure of the quenching process due to water molecules.

$k_2$  is a measure of the quenching process due to water clusters.

$K$  is a measure of the presence of water clusters.

Rose Bengal Decay Rate Dependence  
on Molar Concentration of Water;  
Including Best Fit



$$\lambda = 1.35 + 0.0355 A + 92 B$$

$$K = 7 * 10^{-9}, \text{ std} = 0.138$$

Fig. (4.41)

A few points should be mentioned:

1. The values of  $k_1$ ,  $k_2$ , and  $K$  are not unique for a fit of this quality (goodness); still, the values of constants for any good fit are within an order of magnitude of the values of eq. (4.6.11).  
  
Until we determine the fluorescence lifetime of RB in 87.5% and 100% water more precisely, it is not possible to make a definite fit.
2. The data has been fitted with a 'cluster of four' model. It is possible, however, to fit it with a model of more than four molecules to a cluster. The point that is to be stressed is that there is a deviation from the linear dependence on water concentration signifying the presence of water clusters.
3. If the actual aqueous environment is water molecules and water clusters of four molecules only, then  $K = 7 \cdot 10^{-9}$  is the constant of dynamic equilibrium between the water molecules and the water clusters. This constant can be of importance when describing processes in different types of aqueous chemical reactions.

## Summary

In this chapter, we have used demodulation spectroscopy to measure the lifetimes of Rose Bengal in mixtures of water with ethanol. Rose Bengal in pure ethanol has a lifetime of  $740 \pm 4$  ps.

The measurements were done with great certainty for lifetimes greater than 200 ps. Because of limitations in the detection system, lifetime measurements shorter than 100 ps had imprecision. For this reason, the lifetime measurements of Rose Bengal in pure water was repeated eight times. The average value was found to be 80 ps with 22 ps uncertainty.

The fact that an 800 ps rise time PMT may be used to accurately measure lifetimes as short as 200 ps, without the need of deconvolution or any non-linear processes, is astonishing.

The decay rates of Rose Bengal in water-ethanol mixtures show a non-linear dependence on water molar concentration. This may be explained with a water cluster model where quenching induced by collisions is promoted not only by water molecules, but also by water clusters.

## Conclusion

In this thesis two ring dye lasers have been used to achieve amplitude modulated light of variable frequency.

This was used to study the frequency response of an 800 ps risetime photomultiplier against different parameters. The frequency response of the photomultiplier was found to be independent of intensity of incident light, photocathode illumination shape, laser wavelength in the range 570–593 nm, and polarization of incident laser beam. The higher components of the frequency response were enhanced with increasing photomultiplier operating voltage.

The amplitude modulated light was used to perform demodulation spectroscopy on Rose Bengal. By measuring the demodulation in the fluorescence signal, the fluorescence lifetime of Rose Bengal in pure ethanol was found to be  $740 \pm 4$  ps. The lifetime was then determined in mixtures of water and ethanol. The fluorescence lifetime of Rose Bengal was found to monotonically decrease with increasing water concentration. The Rose Bengal fluorescence lifetime in pure water was found to be  $80 \pm 22$  ps.

The decay rate of Rose Bengal fluorescence showed a nonlinear dependence on water concentration. This could be explained by a water cluster model.

# **APPENDIX I.A**

## **PMT FREQUENCY**

### **RESPONSE MEASUREMENTS**

#### **AGAINST DIFFERENT PARAMETERS**

# **APPENDIX I.A.1**

**FREQUENCY RESPONSE**

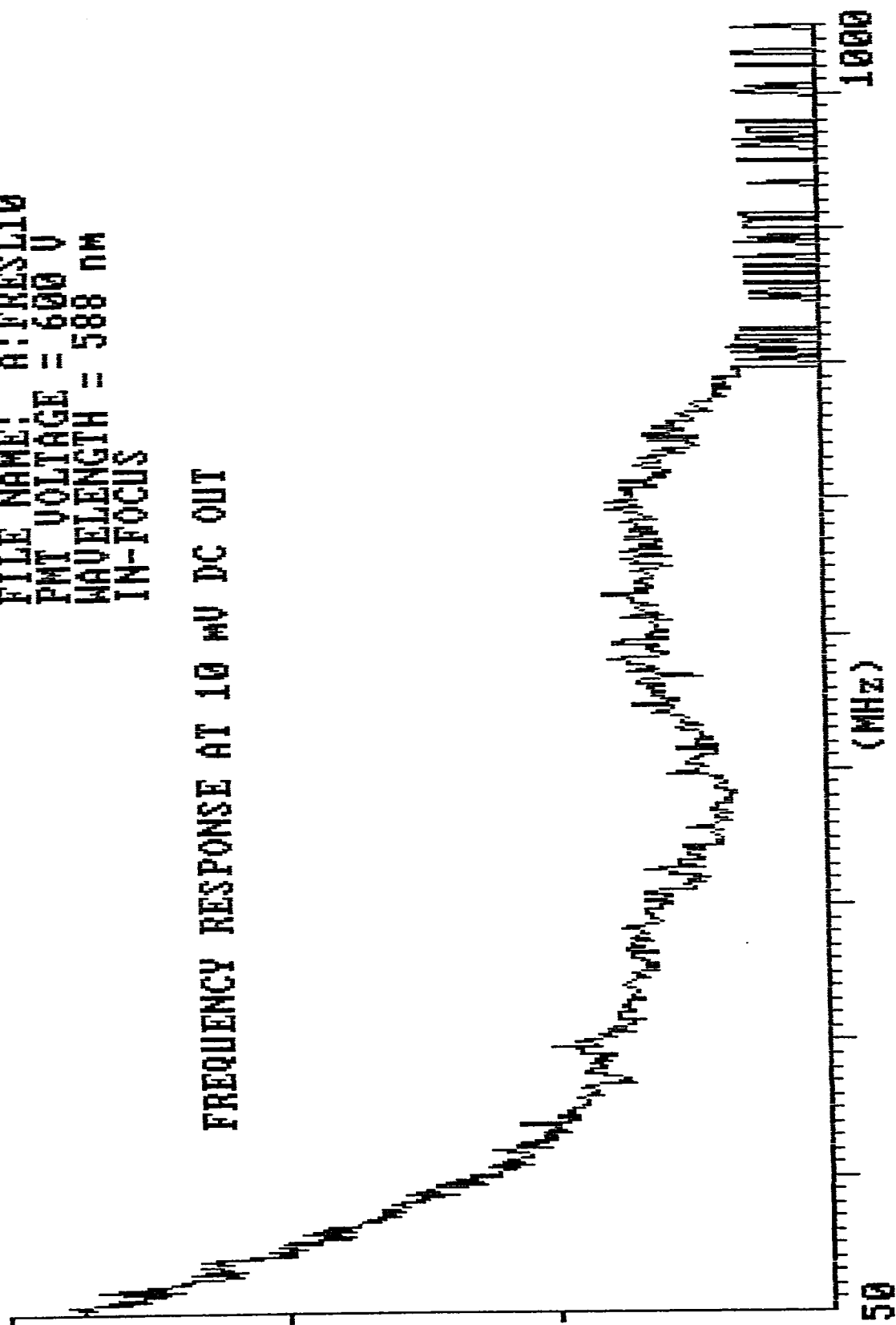
**AT DIFFERENT INCIDENT**

**LASER INTENSITIES**

FILE NAME: A:FRESL10  
PMT VOLTAGE = 600 V  
WAVELENGTH = 588 NM  
IN-FOCUS

3  
RELATIVE  
AMPLITUDE

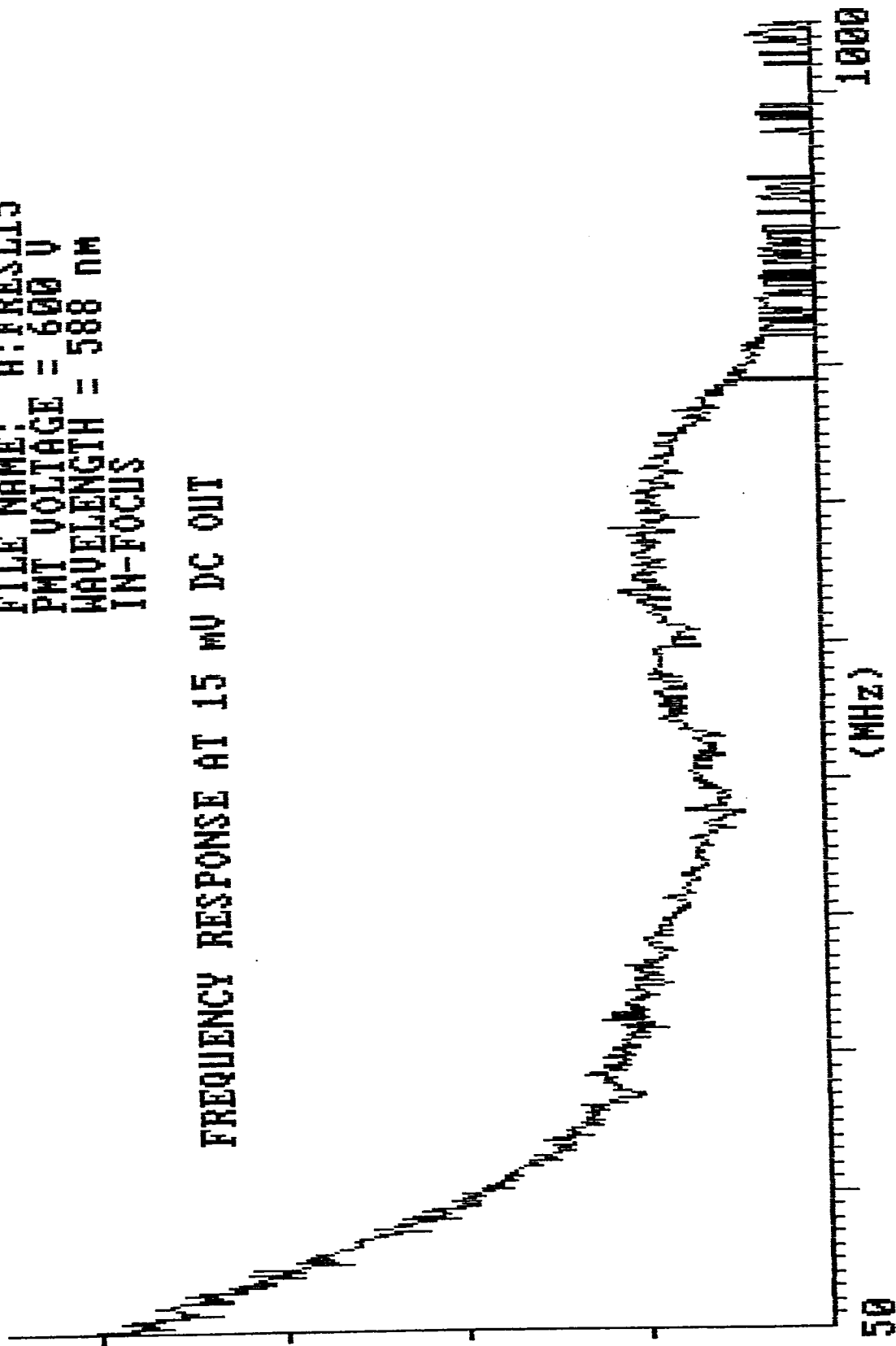
FREQUENCY RESPONSE AT 10 MV DC OUT



FILE NAME: A:FRESL15  
PMT VOLTAGE = 600 V  
WAVELENGTH = 588 NM  
IN-FOCUS

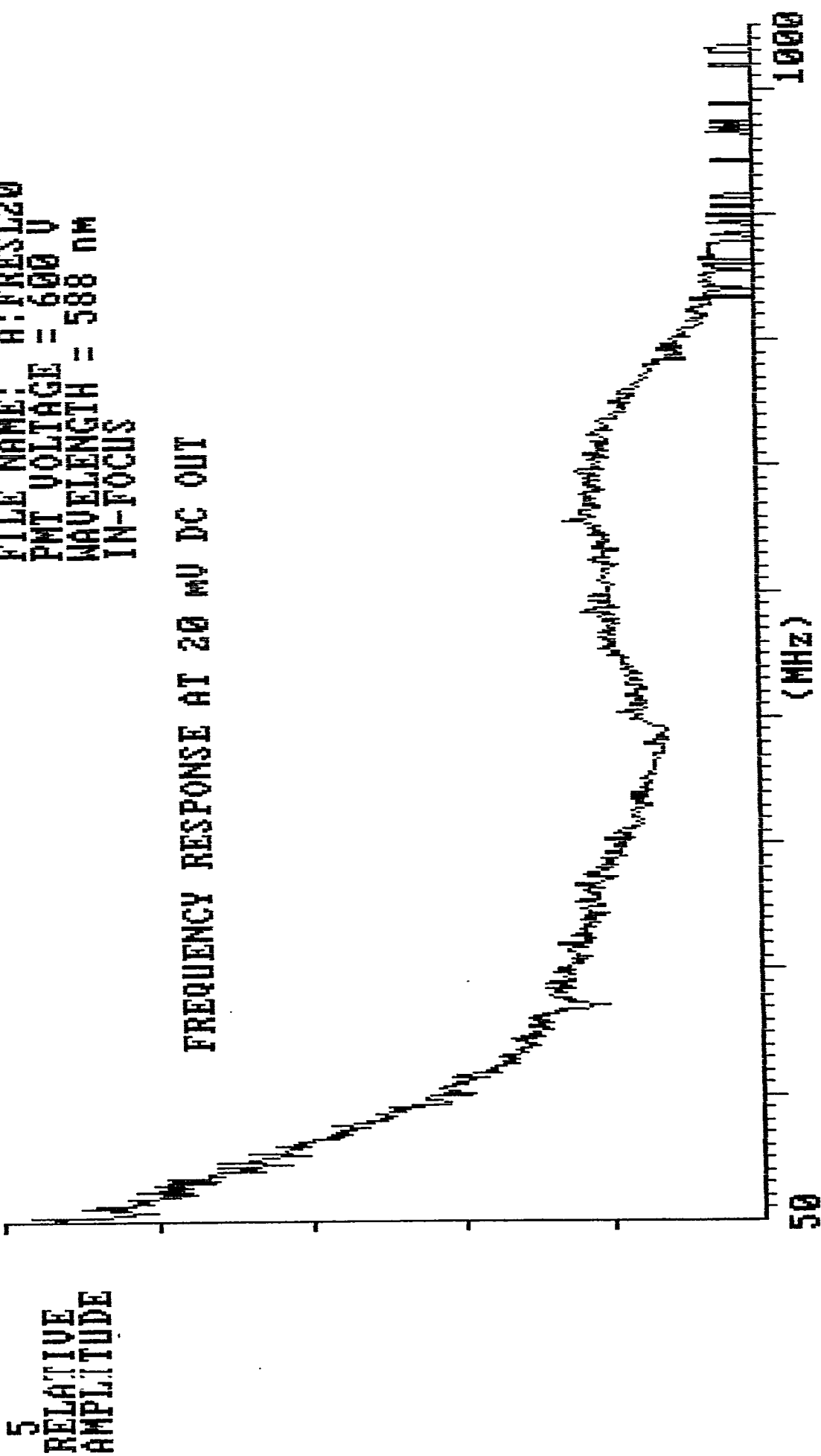
4.5  
RELATIVE  
AMPLITUDE

FREQUENCY RESPONSE AT 15 MV DC OUT



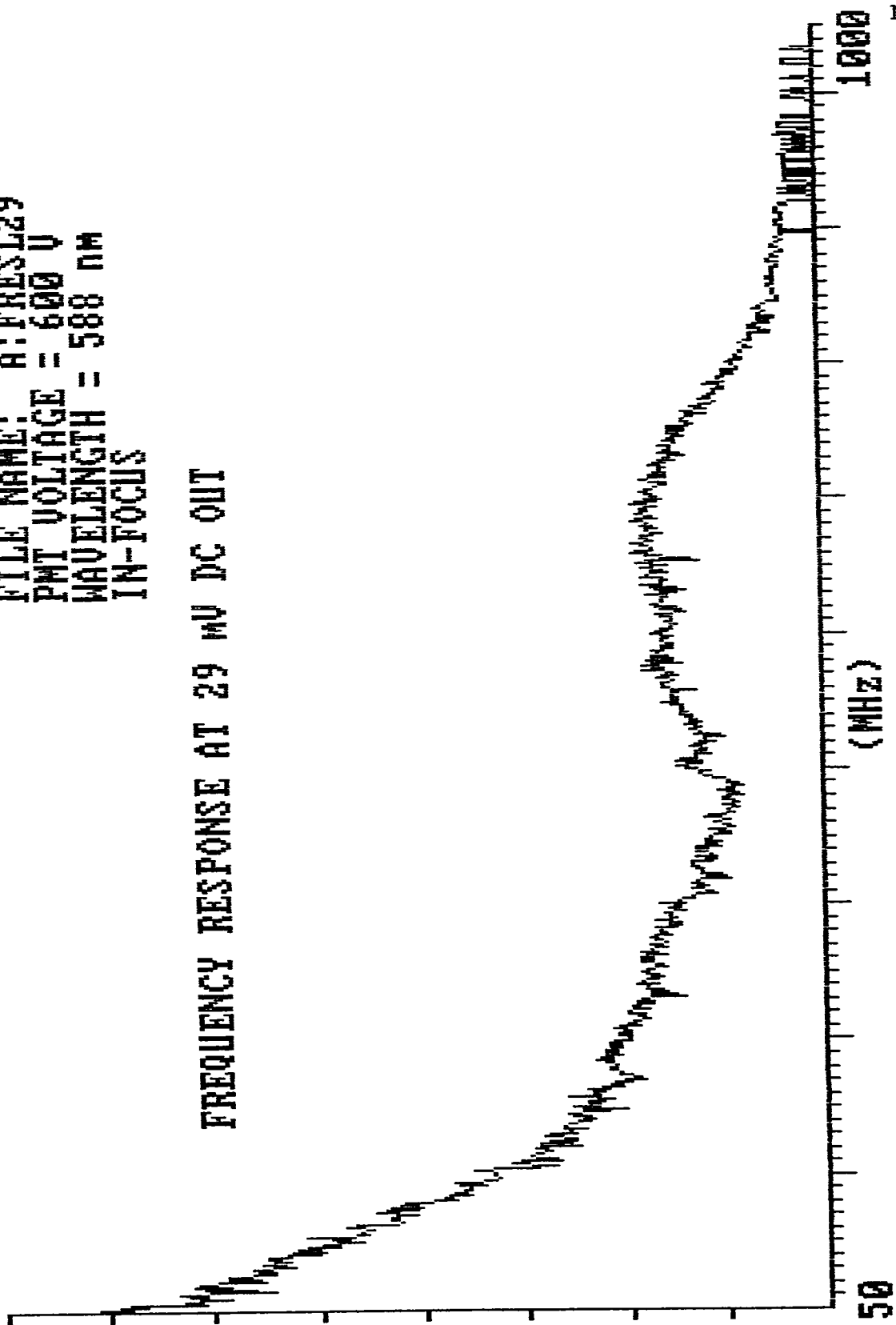
FILE NAME: A:FRESL20  
PMT VOLTAGE = 600 V  
WAVELENGTH = 588 nm  
IN-FOCUS

FREQUENCY RESPONSE AT 20 MV DC OUT



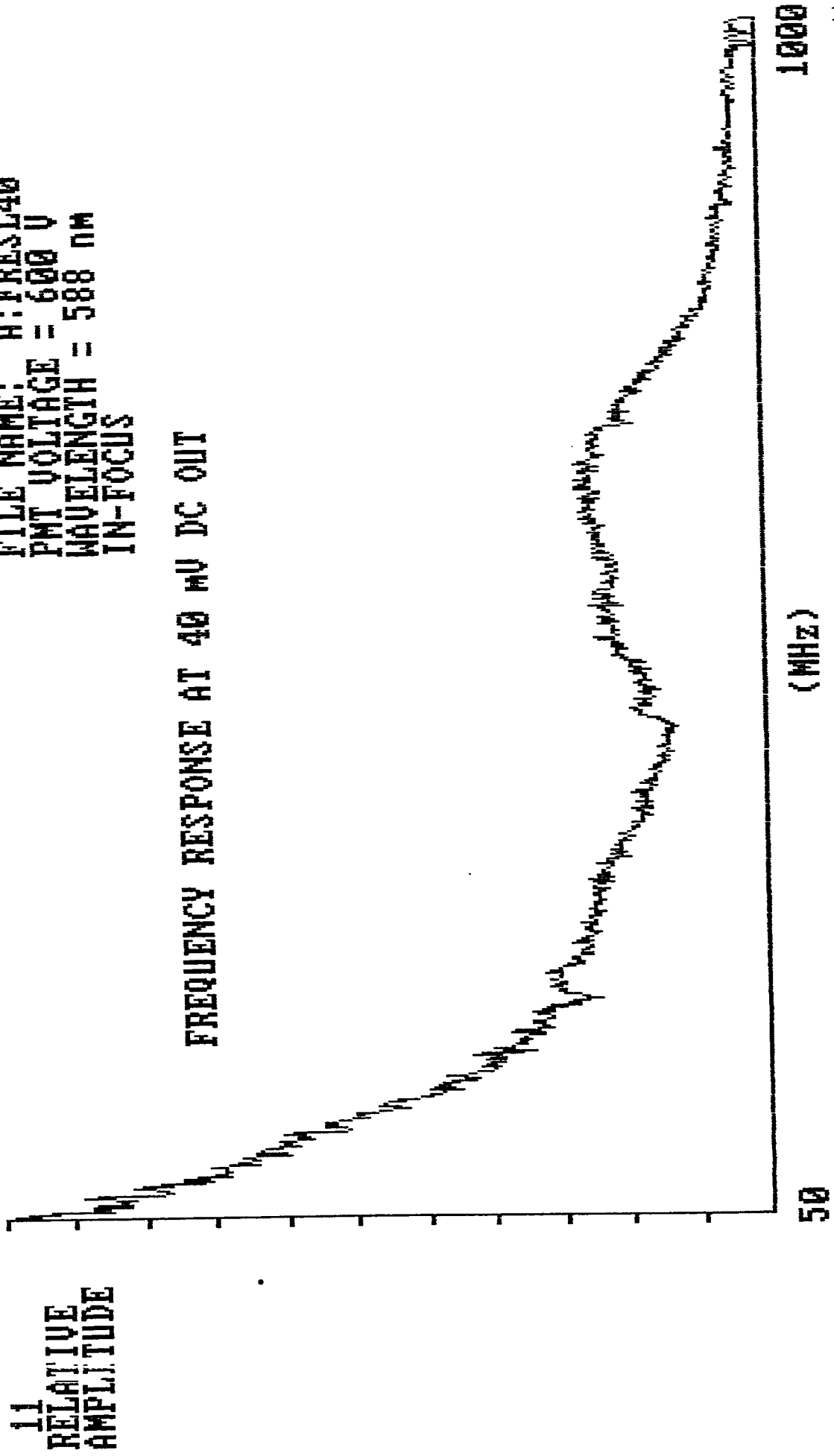
FILE NAME: A:FRESL29  
PMT VOLTAGE = 600 V  
WAVELENGTH = 588 nm  
IN-FOCUS

FREQUENCY RESPONSE AT 29 mV DC OUT



FILE NAME: A:FRESL40  
PMT VOLTAGE = 600 V  
WAVELENGTH = 588 nm  
IN-FOCUS

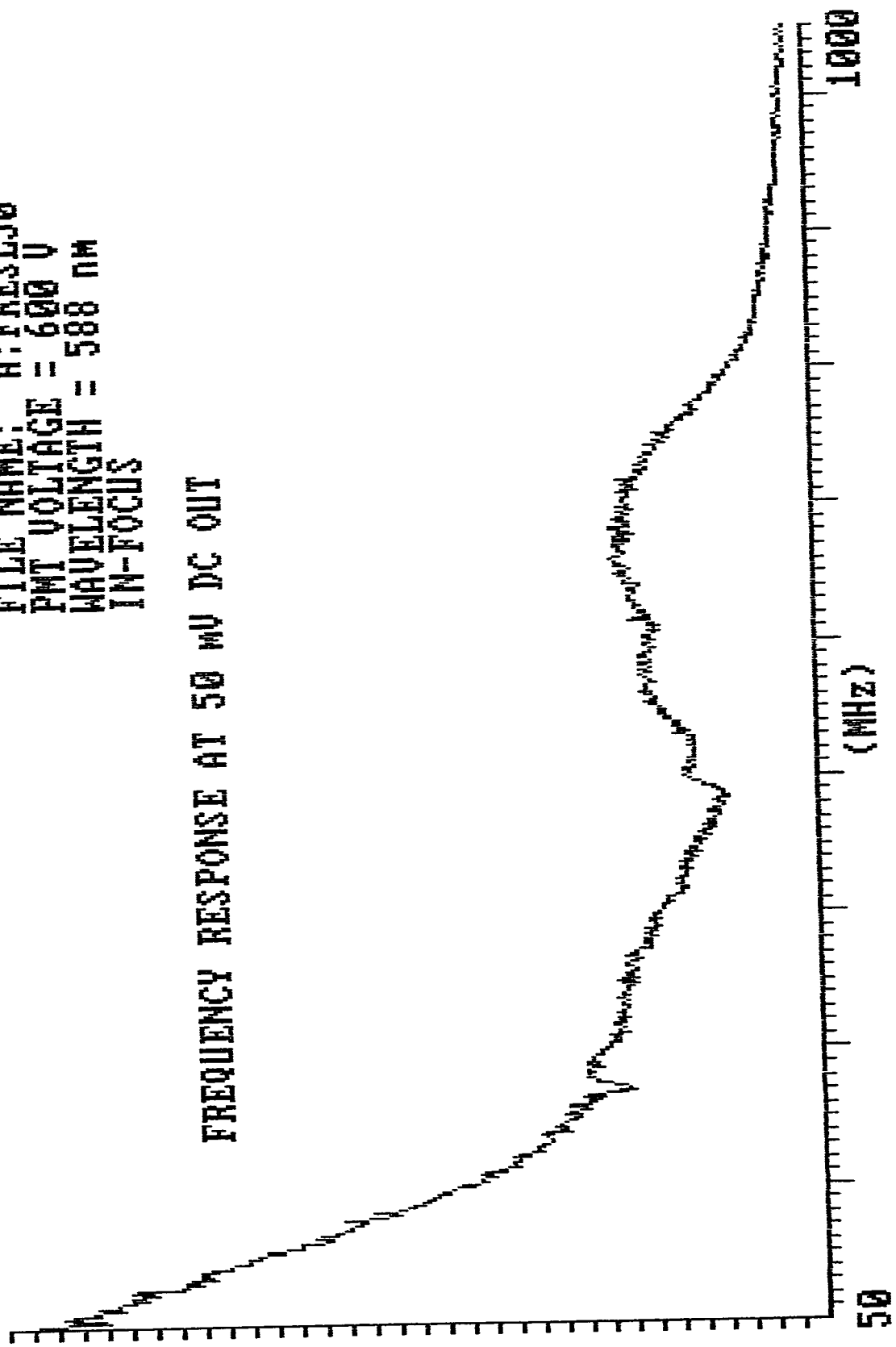
FREQUENCY RESPONSE AT 40 MV DC OUT



FILE NAME: A:FRES150  
PMT VOLTAGE = 600 V  
WAVELENGTH = 588 nm  
IN-FOCUS

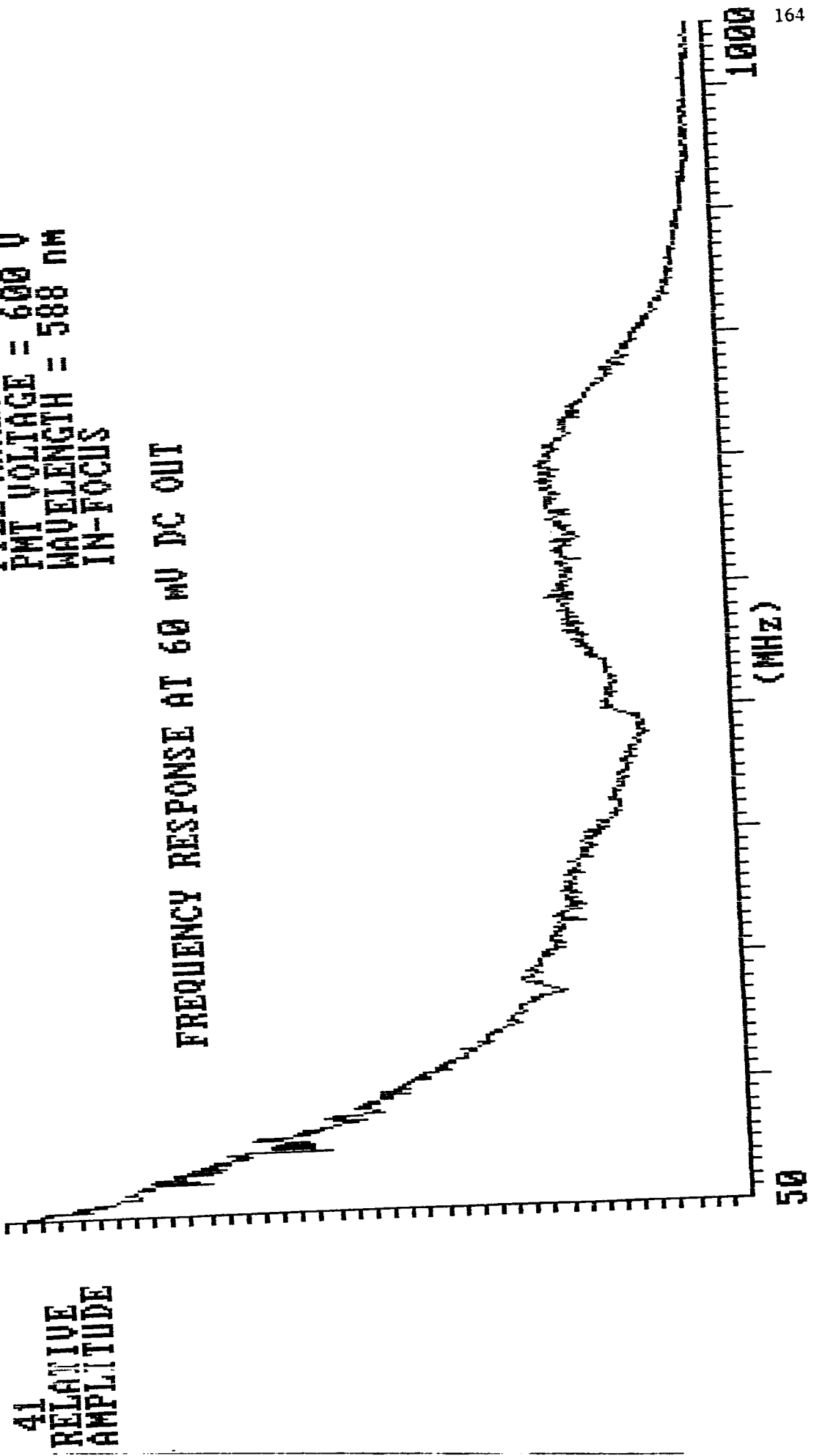
34  
RELATIVE  
AMPLITUDE

FREQUENCY RESPONSE AT 50 mV DC OUT



FILE NAME: A:FRESL60  
PMT VOLTAGE = 600 V  
WAVELENGTH = 588 nm  
IN-FOCUS

FREQUENCY RESPONSE AT 60 MV DC OUT



# **APPENDIX I.A.2**

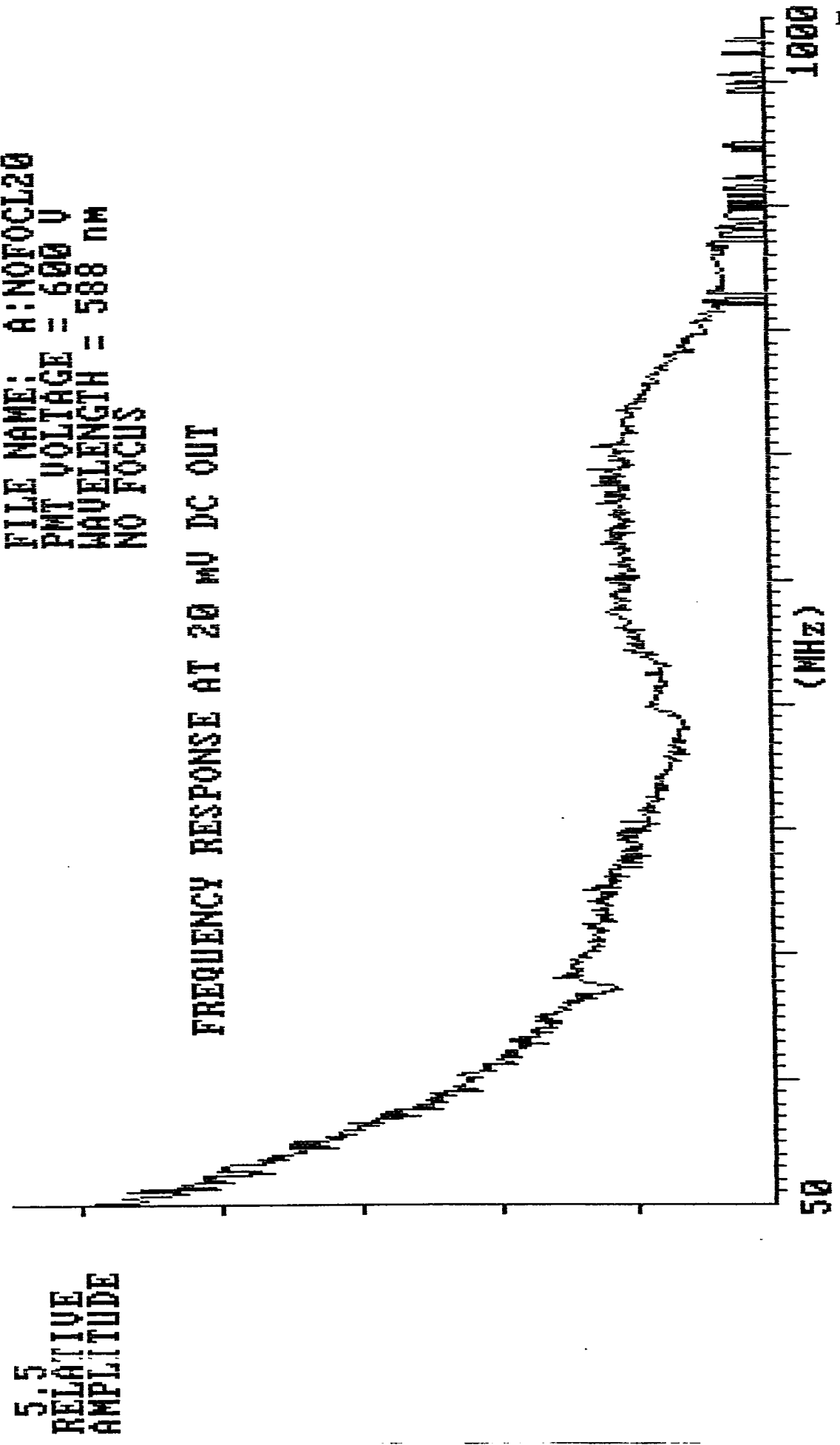
## **FREQUENCY RESPONSE**

### **WITH FOCUS:NON-FOCUS**

#### **PHOTOCATHODE ILLUMINATION**

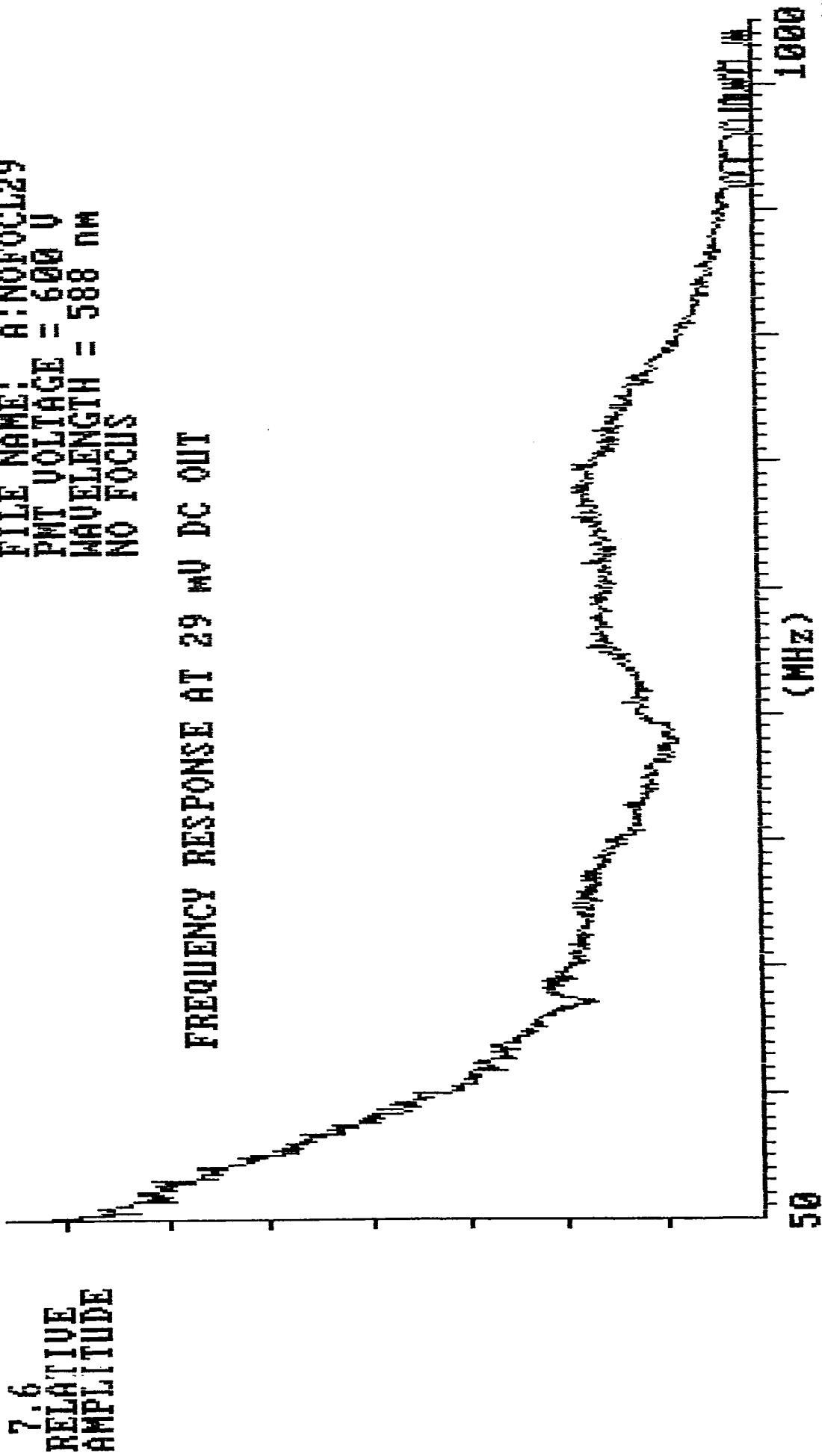
FILE NAME: A:NOFOCL20  
PMT VOLTAGE = 600 V  
WAVELENGTH = 588 nm  
NO FOCUS

FREQUENCY RESPONSE AT 20 mV DC OUT



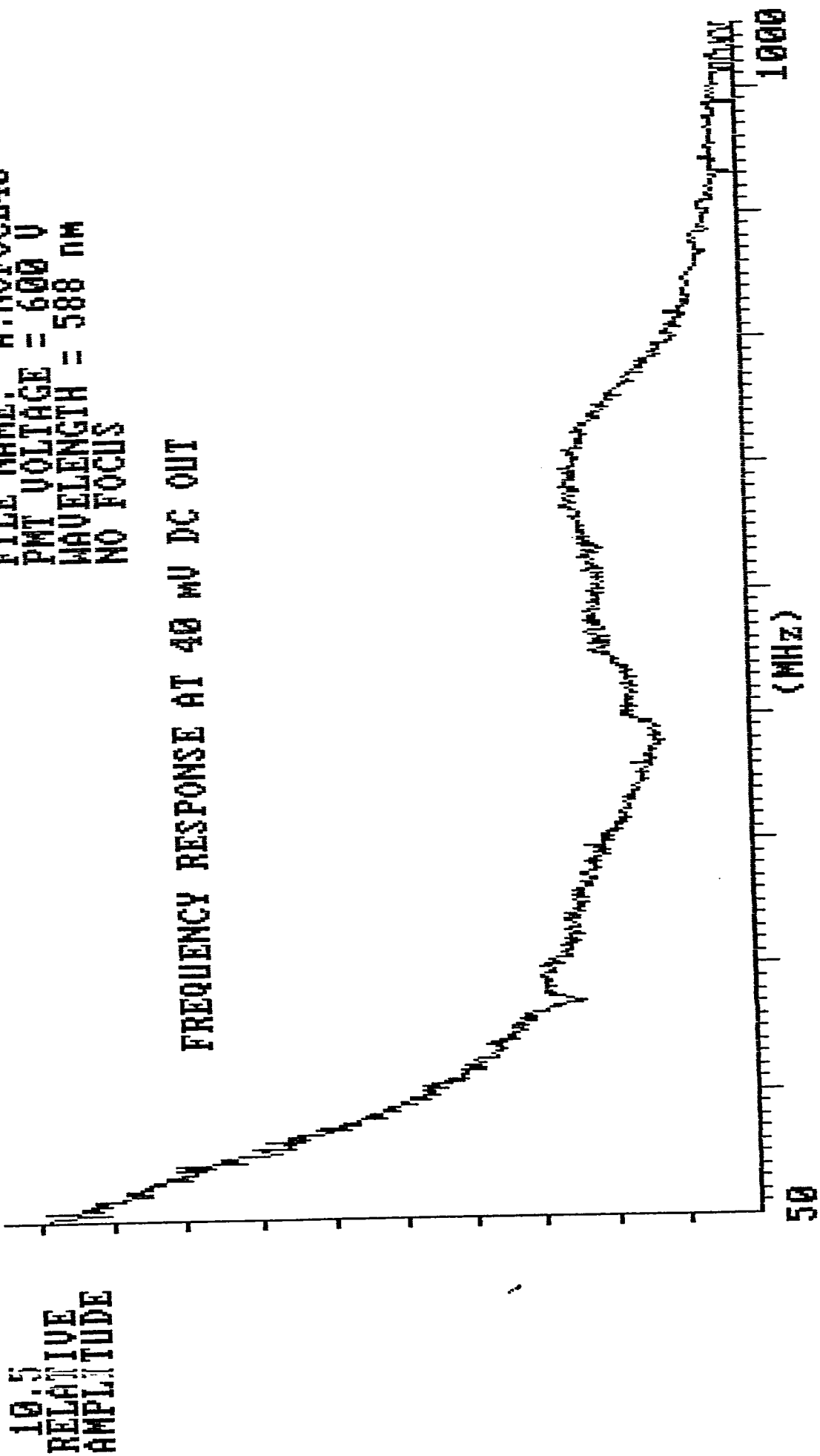
FILE NAME: A:NOFOCL29  
PMT VOLTAGE = 600 V  
WAVELENGTH = 588 NM  
NO FOCUS

FREQUENCY RESPONSE AT 29 MV DC OUT



FILE NAME: A:NOFOCL40  
PMT VOLTAGE = 600 V  
WAVELENGTH = 588 nm  
NO FOCUS

FREQUENCY RESPONSE AT 40 MV DC OUT



# **APPENDIX I.A.3**

## **FREQUENCY RESPONSE**

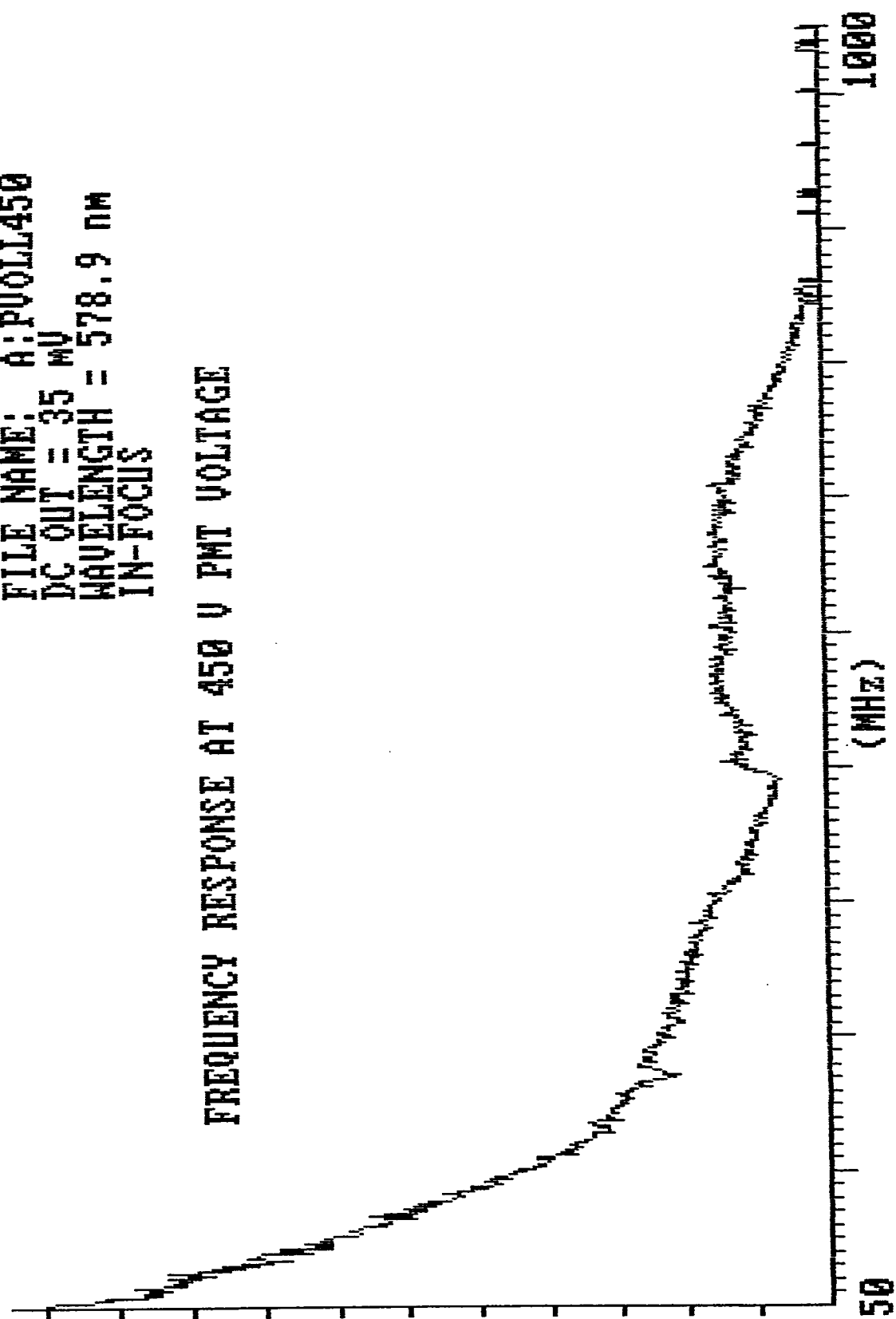
### **AT DIFFERENT PMT**

### **OPERATING VOLTAGES**

FILE NAME: A:PVOLL450  
DC OUT = 35 MV  
WAVELENGTH = 578.9 NM  
IN-FOCUS

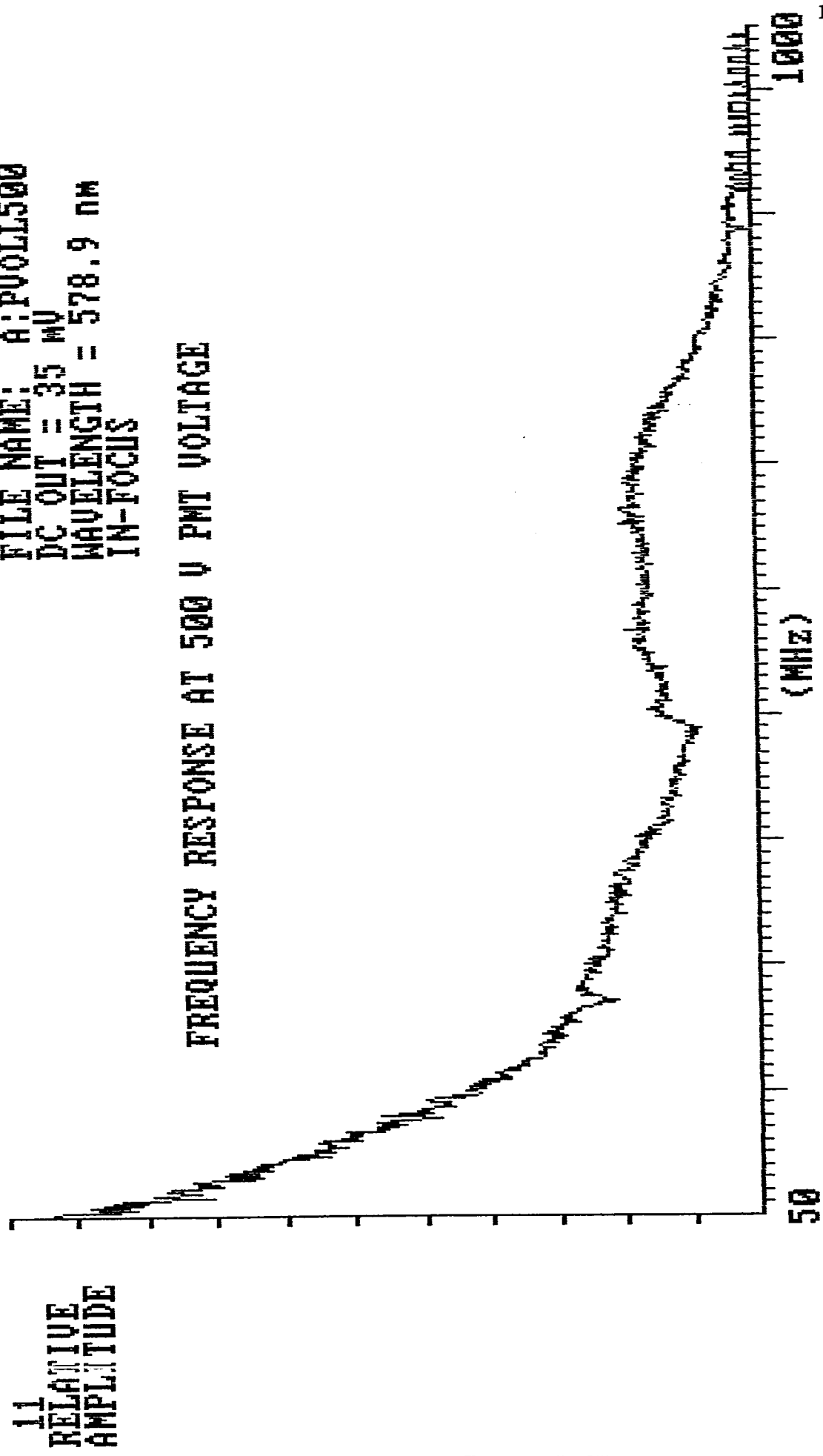
11.5  
RELATIVE  
AMPLITUDE

FREQUENCY RESPONSE AT 450 V PMT VOLTAGE



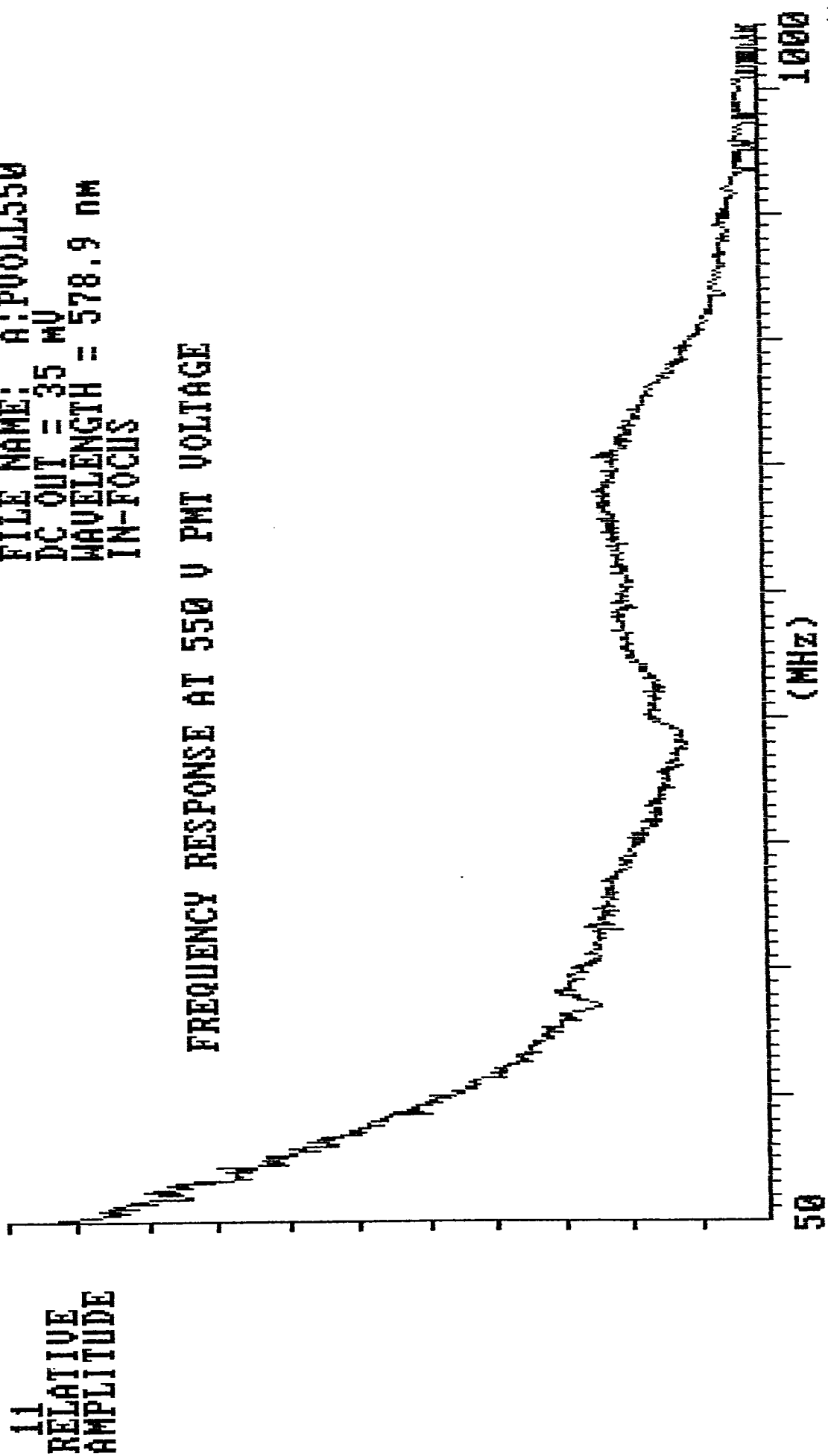
FILE NAME: A:PV011500  
DC OUT = 35 MV  
WAVELENGTH = 578.9 nm  
IN-FOCUS

FREQUENCY RESPONSE AT 500 V PMT VOLTAGE



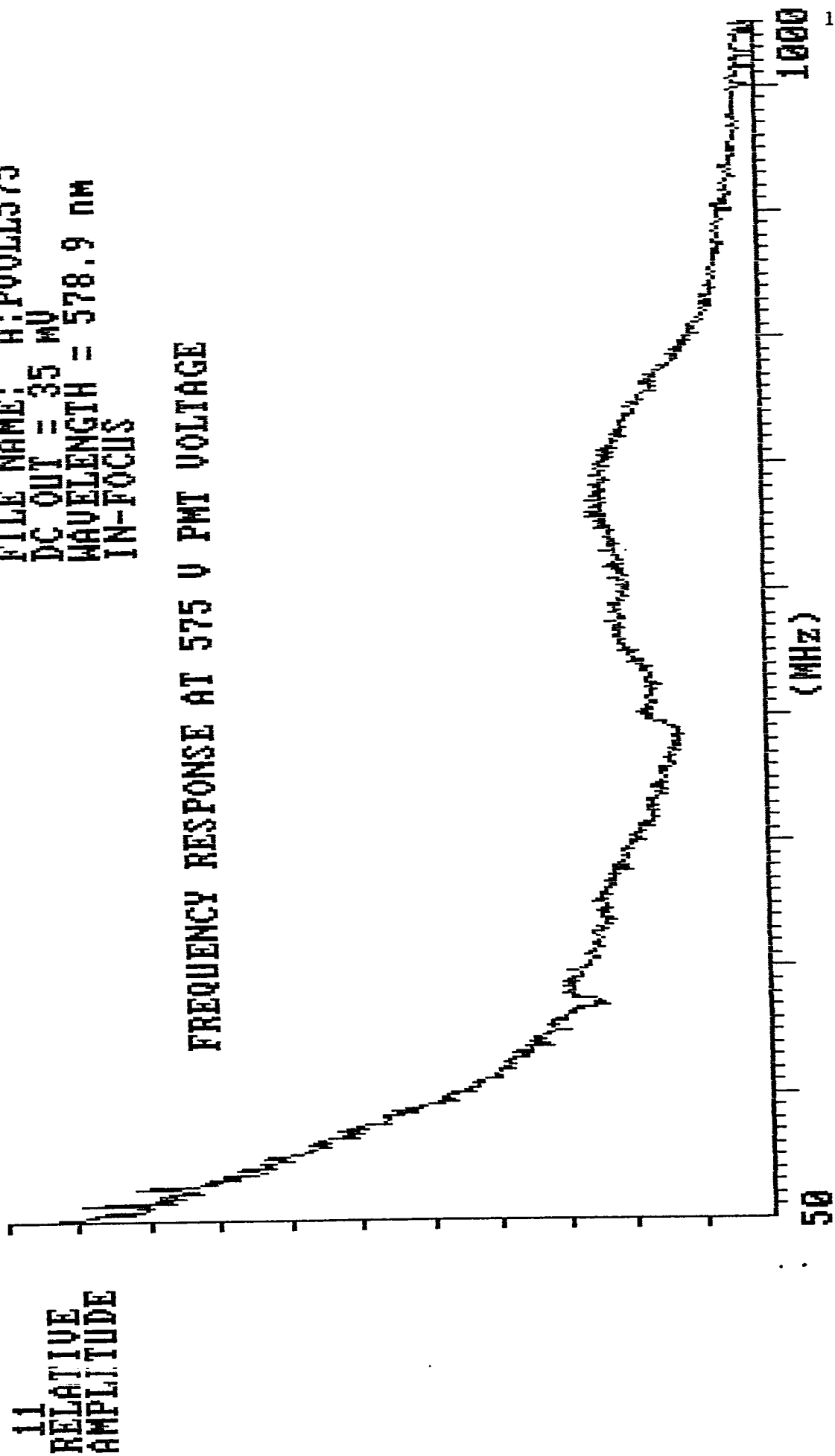
FILE NAME: A:PU01L550  
DC OUT = 35 MV  
WAVELENGTH = 578.9 NM  
IN-FOCUS

FREQUENCY RESPONSE AT 550 V PMT VOLTAGE



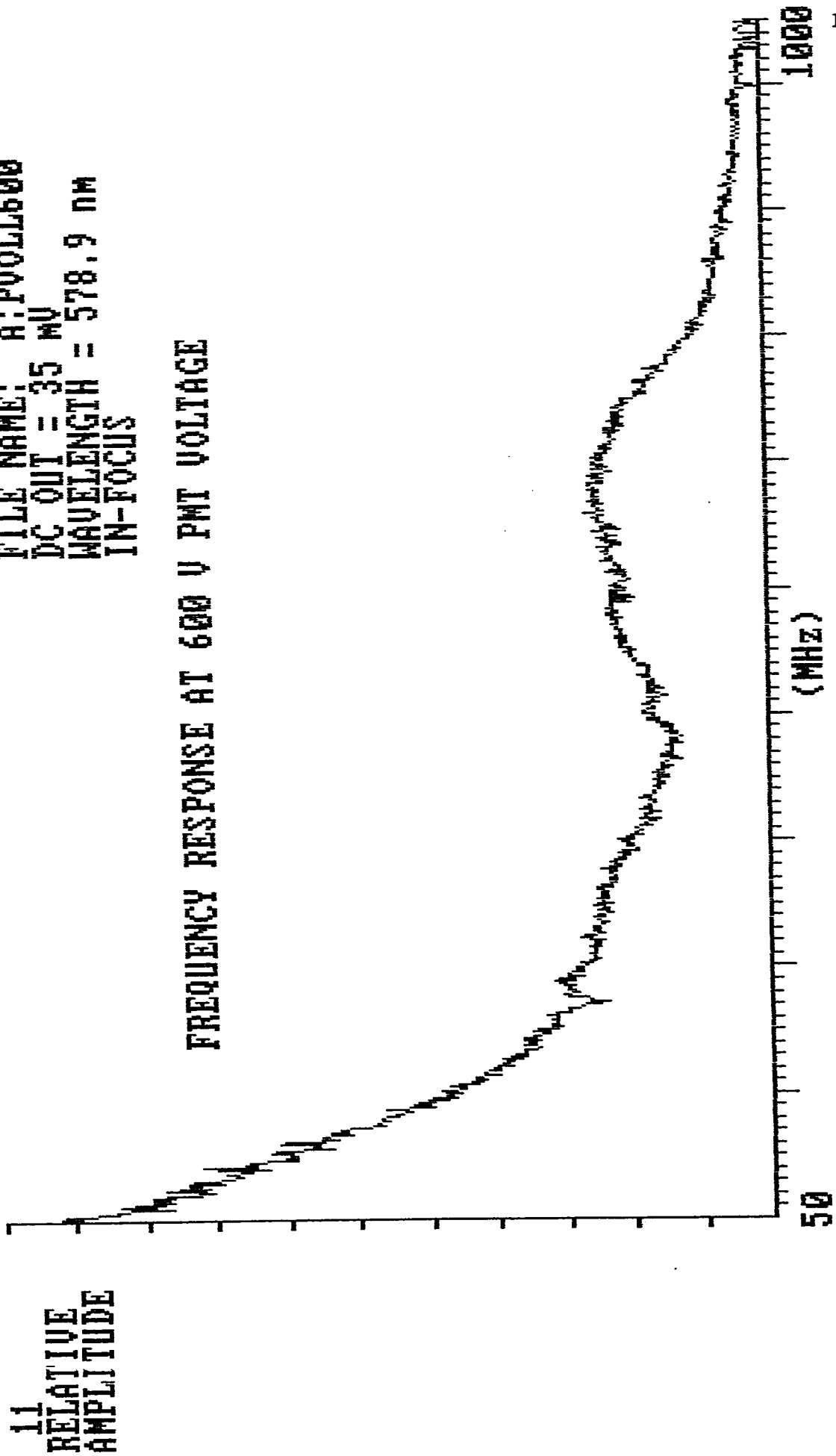
FILE NAME: A:PV011575  
DC OUT = 35 MV  
WAVELENGTH = 578.9 nm  
IN-FOCUS

FREQUENCY RESPONSE AT 575 V PMT VOLTAGE



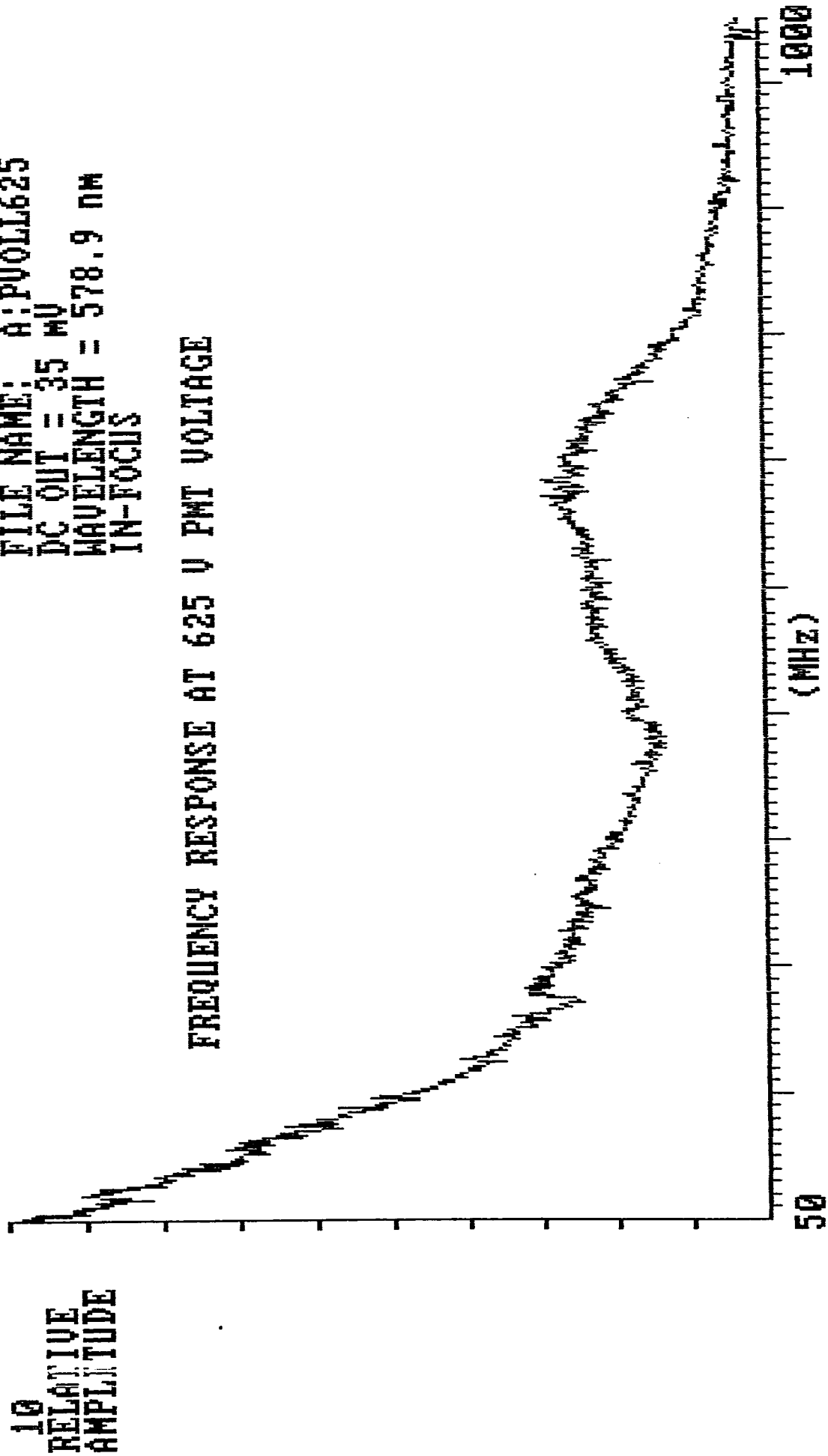
FILE NAME: A:PV01L600  
DC OUT = 35 MV  
WAVELENGTH = 578.9 NM  
IN-FOCUS

FREQUENCY RESPONSE AT 600 V PMT VOLTAGE



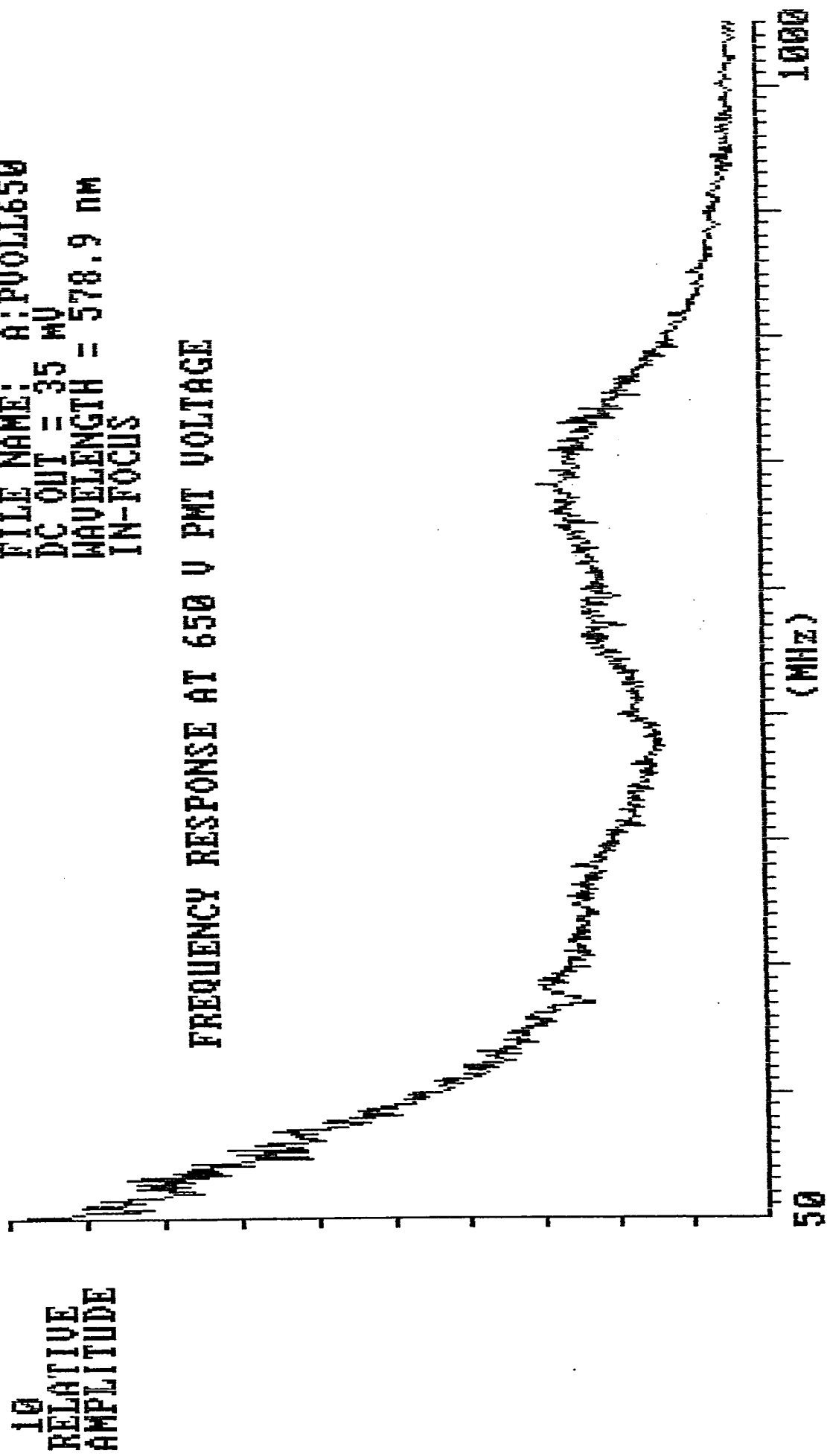
FILE NAME: A:PVOLL625  
DC OUT = 35 MV  
WAVELENGTH = 578.9 NM  
IN-FOCUS

FREQUENCY RESPONSE AT 625 V PMT VOLTAGE



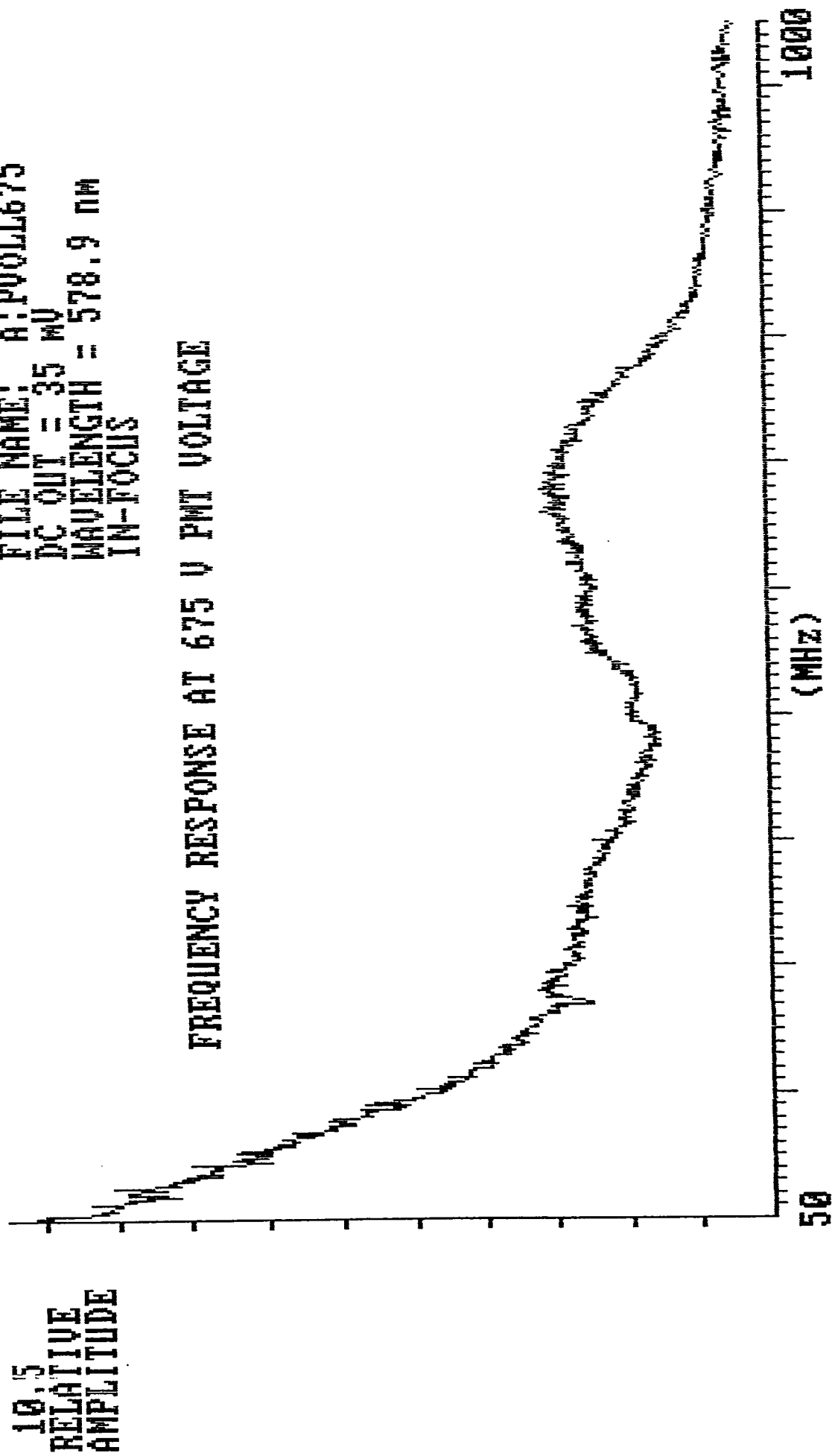
FILE NAME: A:PV01L650  
DC OUT = 35 MV  
WAVELENGTH = 578.9 NM  
IN-FOCUS

FREQUENCY RESPONSE AT 650 V PMT VOLTAGE



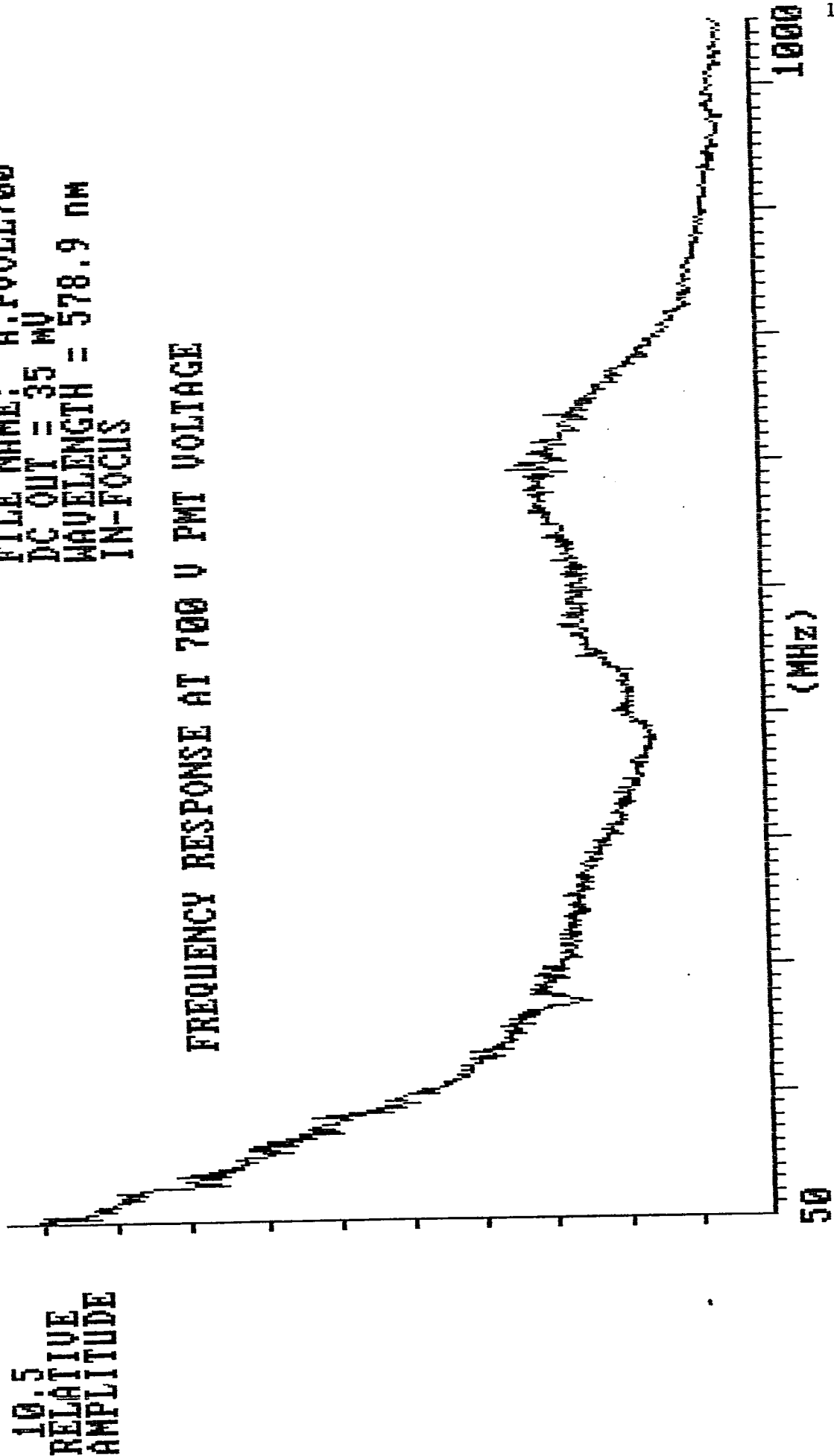
FILE NAME: A:PV01L675  
DC OUT = 35 MV  
WAVELENGTH = 578.9 NM  
IN-FOCUS

FREQUENCY RESPONSE AT 675 V PMT VOLTAGE



FILE NAME: A:PV011700  
DC OUT = 35 MV  
WAVELENGTH = 578.9 nm  
IN-FOCUS

FREQUENCY RESPONSE AT 700 V PMT VOLTAGE



# **APPENDIX I.A.4**

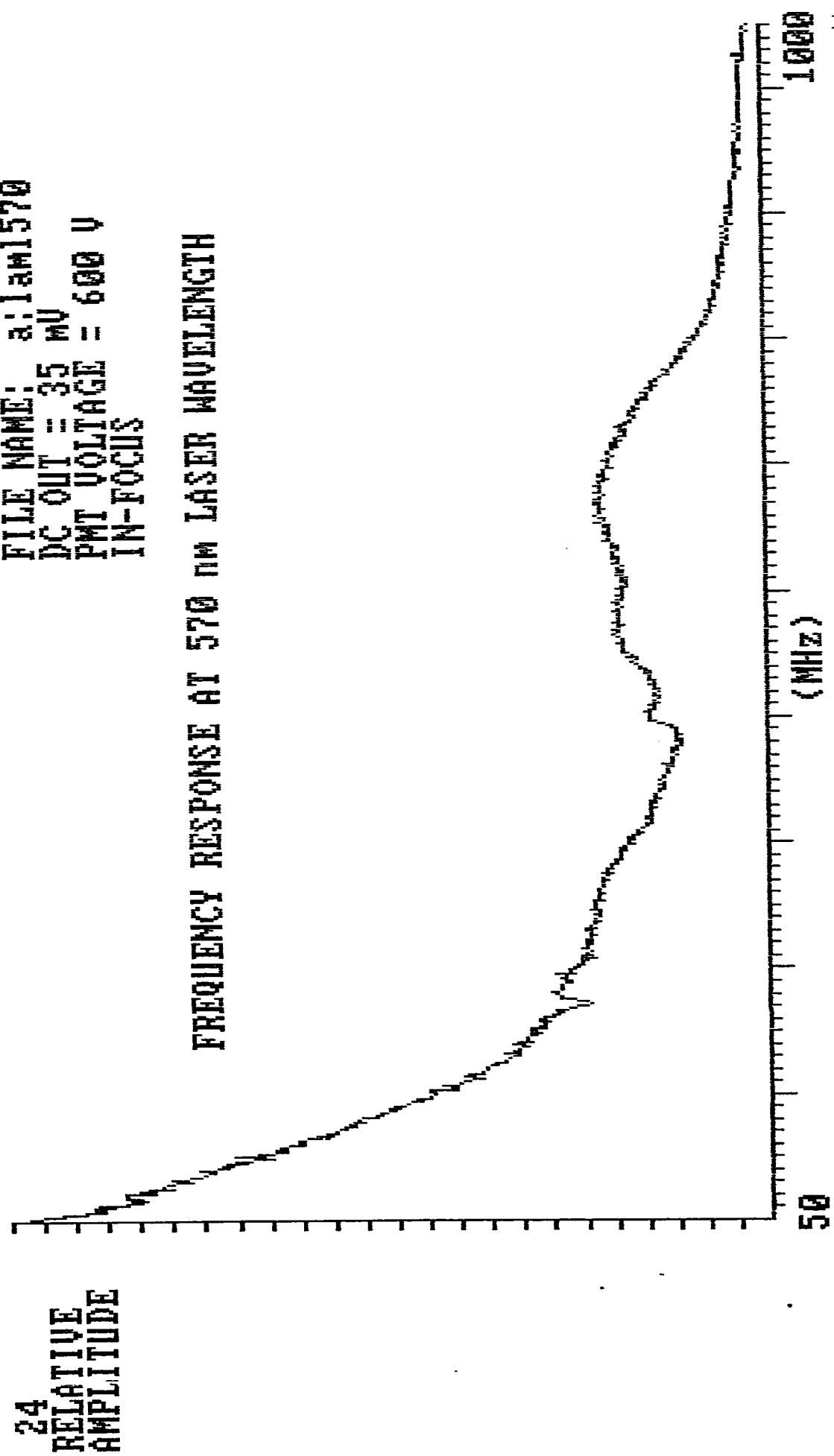
**FREQUENCY RESPONSE**

**AT DIFFERENT INCIDENT**

**LASER WAVELENGTHS**

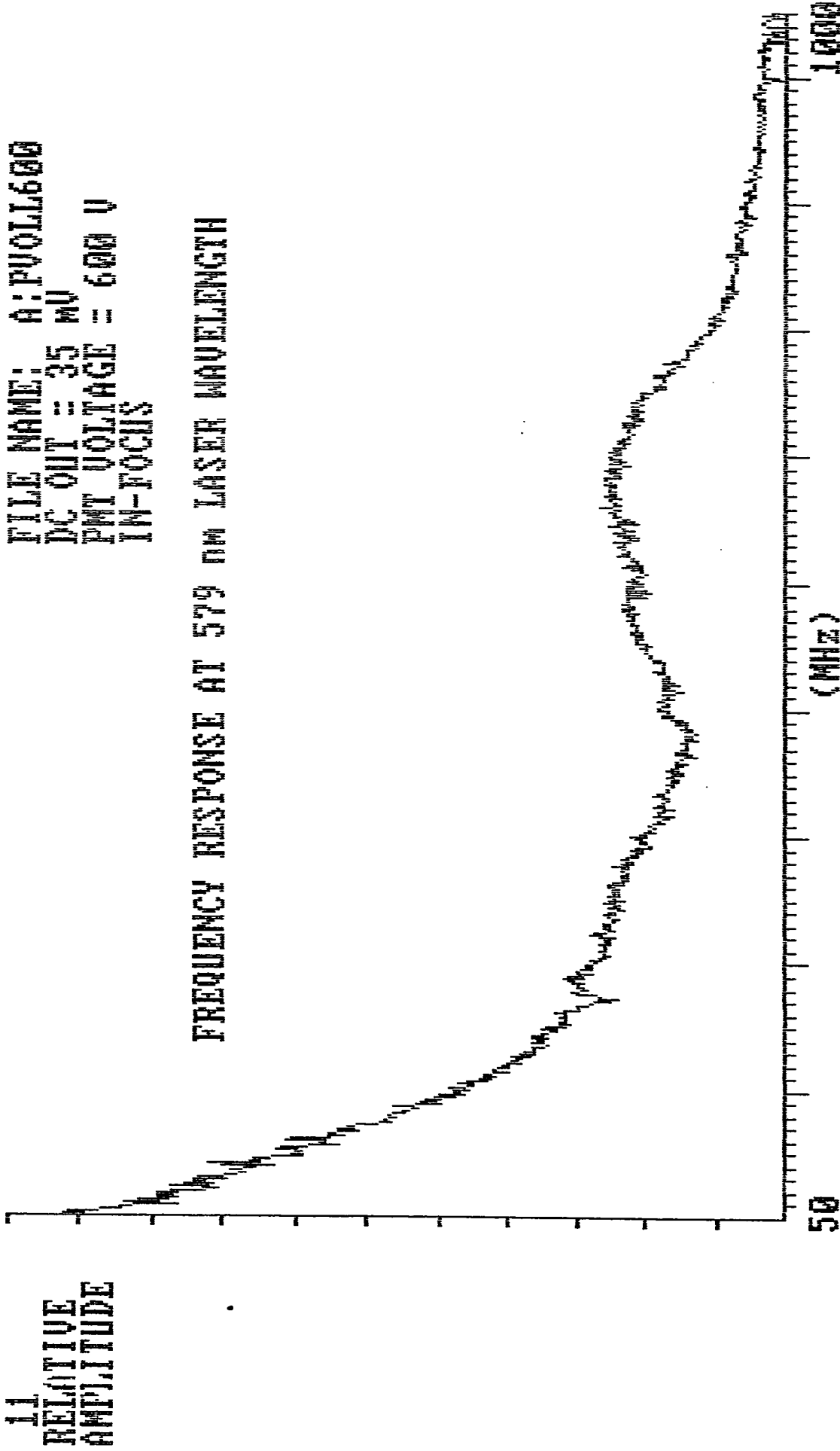
FILE NAME: a:lami570  
DC OUT = 35 MV  
PMT VOLTAGE = 600 V  
IN-FOCUS

FREQUENCY RESPONSE AT 570 nm LASER WAVELENGTH



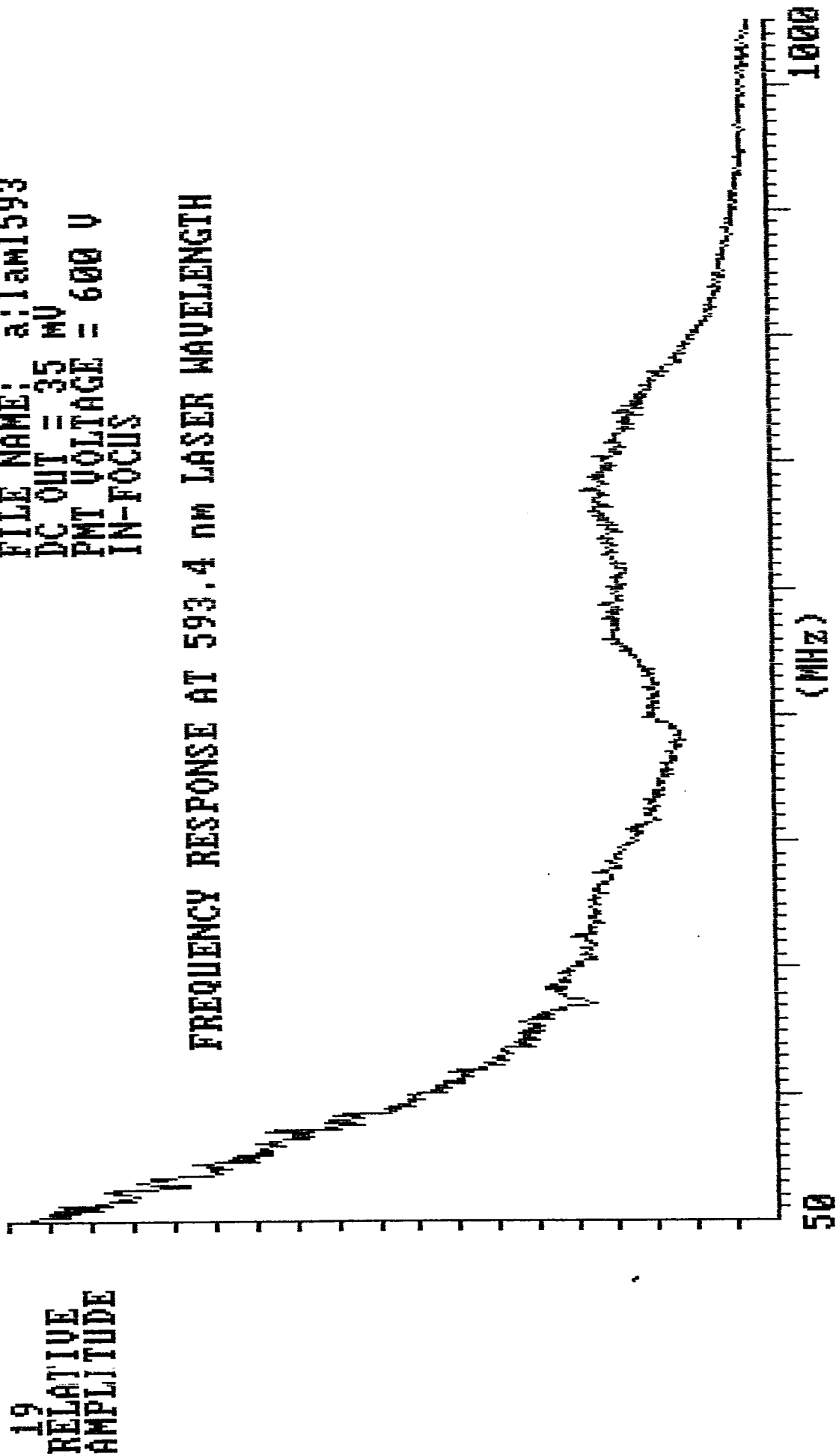
FILE NAME: A:PV01L600  
DC OUT = 35 MV  
PMT VOLTAGE = 600 V  
IN-FOCUS

FREQUENCY RESPONSE AT 579 nm LASER WAVELENGTH



FILE NAME: a:lam1593  
DC OUT = 35 MV  
PMT VOLTAGE = 600 V  
IN-FOCUS

FREQUENCY RESPONSE AT 593.4 nm LASER WAVELENGTH



# **APPENDIX I.A.5**

**FREQUENCY RESPONSE**

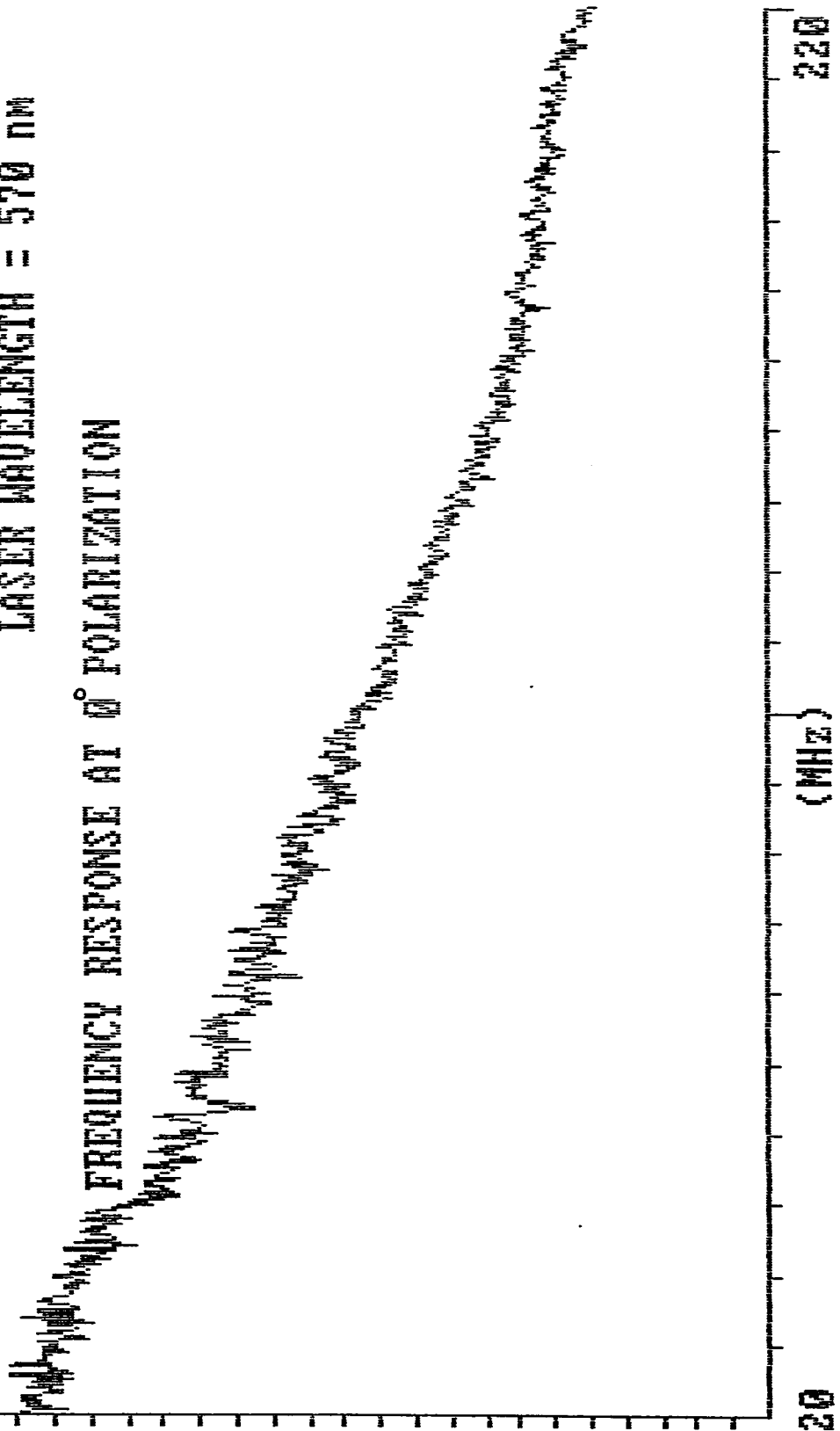
**AT DIFFERENT INCIDENT**

**LIGHT POLARIZATIONS**

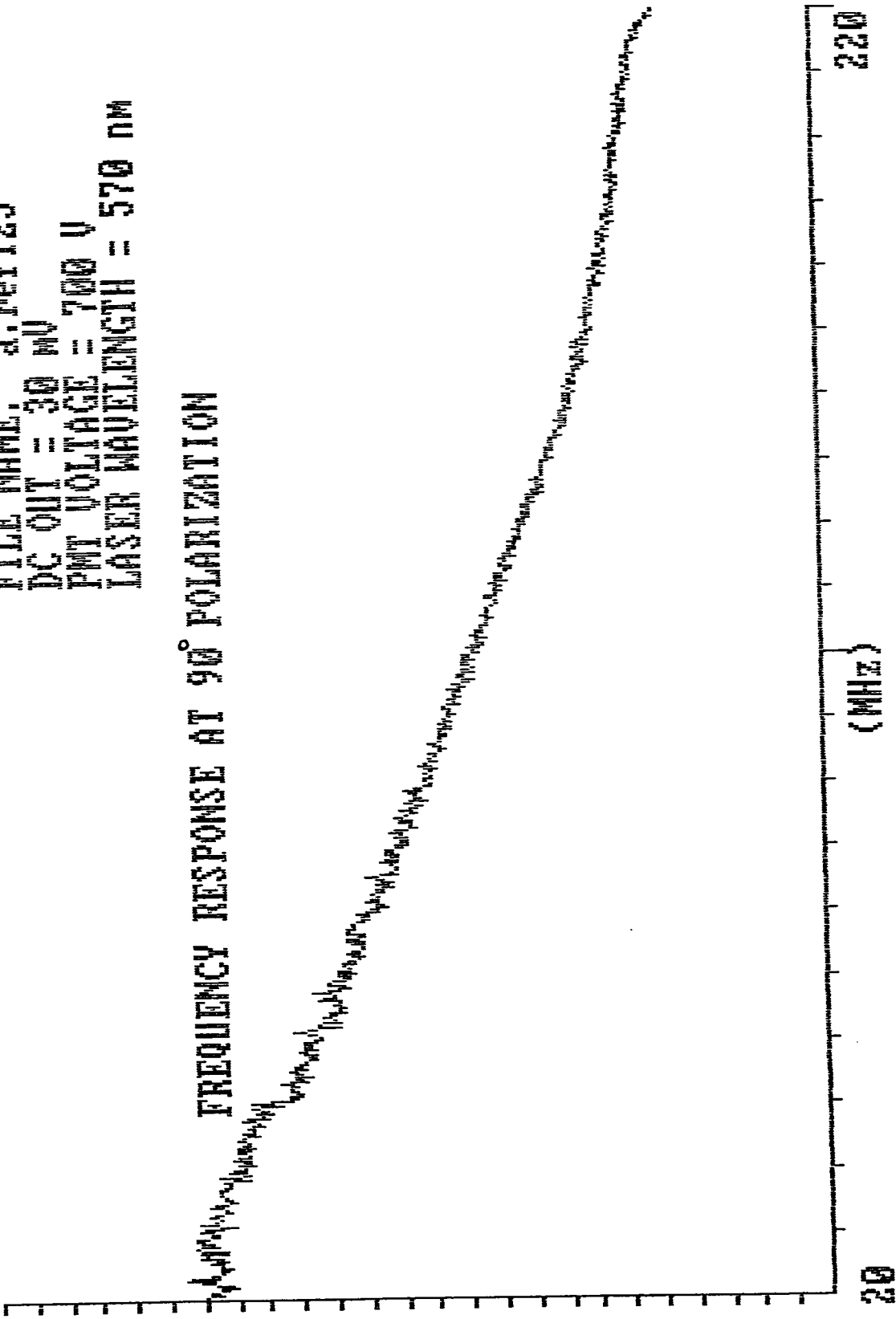
25  
RELATIVE  
AMPLITUDE

FILE NAME: a:ref1254  
DC OUT = 30 MV  
PMT VOLTAGE = 700 V  
LASER WAVELENGTH = 570 nm

FREQUENCY RESPONSE AT 0° POLARIZATION



FILE NAME: a:ref125  
DC OUT = 30 MV  
PMT VOLTAGE = 700 V  
LASER WAVELENGTH = 570 nm



# **APPENDIX I.B**

**ROSE BENGAL FLUORESCENCE**

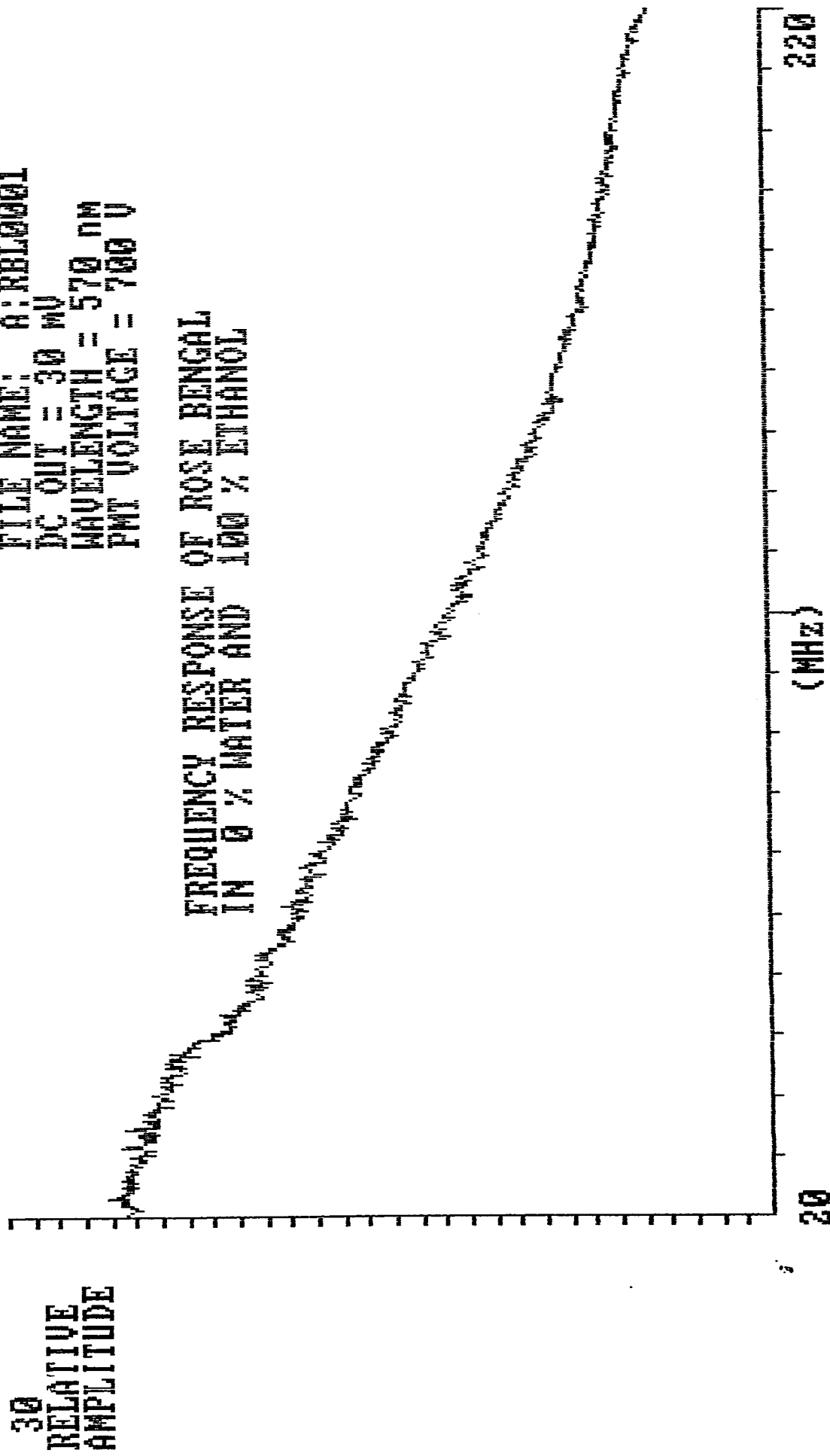
**FREQUENCY RESPONSE SPECTRA**

**AT DIFFERENT**

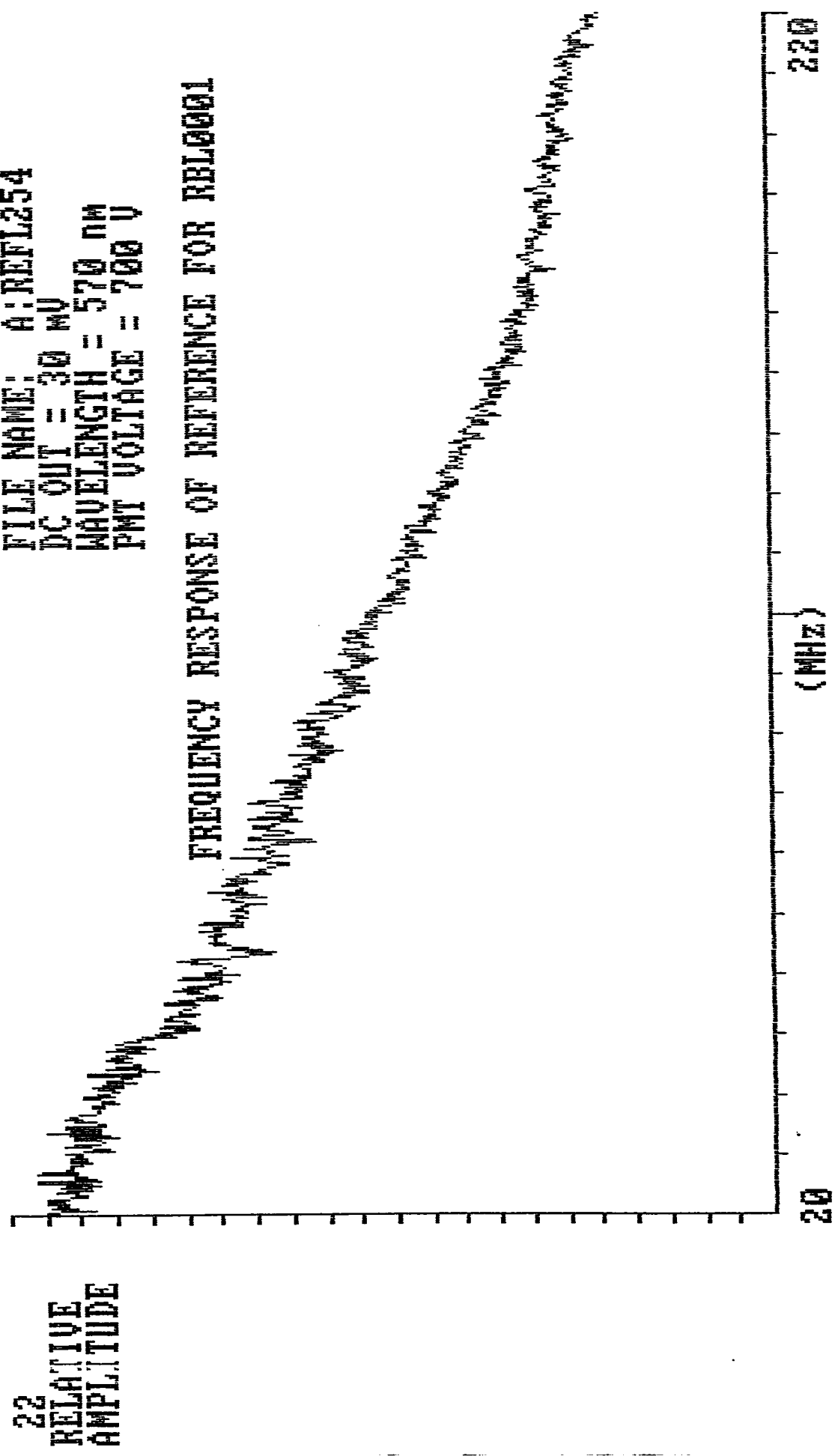
**WATER - ETHANOL MIXTURES**

FILE NAME: A:RBL0001  
DC OUT = 30 MV  
WAVELENGTH = 570 NM  
PMT VOLTAGE = 700 V

FREQUENCY RESPONSE OF ROSE BENGAL  
IN 0% WATER AND 100% ETHANOL

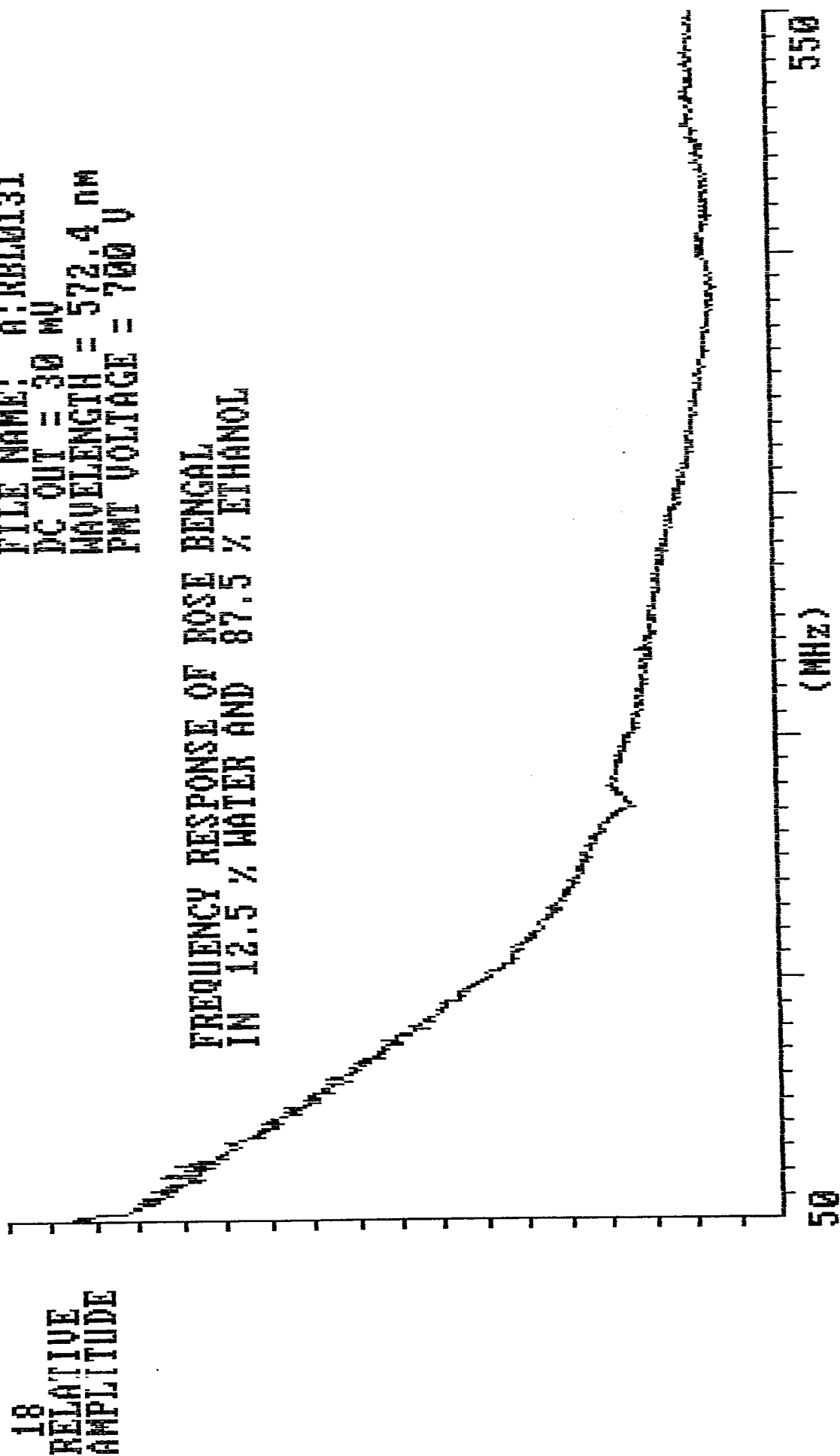


FILE NAME: A:REFL254  
DC OUT = 30 MV  
WAVELENGTH = 570 nm  
PMT VOLTAGE = 700 V



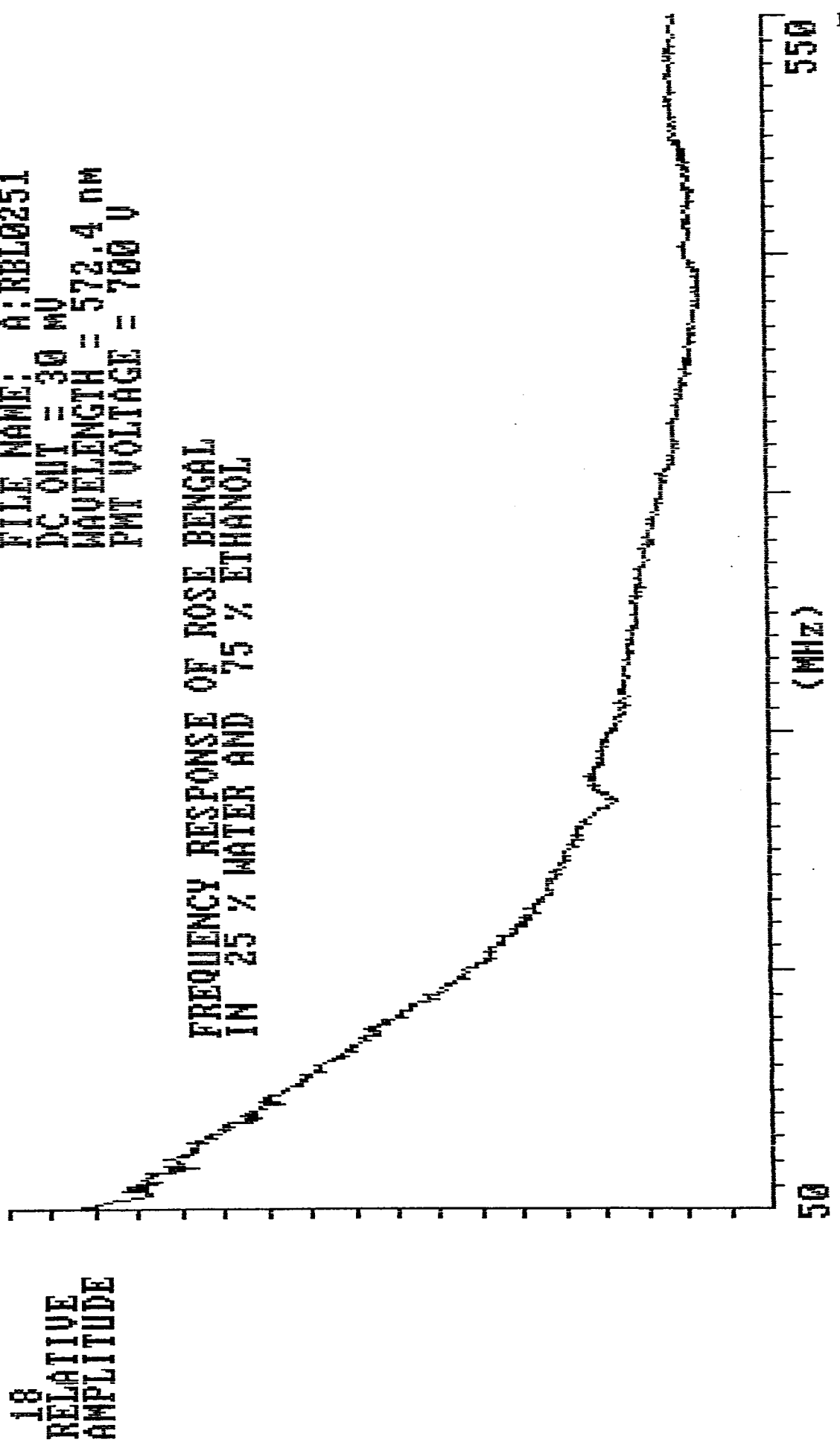
FILE NAME: A:RB10131  
DC OUT = 30 MV  
WAVELENGTH = 572.4 NM  
PMT VOLTAGE = 700 V

FREQUENCY RESPONSE OF ROSE BENGAL  
IN 12.5 % WATER AND 87.5 % ETHANOL



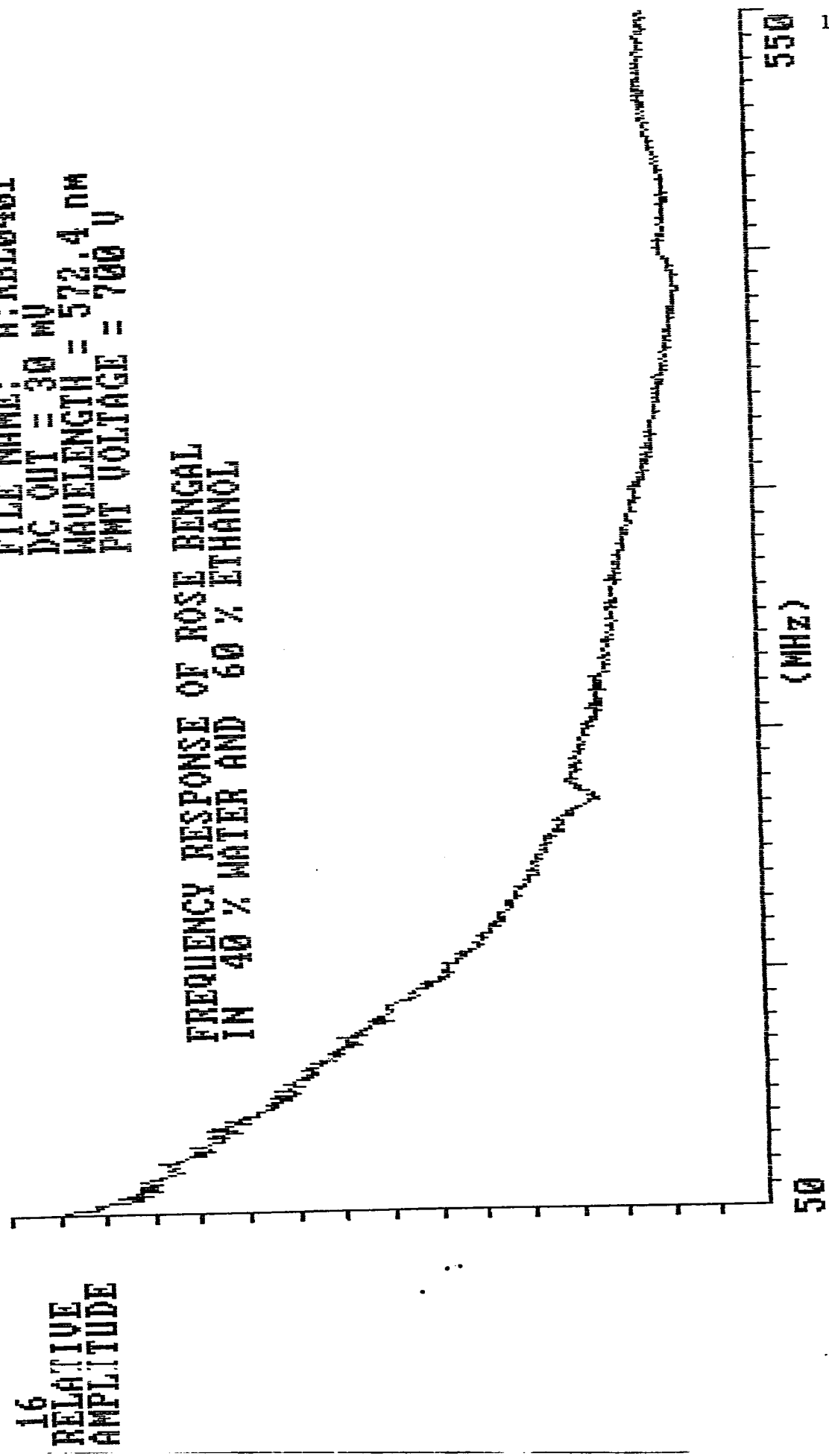
FILE NAME: A:RBL0251  
DC OUT = 30 MV  
WAVELENGTH = 572.4 NM  
PMT VOLTAGE = 700 V

FREQUENCY RESPONSE OF ROSE BENGAL  
IN 25 % WATER AND 75 % ETHANOL



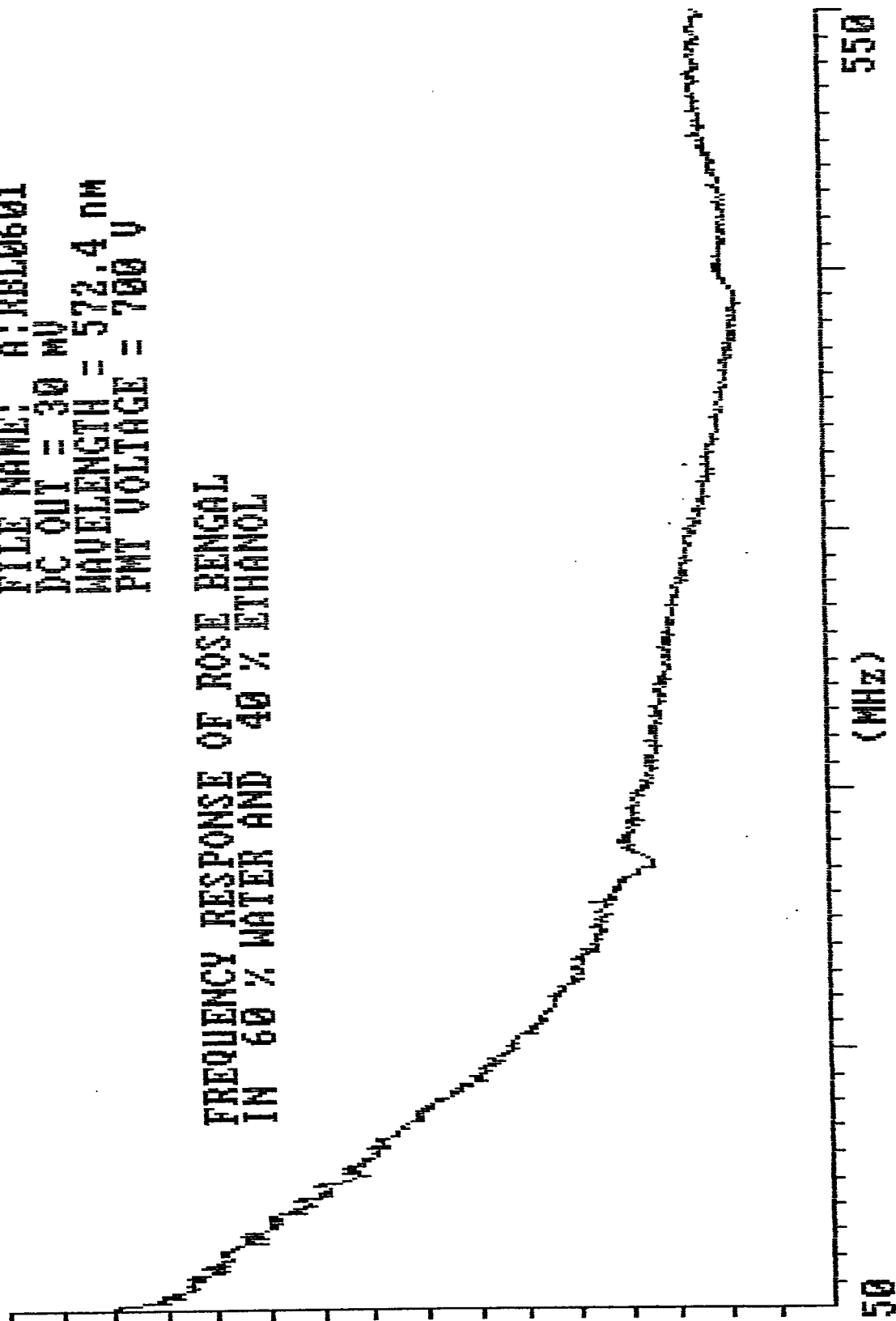
FILE NAME: A:RB10401  
DC OUT = 30 mV  
WAVELENGTH = 572.4 nm  
PMT VOLTAGE = 700 V

FREQUENCY RESPONSE OF ROSE BENGAL  
IN 40 % WATER AND 60 % ETHANOL



FILE NAME: A:HEL0601  
DC OUT = 30 MV  
WAVELENGTH = 572.4 nm  
PMT VOLTAGE = 700 V

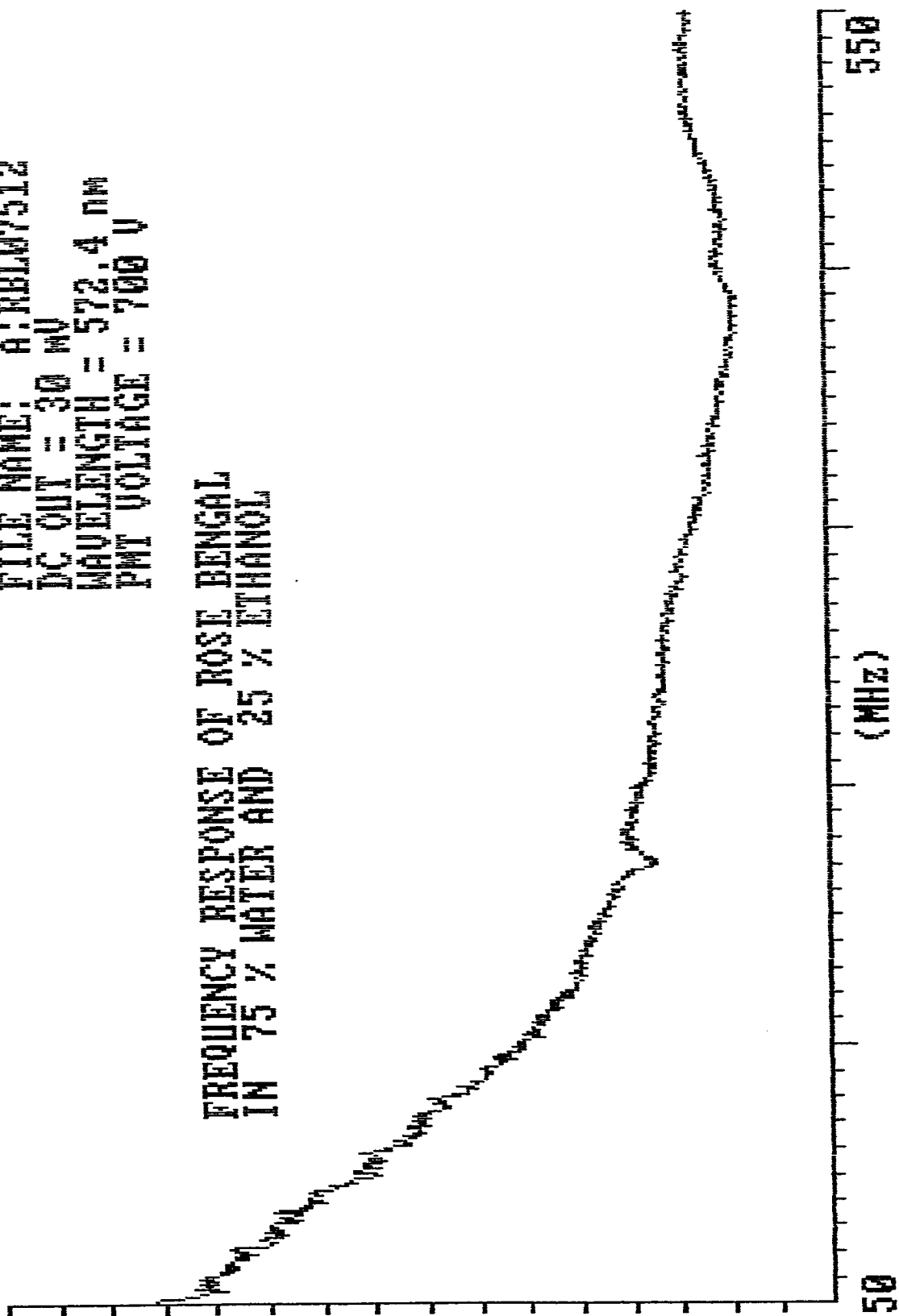
FREQUENCY RESPONSE OF ROSE BENGAL  
IN 60 % WATER AND 40 % ETHANOL



FILE NAME: A:RBL07512  
DC OUT = 30 MV  
WAVELENGTH = 572.4 nm  
PMT VOLTAGE = 700 V

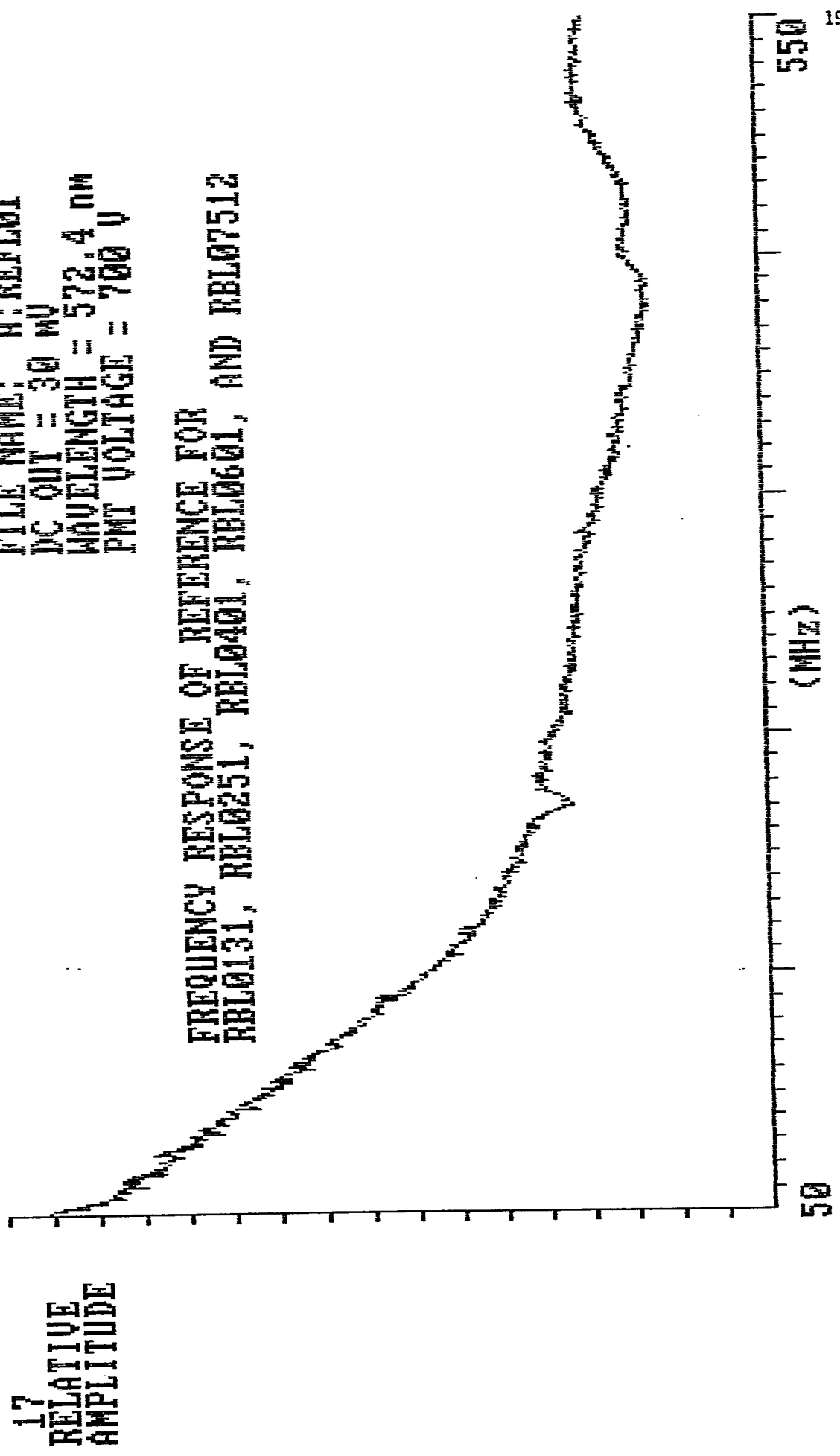
FREQUENCY RESPONSE OF ROSE BENGAL  
IN 75 % WATER AND 25 % ETHANOL

16  
RELATIVE  
AMPLITUDE



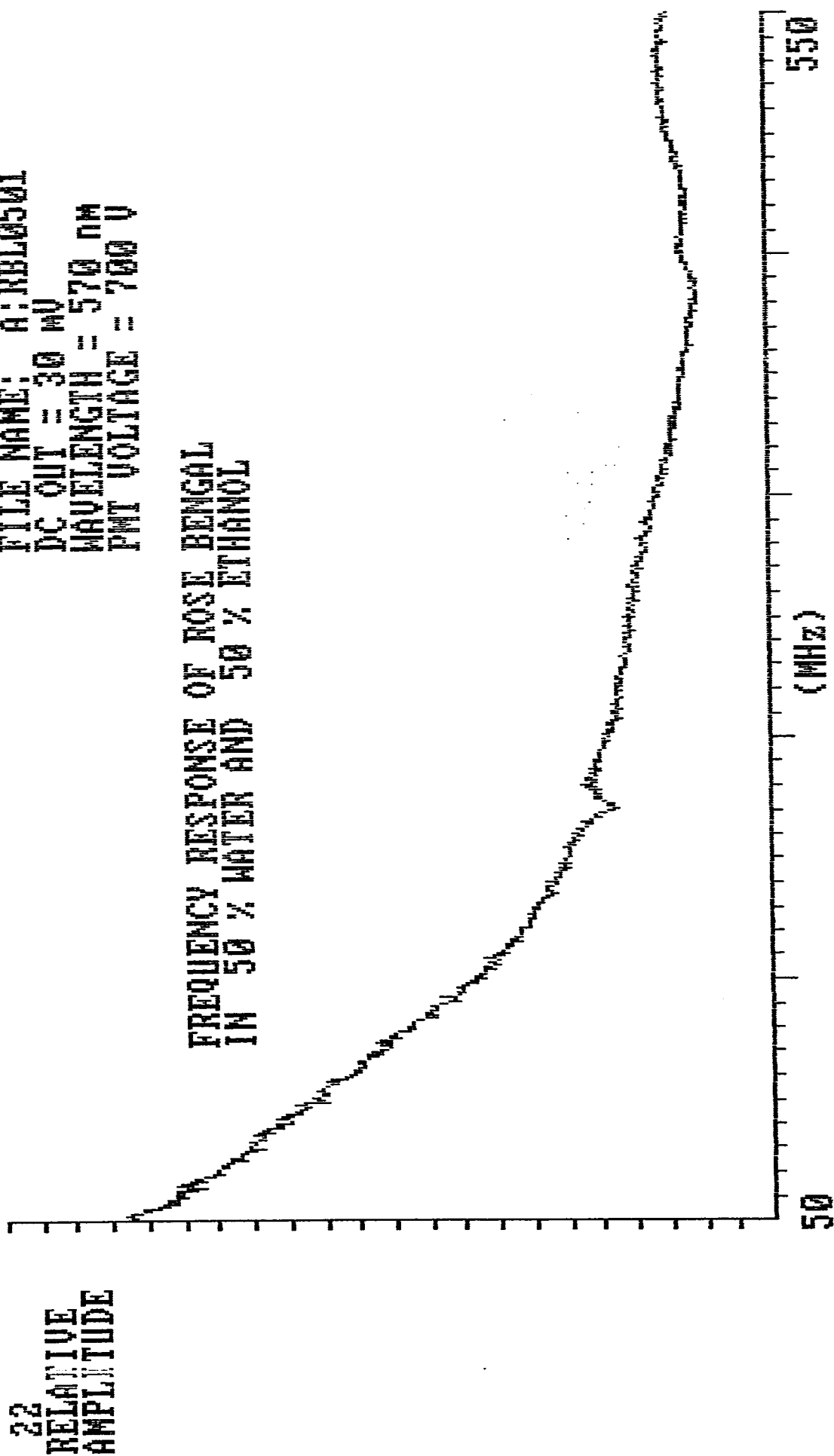
FILE NAME: A:REFL01  
DC OUT = 30 mV  
WAVELENGTH = 572.4 nm  
PMT VOLTAGE = 700 V

FREQUENCY RESPONSE OF REFERENCE FOR  
RBL0131, RBL0251, RBL0401, RBL0601, AND RBL07512



FILE NAME: A:RBL0501  
DC OUT = 30 MV  
WAVELENGTH = 570 NM  
PMT VOLTAGE = 700 V

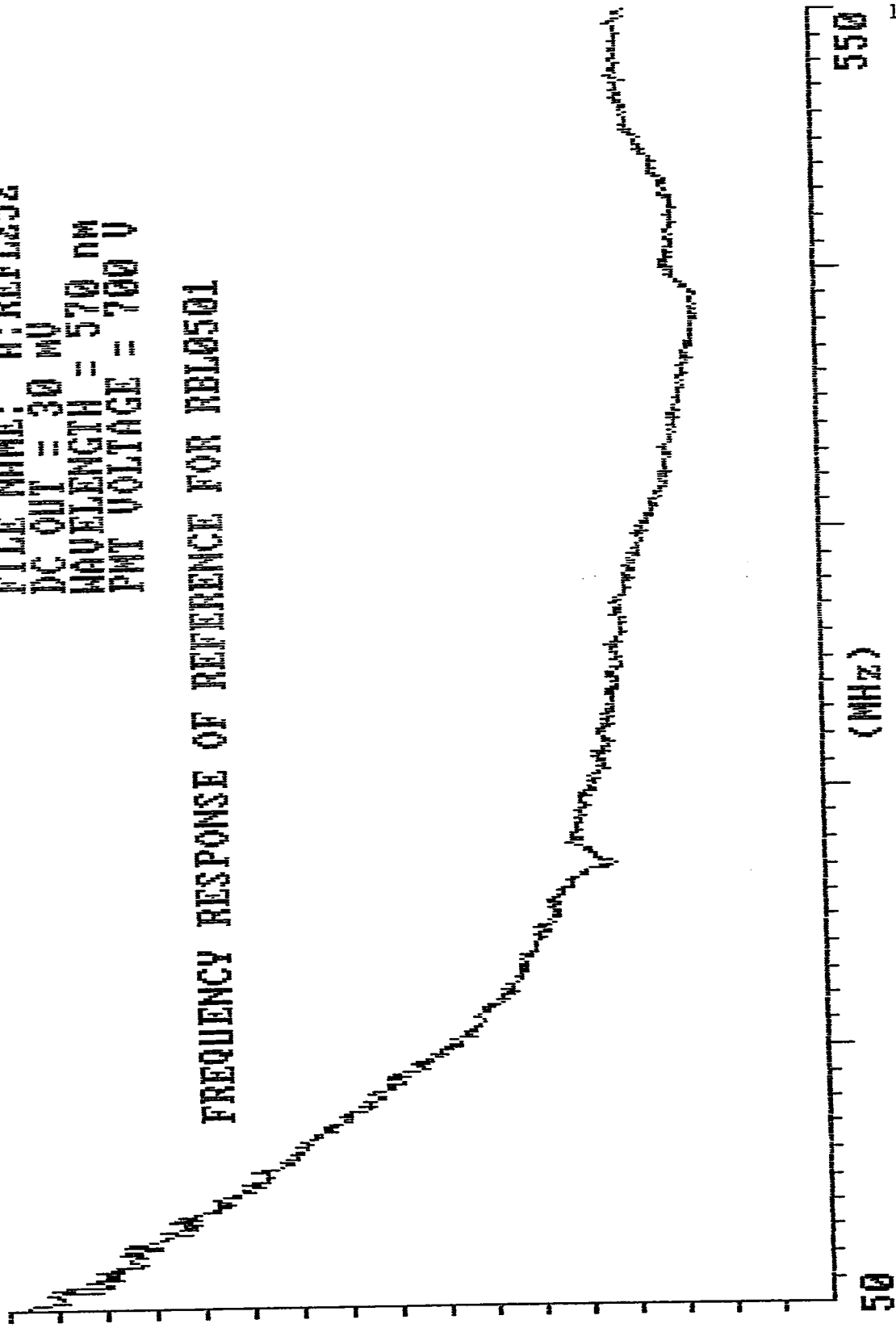
FREQUENCY RESPONSE OF ROSE BENGAL  
IN 50 % WATER AND 50 % ETHANOL



FILE NAME: A:REFL252  
DC OUT = 30 MV  
WAVELENGTH = 570 nm  
PWT VOLTAGE = 700 V

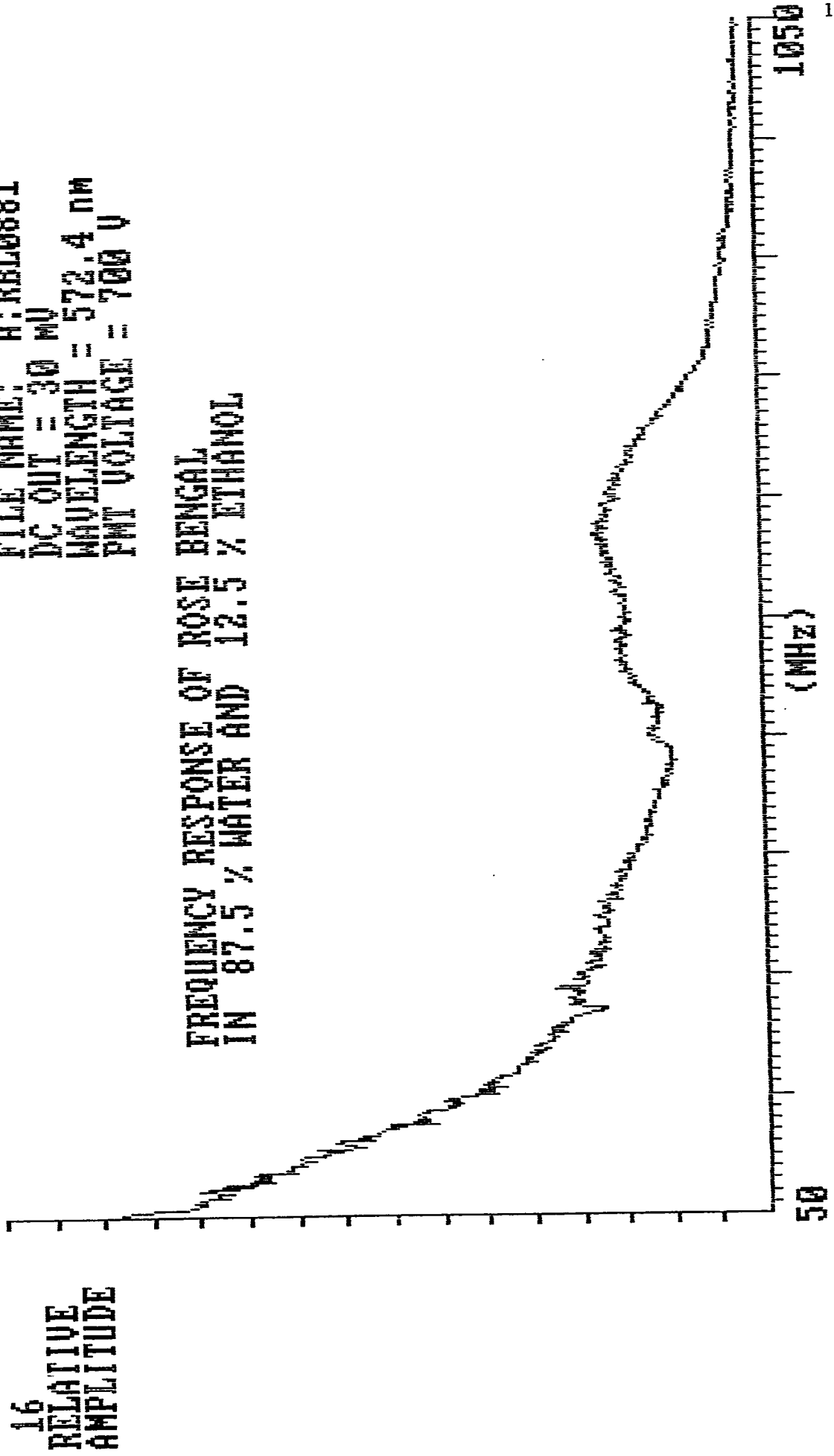
17  
RELATIVE  
AMPLITUDE

FREQUENCY RESPONSE OF REFERENCE FOR RBL0501



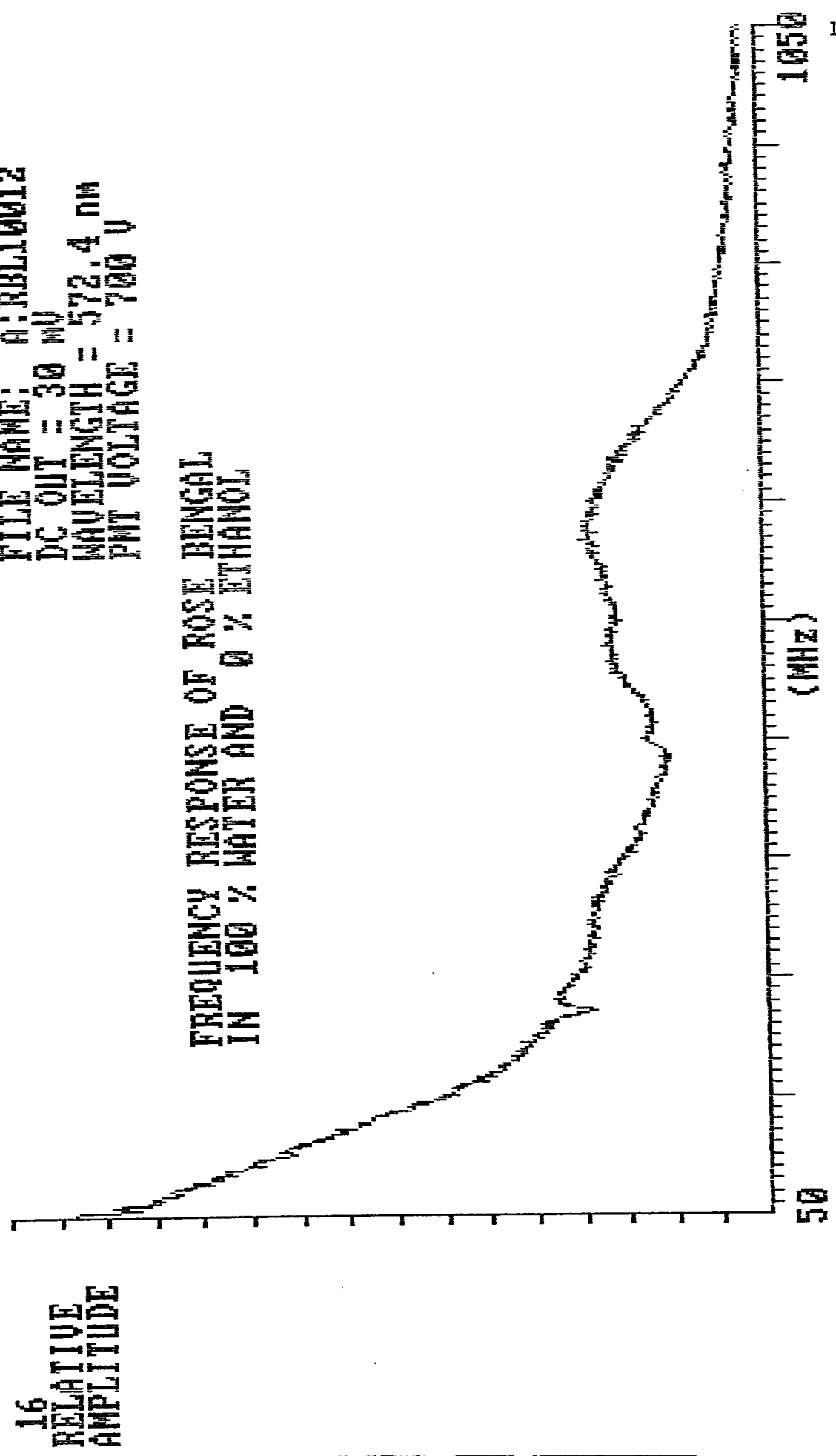
FILE NAME: A:RRL0881  
DC OUT = 30 MV  
WAVELENGTH = 572.4 NM  
PMT VOLTAGE = 700 V

FREQUENCY RESPONSE OF ROSE BENGAL  
IN 87.5 % WATER AND 12.5 % ETHANOL



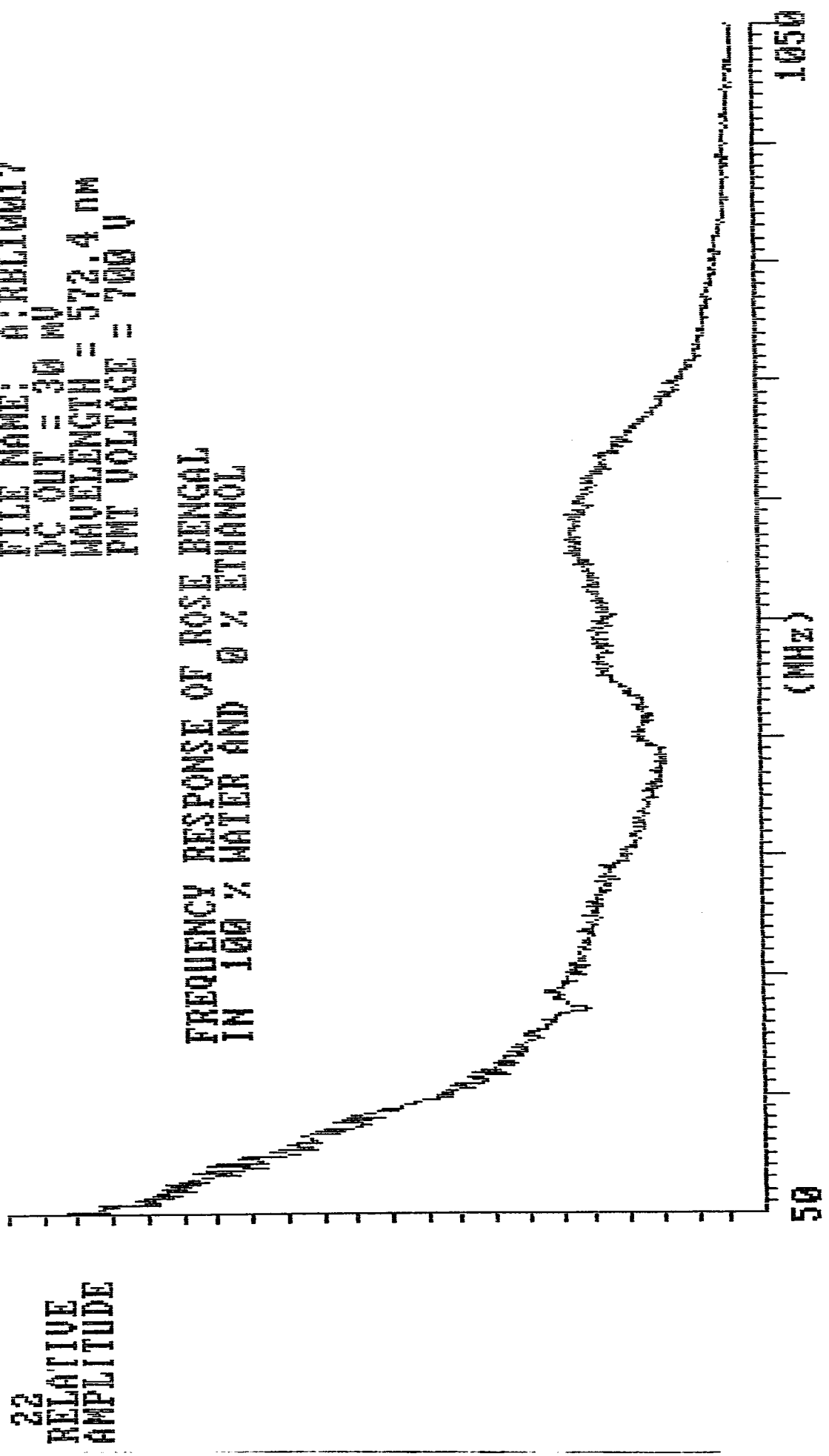
FILE NAME: A:RBL10012  
DC OUT = 30 MV  
WAVELENGTH = 572.4 NM  
PMT VOLTAGE = 700 V

FREQUENCY RESPONSE OF ROSE BENGAL  
IN 100 % WATER AND 0 % ETHANOL



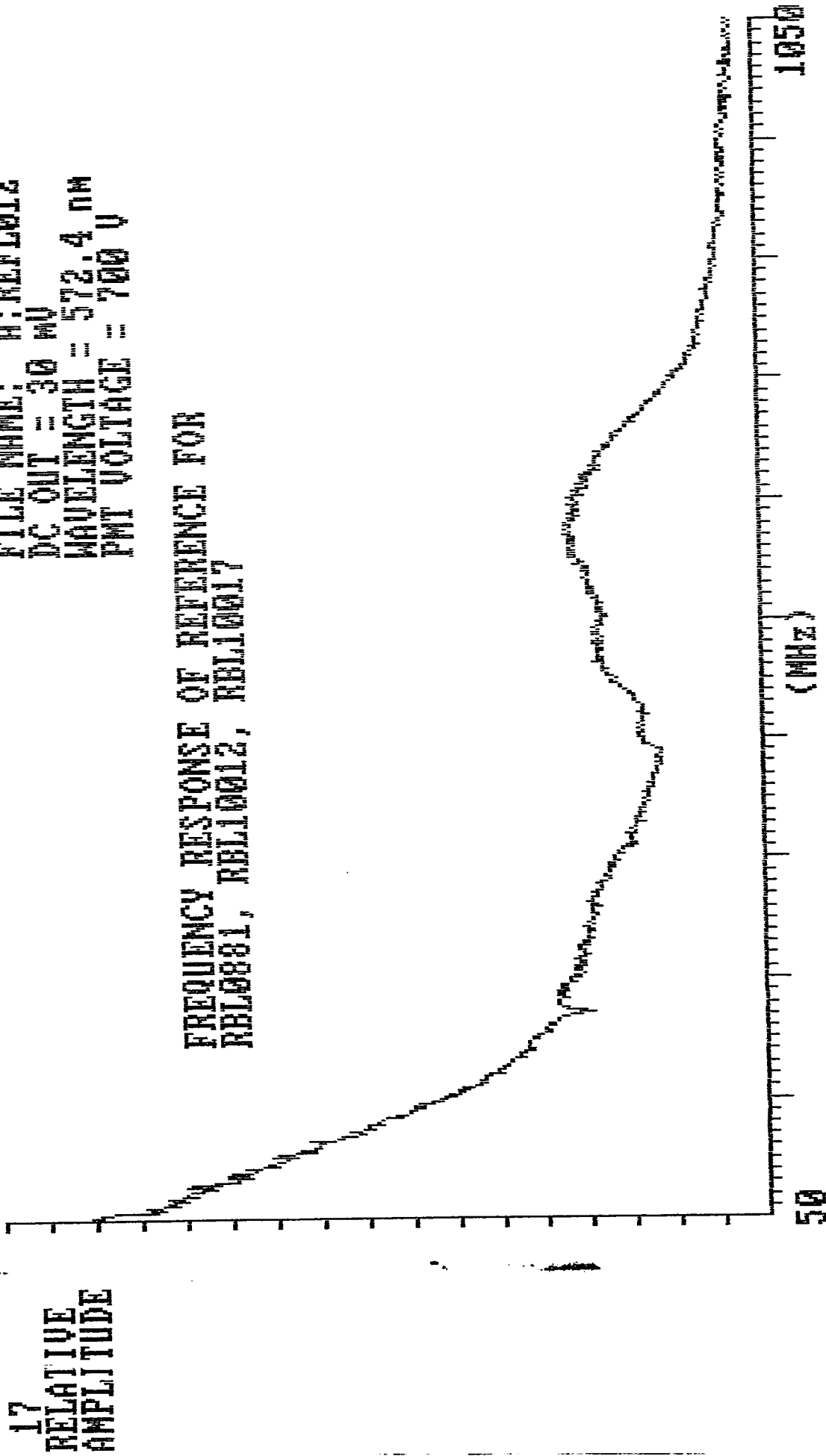
FILE NAME: A:RBL10017  
DC OUT = 30 MV  
WAVELENGTH = 572.4 NM  
PMT VOLTAGE = 700 V

FREQUENCY RESPONSE OF ROSE BENGAL  
IN 100 % WATER AND 0 % ETHANOL



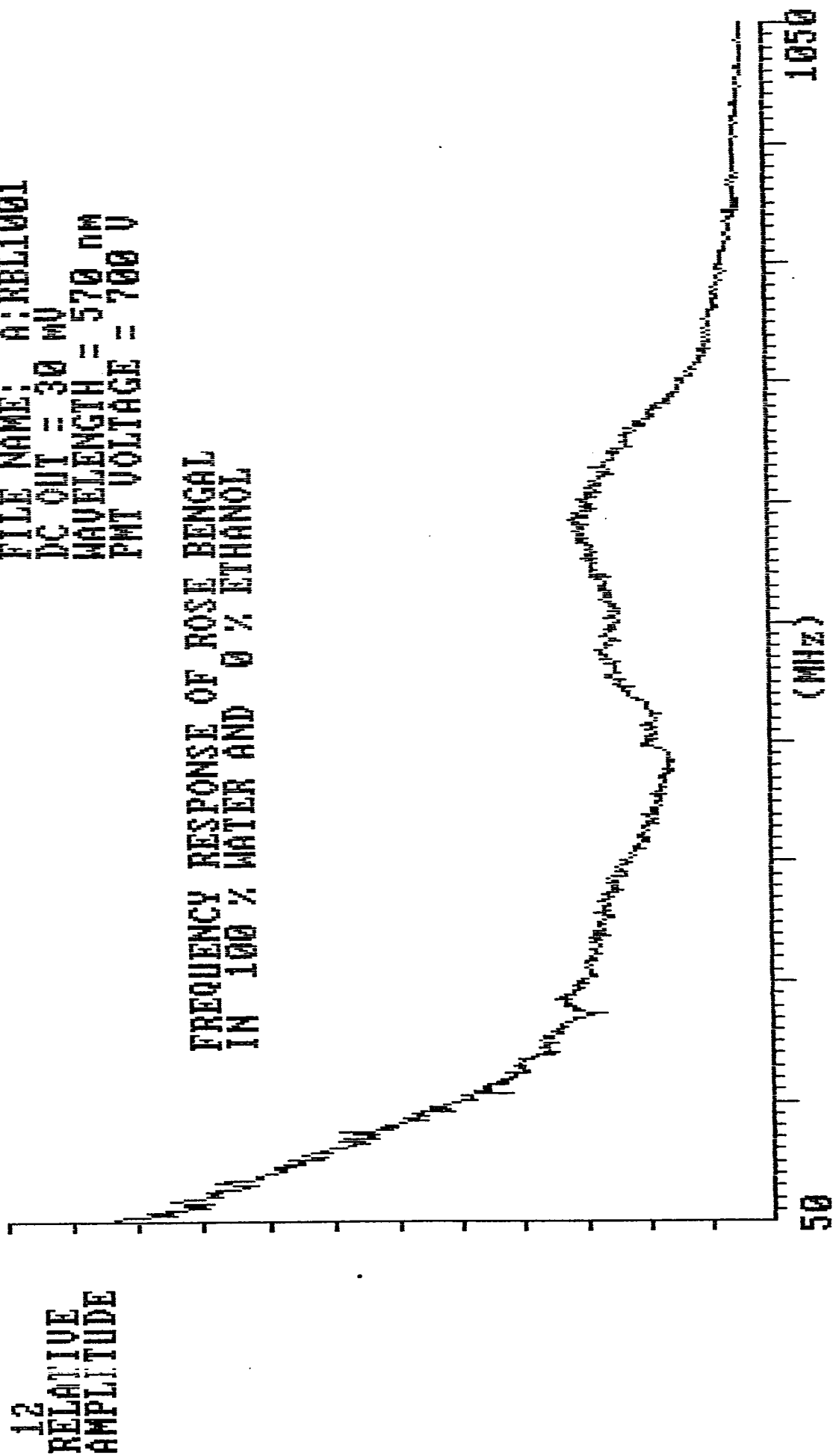
FILE NAME: A:REFL012  
DC OUT = 30 MV  
WAVELENGTH = 572.4 nm  
PMT VOLTAGE = 700 V

FREQUENCY RESPONSE OF REFERENCE FOR  
RBL0881, RBL10012, RBL10017



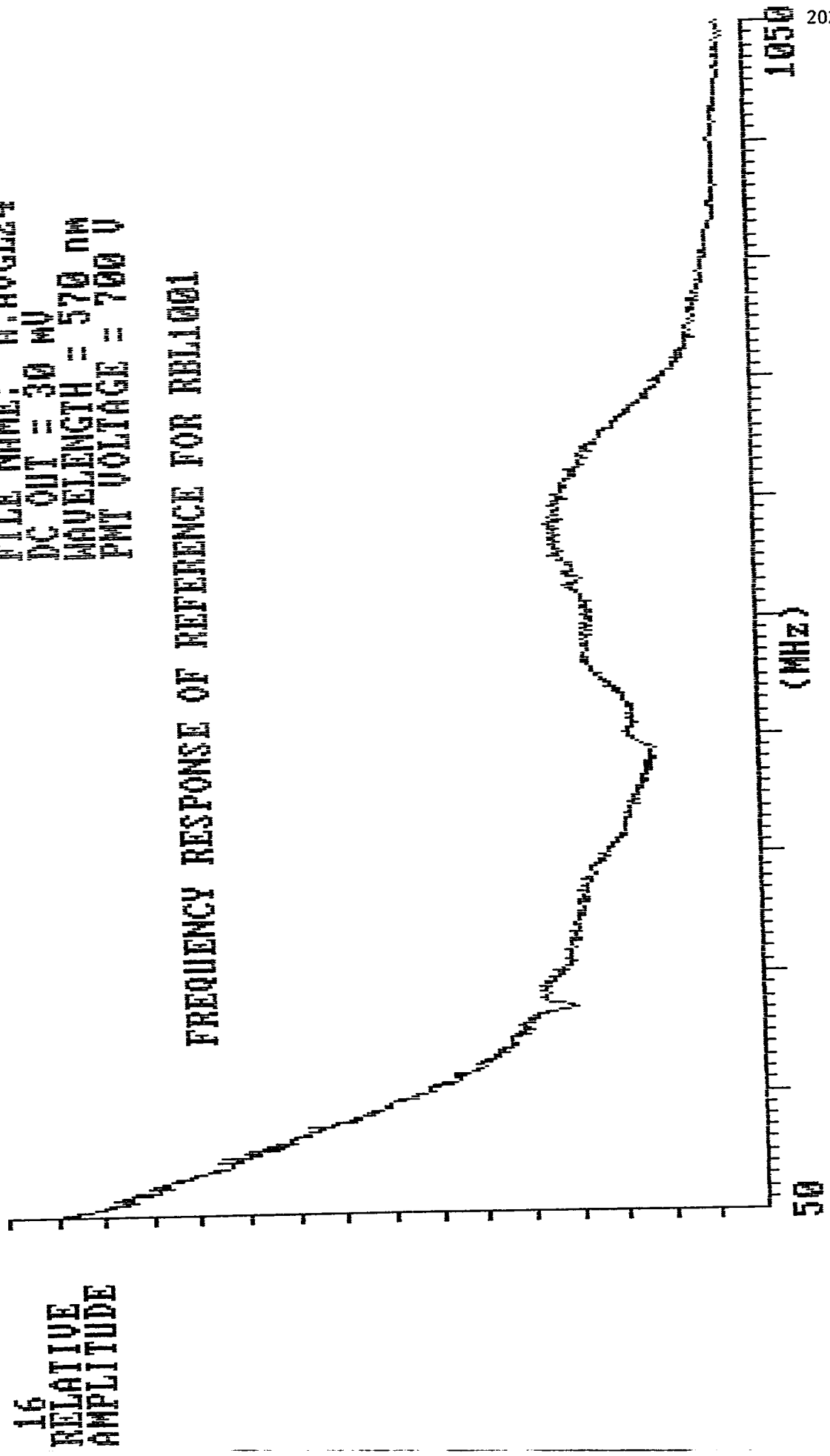
FILE NAME: A:RBL1001  
DC OUT = 30 MV  
WAVELENGTH = 570 nm  
PMT VOLTAGE = 700 V

FREQUENCY RESPONSE OF ROSE BENGAL  
IN 100 % WATER AND 0 % ETHANOL



FILE NAME: 0:AVGL24  
DC OUT = 30 MV  
WAVELENGTH = 570 nm  
PMT VOLTAGE = 700 V

FREQUENCY RESPONSE OF REFERENCE FOR NBL1001



# **APPENDIX II**

**BASIC PROGRAM LISTING**

**FOR**

**SPECTRUM ANALYZER**

**BASELINE SUBTRACTION**

---

```

'READ SIGNAL FILE, AND BASELINE FILE

20 INPUT "ENTER SIGNAL,BASELINE FILES"; S$, B$
   INPUT "NEW FILE NAME"; NSS
   OPEN S$ FOR INPUT AS #1 LEN = 4
   OPEN B$ FOR INPUT AS #2 LEN = 4
   OPEN NSS FOR OUTPUT AS #3 LEN = 4

   INPUT #1, NPTS, START, FINISH
   INPUT #2, A, B, C
   WRITE #3, NPTS, START, FINISH
   PRINT NPTS, START, FINISH
   FOR K = 1 TO NPTS
     INPUT #1, S
     INPUT #2, B

' TO CALUCLATE WHAT IS NEEDED FOR SUBTRACTION WE CAN SAY THAT:
' SUBT(K) = MxD(K) + T ; WHERE D(K) = S(K) - B(K)
' IN EACH REGION : M = (SUBT2-SUBT1)/(D2-D1)
'                   B = SUBT2 - MxD2 OR SUBT1-MxD1

' D(K) IS THE DIFFERENCE BETWEEN SIGNAL AND BASELINE

D = S - B

' NO SUBTRACTION FOR THE FIRST REGION, LITTLE SUBTRACTION FOR THE SECOND
' MORE FOR THE THIRD AND SO ON.
' M, AND T ARE THE SLOPE AND SUBT (ie, y) INTERCEPT OF THE SUBTRACTION

IF D > 28.6 OR D = 28.6 THEN
M = 0: T = 0

ELSEIF D < 28.6 AND D > 21.2 OR D = 21.2 THEN
M = -.014: T = .586

ELSEIF D < 21.2 AND D > 10.8 OR D = 10.8 THEN
M = -.15: T = 3.56

ELSEIF D < 10.8 AND D > 7.6 OR D = 7.6 THEN
M = -.22: T = 4.26

ELSEIF D < 7.6 AND D > 7 OR D = 7 THEN
M = -.66: T = 7.67

```

```
ELSEIF D < 7 AND D > 5.4 OR D = 5.4 THEN  
M = -.25: T = 4.75
```

```
ELSEIF D < 5.4 AND D > 4 OR D = 4 THEN  
M = -.43: T = 5.71
```

```
ELSEIF D < 4 AND D > 3.2 OR D = 3.2 THEN  
M = -1.5: T = 10
```

```
ELSEIF D < 3.2 AND D > 1.2 OR D = 1.2 THEN  
M = -1.05: T = 8.56
```

```
ELSEIF D < 1.2 AND D > 1 OR D = 1 THEN  
M = -3.5: T = 11.5
```

```
END IF
```

```
SUBT = M * D + T
```

```
'NS IS THE NEW SUBTRACTED VALUE
```

```
NS = S - SUBT
```

```
'WHEN THEN DIFFERENCE BETWEEN APPARENT SIGNAL AND  
'BASELINE IS VERY SMALL, SET THE NEW VALUE  
'TO ZERO BECAUSE OF UNRELIABILITY
```

```
IF D < 1 THEN NS = 0
```

```
' WRITE THE NEW VALUE INTO "NEW FILE"
```

```
WRITE #3, NS  
PRINT K, S, B, NS
```

```
NEXT K
```

```
CLOSE #1
```

```
CLOSE #2
```

```
CLOSE #3
```

```
END
```

# REFERENCES

---

## References

1. K.G. Spears, E. Cramer, and L.D. Hoffland, *Rev. Sci. Instrum.* **49**, 255 (1978).
2. H. Walther, *Laser Spectroscopy of Atoms and Molecules*, Springer-Verlag, pp. 1-19 (1976).
3. UWE K. A. Klein, *The Arabian Journal for Science and Engineering*, **9**, 327(1984).
4. J.R. Lacowicz, and I. Gryczynski, *The Arabian Journal for Science and Engineering*, **17**, 261 (1992).
5. A.H. Zewail, *Advances in Laser Chemistry*, Springer-Verlag (1978).
6. M. Nakazawa, T. Nakashima, H. Kubota, and S. Seikai, *Appl. Phys. Lett.* **51**, 10 (1987).
7. C.V. Shank, *Science*, **233**, 1276 (1986).
8. W.R. Ware, L.J. Doemeny and T.L. Nemzek, *J. Phys. Chem.* **77**, 2038 (1973).
9. A.H. Zewail, *Science*, **242**, 1645 (1988).
10. J.G. Fujimoto, *Femtosecond Pulse Generation and Measurement*, Spectra Physics (1988).
11. C.C. Dorsey, M.J. Pelletier, and J.M. Harris, *Rev. Sci. Instrum.* **50**, 333 (1979).
12. K.J. Williams, L. Goldberg, R.D. Esman, M. Dagenais, and J.F. Weller, *Electron. Lett.* **25**, 1242-3 (1989).
13. K.J. Williams, L. Goldberg, and R.D. Esman, *CLEO 90*, CTUH 75.

14. D.C. Neckers, *Journal of Photochemistry and Photobiology, A*, **47**, 1, 1989.
15. G.R. Fleming, J.M. Morris, and G.W. Robinson, *Chemical Physics*, **17**, 91 (1976).
16. G.A. Epling and M.L. Jackson, *Tetrahedron Letters*, **32**, 7507 (1991).
17. M.A.J. Rodgers, *Chemical Physics Letters*, **78**, 509 (1981).
18. M.A.J. Rodgers, *Phys. Chem.* **85**, 3372 (1981).
19. M.A.J. Rodgers, and H.D. Burrows, *Chemical Physics Letters*, **66**, 238 (1979).
20. E.W. Small, L.J. Libertini, D.W. Brown, and J.R. Small, *Optical Engineering*, **30**, 1345 (1991).
21. D.P. Shoemaker, C.W. Garland, and J.W. Nipler, *Experiments in Physical Chemistry*, McGraw-Hill (1989).
22. J. Lee, R.D. Griffin, and G.W. Robinson, *J. Chem. Phys.* **82**, 4920 (1985).
23. J. Lee, G.W. Robinson, S.P. Webb, L.A. Philips, and J.H. Clark, *J. Am. Chem. Soc.* **108**, 6538 (1986).
24. J. Lee, *J. Am. Chem. Soc.* **111**, 427 (1989).
25. T.G. Fillingim, N. Luo, J. Lee, and G.W. Robinson, *J. Phys. Chem.* **94**, 6368 (1990).
26. R. Krishnan, T.G. Fillingim, J. Lee, and G.W. Robinson, *J. Am. Soc.* **112**, 1353 (1990).